BULLETIN OF RUSSIAN STATE MEDICAL UNIVERSITY

BIOMEDICAL JOURNAL OF PIROGOV RUSSIAN NATIONAL RESEARCH MEDICAL UNIVERSITY

SUBMISSION http://vestnikrgmu.ru/login?lang=en
CORRESPONDENCE editor@vestnikrgmu.ru
COLLABORATION manager@vestnikrgmu.ru
ADDRESS ul. Ostrovityanova, d. 1, Moscow, Russia, 117997

Indexed in Scopus. CiteScore 2022: 0.5

Indexed in WoS. JCR 2021: 0.5

Five-year h-index is 8

SCImago Journal & Country Rank 2020: 0.14

Listed in HAC 31.01.2020 (№ 507)

Open access to archive

Issue DOI: 10.24075/brsmu.2023-04
The mass media registration certificate № 012769 issued on July 29, 1994
Founder and publisher is Pirogov Russian National Research Medical University (Moscow, Russia)

Approved for print 31.08.2023
Circulation: 100 copies. Printed by Print.Formula
www.print-formula.ru

ВЕСТНИК РОССИЙСКОГО ГОСУДАРСТВЕННОГО МЕДИЦИНСКОГО УНИВЕРСИТЕТА

НАУЧНЫЙ МЕДИЦИНСКИЙ ЖУРНАЛ РНИМУ ИМ. Н. И. ПИРОГОВА

ГЛАВНЫЙ РЕДАКТОР Денис Ребриков, д. б. н., профессор

ЗАМЕСТИТЕЛЬ ГЛАВНОГО РЕДАКТОРА Александр Эттингер, д. м. н., профессор

РЕДАКТОРЫ Валентина Гейдебрехт, к. б. н.; Надежда Тихомирова

ТЕХНИЧЕСКИЙ РЕДАКТОР Евгений Лукьянов

ПЕРЕВОДЧИКИ Надежда Тихомирова, Вячеслав Витюк

ДИЗАЙН И ВЕРСТКА Марины Дорониной

ПОДАЧА РУКОПИСЕЙ http://vestnikrgmu.ru/login
ПЕРЕПИСКА С РЕДАКЦИЕЙ editor@vestnikrgmu.ru
СОТРУДНИЧЕСТВО manager@vestnikrgmu.ru
АДРЕС РЕДАКЦИИ ул. Островитянова, д. 1, г. Москва, 117997

Журнал включен в Scopus. CiteScore 2022: 0,5

Журнал включен в WoS. JCR 2021: 0,5

Индекс Хирша (h^5) журнала по оценке Google Scholar: 8

SCImago Journal & Country Rank 2020: 0,14

Журнал включен в Перечень 31.01.2020 (№ 507)

Здесь находится открытый архив журнала

DOI выпуска: 10.24075/vrgmu.2023-04
Свидетельство о регистрации средства массовой информации № 012769 от 29 июля 1994 г.
Учредитель и издатель — Российский национальный исследовательский медицинский университет имени Н. И. Пирогова (Москва, Россия)

Подписано в печать 31.08.2023
Тираж 100 экз. Отпечатано в типографии Print.Formula
www.print-formula.ru

BULLETIN OF RSMU **4, 2023**
ВЕСТНИК РГМУ

Contents
Содержание

ASSESSMENT OF METASTATIC TRAITS OF THE CELLS WITH HYBRID PHENOTYPE IN BREAST CANCER

Mukhamedzhanov RK[1,4], Grigoryeva ES[2], Tashireva LA[2], Perelmuter VM[2], Zavyalova MV[1,2], Savelieva OE[2,3] ✉

[1] Siberian State Medical University, Tomsk, Russia
[2] Cancer Research Institute, Tomsk National Research Medical Center, Russian Academy of Sciences, Tomsk, Russia
[3] Saint-Petersburg State Pediatric Medical University, Saint-Petersburg, Russia
[4] Regional Children's Clinical Hospital, Vladimir, Russia

Nowadays, great attention is paid to the study of circulating tumor cells (CTCs) due to their key role in distant metastasis. At the same time there is little data on the properties of circulating cells showing simultaneous expression of the leukocyte and epithelial markers and their possible role in tumor progression and chemotherapy resistance. The study was aimed to assess subpopulations of cells with hybrid epithelial/leukocyte phenotype and estimate the features of stemness, epithelial–mesenchymal transition (EMT), and integrin interface, which determine the cells' possible metastatic properties in breast cancer (BC). The survey data from 128 patients with invasive breast carcinoma of no special type were included. Multicolor flow cytometry was used to assess the population structure and metastatic potential of the cells circulating in blood and primary tumor cells with hybrid phenotype. The primary tumor cell suspension was prepared by mechanical disaggregation. The high degree of heterogeneity was noted in the population of cells with hybrid phenotype, including the combination of the stemness and EMT features, and diverse integrin interface. Cells with hybrid phenotype are involved in the mechanisms underlying lymph node and distant metastasis. In lymph node metastasis, metastatic potential of these cells is associated with the stemness features (p = 0.0422) and co-expression of β3-, β4-, and αVβ5-integrins (p = 0.0338). In distant metastasis, metastatic potential of hybrid cells is associated with the stemness features (p = 0.015) and is not associated with the EMT features and integrin expression.

Keywords: hybrid cells, circulating tumor cells, metastasis, stemness, epithelial-mesenchymal-transition, integrins

Funding: the study was supported by the RSF grant № 21-15-00140.

Author contribution: Mukhamedzhanov RK — literature analysis, data acquisition and statistical processing, manuscript writing; Grigoryeva ES — data acquisition and analysis, manuscript writing; Tashireva LA — study design, manuscript editing; Perelmuter VM — data interpretation, manuscript editing; Zavyalova MV — study planning, manuscript editing; Savelieva OE — study planning and management, data analysis and interpretation, manuscript writing.

Compliance with the ethical standards: the study was approved by the Ethics Committee of the Cancer Research Institute, Tomsk National Research Medical Center (protocol № 10 of 24 April 2015) and conducted in accordance with the Federal Laws of the Russian Federation (№ 152, 323, etc.), the Declaration of Helsinki (1964) and all subsequent amendments and supplements regulating the research involving human biomaterials. The informed consent to study participation was submitted by all subjects.

✉ **Correspondence should be addressed:** Olga E. Savelieva
Litovskaya, 2, Saint-Petersburg, 194100; olga_chechina@mail.ru

Received: 04.07.2023 **Accepted:** 22.08.2023 **Published online:** 31.08.2023

DOI: 10.24075/brsmu.2023.033

ОЦЕНКА МЕТАСТАТИЧЕСКИХ ХАРАКТЕРИСТИК КЛЕТОК С ГИБРИДНЫМ ФЕНОТИПОМ ПРИ РАКЕ МОЛОЧНОЙ ЖЕЛЕЗЫ

Р. Х. Мухамеджанов[1,4], Е. С. Григорьева[2], Л. А. Таширева[2], В. М. Перельмутер[2], М. В. Завьялова[1,2], О. Е. Савельева[2,3] ✉

[1] Сибирский государственный медицинский университет, Томск, Россия
[2] Научно-исследовательский институт онкологии, Томский национальный исследовательский медицинский центр Российской академии наук, Томск, Россия
[3] Санкт-Петербургский государственный педиатрический медицинский университет, Санкт-Петербург, Россия
[4] Областная детская клиническая больница, Владимир, Россия

Изучению циркулирующих опухолевых клеток (ЦОК) в последнее время уделяют большое внимание, благодаря их ведущей роли в формировании отдаленных метастазов. В то же время мало данных о свойствах циркулирующих клеток с одновременной экспрессией лейкоцитарных и эпителиальных маркеров и их возможной роли в опухолевой прогрессии и резистентности к химиотерапии. Целью исследования было изучить субпопуляции клеток с гибридным эпителиально-лейкоцитарным фенотипом, а также оценить признаки стволовости, эпителиально-мезенхимальный переход (ЭМП) и интегриновый интерфейс, обусловливающие их возможные метастатические свойства при раке молочной железы (РМЖ). В работу включены данные исследования 128 больных инвазивной карциномой неспецифического типа молочной железы. Для оценки популяционного состава и метастатического потенциала циркулирующих в крови клеток и клеток первичной опухоли с гибридным фенотипом использовали метод многоцветной проточной цитометрии. Суспензию клеток первичной опухоли готовили методом механической дезагрегации. В популяции клеток с гибридным фенотипом отмечена высокая степень гетерогенности, включая комбинацию признаков стволовости, ЭМП и разнообразный интегриновый интерфейс. Клетки с гибридным фенотипом принимают участие в механизмах лимфогенного и гематогенного метастазирования. При лимфогенном метастазировании метастатический потенциал этих клеток ассоциирован с признаками стволовости (p = 0,0422) и коэкспрессией β3-, β4- и αVβ5-интегринов (p = 0,0338). При гематогенном метастазировании метастатический потенциал гибридных клеток ассоциирован с признаками стволовости (p = 0,015) и не связан с признаками ЭМП и экспрессией интегринов.

Ключевые слова: гибридные клетки, циркулирующие опухолевые клетки, метастазы, стволовость, эпителиально-мезенхимальный переход, интегрины

Финансирование: работа выполнена при финансовой поддержке гранта РНФ 21-15-00140.

Вклад авторов: Р. Х. Мухамеджанов — анализ литературы, получение и статистическая обработка результатов, написание статьи; Е. С. Григорьева — получение и анализ данных, написание статьи; Л. А. Таширева — дизайн исследования, редактирование статьи; В. М. Перельмутер — интерпретация результатов, редактирование статьи; М. В. Завьялова — планирование исследования, редактирование статьи; О. Е. Савельева — планирование и руководство исследованием, анализ и интерпретация результатов, написание статьи.

Соблюдение этических стандартов: исследование одобрено этическим комитетом НИИ онкологии Томского НИМЦ (протокол № 10 от 24 апреля 2015 г.), проведено в соответствии с федеральными законами Российской Федерации (№ 152, 323 и др.) и Хельсинкской декларацией 1964 г. и всеми последующими дополнениями и изменениями, регламентирующими научные исследования на биоматериале, полученном у людей. Все участники подписали информированное добровольное согласие об участии в исследовании.

✉ **Для корреспонденции:** Ольга Евгеньевна Савельева
ул. Литовская, д. 2, г. Санкт-Петербург, 194100; olga_chechina@mail.ru

Статья получена: 04.07.2023 **Статья принята к печати:** 22.08.2023 **Опубликована онлайн:** 31.08.2023

DOI: 10.24075/vrgmu.2023.033

Nowadays, great attention is paid to the study of circulating tumor cells (CTCs). This is due to their key role in distant metastasis and, therefore, in adverse outcomes of cancer. Today, the data are available on their subpopulation composition [1], stem-like properties [2], epithelial–mesenchymal transition (EMT) [3], chemotherapy resistance [4]; the genomic profiling data of CTCs have been also published [5]. Furthermore, the importance of integrin expression in CTCs for metastasis in breast cancer (BC) has been shown; the CTC integrin interface can be associated with the location of distant metastases [6–7]. The data on the correlation of peripheral blood levels of these cells with the survival rate and the risk of distant metastasis in BC [8], lung cancer [9], ovarian cancer [10], colorectal cancer [11], etc. are provided. Thus, in 2019 it was shown that the presence of CTCs showing stemness and partial EMT features was associated with adverse disease outcomes and reduced overall survival rate. Cells with the same phenotype turned out to be resistant to chemotherapy [12].

When studying various CTC populations, we have found unusual cells showing simultaneous expression of the CD45 leukocyte and CD326 (EpCAM) epithelial markers. It turned out that other researchers obtained similar results. Thus, cells with the $CD45^{+}CK^{+}EpCAM^{+}$ phenotype were found in blood of patients with BC, and in 90% of cases expression of the CD68 macrophage marker was also noted [13]. Cells with the $CD45^{+}EpCAM^{+}$ phenotype were found in primary tumors and pleural effusion of all surveyed patients with non-small cell lung cancer. Moreover, the higher percentage of such cells was associated with adverse outcome [14].

Hybridization (cell fusion) between tumor cells and macrophages or leukocytes is the most probable mechanism underlying generation of cells showing simultaneous expression of the leukocyte and epithelial markers. It has been noted that formation of hybrid cells is associated with many body's physiological processes, such as muscle and bone tissue formation, wound healing [15]. The $CD45^{+}EpCAM^{+}$ cells' physiological role is confirmed by detection of these cells in blood of healthy donors. However, biological value of these cells together with their role in physiological and disease processes is poorly understood.

Due to the lack of knowledge about the cells showing simultaneous expression of the leukocyte and epithelial markers and the data on their possible role in tumor progression and chemotherapy resistance [16], our study was aimed to assess subpopulations of cells with hybrid epithelial/leukocyte phenotype and estimate the features of stemness, EMT, and integrin interface, which determine the cells' possible metastatic properties in breast cancer (BC).

METHODS

Patients

Survey results of 128 patients treated in the clinics of the Cancer Research Institute, Tomsk National Research Medical Center, in 2015–2020 were included in the study. Inclusion criteria: invasive breast carcinoma of no special type; age 29–76 years (average age: 52.56 ± 11.57; $T1^{-}4N0^{-}3M0^{-}1$). Exclusion criteria: breast cancer of other histological type; multiple primary malignant tumors; exacerbation of chronic inflammatory disorder. To assess the population structure and metastatic traits of the circulating cells with hybrid phenotype, venous blood was collected from 108 patients before neoadjuvant chemotherapy. The association between cells with hybrid phenotype and lymph node or distant metastasis was estimated in the group of patients without neoadjuvant chemotherapy (n = 79). To assess properties of the cell populations with the primary tumor hybrid phenotype, surgical material obtained from 35 patients during surgical treatment (radical mastectomy or sectoral resection) was studied. These patients were not prescribed neoadjuvant therapy. The basic clinical and morphological parameters are provided in Table. 1.

Sample preparation for flow cytometry

The patients' venous blood was collected before the course of neoadjuvant chemotherapy and surgical treatment in the morning in the fasting state: 12 mL in the EDTA vacuum tubes. The entire volume of blood was used to prepare cell concentrate by sedimentation at 37 °C for 90 min at an angle of 45° with subsequent collection of buffy coat with cells on the boundary between the erythrocyte sediment and the separated blood plasma, as well as the entire supernatant, in accordance with the method by R.A. Pospelova [17].

Fresh cancer tissue samples were mechanically disaggregated using the BD Medimachine System (BD; USA) for cell suspensions. The total cell count of the resulting suspensions was determined using the Luna-II Cell Counter system (Logos Biosystems; Korea).

Flow cytometry of samples and data processing

After Fc blocking with the Human TruStain FcX™ Fc Receptor Blocking Solution (Biolegend; USA), 5 μL of the BV570 anti-human CD45 (clone HI30; Sony Biotechnology, USA), BV650 anti-human CD326 (EpCAM) (clone 9C4; Sony Biotechnology, USA), BV510 anti-human CD44 (clone G44-26; BD Horizon, USA), PerCP/Cy5.5 anti-human CD24 (clone ML5; Sony Biotechnology, USA), PE/Cy7 anti-human N-Cadherin (clone 8C11; Sony Biotechnology, USA) monoclonal antibodies and 7-AAD Viability Staining Solution (Sony Biotechnology; USA) were added to the primary tumor cell concentrate and/or cell suspension and incubated in the dark at room temperature for 20 min. Cell concentrate was also supplemented with 5 μL of the BV 421-anti-β3 integrin (clone VI-PL2; BD Biosciences, USA), Alexa Fluor 488-anti-β4 integrin (clone 422325; R&D Systems, USA), BV Alexa Fluor 750-anti-αVβ5 integrin (clone P5H9; R&D Systems, USA) monoclonal antibodies. The unstained control was processed in parallel. After incubation, 500 μL of the OptiLyse C buffer (Beckman Coulter; France) were added to the samples for erythrocyte lysis, then the samples were washed in 2 mL of the CellWASH solution (BD Biosciences; USA) for 10 min at 300 g with subsequent removal of supernatant. During the intracellular staining phase each stained sample was supplemented with 250 μL of the BD Cytofix/Cytoperm solution (BD Biosciences; USA), incubated in the dark for 30 min at 4 °C, and then twice washed in 1 mL of the BD Perm/Wash buffer (BD Biosciences; USA) when centrifuged at 300 g for 6 min. A total of 50 μL of the BD Perm/Wash buffer (BD Biosciences; USA) were added to the samples, the stained sample was supplemented with 5 μL of the AF647-anti-human CK7/8 antibody (clone CAM5.2; BD Pharmingen, USA) and incubated at 4 °C for 20 min. After that each sample was washed in 1 mL of the CellWASH buffer (BD Biosciences; USA) by centrifugation at 300 g for 6 min. In the final phase 500 μL of the Cell Staining Buffer (Sony Biotechnology; USA) were added to precipitate, and the sample was resuspended.

Nonspecific staining was controlled using appropriate isotype antibodies. The BC MCF-7 cell line was used as a positive control for antibodies against epithelial markers EpCAM

Table 1. Characteristics of patients with invasive breast carcinoma of no special type

Parameter	Parameter value	Frequency, % (abs.)
Age	52.56 ± 11.57	
Molecular subtype	Luminal A	32.8% (42/128)
	Luminal B	47.7% (61/128)
	Triple negative	15.6% (20/128)
	HER2neu+	3.9% (5/128)
Stage	I	25.0% (32/128)
	IIA	48.4% (62/128)
	IIB	17.2% (22/128)
	IIIA	1.6% (2/128)
	IIIB	4.7% (6/128)
	IIIC	3.1% (4/128)
Lymph node metastasis	Yes	34.4% (44/128)
	No	65.6% (84/128)
Distant metastasis	Yes	9.4% (12/128)
	No	90.6% (116/128)
Estrogen receptors	Positive	80.5% (103/128)
	Negative	19.5% (25/128)
Progesterone receptors	Positive	71.9% (92/128)
	Negative	28.1% (36/128)
HER2 receptors	Positive	51.6% (66/128)
	Negative	48.4% (62/128)
Ki67 expression	< 20%	35.9% (46/128)
	>20%	64.1% (82/128)
Tumor size	< 2 cm	28.1% (36/128)
	2–5 cm	67.2% (86/128)
	> 5 cm	4.7% (6/128)
Menstrual status	Postmenopausal	41.4% (53/128)
	Premenopausal	54.7% (70/128)
	Perimenopausal	3.9% (5/128)
Neoadjuvant chemotherapy	Yes	38.3% (49/128)
	No	61.7% (79/128)
Tumor grade	1	17.2% (22/128)
	2	63.3% (81/128)
	3	19.5% (25/128)
Recurrence	Yes	5.5% (7/128)
	No	94.5% (121/128)

and CK7/8 and a negative control for CD45. The histiocytic lymphoma U937 cell line was used as a negative control for antibodies against the above epithelial markers and a positive control for CD45.

The samples were analyzed in the Novocyte 3000 flow cytometer (ACEA Biosciences; USA) using NovoExpress 1.3.0 (ACEA Biosciences; USA). The concentration of circulating cells per 1 mL of blood and the concentration of primary tumor cells per 1000 tumor cells were calculated. When gating cells with hybrid phenotype, the cells were first analyzed in the FSC vs. SSC mode, then singlets were isolated in the FSC-A vs. FSC-H mode. After that viable cells were isolated based on the 7-AAD negative stain, and then cell fluorescence parameters were analyzed in appropriate channels. The gating strategy for cells with hybrid phenotype is provided in Fig. 1.

Statistical analysis

Statistical processing of the results was performed using the IBM SPSS Statistics 22 (Armonk; USA) and GraphPad Prism 8.3.1 (GraphPad Software; USA) software packages. All the studied parameters were tested for normality using the Shapiro–Wilk test. Parameters were described using median (Me) and interquartile range (Q_1–Q_3). The differences in parameters were assessed using the Mann–Whitney U test and the Wilcoxon signed-rank test. Fisher's exact test was used to estimate the differences in the traits' frequency. Spearman's rank correlation coefficient was calculated to determine the relationships between the traits. The differences were considered significant at $p < 0.05$ (5%).

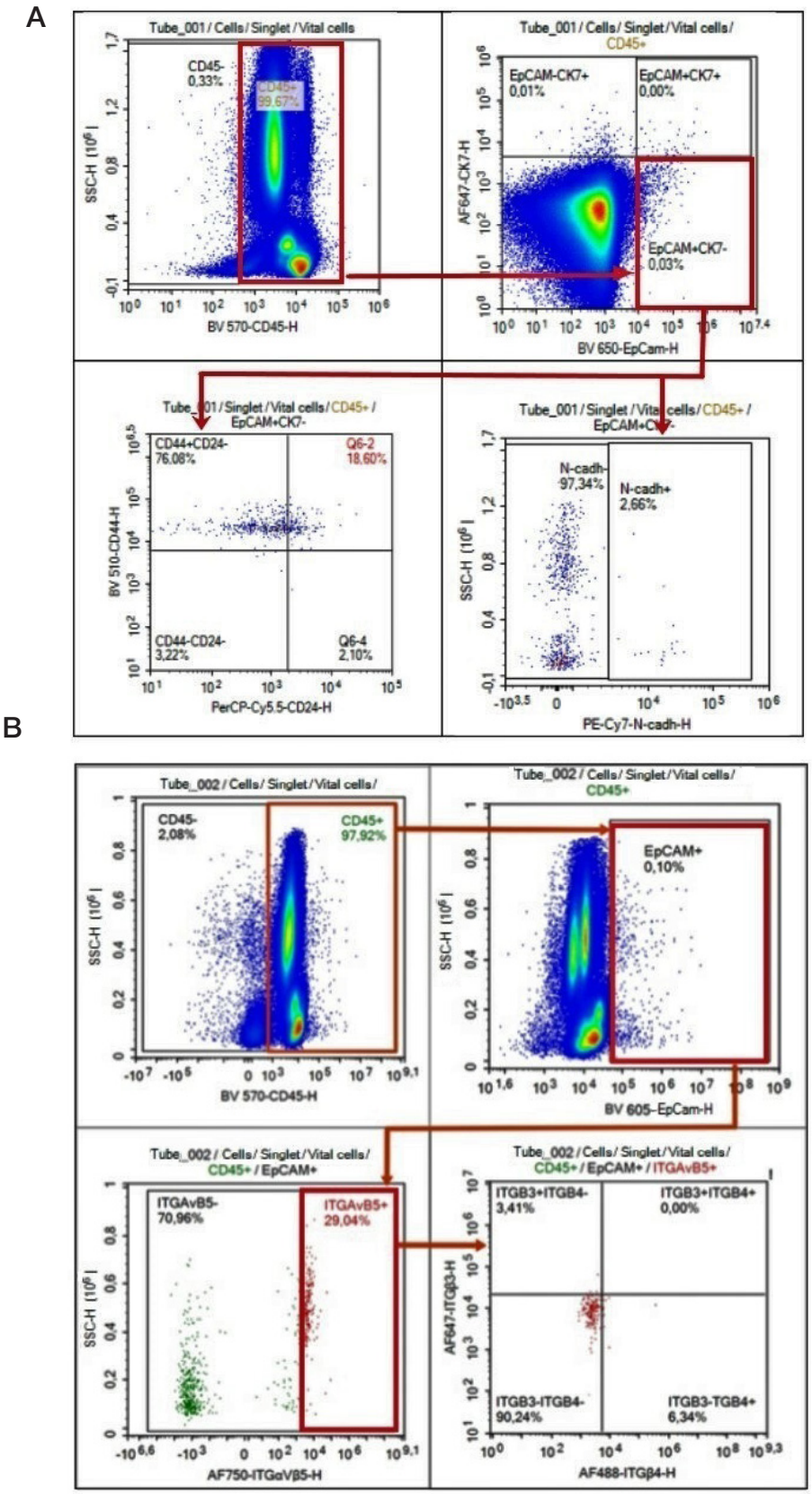

Fig. 1. Gating strategy for the populations of cells with hybrid phenotype and expression of the leukocyte, epithelial, stem and EMT markers (**A**), and integrin receptors (**B**) exemplified by the cells circulating in blood

Logistic regression was used as a multivariate method to assess the relationships between the traits and build the prognostic models. When building mathematical models, the threshold values were determined by ROC analysis. The probability of an event was calculated using the following formula: $P = e^Y/(1+e^Y)$, where P was the probability of a trait; Y was a regression equation value; e was a mathematical constant equal to 2.72. When the probability $P \geq 50\%$, the risk of the event was considered to be high; when the probability $P < 50\%$, the risk was considered to be low. The differences were considered significant at $p < 0.05$ (5%).

Table 2. Frequency of cells with hybrid phenotype in patients with breast cancer

№	Phenotype	Frequency, %	Significance level
Blood			
1	$CD45^+EpCAM^+CK7/8^-$	93.5% (101/108)	$p_{1-2} = 0.1137$; $p_{1-3} = 0.0045$
2	$CD45^+EpCAM^+CK7/8^+$	86.1% (93/108)	$p_{2-3} = 0.2785$
3	$CD45^+EpCAM^-CK7/8^+$	79.6% (86/108)	
Primary tumor			
4	$CD45^+EpCAM^+CK7/8^-$	94.6% (35/37)	$p_{4-1} = 1.0000$; $p_{4-5} = 0.0123$; $p_{4-6} = 0.0001$
5	$CD45^+EpCAM^+CK7/8^+$	70.3% (26/37)	$p_{5-2} = 0.0452$; $p_{5-6} = 0.2305$
6	$CD45^+EpCAM^-CK7/8^+$	54.1% (20/37)	$p_{6-3} = 0.0046$

RESULTS

Subpopulation composition of cells with hybrid phenotype

Flow cytometry was used to estimate the expression of the CD45 leukocyte marker and the EpCAM and CK7/8 epithelial markers in the circulating cells and primary tumor cells. The $CD45^+$ cell populations showing co-expression of two epithelial markers ($CD45^+EpCAM^+CK7/8^+$) and mono-expression of one epithelial marker ($CD45^+EpCAM^+CK7/8^-$, $CD45^+EpCAM^-CK7/8^+$) were found in blood and primary tumors of the majority of patients (Table 2).

The largest population most often found in both blood and primary tumor was represented by cells with the $CD45^+EpCAM^+CK7/8^-$ phenotype (Table 2; Fig. 2A).

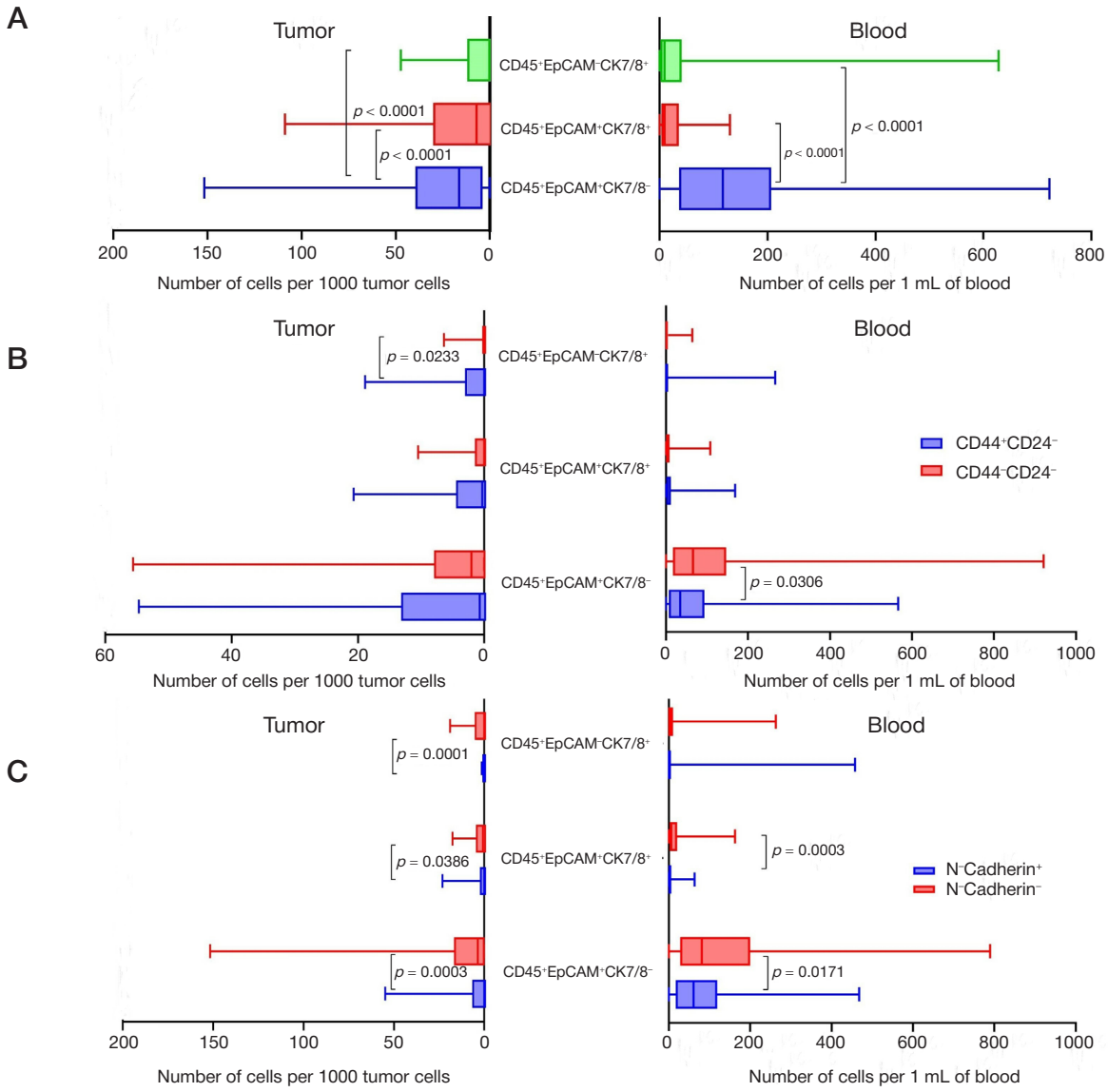

Fig. 2. Number of cells with hybrid phenotype in blood and primary tumors of patients with breast cancer. **A**. Number of cells with various combinations of the CD45 leukocyte and EpCAM and CK7/8 epithelial markers expression. **B**. Number of cells showing stem features. **C**. Number of cells showing features of epithelial–mesenchymal transition

Table 3. Frequency of cells with hybrid phenotype showing stem features in patients with breast cancer

	№	Phenotype	Frequency, %	Significance level
Blood	CD45$^+$EpCAM$^+$CK7/8$^-$			
	1	CD44$^+$CD24$^-$	85.7% (54/63)	$p_{1-2} = 0.0540$
	2	CD44$^-$CD24$^-$	96.8% (61/63)	
	CD45$^+$EpCAM$^+$CK7/8$^+$			
	3	CD44$^+$CD24$^-$	77.8% (49/63)	$p_{3-4} = 0.4179$
	4	CD44$^-$CD24$^-$	69.8% (44/63)	
	CD45$^+$EpCAM$^-$CK7/8$^+$			
	5	CD44$^+$CD24$^-$	47.6% (30/63)	$p_{5-6} = 0.4760$
	6	CD44$^-$CD24$^-$	55.6% (35/63)	
Primary tumor	CD45$^+$EpCAM$^+$CK7/8$^-$			
	7	CD44$^+$CD24$^-$	62.2% (23/37)	$p_{7-8} = 0.2030$; $p_{7-1} = 0.0126$
	8	CD44$^-$CD24$^-$	78.4% (29/37)	$p_{8-2} = 0.0048$
	CD45$^+$EpCAM$^+$CK7/8$^+$			
	9	CD44$^+$CD24$^-$	51.4% (19/37)	$p_{9-10} = 0.3497$; $p_{9-3} = 0.0081$
	10	CD44$^-$CD24$^-$	37.8% (14/37)	$p_{10-4} = 0.0030$
	CD45$^+$EpCAM$^-$CK7/8$^+$			
	11	CD44$^+$CD24$^-$	43.2% (16/37)	$p_{11-12} = 0.0811$; $p_{11-5} = 0.6842$
	12	CD44$^-$CD24$^-$	21.6% (8/37)	$p_{12-6} = 0.0015$

No significant correlations were revealed for the number of cells with hybrid phenotype in blood and primary tumors of BC patients.

Assessment of the metastatic traits in cells with hybrid phenotype

Acquisition of the stemness and EMT features by tumor cells, including CTCs, is associated with their capability of self-renewal, anticancer therapy resistance, and metastatic potential increase [3, 12, 18]. Furthermore, the integrin expression in CTCs plays an important role in metastasis and is likely to promote targeting distant organs by these cells, thereby determining the location of prospective metastases [6–7]. The same properties can be possessed by CTCs with hybrid phenotype. In this regard we have analyzed metastatic potential of the cells with hybrid phenotype circulating in blood and primary tumor cells by assessing the features of stemness, EMT, and expression of integrin receptors.

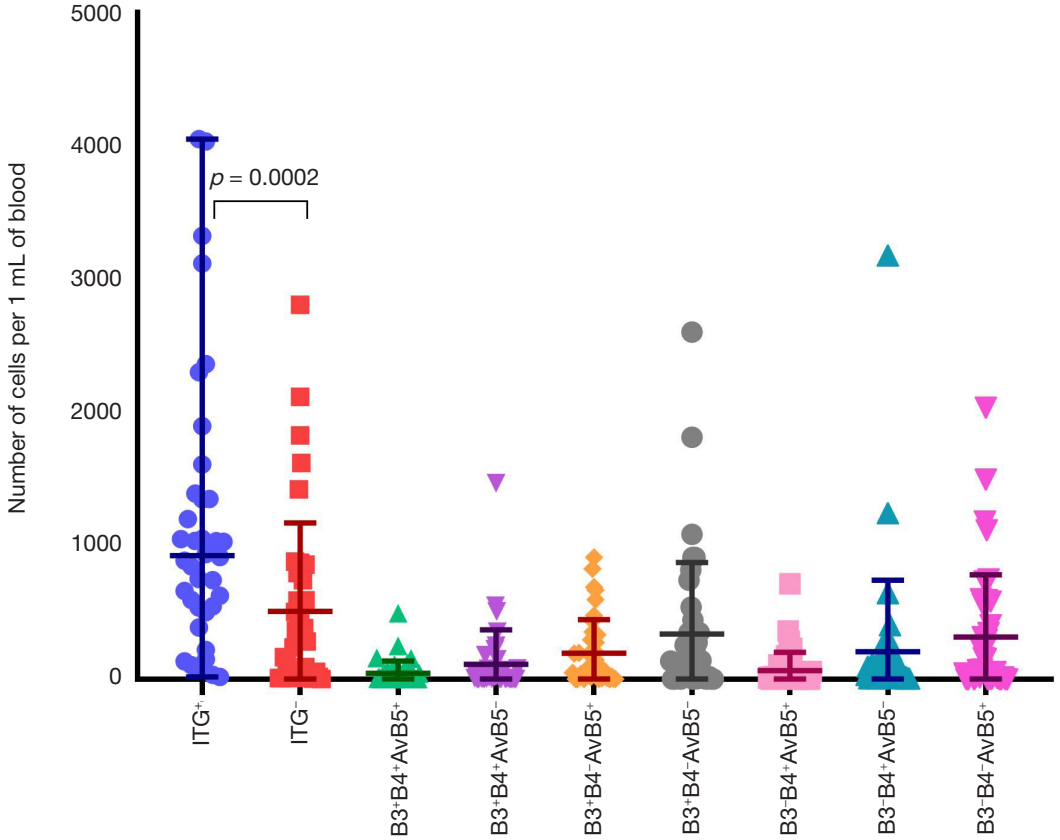

Fig. 3. Number of cells with hybrid phenotype showing expression of β3, β4, and αVβ5 integrin molecules in blood of patients with breast cancer

Table 4. Frequency of cells with hybrid phenotype showing EMT features in patients with breast cancer

	№	Phenotype	Frequency, %	Significance level
Blood	CD45⁺EpCAM⁺CK7/8⁻			
	1	N-cadherin⁺	92.1% (58/63)	$p_{1-2} = 0.7175$
	2	N-cadherin⁻	95.2% (60/63)	
	CD45⁺EpCAM⁺CK7/8⁺			
	3	N-cadherin⁺	65.1% (41/63)	$p_{3-4} = 0.0235$
	4	N-cadherin⁻	84.1% (53/63)	
	CD45⁺EpCAM⁻CK7/8⁺			
	5	N-cadherin⁺	52.4% (33/63)	$p_{5-6} = 0.5909$
	6	N-cadherin⁻	58.7% (37/63)	
Primary tumor	CD45⁺EpCAM⁺CK7/8⁻			
	7	N-cadherin⁺	45.9% (17/37)	$p_{7-8} = 0.0004$; $p_{7-1} = 0.0000$
	8	N-cadherin⁻	86.5% (32/37)	$p_{8-2} = 0.1419$
	CD45⁺EpCAM⁺CK7/8⁺			
	9	N-cadherin⁺	29.7% (11/37)	$p_{9-10} = 0.0340$; $p_{9-3} = 0.0009$
	10	N-cadherin⁻	56.8 (21/37)	$p_{10-4} = 0.0042$
	CD45⁺EpCAM⁻CK7/8⁺			
	11	N-cadherin⁺	5.4% (2/37)	$p_{11-12} = 0.0001$; $p_{11-5} = 0.0000$
	12	N-cadherin+⁻	45.9% (17/37)	$p_{12-6} = 0.2988$

Detection of the stemness features

The results of the analysis of the stemness features in the populations of cells with hybrid phenotype in blood and primary tumor by flow cytometry are provided in Table 3 and Fig. 2B. It was determined that the stemness features were found in all populations of cells with hybrid phenotype, in both blood and primary tumor. However, no significant differences in the frequency of cells possessing and not possessing stem-like properties were revealed. Cells with the CD45⁺EpCAM⁺CK7/8⁻CD44⁺CD24⁻ and CD45⁺EpCAM⁺CK7/8⁺CD44⁺CD24⁻ phenotypes were less common in primary tumor than in blood ($p = 0.0126$ and $p = 0.0081$, respectively) (Table 3).

Quantification of the cell populations with hybrid phenotype demonstrated that the CD45⁺EpCAM⁺CK7/8⁻CD44⁻CD24⁻cells showing mono-expression of the EpCAM epithelial marker and no stemness features prevailed in blood ($p = 0.0306$); there were significantly more hybrids possessing stem-like properties among the CD45⁺EpCAM⁻CK7/8⁺ cells of the tumor ($p = 0.0233$) (Fig. 2B).

Detection of the EMT features

The EMT features in the populations of cells with hybrid phenotype were estimated via detection of N-cadherin in the cells by flow cytometry (Table 4; Fig. 2C).

Expression of N-cadherin was found in all populations of cells with hybrid phenotype, in both blood and primary tumor. However, N-cadherin-positive cells were significantly less common than N-cadherin-negative cells (Table 4).

Quantification of cells showing EMT features demonstrated that the number of cells with hybrid phenotype showing N-cadherin expression in both blood and primary tumor was significantly lower than the number of cells with no N-cadherin expression (Fig. 2C).

Integrin interface assessment

The results of analysis of the β3, β4, and αVβ5 integrin expression in circulating cells with hybrid phenotype by flow cytometry are provided in Table 5 and Fig. 3. Estimation of the studied cells' frequency showed that cells with the β3⁺β4⁺αVβ5⁺ phenotype were the least common ($p = 0.0003$) (Table 5).

Table 5. Frequency of cells with hybrid phenotype showing integrin expression in patients with breast cancer

№	Phenotype	Frequency, %	Significance level
1	β3⁺β4⁺αVβ5⁺	64.1% (25/39)	$p_{1-8} = 0.0003$
2	β3⁺β4⁺αVβ5⁻	82.1% (32/39)	$p_{2-8} = 0.0564$
3	β3⁺β4⁻αVβ5⁺	92.3% (36/39)	$p_{3-8} = 0.6151$
4	β3⁺β4⁻αVβ5⁻	87.2% (34/39)	$p_{4-8} = 0.2002$
5	β3⁻β4⁺αVβ5⁺	82.1% (32/39)	$p_{5-8} = 0.0564$
6	β3⁻β4⁺αVβ5⁻	97.4% (38/39)	$p_{6-8} = 1.0000$
7	β3⁻β4⁻αVβ5⁺	97.4% (38/39)	$p_{7-8} = 1.0000$
8	β3⁻β4⁻αVβ5⁻	97.4% (38/39)	

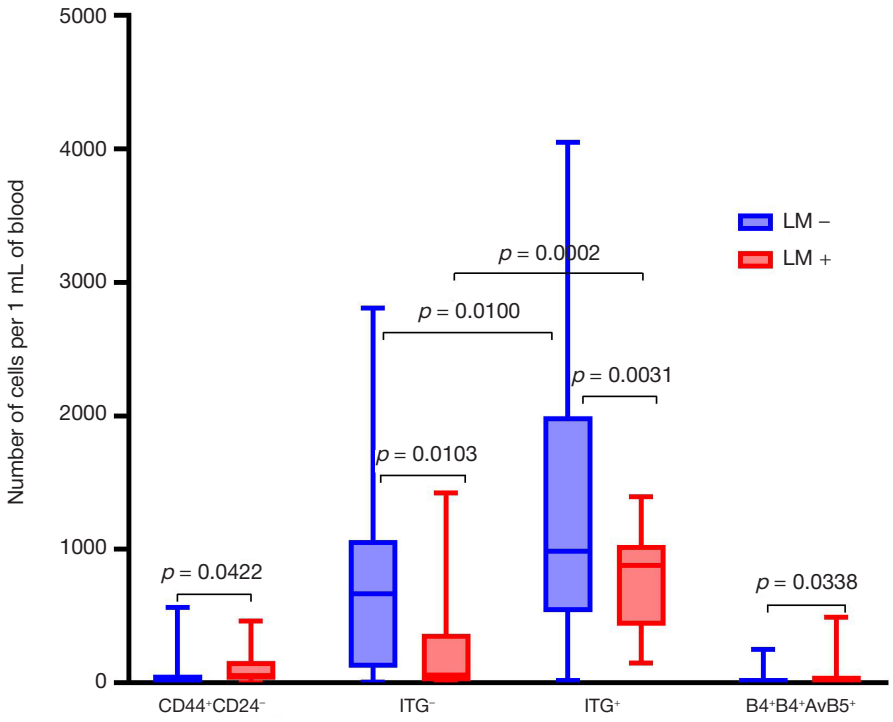

Fig. 4. Stem features and integrin expression in circulating cells with hybrid phenotype in breast cancer patients with lymph node metastasis

The number of circulating cells with hybrid phenotype showing expression of the β3- and/or β4- and/or αVβ5 integrin receptors (ITG+) was significantly higher ($p = 0.0002$) than the number of cells showing no expression of these molecules (ITG–) (Fig. 3).

Association between metastatic traits of cells with hybrid phenotype and lymph node metastasis

Comparative analysis of the metastatic traits in cells with hybrid phenotype revealed the association of the cells showing the stemness features and the expression of integrin molecules with lymph node metastasis (LM).

Thus, the level of "stem" $CD45^+EpCAM^+CK7/8^-CD44^+CD24^-$ cells in blood turned out to be significantly higher ($p = 0.0422$) in patients with LM than in patients with no LM (Fig. 4).

The levels of ITG^- and ITG^+ cells with hybrid phenotype were significantly higher in patients with no LM than in patients with LM ($p = 0.0103$ and $p = 0.0031$, respectively) (Fig. 4). At the same time, patients with LM has a significantly larger number of ITG^+ cells ($p = 0.0002$) relative the number of ITG^- cells. The increase in the number of $\beta3^+\beta4^+\alpha V\beta5^+$ cells ($p = 0.0338$) compared to patients with no metastasis was found in blood of patients with LM (Fig. 4).

The logistic regression models confirmed the role in lymph node metastasis played by cells with hybrid phenotype.

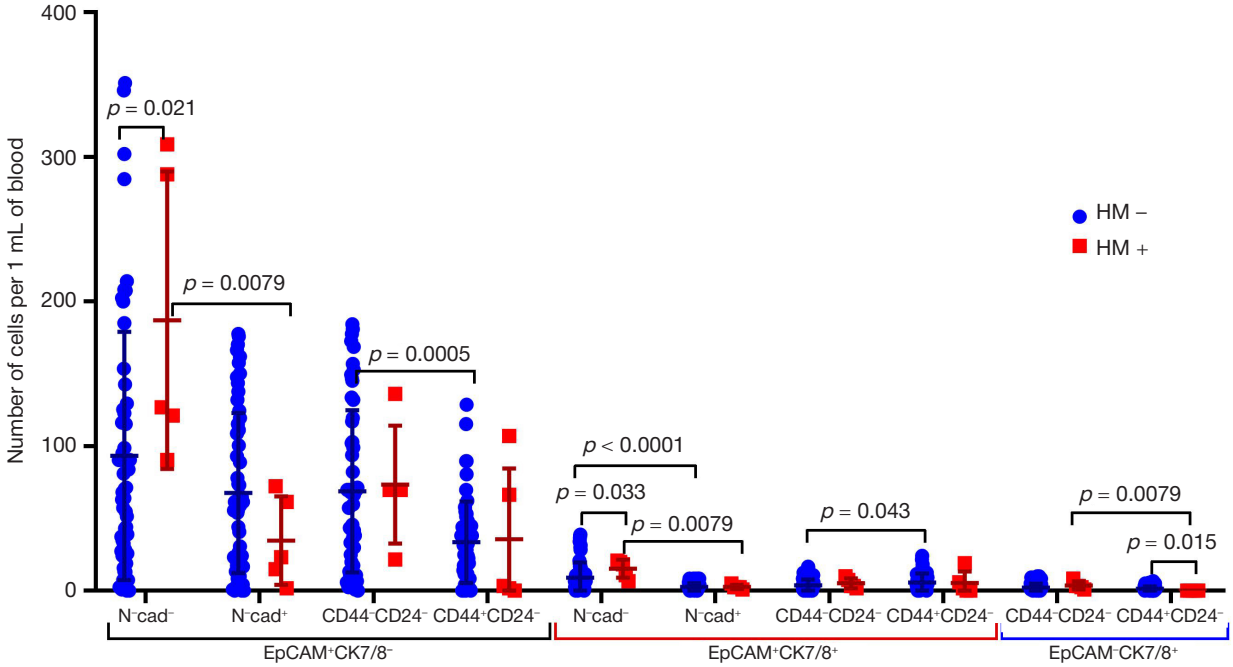

Fig. 5. Stem and EMT features in circulating cells with hybrid phenotype in breast cancer patients with distant metastasis

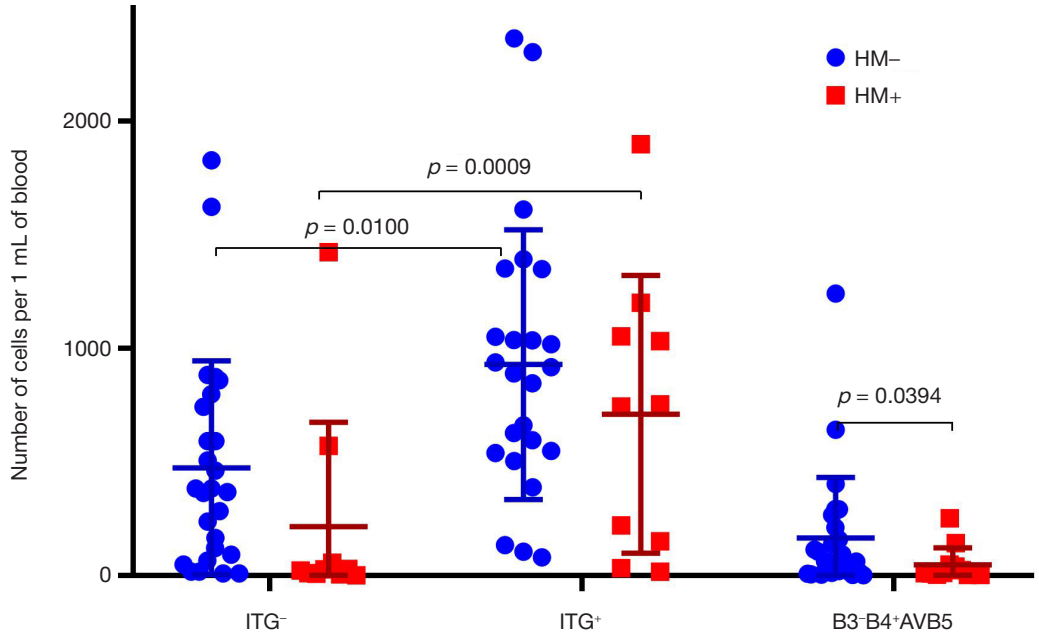

Fig. 6. Integrin expression by cells with hybrid phenotype in breast cancer patients with distant metastasis

Thus, the risk of LM in BC patients turned out to be associated with the presence of cells with the $CD45^+EpCAM^+CK7/8^+$ and $CD45^+EpCAM^-CK7/8^+$ phenotypes showing stemness features in blood. The mathematical model is as follows:

$$Y = -2.4 + 2.7X_1 - 1.0X_2,$$

where Y is the regression equation value; –2.4 is the regression coefficient of the constant term; X_1 is the level of $CD45^+EpCAM^+CK7/8^+$ hybrid cells in blood ($X_1 = 1$ when the frequency is less than 14.94 cells per 1 mL of blood, $X_1 = 2$ when the frequency exceeds 14.94 cells per 1 mL of blood); 2.7 is the regression coefficient of this trait; X_2 is the level of $CD45^+EpCAM^-CK7/8^+CD44^+CD24^-$ cells in blood ($X_2 = 1$ when the frequency exceeds 2.49 cells per 1 mL of blood, $X_2 = 2$ when the frequency is less than 2.49 cells per 1 mL of blood); –1.0 is the regression coefficient of this trait.

The model's sensitivity is 79% and specificity is 85% ($\chi^2 = 18.49$; $p = 0.0001$).

Thus, the study has shown that cells with hybrid phenotype have such properties, as stemness and co-expression of β3-, β4-, and αVβ5-integrins, that are likely to contribute to the mechanisms underlying lymph node metastasis in BC.

Association between metastatic traits of cells with hybrid phenotype and distant metastasis

Comparative analysis of the metastatic traits of cells with hybrid phenotype showed that cells with no features of EMT or stemness were associated with distant metastasis (DM).

Thus, patients with DM showed a significant increase in the frequency of $CD45^+EpCAM^+CK7/8^-N\text{-}cadh^-$ and $CD45^+EpCAM^+CK7/8^+N\text{-}cadh^-$ cells ($p = 0.021$ and $p = 0.033$, respectively) compared to patients with no DM, and the decrease in the frequency of $CD45^+EpCAM^+CK7/8^-N\text{-}cadh^+$ and $CD45^+EpCAM^+CK7/8^+N\text{-}cadh^+$ cells ($p = 0.0079$ and $p = 0.0079$, respectively) relative to N-cadherin-negative cells (Fig. 5).

The number of $CD45^+EpCAM^-CK7/8^+CD44^+CD24^-$ cells in individuals with DM was significantly lower than the number of $CD45^+EpCAM^-CK7/8^+CD44^-CD24^-$ cells ($p = 0.015$) (Fig. 5).

No significant differences in the frequency of cells with hybrid phenotype showing and not showing features of stemness and EMT were found in primary tumors of individuals with DM.

Comparative analysis of the properties possessed by cells with hybrid phenotype in individuals with DM revealed an increase in the frequency of cells showing integrin expression (Fig. 6).

The number of ITG^- cells was significantly lower than the number of ITG^+ cells in patients with no DM or patients with DM ($p = 0.0100$ and $p = 0.0009$, respectively) (Fig. 6). The decrease in the number of β3–β4+αVβ5– circulating cells ($p = 0.0394$) associated with DM relative to no DM was also found (Fig. 6).

The risk of DM in BC patients turned out to be associated with the presence of $CD45^+EpCAM^+CK7/8^+$ cells in blood, regardless of the presence of the features of stemness or EMT, and $CD45^+EpCAM^-CK7/8^+$ cells showing stemness features. The mathematical model is as follows:

$$Y = 63.5 - 31.8X_1 - 30.0X_2,$$

where Y is the regression equation value; 63.5 is the regression coefficient of the constant term; X_1 is the frequency of $CD45^+EpCAM^+CK7/8^+$ hybrid cells in blood ($X_1 = 1$ when the frequency is less than 14.94 cells per 1 mL of blood, $X_1 = 2$ when the frequency exceeds 14.53 cells per 1 mL of blood); –31.8 is the regression coefficient of this trait; X_2 is the frequency of $CD45^+EpCAM^-CK7/8^+CD44^+CD24^-$ cells in blood ($X_2 = 1$ when the frequency exceeds 2.49 cells per 1 mL of blood, $X_2 = 2$ when the frequency is less than 2.49 cells per 1 mL of blood); –30.0 is the regression coefficient of this trait.

The model's sensitivity is 100.0% and specificity is 98.3% ($\chi^2 = 29.52$; $p = 0.0000004$).

DISCUSSION

A biological phenomenon of hybridization in cancer is still a source of debate. Despite numerous in vitro and in vivo studies conducted in the recent decades, there is still no evidence that hybrid tumor cells can cause tumor progression.

Fusion of normal cells and cancer cells is considered to be the most probable mechanism underlying hybrid cell

generation. Thus, *in vitro* studies revealed spontaneous fusion of normal breast epithethelial cells and cancer cells, cancer cells only, epithelial tumor cells and endothelial cells, epithelial tumor cells and stromal cells [19]. It was also noted that the processes of cell fusion and hybrid cell generation were enhanced after using radiotherapy and chemotherapy due to local inflammation in the tumor microenvironment and tissue regeneration processes [20–21]. Discovering the biological nature of cells with hybrid phenotype is still a pressing issue.

Subpopulation analysis of cells with hybrid phenotype has shown that these cells can express one epithelial marker (EpCAM or CK7/8) or both markers. According to modern concepts, the EpCAM and CK7/8 markers are expressed mainly by epithelial cells [22]. However, there is evidence of the EpCAM expression in the bone marrow-derived precursor cells, such as early erythroid precursors [23]. Under physiologic conditions, precursor cells are recruited from the bone marrow during reparative regeneration if needed [24]. In tumor process, these cells are involved in generation and maintenance of the tumor and premetastatic niches and, therefore, contribute to the emergence of metastatic foci in distant organs [25].

Thus, the cells showing expression of CK7/8 and CD45 ($CD45^+EpCAM^+CK7/8^+$ and $CD45^+EpCAM^-CK7/8^+$) are likely to by hybrids of leukocytes/macrophages and epithelial tumor cells, while the $CD45^+EpCAM^+CK7/8^-$ cell population can be represented by both leukocyte-epithelial hybrids and bone marrow-derived hematopoietic progenitor cells.

Assessment of the metastatic traits of cells with hybrid phenotype has shown that these cells are involved in the mechanisms underlying LM and DM. Thus, the logistic regression data suggest that both metastasis types are associated with the same patterns: the increase in the number of circulating $CD45^+EpCAM^+CK7/8^+$ cells and the decrease in the number of $CD45^+EpCAM^-CK7/8^+$ cells showing stemness features. Furthermore, in LM, the increase in blood levels of $CD45^+EpCAM^+CK7/8^-$ cells showing stemness features and $CD45^+EpCAM^+$ cells showing co-expression of β3-, β4-, and αVβ5-integrins is observed. In DM, there is an increase in the number of $CD45^+EpCAM^+CK7/8^-$ and $CD45^+EpCAM^+CK7/8^+$ cells showing no EMT features along with the decrease in the number of the same cells showing EMT features and $CD45^+EpCAM^+$ cells showing mono-expression of β4-integrin.

Acquisition of stem-like properties by hybrid cells can (by analogy with CTCs) contribute to their anticancer therapy resistance and metastatic potential enhancement. The increase in the number of β3-, β4-, and αVβ5-expressing cells with hybrid phenotype observed in LM also suggests enhancement of their metastatic potential. Integrin β3, expressed mainly by platelets, hematopoietic cells, and angiogenic endothelial cells, is responsible for adhesion in hemostasis, wound healing, and angiogenesis. The association of integrin β3 with tumor growth, lymph node and bone marrow metastasis, as well as reduced patient survival, has been shown [26]. Integrin β4 is expressed mainly by epithelial cells. In BC, integrin β4 promotes tumor invasion, increases tumor cell viability, and contributes to angiogenesis [27]. Integrin αVβ5 is a positive regulator of the tumor cells' stemness, it contributes to their growth and invasion [28]. As we have earlier reported, CTCs express the CXCR4 pro-migratory marker [29]. Elevated expression of CXCR4 and integrin molecules in tumor cells can ensure their high migration potential and promote dissemination to various organs. As a result, the hybrid cells can acquire properties that are necessary for metastasis [30].

Today, it is unknown whether the hybrids of leukocytes and epithelial tumor cells can divide indefinitely to form tumors in distant organs, i.e. play the role of tumor seeds. It is not known whether hybrid circulating cells can have a function of niche formation. However, it is already clear that hybrid cells of the tumor and peripheral blood are associated with both LM and DM.

CONCLUSIONS

Thus, the population of cells with hybrid phenotype, just like CTCs, is characterized by high degree of heterogeneity, including the combination of the features of stemness, EMT, and diverse integrin interface. Cells with hybrid phenotype are involved in lymph node and distant metastasis. LM is associated with such metastatic traits of the circulating cells with hybrid phenotype, as the stemness features and co-expression of β3-, β4-, and αVβ5-integrins. In DM, metastatic traits of cells with hybrid phenotype are associated with the stemness features, but not with the EMT features and integrin expression. Understanding of the involvement of cells with hybrid phenotype in metastasis can be useful in terms of improving anti-metastatic therapy.

References

1. Ruiz-Rodríguez AJ, Molina-Vallejo MP, Aznar-Peralta I, González Puga C, Cañas García I, González E, et al. Deep Phenotypic Characterisation of CTCs by Combination of Microfluidic Isolation (IsoFlux) and Imaging Flow Cytometry (ImageStream). Cancers (Basel). 2021; 13 (24): 6386.
2. Zhang Q, Kong D, Yang Z, Li G, Cheng S, Feng L, et al. Prognostic value of stem-like circulating tumor cells in patients with cancer: a systematic review and meta-analysis. Clin Exp Med. 2023. DOI: 10.1007/s10238-023-01009-0.
3. Orrapin S, Udomruk S, Lapisatepun W, Moonmuang S, Phanphaisarn A, Phinyo P, et al. Clinical Implication of Circulating Tumor Cells Expressing Epithelial Mesenchymal Transition (EMT) and Cancer Stem Cell (CSC) Markers and Their Perspective in HCC: A Systematic Review. Cancers (Basel). 2022; 14 (14): 3373.
4. Grigoryeva ES, Tashireva LA, Alifanov VV, Savelieva OE, Vtorushin SV, Zavyalova MV, et al. Molecular subtype conversion in CTCs as indicator of treatment adequacy associated with metastasis-free survival in breast cancer. Sci Rep. 2022; 12 (1): 20949.
5. Fina E, Cleris L, Dugo M, Lecchi M, Ciniselli CM, Lecis D, et al. Gene signatures of circulating breast cancer cell models are a source of novel molecular determinants of metastasis and improve circulating tumor cell detection in patients. J Exp Clin Cancer Res. 2022; 41 (1): 78.
6. Grigoryeva ES, Tashireva LA, Savelieva OE, Zavyalova MV, Popova NO, Kuznetsov GA, et al. The Association of Integrins β3, β4, and αVβ5 on Exosomes, CTCs and Tumor Cells with Localization of Distant Metastasis in Breast Cancer Patients. Int J Mol Sci. 2023; 24 (3): 2929.
7. Hoshino A, Costa-Silva B, Shen TL, Rodrigues G, Hashimoto A, Tesic Mark M, et al. Tumour exosome integrins determine organotropic metastasis. Nature. 2015; 527 (7578): 329–35.
8. Guan X, Ma F, Li C, Wu S, Hu S, Huang J, et al. The prognostic and therapeutic implications of circulating tumor cell phenotype detection based on epithelial-mesenchymal transition markers in the first-line chemotherapy of HER2-negative metastatic breast cancer. Cancer Commun (Lond). 2019; 39 (1): 1.
9. Wankhede D, Grover S, Hofman P. Circulating Tumor Cells as a Predictive Biomarker in Resectable Lung Cancer: A Systematic Review and Meta-Analysis. Cancers (Basel). 2022; 14 (24): 6112.
10. Jou HJ, Ling PY, Hsu HT. Circulating tumor cells as a "real-time

liquid biopsy": Recent advances and the application in ovarian cancer. Taiwan J Obstet Gynecol. 2022; 61 (1): 34–39.
11. Li H, Liu Q, Liang S, Yao P, Lv J, Wang G, et al. Circulating tumor cells and neutrophil-lymphocyte ratio are predictive markers for metastatic colorectal cancer patients. Transl Cancer Res. 2021; 10 (1): 288–97.
12. Papadaki MA, Stoupis G, Theodoropoulos PA, Mavroudis D, Georgoulias V, Agelaki S. Circulating Tumor Cells with Stemness and Epithelial-to-Mesenchymal Transition Features Are Chemoresistant and Predictive of Poor Outcome in Metastatic Breast Cancer. Mol Cancer Ther. 2019; 18 (2): 437–47.
13. Lustberg MB, Balasubramanian P, Miller B, Garcia-Villa A, Deighan C, Wu Y, et al. Heterogeneous atypical cell populations are present in blood of metastatic breast cancer patients. Breast Cancer Res. 2014; 16 (2): R23.
14. Ishizawa K, Yamanaka M, Saiki Y, Miyauchi E, Fukushige S, Akaishi T, et al. CD45+CD326+ Cells are Predictive of Poor Prognosis in Non-Small Cell Lung Cancer Patients. Clin Cancer Res. 2019; 25 (22): 6756–63.
15. Dittmar T, Zänker KS. Introduction. In: Dittmar T, Zänker KS. Cell Fusion in Health and Disease. Advances in Experimental Medicine and Biology, vol 950. Dordrecht: Springer, 2011; p. 1–3.
16. Laberge GS, Duvall E, Haedicke K, Pawelek J. Leukocyte-Cancer Cell Fusion-Genesis of a Deadly Journey. Cells. 2019; 8 (2): 170.
17. Pospelova RA. Lejkokoncentraciya v klinicheskoj praktike: diagnosticheskoe znachenie. M.: Medicina, 1973; 88 s. Russian.
18. Agnoletto C, Corrà F, Minotti L, Baldassari F, Crudele F, Cook WJJ, et al. Heterogeneity in Circulating Tumor Cells: The Relevance of the Stem-Cell Subset. Cancers (Basel). 2019; 11 (4): 483.
19. Noubissi FK, Ogle BM. Cancer Cell Fusion: Mechanisms Slowly Unravel. Int J Mol Sci. 2016; 17 (9): 1587.
20. Kaur E, Rajendra J, Jadhav S, Shridhar E, Goda JS, Moiyadi A, et al. Radiation-induced homotypic cell fusions of innately resistant glioblastoma cells mediate their sustained survival and recurrence. Carcinogenesis. 2015; 36 (6): 685–95.
21. Yan B, Wang J, Liu L. Chemotherapy promotes tumour cell hybridization in vivo. Tumour Biol. 2016; 37 (4): 5025–30.
22. Gires O, Pan M, Schinke H, Canis M, Baeuerle PA. Expression and function of epithelial cell adhesion molecule EpCAM: where are we after 40 years? Cancer Metastasis Rev. 2020; 39 (3): 969–87.
23. Fidanza A, Stumpf PS, Ramachandran P, Tamagno S, Babtie A, Lopez-Yrigoyen M et al. Single-cell analyses and machine learning define hematopoietic progenitor and HSC-like cells derived from human PSCs. Blood. 2020; 136 (25): 2893–904.
24. Rodrigues M, Kosaric N, Bonham CA, Gurtner GC. Wound Healing: A Cellular Perspective. Physiol Rev. 2019; 99 (1): 665–706.
25. Psaila B, Lyden D. The metastatic niche: adapting the foreign soil. Nat Rev Cancer. 2009; 9 (4): 285–93.
26. Pan B, Guo J, Liao Q, Zhao Y. β1 and β3 integrins in breast, prostate and pancreatic cancer: A novel implication. Oncol Lett. 2018; 15 (4): 5412–6.
27. Abdel-Ghany M, Cheng HC, Elble RC, Pauli BU. The breast cancer beta 4 integrin and endothelial human CLCA2 mediate lung metastasis. J Biol Chem. 2001; 276 (27): 25438–46.
28. Liu F, Wu Q, Dong Z, Liu K. Integrins in cancer: Emerging mechanisms and therapeutic opportunities. Pharmacol Ther. 2023; 247: 108458.
29. Savelieva OE, Tashireva LA, Buldakov MA, Mukhamedzhanov RK, Kaigorodova EV, Denisov EV, et al. CXCR4 expression in different subsets of CTCs and single (detached) breast cancer cells. Siberian journal of oncology. 2018; 17 (4): 75–80.
30. Ramakrishnan M, Mathur SR, Mukhopadhyay A. Fusion-derived epithelial cancer cells express hematopoietic markers and contribute to stem cell and migratory phenotype in ovarian carcinoma. Cancer Res. 2013; 73 (17): 5360–70.

Литература

1. Ruiz-Rodríguez AJ, Molina-Vallejo MP, Aznar-Peralta I, González Puga C, Cañas García I, González E, et al. Deep Phenotypic Characterisation of CTCs by Combination of Microfluidic Isolation (IsoFlux) and Imaging Flow Cytometry (ImageStream). Cancers (Basel). 2021; 13 (24): 6386.
2. Zhang Q, Kong D, Yang Z, Li G, Cheng S, Feng L, et al. Prognostic value of stem-like circulating tumor cells in patients with cancer: a systematic review and meta-analysis. Clin Exp Med. 2023. DOI: 10.1007/s10238-023-01009-0.
3. Orrapin S, Udomruk S, Lapisatepun W, Moonmuang S, Phanphaisarn A, Phinyo P, et al. Clinical Implication of Circulating Tumor Cells Expressing Epithelial Mesenchymal Transition (EMT) and Cancer Stem Cell (CSC) Markers and Their Perspective in HCC: A Systematic Review. Cancers (Basel). 2022; 14 (14): 3373.
4. Grigoryeva ES, Tashireva LA, Alifanov VV, Savelieva OE, Vtorushin SV, Zavyalova MV, et al. Molecular subtype conversion in CTCs as indicator of treatment adequacy associated with metastasis-free survival in breast cancer. Sci Rep. 2022; 12 (1): 20949.
5. Fina E, Cleris L, Dugo M, Lecchi M, Ciniselli CM, Lecis D, et al. Gene signatures of circulating breast cancer cell models are a source of novel molecular determinants of metastasis and improve circulating tumor cell detection in patients. J Exp Clin Cancer Res. 2022; 41 (1): 78.
6. Grigoryeva ES, Tashireva LA, Savelieva OE, Zavyalova MV, Popova NO, Kuznetsov GA, et al. The Association of Integrins β3, β4, and αVβ5 on Exosomes, CTCs and Tumor Cells with Localization of Distant Metastasis in Breast Cancer Patients. Int J Mol Sci. 2023; 24 (3): 2929.
7. Hoshino A, Costa-Silva B, Shen TL, Rodrigues G, Hashimoto A, Tesic Mark M, et al. Tumour exosome integrins determine organotropic metastasis. Nature. 2015; 527 (7578): 329–35.
8. Guan X, Ma F, Li C, Wu S, Hu S, Huang J, et al. The prognostic and therapeutic implications of circulating tumor cell phenotype detection based on epithelial-mesenchymal transition markers in the first-line chemotherapy of HER2-negative metastatic breast cancer. Cancer Commun (Lond). 2019; 39 (1): 1.
9. Wankhede D, Grover S, Hofman P. Circulating Tumor Cells as a Predictive Biomarker in Resectable Lung Cancer: A Systematic Review and Meta-Analysis. Cancers (Basel). 2022; 14 (24): 6112.
10. Jou HJ, Ling PY, Hsu HT. Circulating tumor cells as a "real-time liquid biopsy": Recent advances and the application in ovarian cancer. Taiwan J Obstet Gynecol. 2022; 61 (1): 34–39.
11. Li H, Liu Q, Liang S, Yao P, Lv J, Wang G, et al. Circulating tumor cells and neutrophil-lymphocyte ratio are predictive markers for metastatic colorectal cancer patients. Transl Cancer Res. 2021; 10 (1): 288–97.
12. Papadaki MA, Stoupis G, Theodoropoulos PA, Mavroudis D, Georgoulias V, Agelaki S. Circulating Tumor Cells with Stemness and Epithelial-to-Mesenchymal Transition Features Are Chemoresistant and Predictive of Poor Outcome in Metastatic Breast Cancer. Mol Cancer Ther. 2019; 18 (2): 437–47.
13. Lustberg MB, Balasubramanian P, Miller B, Garcia-Villa A, Deighan C, Wu Y, et al. Heterogeneous atypical cell populations are present in blood of metastatic breast cancer patients. Breast Cancer Res. 2014; 16 (2): R23.
14. Ishizawa K, Yamanaka M, Saiki Y, Miyauchi E, Fukushige S, Akaishi T, et al. CD45+CD326+ Cells are Predictive of Poor Prognosis in Non-Small Cell Lung Cancer Patients. Clin Cancer Res. 2019; 25 (22): 6756–63.
15. Dittmar T, Zänker KS. Introduction. In: Dittmar T, Zänker KS. Cell Fusion in Health and Disease. Advances in Experimental Medicine and Biology, vol 950. Dordrecht: Springer, 2011; p. 1–3.
16. Laberge GS, Duvall E, Haedicke K, Pawelek J. Leukocyte-Cancer Cell Fusion-Genesis of a Deadly Journey. Cells. 2019; 8 (2): 170.
17. Поспелова Р. А. Лейкоконцентрация в клинической практике: диагностическое значение. М.: Медицина, 1973; 88 с.
18. Agnoletto C, Corrà F, Minotti L, Baldassari F, Crudele F, Cook WJJ, et al. Heterogeneity in Circulating Tumor Cells: The Relevance of the Stem-Cell Subset. Cancers (Basel). 2019; 11 (4): 483.
19. Noubissi FK, Ogle BM. Cancer Cell Fusion: Mechanisms Slowly Unravel. Int J Mol Sci. 2016; 17 (9): 1587.
20. Kaur E, Rajendra J, Jadhav S, Shridhar E, Goda JS, Moiyadi A, et

al. Radiation-induced homotypic cell fusions of innately resistant glioblastoma cells mediate their sustained survival and recurrence. Carcinogenesis. 2015; 36 (6): 685–95.
21. Yan B, Wang J, Liu L. Chemotherapy promotes tumour cell hybridization in vivo. Tumour Biol. 2016; 37 (4): 5025–30.
22. Gires O, Pan M, Schinke H, Canis M, Baeuerle PA. Expression and function of epithelial cell adhesion molecule EpCAM: where are we after 40 years? Cancer Metastasis Rev. 2020; 39 (3): 969–87.
23. Fidanza A, Stumpf PS, Ramachandran P, Tamagno S, Babtie A, Lopez-Yrigoyen M et al. Single-cell analyses and machine learning define hematopoietic progenitor and HSC-like cells derived from human PSCs. Blood. 2020; 136 (25): 2893–904.
24. Rodrigues M, Kosaric N, Bonham CA, Gurtner GC. Wound Healing: A Cellular Perspective. Physiol Rev. 2019; 99 (1): 665–706.
25. Psaila B, Lyden D. The metastatic niche: adapting the foreign soil. Nat Rev Cancer. 2009; 9 (4): 285–93.
26. Pan B, Guo J, Liao Q, Zhao Y. β1 and β3 integrins in breast, prostate and pancreatic cancer: A novel implication. Oncol Lett. 2018; 15 (4): 5412–6.
27. Abdel-Ghany M, Cheng HC, Elble RC, Pauli BU. The breast cancer beta 4 integrin and endothelial human CLCA2 mediate lung metastasis. J Biol Chem. 2001; 276 (27): 25438–46.
28. Liu F, Wu Q, Dong Z, Liu K. Integrins in cancer: Emerging mechanisms and therapeutic opportunities. Pharmacol Ther. 2023; 247: 108458.
29. Savelieva OE, Tashireva LA, Buldakov MA, Mukhamedzhanov RK, Kaigorodova EV, Denisov EV, et al. CXCR4 expression in different subsets of CTCs and single (detached) breast cancer cells. Siberian journal of oncology. 2018; 17 (4): 75–80.
30. Ramakrishnan M, Mathur SR, Mukhopadhyay A. Fusion-derived epithelial cancer cells express hematopoietic markers and contribute to stem cell and migratory phenotype in ovarian carcinoma. Cancer Res. 2013; 73 (17): 5360–70.

MULTIDISCIPLINARY APPROACH TO TREATMENT OF A PATIENT WITH UNRESECTABLE METASTATIC LIVER LESION SPAWNED BY HER2+ GASTRIC ADENOCARCINOMA GIVING

Kolomiets KV ✉, Isaev IV, Kovalev VV, Grishchenko NV, Kokovihina DI, Morozova AA, Torosyan AR, Shashkova VV, Snegireva PV

Rostov State Medical University of the Ministry of Health of the Russian Federation, Rostov-on-Don, Russia

In 85% of patients worldwide, gastric cancer (GC) metastasizes from the very beginning or within three years. In 30–50% of cases, metastases, both synchronous and metachronous, grow into liver. Multifocal liver metastases translate into an unfavorable prognosis: the median survival period is 10–15 months, with less than 10% of the patients surviving past three years. In such cases, the palliative treatment option is systemic chemotherapy. Combined with immunotherapy, transarterial chemoembolization (TACE), a relatively new method of local treatment of metastatic foci, offer new options of combating liver metastases. This work presents a clinical case of application of this combination coupled with chemotherapy to treat a patient with unresectable liver metastases spawned by HER2+ gastric adenocarcinoma. From the day of diagnosis, the patient's life expectancy was 42 months.

Keywords: gastric cancer, liver metastases of gastric cancer, transarterial chemoembolization, immunotherapy, chemotherapy

Author contribution: Kolomiets KV — article authoring, editing; Isaev IV, Snegireva PV — article authoring, literature review, data analysis; Kovalev VV, Grishchenko NV — article authoring, literature review, data collection; Kokovikhina DI, Morozova AA — article authoring, literature review, study concept and design; Torosyan AR, Shashkova VV — article authoring, literature review, article revision.

Compliance with ethical standards: the patient has signed a voluntary informed consent to publication of anonymized medical information.

✉ **Correspondence should be addressed:** Karina V. Kolomiets
Krasnoarmeyskaya, 198, Novocherkassk, 346400, Russia; karina_kolomiets_99@mail.ru

Received: 27.06.2023 **Accepted:** 12.08.2023 **Published online:** 29.08.2023

DOI: 10.24075/brsmu.2023.031

МУЛЬТИДИСЦИПЛИНАРНЫЙ ПОДХОД К ЛЕЧЕНИЮ ПАЦИЕНТА С НЕРЕЗЕКТАБЕЛЬНЫМ МЕТАСТАТИЧЕСКИМ ПОРАЖЕНИЕМ ПЕЧЕНИ HER2+ АДЕНОКАРЦИНОМОЙ ЖЕЛУДКА

К. В. Коломиец ✉, И. В. Исаев, В. В. Ковалев, Н. В. Грищенко, Д. И. Коковихина, А. А. Морозова, А. Р. Торосян, В. В. Шашкова, П. В. Снегирева

Ростовский государственный медицинский университет, Ростов-на-Дону, Россия

У 85% больных во всем мире сразу или в течение трех лет рак желудка (РЖ) переходит в метастатическую форму. Печень является органом метастазирования РЖ с частотой 30–50%, включая как синхронные, так и метахронные метастазы. При наличии мультифокальных метастазов печени прогноз для пациентов весьма неблагоприятен: медиана выживаемости составляет около 10–15 месяцев, а трехлетняя выживаемость — менее 10%, и паллиативным вариантом лечения в таких случаях является системная химиотерапия. Внедрение относительно молодого локального метода воздействия на метастатические очаги — трансартериальной химиоэмболизации (ТАХЭ) в комбинации с иммунотерапией открыло новые возможности лечения метастазов в печень. Представлен клинический случай использования методики ТАХЭ в комбинации с иммунотерапией, а также химиотерапией у пациента при нерезектабельном метастатическом поражении печени HER2+ аденокарциномой желудка с продолжительностью жизни 42 месяца с момента установления диагноза.

Ключевые слова: рак желудка, метастазы рака желудка в печень, трансартериальная химиоэмболизация, иммунотерапия, химиотерапия

Вклад авторов: К. В. Коломиец — написание статьи, редактирование; И. В. Исаев, П. В. Снегирева — написание статьи, обзор литературы, анализ данных; В. В. Ковалев, Н. В. Грищенко — написание статьи, обзор литературы, сбор данных; Д. И. Коковихина, А. А. Морозова — написание статьи, обзор литературы, концепция и дизайн; А. Р. Торосян, В. В. Шашкова — написание статьи, обзор литературы, переработка статьи.

Соблюдение этических стандартов: пациент подписал добровольное информированное согласие на публикацию персональной медицинской информации в обезличенной форме.

✉ **Для корреспонденции:** Карина Викторовна Коломиец
ул. Красноармейская, д. 198, г. Новочеркасск, 346400, Россия; karina_kolomiets_99@mail.ru

Статья получена: 27.06.2023 **Статья принята к печати:** 12.08.2023 **Опубликована онлайн:** 29.08.2023

DOI: 10.24075/vrgmu.2023.031

In the worldwide cancer rating, gastric cancer (GC) is on the 5th place in terms of morbidity, and 3rd in terms of mortality [1]. Over 700 thousand people die from GC every year throughout the world, since in most cases this disease is diagnosed at late stages, when the neoplasm has already spawned metastases [2, 3]. In the Russian Federation (RF), the incidence of GC is slightly lower: in 2019, it was on the 7th place of the oncological morbidity rating (5.7% of all cancer cases). However, in terms of mortality, GC in RF is a more common cause of death than worldwide: it holds the 2nd place in the respective rating, being the reason of 9.8% of deaths from malignant neoplasms. In RF, the share of late stage diagnoses is noticeably high. In 2019, GC was the third type of cancer most often diagnosed untimely, i.e., when it had already progressed to stage IV, and 45.8% of first-time GC patients died within a year from the day of diagnosis [2, 4]. Approximately similar number of patients have the tumor growing after treatment. As a result, in 85% of GC patients the disease turns metastatic immediately or within three years, which translates into an unfavorable prognosis [5].

Most often, GC spawns metastases into liver: it happens in 30–50% of cases, counting both synchronous and metachronous metastases. At the time of diagnosis, 35% of patients have signs of remote metastases, and in 4–14% the tumor metastasizes into liver; 25–30% have metachronous metastases after therapeutic gastrectomy, and 80% of them appear within the first two years after surgery. Patients with metachronous GC metastasizing into liver survive for 11 months on average, and less than 20% of them survive past the 5-year mark. Excision of primary tumors and liver metastases can increase the five-year survival rate to 23.8% [6].

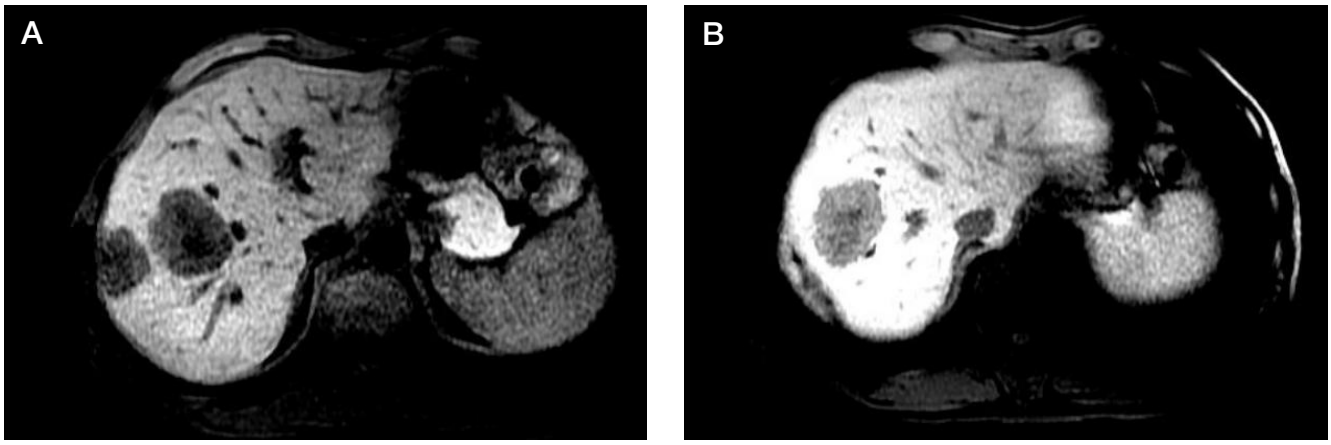

Fig. 1. A, B. MRI scan, abdominal cavity, 07.12.2019

Multifocal liver metastases translate into an unfavorable prognosis: the median survival period is 10–15 months, with less than 10% of the patients surviving past three years. In such cases, the palliative treatment option is systemic chemotherapy.

Combined with immunotherapy, transarterial chemoembolization (TACE), a method of local treatment of metastatic foci, offer new options of combating liver metastases. This method allows solving several tasks at once: achieving the optimal concentration of antitumor drugs directly in the tumor node and optimization of the neoplasm's exposure thereto; inducing ischemic necrosis of tumor tissue through impairment of vascularization; reducing systemic toxicity of cytostatic drugs by keeping their concentration in the systemic bloodstream low [5, 9–11]. There are studies that have demonstrated the effectiveness of TACE in GC patients with liver metastases, but they are few. One of the retrospective studies cites mean survival rate (MSR) of such patients after first TACE with mitomycin only at 6 months and 25.5 months, respectively, MSR after first TACE with mitomycin and gemcitabine — at 8.1 and 11.4 months, respectively, and MSR after TACE with mitomycin in combination with gemcitabine and cisplatin — at 15.3 and 30.5 months, respectively [2, 12–14].

About 10–15% of GC cases are associated with activation of HER2 (human epidermal growth factor receptor 2). It is the overexpression of HER2 that indicates an aggressive course of the disease and promises unfavorable prognosis: various studies report a correlation between amplification of the HER2 gene (HER2+ status) and low overall survival rates of GC patients. This fact necessitates introduction of more effective antitumor drugs into clinical practice. The most promising among the recent malignant neoplasm treatment methods is the immune checkpoint therapy (ICT), which proved highly effective against many types of tumors, including GC [15].

In this clinical observation, we assess the efficacy of a multidisciplinary approach to treatment of an HER2+ GC spawning unresectable metastases into liver: TACE with fluorouracil combined with immunotherapy and platinum-based drugs.

Clinical case description

Patient K., born in 1967, self-referred to the clinic of Rostov State Medical University in July 2019, complaints — unmotivated weight loss, heaviness in the right hypochondrium. He considers himself ill since July 2018, when a checkup at a local clinic revealed GC; after the diagnosis, on 16.07.2018, he underwent gastrectomy and plastic reconstruction at the Stavropol Regional Clinical Oncology Dispensary.

Computed tomography of the abdominal cavity organs on 01.07.2019 revealed two metastatic foci in the right lobe of liver. Samples of the metastases were taken (needle core biopsy) on 20.07.2019, their histological analysis yielded the conclusion: glandular carcinoma. The diagnosis read: C78.7 secondary metastatic liver lesion; gastric cancer, pT3N1M0, st. IIIB, condition after gastrectomy on 16.07.2018, cl. gr. 2.

On 24.07.2019, the central venous port was implanted. Then the patient received 7 courses of chemotherapy, Ramucirumab with FOLFIRI: irinotecan 180 mg/m^2 + calcium folinate 400 mg + fluorouracil 400 mg/m^2 as bolus + fluorouracil 2400 mg/m^2 intravenously, 48-hour infusion + ramucirumab 8 mg/kg on the 1st and 15th days every 28 days.

Control examination of 22.10.2019 revealed the level of CEA at 21.50 ng/ml (reference values: 0–5.0) and CA at 19–9 — 44.56 units/ml (reference values: 0 × 37.0). During the courses of systemic chemotherapy, the patient assessed his condition as moderately severe, complaining of vomiting, diarrhea, dizziness, fatigue.

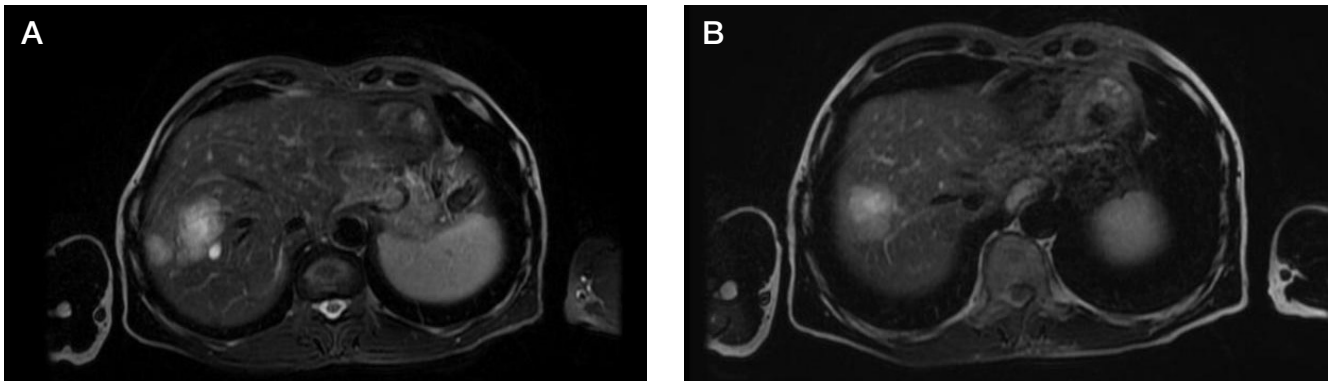

Fig. 2. A, B. MRI scan, abdominal cavity, 18.02.2020

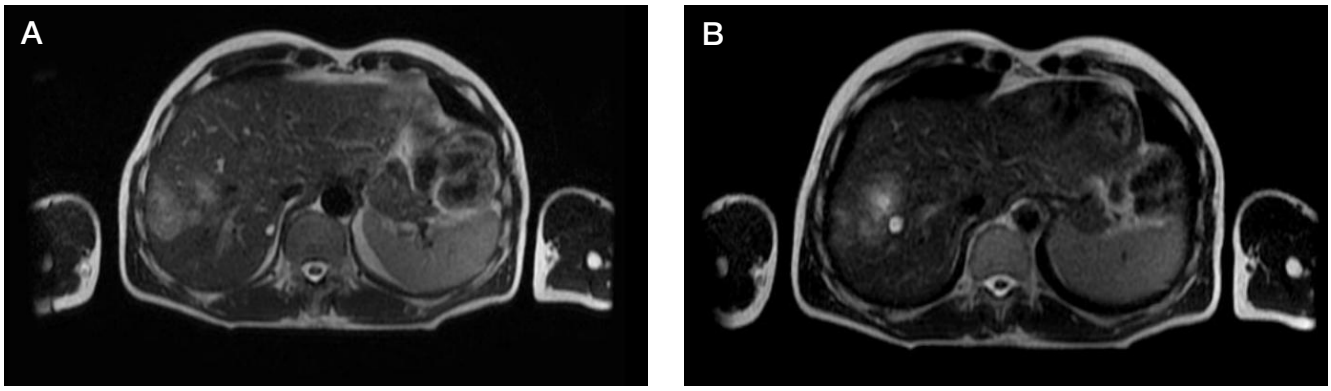

Fig. 3. A, B. MRI scan, abdominal cavity, 15.07.2020

Results of MRI of the abdominal cavity organs of 07.12.2019: locus measuring up to 45 × 48 mm in the right lobe of liver, S7–S8; locus measuring 31 × 37 mm in S7, on the lateral surface; locus measuring 8 × 10 mm in the posteromedial surface of S8; fuzzy 7-mm locus in the capsule of lower surface of S6; no data indicates recurrence or carcinomatosis of peritoneum (Fig. 1A, B). The patient considered his condition to be satisfactory. Factoring in the volume of damage to the liver, prevalence and negative dynamics, on 19.12.2019 the patient underwent another TACE with oxaliplatin 100 mg and fluorouracil 1000 mg.

The postoperative supportive pharmacotherapy course prescribed comprised:

– for analgesia — diclofenac 75 mg 2 times, IM, for 5 days;

– drotaverine hydrochloride 40 mg, 2 times a day, IM, for 5 days;

– octreotide 300 mcg, 2 times a day, SC, for 7 days;

– to prevent thromboembolic complications — enoxaparin sodium 0.4 mg, SC, once a day for 7 days;

– infusion therapy — glucose 5% 500 ml + insulin 6 units, once a day, IV, for 3 days; NaCl 0.9% 500 ml + 40 mg omeprazole, twice a day, IV, for 3 days.

– additionally, as prescribed by the vascular surgeon — thioctic acid 600 mg + NaCl 0.9%, 100 ml once a day, IV, for 5 days; deproteinized calf blood derivate 10 ml + NaCl 0.9%, 100 ml once a day, IV, for 5 days; meldonium 10 ml + NaCl 0.9%, 100 ml once a day, IV, for 5 days; sulodexide 2 ml once a day, IM, for 5 days.

When discharged, the patient assessed his condition as satisfactory, despite the volume of metastatic foci; his body temperature was slightly elevated during the first 2 days after the TACE.

Report of the IHC examination of 19.01.2020: the liver biopsy material contains adenocarcinoma metastases with extensive foci of necrosis and focal lymphoid infiltration. Given the clinical data, the likely situation is a gastric adenocarcinoma metastasizing into liver. Conclusion: $HER2^+$ gastric adenocarcinoma spawning metastases to liver.

Afterwards, the patient received chemotherapy courses in his local clinic. Control examination revealed positive dynamics: MRI of the abdominal cavity of 18.02.2020 had shown that liver was enlarged, the bilobed size was 188 × × 16 mm, parenchyma unevenly diffusely changed by signal; the MRI picture was that of a metastatic lesion, in the right lobe the focus measured up to 34 × 54 mm (previously 45 × 48 mm) in S7–S8, with the S7 focus, lateral surface, measuring 28 × 29 mm (previously 31 × 37 mm), and the S8 focus, posteromedial surface, measuring up to 5 × 10 mm (previously 8 × 10 mm), while the focus in the capsule of the lower surface of S6 could not be detected at all (previously 7 mm) (Fig. 2A, B).

On 19.02.2020, as planned, the patient consulted with a chemotherapist. Conclusion: as supportive therapy, the patient may receive a course of paclitaxel 175 mg/m^2 on day 1 + trastuzumab 6 mg/kg, loading dose 8 mg/kg, on day 1, cycling for 21 day. The patient underwent 3 courses of such chemotherapy.

Results of MRI of the abdominal cavity, 30.04.2020: growing single (2) metastases in the liver's right lobe, neoplasms tend to merge (negative dynamics), contours of the liver are smooth; the vertical size of the right lobe is 18.2 cm, left lobe is 5.1 cm, liver cysts S7, S6 measuring up to 9 × 12 mm. In S8, S7 — tumor nodes of measuring 39 × 60 and 27 × 44 mm (previously 35 × 54 and 28 × 29 mm), merging into a conglomerate.

With the extent of damage to the liver, prevalence and negative dynamics of the process, complaints of heaviness in the right hypochondrium accounted for, and given the satisfactory condition of the patient, it was decided to keep liver TACE in the treatment plan.

The patient was prescribed 5-day preoperative cardio and hepatotropic preparatory course: thioctic acid 600 mg + NaCl 0.9% 100 ml, IV, once a day, for 5 days; meldonium 5 ml + glucose 250 ml, IV, once a day, ademetionine 400 mg + glucose 250 ml, IV, once a day.

On 05.05.2020, the patient underwent TACE: lipiodol 10 ml + fluorouracil 1000 mg + 100 ml oxaliplatin. HydroPearl spheres (800 nm) were used for arterial embolization. The patient was prescribed post-surgery supportive pharmacotherapy.

From May to July 2020, the patient received 2 courses of immunotherapy at his local clinic: nivolumab 210 mg IV, once every 2 weeks. Results of MRI scanning, 15.07.2020: in S8, S7 — tumor nodes, measuring 49 × 57 and 41 × 61 mm (previously 39 × 60 and 27 × 44 mm), merging into a single conglomerate (Figure 3A, B), which indicates progression.

With the extent of damage to the liver, prevalence and negative dynamics of the process accounted for, the patient underwent liver TACE with lipiodol 10 ml + cisplatin 100 mg on 07.08.2020. Post-surgery, he received supportive pharmacotherapy.

Then, the patient underwent a course of chemotherapy (paclitaxel 175 mg/m^2 on day 1 + trastuzumab 6 mg/kg, loading dose 8 mg/kg) on day 1; cycle 21 days) combined with a course of immunotherapy (nivolumab 210 mg infused IV once every 2 weeks in the local clinic). During the courses, the patient noted the following side effects: itching around knees, skin redness, intermittent diarrhea and nausea.

Results of MRI of the abdominal cavity, 13.11.2020: a lesion measuring 54 × 78 × 52 mm found in the liver's S7, which indicated progression.

On 16.11.2020, the patient underwent parenchymal chemoembolization of the arteries supplying the foci (lipiodol

10 ml + fluorouracil 1000 mg) and arterial chemoembolization with 800 nm HydroPearl spheres (2 ml — 1 syringe) + 100 mg cisplatin. The patient was prescribed post-surgery supportive pharmacotherapy.

Afterwards, the patient received immunotherapy: nivolumab 210 mg, IV, once every 2 weeks. Control examination of 18.12.2020 revealed stabilization of the metastatic focus. MRI scanning results, abdominal cavity, 18.12.2020: tumor nodes measuring 49 × 57 and 41 × 52 mm in S8, S7, merging into a single conglomerate.

On 12.01.2021, the patient underwent TACE: EmboSphere microspheres (500–700 nm) + fluorouracil 1000 mg + cisplatin 100 mg. Post-surgery, he received supportive pharmacotherapy.

Results of MRI of abdominal cavity, 04.03.2021: solid formations measuring 98 × 61 × 70 mm (previously 49 × 57 mm) and 28 × 32 × 17 mm (previously not found) in S7; a cystic component therein measuring 16 × 11 × 14 cm, a solid formation 22 × 13 mm (previously not found) on the anterior diaphragmatic surface of the liver. Results of radiography of thoracic organs, 14.03.2021: no pathological changes detected in the lungs.

On 16.03.2021, the patient underwent TACE: HydroPearl microspheres (500–700 nm) + fluorouracil 1000 mg + cisplatin 100 mg. The patient was prescribed post-surgery supportive pharmacotherapy.

On 08.07.2021, the patient was admitted to the hospital for repeated TACE. Four courses of immunotherapy were conducted. Results of MRI of abdominal cavity, 05.07.2021: solid formations measuring 89 × 54 × 72 mm (previously 98 × 61 × 70 mm) and 24 × 29 × 14 mm (previously 28 × 32 × × 17 mm) in S7; a cystic component therein measuring 11 × 9 × × 12 cm, a solid formation 17 × 11 mm (previously 22 × 13 mm) on the anterior diaphragmatic surface of the liver.

With the extent of damage to the liver, prevalence and negative dynamics of the process accounted for, the patient underwent liver TACE with lipiodol 20 ml + fluorouracil 1000 mg + oxaliplati cisplatin 100 mg on 09.07.2021. Arterial embolization was done with hemostatic sponge suspension. Post-surgery, he received supportive pharmacotherapy.

To date, the patient is in a satisfactory condition, leads an active lifestyle and takes courses of systemic chemotherapy under the FOLFIRI regimen, despite a slight shrinking of metastatic foci in the liver.

Clinical case discussion

Surgical intervention against liver metastases spawned by HER2+ GC, which involved TACE with microspheres, allowed blocking arterial inflow to the tumor and enabled gradual release of the chemotherapy drug in the metastasis area, its cytostatic action selective, which translated into minimization of systemic side effects.

In turn, ICT inhibition is an important recent achievement in the field of antitumor therapy. Used against some malignant neoplasms, it shows encouraging results and significantly improves the prognosis for patients. Inhibition as part of ICT is advisable in late-stage GC cases, since GC is often resistant to chemotherapy. One of the inhibitors used in ICT is pembrolizumab, which was approved by the FDA in 2017 based on the results of KEYNOTE-059 study as the 3rd line therapy for metastatic GC/CEC with PD-L1 expression [8]. GC patients are also involved in a large number of clinical studies investigating other therapy regimens that rely on ICT inhibitors. Their combinations with targeted drugs and chemotherapy are among the most promising regimens [15].

CONCLUSION

New composite methods of treatment that combine TACE, molecular targeted therapy (trastuzumab in the described case) and inhibition in ICT are based on individual characteristics of the tumor, its HER2+ status in particular. The intratumor activity of gastric is pronounced, and its primary tumor and metastases are heterogeneous; thus intracancerous heterogeneity in the expression of HER2+ may signal of decreased effectiveness of treatment. Determination of biomarkers or gene signatures that can be translated into clinically significant prognostic indicators of response to TACE is an important subject requiring investigation.

The multidisciplinary approach involving TACE, immuno- and chemotherapy in a patient with unresectable metastatic liver lesions spawned by HER2+ GC allowed controlling the course of the disease for 42 months, which is virtually 4 times longer than the median survival period in such cases. This is a solid confirmation of efficacy of the composite therapy this patient has received.

References

1. Panda SK, Sahoo PK, Agarwala SK, Houghton TT, Chandrapattan PP, Sankar KV, Nag R. Evolution of treatment in gastric cancer- a systematic review. J Egypt Natl Canc Inst. 2022; 34 (1); DOI: 10.1186/s43046-022-00114-7.
2. Malihova OA, Ryabova VE, Lozovaya VV, i dr. Rannij rak zheludka: klinicheskoe nablyudenie. RMZh. Medicinskoe obozrenie. 2022; 6 (6): 334–40; DOI: 10.32364/2587-6821-2022-6-6-334-340. Russian.
3. Bray F, Ferlay J, Soerjomataram I, Siegel RL, Torre LA, Jemal A. Global cancer statistics 2018: GLOBOCAN estimates of incidence and mortality worldwide for 36 cancers in 185 countries. CA Cancer J Clin. 2018; 68 (6): 394–424.
4. Rykov OV, Parshin DV, Cxovrebov AT, Mirzoyan OS, Fyodorov DN, Tarasova IA, i dr. Rezul'taty lecheniya raka zheludka i metaxromnyh metastazov v pecheni i legkih. Hirurgiya. Zhurnal imeni N. I. Pirogova. 2017; (6): 69–71. Russian.
5. Kuhlmann JB, Euringer W, Spangenberg HC, Breidert M, Blum HE, Harder J, et al. Treatment of unresectable cholangiocarcinoma: conventional transarterial chemoembolization compared with drug eluting bead-transarterial chemoembolization and systemic chemotherapy. Eur J Gastroenterol Hepatol. 2012; 24 (4): 437–43; DOI: 10.1097/MEG.0b013e3283502241.
6. Kawahara K, Makino H, Kametaka H, Hoshino I, Fukada T, Seike K, et al. Outcomes of surgical resection for gastric cancer liver metastases: a retrospective analysis. World J Surg Oncol. 2020; 18 (1), 41; DOI: 10.1186/s12957-020-01816-9.
7. Patetta MA, Isaacson AJ, Stewart JK. Initial experience with HydroPearl microspheres for uterine artery embolization for the treatment of symptomatic uterine fibroids. CVIR Endovasc. 2021; 4 (1): 32; DOI: 10.1186/s42155-021-00223-9.
8. Sakaue M, Sugimura K, Masuzawa T, et al. Long-term survival of HER2 positive gastric cancer patient with multiple liver metastases who obtained pathological complete response after systemic chemotherapy: A case report. Int J Surg Case Rep. 2022; 94: 107097; DOI: 10.1016/j.ijscr.2022.107097.
9. Abramov ME, Mashhelueva AYu, Chichikov EI. Ehffektivnaya farmakot. 2010; 3 (22): 46–49. Russian.
10. Safronenko AV, Gancgorn EV, Kolomiec KV. Ehffektivnost'

transarterial'noj himioehmbolizacii s bevacizumabom pri nerezektabel'nom metastaticheskom kolorektal'nom rake pecheni. Ehksperimental'naya i klinicheskaya farmakologiya. 2021; 84 (10): 25–28; DOI: 10.30906/0869-2092-2021-84-10-25-28. Russian.
11. Hochenkov DA, Volkova MI, Timofeev IV, Olshanskaya AS, Hochenkova YuA, Solomko Eh. Sh., i dr. Ehkspressiya faktora rosta ehndoteliya sosudov i ego receptorov pervogo i vtorogo tipov v kletkah pervichnoĭ opuholi u bol'nyh rakom pochki. Sibirskiĭ onkologicheskiĭ zhurnal. 2021; 20 (4): 64–72. DOI: 10.21294/1814-4861-2021-20-4-64-72. Russian.
12. Ciaffaglione V, Modica MN, Pittalà V, et al. Mutual prodrugs of 5-Fluorouracil: from a classic chemotherapeutic agent to novel potential anticancer drugs. Chem Med Chem. 2021; 16 (23): 3496–512; DOI: 10.1002/cmdc.202100473.
13. Mizusawa J, Morizane C, Okusaka T, Katayama H, Ishii H, Fukuda H, et al. Hepatobiliary and Pancreatic Oncology Group of the Japan Clinical Oncology Group. Randomized Phase III study of gemcitabine plus S-1 versus gemcitabine plus cisplatin in advanced biliary tract cancer: Japan Clinical Oncology Group Study (JCOG1113, FUGA-BT). Jpn J Clin Oncol. 2016; 46 (4): 385–88; DOI: 10.1093/jjco/hyv213.
14. Mosconi C, Calandri M, Javle M, Odisio BC. Interventional radiology approaches for intra-hepatic cholangiocarcinoma. Chin Clin Oncol. 2020; 9 (1); DOI: 10.21037/cco.2019.12.15.
15. Rahnemai-Azar AA, Weisbrod AB, Dillhoff M, Schmidt C, Pawlik TM. Intrahepatic cholangiocarcinoma: current management and emerging therapies. Expert Rev Gastroenterol Hepatol. 2017; 11 (5): 439–49; DOI: 10.1080/17474124.2017.1309290.

Литература

1. Panda SK, Sahoo PK, Agarwala SK, Houghton TT, Chandrapattan PP, Sankar KV, Nag R. Evolution of treatment in gastric cancer- a systematic review. J Egypt Natl Canc Inst. 2022; 34 (1); DOI: 10.1186/s43046-022-00114-7.
2. Малихова О. А., Рябова В. Е., Лозовая В. В. и др. Ранний рак желудка: клиническое наблюдение. РМЖ. Медицинское обозрение. 2022; 6 (6): 334–40; DOI: 10.32364/2587-6821-2022-6-6-334-340.
3. Bray F, Ferlay J, Soerjomataram I, Siegel RL, Torre LA, Jemal A. Global cancer statistics 2018: GLOBOCAN estimates of incidence and mortality worldwide for 36 cancers in 185 countries. CA Cancer J Clin. 2018; 68 (6): 394–424.
4. Рыков О. В., Паршин Д. В., Цховребов А. Т., Мирзоян О. С., Фёдоров Д. Н., Тарасова И. А., и др. Результаты лечения рака желудка и метахромных метастазов в печени и легких. Хирургия. Журнал имени Н. И. Пирогова. 2017; (6): 69–71.
5. Kuhlmann JB, Euringer W, Spangenberg HC, Breidert M, Blum HE, Harder J, et al. Treatment of unresectable cholangiocarcinoma: conventional transarterial chemoembolization compared with drug eluting bead-transarterial chemoembolization and systemic chemotherapy. Eur J Gastroenterol Hepatol. 2012; 24 (4): 437–43; DOI: 10.1097/MEG.0b013e3283502241.
6. Kawahara K, Makino H, Kametaka H, Hoshino I, Fukada T, Seike K, et al. Outcomes of surgical resection for gastric cancer liver metastases: a retrospective analysis. World J Surg Oncol. 2020; 18 (1), 41; DOI: 10.1186/s12957-020-01816-9.
7. Patetta MA, Isaacson AJ, Stewart JK. Initial experience with HydroPearl microspheres for uterine artery embolization for the treatment of symptomatic uterine fibroids. CVIR Endovasc. 2021; 4 (1): 32; DOI: 10.1186/s42155-021-00223-9.
8. Sakaue M, Sugimura K, Masuzawa T, et al. Long-term survival of HER2 positive gastric cancer patient with multiple liver metastases who obtained pathological complete response after systemic chemotherapy: A case report. Int J Surg Case Rep. 2022; 94: 107097; DOI: 10.1016/j.ijscr.2022.107097.
9. Абрамов М. Е., Мащелуева А. Ю., Чичиков Е. И. Эффективная фармакот. 2010; 3 (22): 46–49.
10. Сафроненко А. В., Ганцгорн Е. В., Коломиец К. В. Эффективность трансартериальной химиоэмболизации с бевацизумабом при нерезектабельном метастатическом колоректальном раке печени. Экспериментальная и клиническая фармакология. 2021; 84 (10): 25–28; DOI: 10.30906/0869-2092-2021-84-10-25-28.
11. Хоченков Д. А., Волкова М. И., Тимофеев И. В., Ольшанская А. С., Хоченкова Ю. А., Соломко Э. Ш., и др. Экспрессия фактора роста эндотелия сосудов и его рецепторов первого и второго типов в клетках первичной опухоли у больных раком почки. Сибирский онкологический журнал. 2021; 20 (4): 64–72. DOI: 10.21294/1814-4861-2021-20-4-64-72.
12. Ciaffaglione V, Modica MN, Pittalà V, et al. Mutual prodrugs of 5-Fluorouracil: from a classic chemotherapeutic agent to novel potential anticancer drugs. Chem Med Chem. 2021; 16 (23): 3496–512; DOI: 10.1002/cmdc.202100473.
13. Mizusawa J, Morizane C, Okusaka T, Katayama H, Ishii H, Fukuda H, et al. Hepatobiliary and Pancreatic Oncology Group of the Japan Clinical Oncology Group. Randomized Phase III study of gemcitabine plus S-1 versus gemcitabine plus cisplatin in advanced biliary tract cancer: Japan Clinical Oncology Group Study (JCOG1113, FUGA-BT). Jpn J Clin Oncol. 2016; 46 (4): 385–88; DOI: 10.1093/jjco/hyv213.
14. Mosconi C, Calandri M, Javle M, Odisio BC. Interventional radiology approaches for intra-hepatic cholangiocarcinoma. Chin Clin Oncol. 2020; 9 (1); DOI: 10.21037/cco.2019.12.15.
15. Rahnemai-Azar AA, Weisbrod AB, Dillhoff M, Schmidt C, Pawlik TM. Intrahepatic cholangiocarcinoma: current management and emerging therapies. Expert Rev Gastroenterol Hepatol. 2017; 11 (5): 439–49; DOI: 10.1080/17474124.2017.1309290.

POSSIBLE LINKS OF WILDFIRES WITH ONCOLOGICAL DISEASES OF CHILDREN AND ADULTS IN THE RUSSIAN FAR EAST

Pinaev SK[1,8] ✉, Venevsky S[2,3], Chakov VV[1], Tian L[4], Gong P[4], Kaprin AD[5], Starinsky VV[5], Chizhov AYa[6,7], Pinaeva OG[8]

[1] Khabarovsk Federal Research Center, Far Eastern branch of the Russian Academy of Sciences, Khabarovsk, Russia
[2] Tsinghua University, Beijing, China
[3] The Southern Scientific Centre of the Russian Academy of Sciences, Rostov-on-Don, Russia
[4] The University of Hong Kong, Hong Kong
[5] National Medical Research Radiological Centre of the Ministry of Health of the Russian Federation. Moscow, Russia
[6] Peoples' Friendship University of Russia, Moscow, Russia
[7] State Research Center — Burnasyan Federal Medical Biophysical Center of Federal Medical Biological Agency, Moscow, Russia
[8] Far Eastern State Medical University, Khabarovsk, Russia

Russian Federal Far East District is a continental scale area where wildfires are frequent. We aimed to a) determine whether wildfires are related statistically to cancer for children and adults in the Russian Federal Far East District (FFED); b) to estimate time lags of such relationships and c) to find out which age groups are most vulnerable for wildfires. Annual number of fires (NF) in administrative units (AUs), normalized to the maximum value for all AUs in observation period 1992–2019, was taken as a characteristic of wildfires in our analysis. Annual cancer incidence (CI) for five cancer types for children up to 14 years and the entire population, normalized similarly to NF, was compared to normalized NF. ARIMA models were used for time series analysis for the period 1992–2019. Linear statistical analysis was done for NF and CI for short time series (10–12 years) for the central AU of FFED for "children up to 4 years"; Three additional embryonal types of cancer and five benign types of tumors were also focused in linear statistical analysis. ARIMA analysis revealed 27 associations between NF and CI with a lag from 0 to 3 years for two age groups, and five cancer types (p-values between 0.002 and 0.1). Linear statistical analysis for "children up to 4 years" revealed correlations for two from three embryonal types of cancer and three from five benign tumors ($0.002 < p < 0.046$). Incidences of hematopoietic, lymphoid, vascular, and soft tissue neoplasms, as well as CNS tumors had associations with wildfires for "children up to 4 years", for "children up to 14 years" and "the entire population" age groups in many cases. Entire population and children up to 4 years in the central AU of FFED are most sensitive to wildfire — cancer interactions. Associations "number of fires — cancer incidence" as a rule have time lags from 0 to 3 years.

Keywords: wildfires, cancer incidence, ARIMA analysis, Far Eastern Federal district of Russian Federation

Acknowledgments: we thank Professor N.E. Kosykh from Far Eastern Medical University for their help in collecting data on the updated incidence of malignant neoplasms in children in Khabarovskij Kraj. We acknowledged Olga P. Gretsova for preparing the data for analysis. S. Venevsky acknowledges the support from the Russian State Assignment of the Federal Research Centre of the Southern Scientific Centre of the Russian Academy of Sciences (SSC RAS) (122013100131-9) and Department of Earth System Sciences of Tsinghua University.

Author contribution: Pinaev SK — author of the general idea and the main design of the study, collection and analysis of data, and formation of hypotheses; Venevsky S — developed method of spatial and non-linear temporal analysis, presentation and interpretation of results of this analysis and made conclusions; Chakov VV — collection and analysis of information about the fire situation in the Far Eastern Federal district on the basis of data presented in the public domain; Tian L — run ARIMA analysis; Chizhov AYa, Gong P, Pinaeva OG — participated in the planning of the study and discussion of the results; Kaprin AD, Venevsky S — Participation in research planning and formation of data on CI based on the national cancer registry of Russia; Venevsky S, Pinaev SK — wrote the manuscript.

✉ **Correspondence should be addressed:** Sergey K. Pinaev
Muravyova-Amuskogo, 35, Khabarovsk, 680000, Russia; pinaev@mail.ru

Received: 25.04.2023 **Accepted:** 29.07.2023 **Published online:** 26.08.2023

DOI: 10.24075/brsmu.2023.028

ВЛИЯНИЕ ЛЕСНЫХ ПОЖАРОВ НА ОНКОЛОГИЧЕСКИЕ ЗАБОЛЕВАНИЯ У НАСЕЛЕНИЯ ДАЛЬНЕГО ВОСТОКА

С. К. Пинаев[1,8] ✉, С. Веневский[2,3], В. В. Чаков[1], Л. Тянь[4], П. Гонг[4], А. Д. Каприн[5], В. В. Старинский[5], А. Я. Чижов[6,7], О. Г. Пинаева[8]

[1] Хабаровский Федеральный исследовательский центр Дальневосточного отделения Российской академии наук, Хабаровск, Россия
[2] Университет Цинхуа, Пекин, Китай
[3] Южный научный центр Российской академии наук, Ростов-на-Дону, Россия
[4] Гонконгский университет, Гонконг
[5] Национальный медицинский исследовательский центр радиологии Минздрава России, Москва, Россия
[6] Российский университет дружбы народов, Москва, Россия
[7] Федеральный медицинский биофизический центр имени А. И. Бурназяна Федерального медико-биологического агентства, Москва, Россия
[8] Дальневосточный государственный медицинский университет, Хабаровск, Россия

Дальневосточный федеральный округ (ДФО) России подвержен частым лесным пожарам. Целью работы было выявить связь между онкологическими заболеваниями и лесными пожарами на территории ДФО; оценить временные лаги указанных связей; выявить возрастные группы, статистически наиболее чувствительные к воздействию пожаров. Число пожаров (ЧП) за год на территории административных единиц (АЕ), приведенное к максимальному значению для всех АЕ за период наблюдения 1992–2019 гг., использовали в качестве показателя лесных пожаров. Показатели заболеваемости пятью видами рака (ЗР) за год среди детей в возрасте до 14 лет и населения в целом нормировали аналогично ЧП и сопоставляли с нормированными показателями ЧП. Все комбинации из семи АЕ ДФО исследовали на наличие статистических связей между нормированными показателями ЧП и ЗР. Модели ARIMA использовали для анализа временных рядов ЧП и ЗР за период 1992–2019 гг. Линейный статистический анализ применяли для более коротких временных рядов ЧП и ЗР (10–12 лет) на территории центральной АЕ ДФО для детей в возрасте до 4 лет. При этом кроме перечисленных пяти видов детского рака для категории «дети младшего возраста (0–4 лет)» были рассмотрены три дополнительных вида рака, а также пять доброкачественных новообразований. Анализ с применением модели ARIMA позволил выявить 27 связей между ЧП и ЗР с лагом от 0 до 3 лет в двух возрастных группах для пяти видов рака ($0,002 < p < 0,1$). Линейный статистический анализ в группе «дети младшего возраста (0–4 года)» показал корреляции для трех из пяти видов рака, для двух из трех видов эмбрионального рака и трех из пяти видов доброкачественных опухолей ($0,002 < p < 0,046$). Выводы: колебания заболеваемости опухолями гемопоэтических, лимфоидных тканей, сосудистыми опухолями, опухолями мягких тканей и ЦНС среди детей младшего возраста (0–4 года), детей/подростков в возрасте 0–14 лет и населения ДФО в целом отчасти связаны с лесными пожарами. Население ДФО в целом и дети в возрасте до 4 лет на территории центральной АЕ ДФО наиболее чувствительны к воздействию лесных пожаров. Связь «число пожаров — заболеваемость раком», как правило, имеет временной лаг от 0 до 3 лет.

Ключевые слова: лесные пожары, заболеваемость раком, модель ARIMA, Дальневосточный федеральный округ Российской Федерации

Благодарности: авторы благодарят профессора Н. Е. Косых из ДГМУ за помощь в сборе данных о заболеваемости злокачественными новообразованиями среди детей в Хабаровском крае, а также О. П. Грецову за подготовку данных для анализа. С. Веневский выражает благодарность за поддержку Федеральному исследовательскому центру Южного научного центра РАН, оказанную в рамках Российского государственного задания (122013100131-9), и Департаменту системных наук о Земле Университета Циньхуа

Вклад авторов: С. К. Пинаев — идея, дизайн, сбор данных, формулировка гипотез; С. Веневский — разработка метода нелинейного статистического анализа связей числа пожаров и заболеваемости раком, интерпретация результатов, выводы; В. В. Чаков — сбор информации о пожарной ситуации в ДФО; Л. Тянь — програмирование модели ARIMA; А. Я. Чижов, П. Гонг, О. Г. Пинаева — планирование исследования, обсуждение результатов; А. Д. Каприн, В. В. Старинский — планирование исследования, формирование базы данных по заболеваемости раком на основе национального регистра онкологических заболеваний России; С. Веневский, С. К. Пинаев — написание статьи.

✉ **Для корреспонденции:** Сергей Константинович Пинаев
ул. Муравьева-Амурского, д. 35, г. Хабаровск, 680000, Россия; pinaev@mail.ru

Статья получена: 25.04.2023 **Статья принята к печати:** 29.07.2023 **Опубликована онлайн:** 26.08.2023

DOI: 10.24075/vrgmu.2023.028

Growth of cancer incidence (CI) worldwide is related not only to the growth and aging of the population [1], but as well to the growth of some environmental risks associated with socioeconomic development and climate change. Studies at large spatial scales — the global, national, and regional levels — are necessary to understand the relationship between CI and environmental conditions. Such studies are conducted [2], but their number is still not sufficient.

Russia had a slightly smaller increase in age-standardized CI rates in both sexes for all cancers in 195 countries or territories from 2005 to 2015 (0% to 10%) in comparison with other countries with high Human Development Index (HDI) (10% to 20%) [3]. Inter-regional comparison of CI rates in Russia demonstrates, however, that not only is the aging of the population in Russia is responsible for cancers, but also other factors which likely include environmental air pollution. Indeed, a comparison of all cancers age-standardized CI in the Russian Federation in total with the one in the Far East Federal District (FEFD) in 2019 revealed that level of all cancer incidences in FEFD is more than in Russia (269.15 against 249.54 per 100,000) [4]. Meanwhile, average age of population is lowest in FEFD in relation to the other federal districts (and 2 years lower than for the entire Russia [5]). Wildfires could be one of the factors promoting cancers in FEFD. Indeed, remote sensing analysis confirms that areas burnt in forested areas in Russia had a significant increasing trend from 2000 to 2016 [5] which continues until now, presumably due to ongoing climate change. The major input to the burned areas comes from the Far East and East Siberian Federal Districts; major ignitions occur near large cities in these districts, especially near the southern border of the Asian part of the Russian Federation [6]. Wildfire smoke contains particulate matter PM2.5/ PM4 and carcinogens, such as benzene and formaldehyde, which have been shown to increase cancer risk in American firefighters [7]. Air pollution in FEFD [8] and tobacco consumption are close an average for Russia here [9]. Thus, exposure to wildfires smoke of population in southern settlements of FEFD may explain excess of CI in the district.

Smoke from wildfires was found to have variety of negative effects to human health [7], increasing both mortality and morbidity to cardiovascular, respiratory and other diseases. Particulate matter in smoke were found to be most important stressors, affecting human health through pulmonary oxidative stress, which can cause cell death or DNA damage, and inflammation [10]. Both oxidative stress and inflammation are major modulators of cancers, thus, airborne particulate matter was classified by the International Agency for Research on Cancer as carcinogen of Group I for lung cancer and potentially to other cancers [11]. Thus, long term exposure of humans to PM and other carcinogens in wildfire smoke may affect cancer mortality and/or cancer incidence.

For the first time V.A. Dobrykh and T.A. Zakharycheva pointed out the connection between forest fires and malignant neoplasms of the respiratory organs [12]. Subsequently, this was confirmed by researchers from Canada, who also established the effect of natural fire smoke on the incidence of brain tumors [13]. We have previously reported on the relationship between forest fires and the frequency of various neoplasms in children and adults [14, 15].

Cancer is a complex phenomenon. It represents a class of diseases that manifests in different forms and presentations. Cancer destroys different target tissues and has a wide variety of etiologies. In addition, age-specific global contributions of cancer types to the total CI are quite different for young children up to 4 years, children/teenagers up to 14 years and the entire population [3]. Thus, analysis of at least two age population groups (children/teens up to 14 years and the entire population) for CI in conditions of airborne pollution can provide a full picture of relationships between different cancer types and wildfires. Here, we studied spatial and temporal associations of wildfires with cancer incidence for the period 1992–2019 years in two age population groups (children/teenagers up to 14 years and the entire population) for the Far East Federal district in Russia prone to wildfires using an annual total number of fires as a proxy for long term exposure of humans to smoke. We also analyzed the relationship between the number of fires (NF) and CI in one age cohort of young children (0–4 years) for the period 1972–1986 in Khabarovskij Kraj (central AU of the FFED until 2018). This study has an objective a) to investigate if statistically significant temporal associations exist between the incidence of different types of cancer and NF in the Far East Federal district in one age cohort (young children) and in two population groups (children/teens 0–14 year and the entire population) for NF and CI and b) to estimate what are time lags in these associations and c) to find out what age group is most vulnerable to impact of wildfires. Existence of large geographical regions, for which statistical relations between wildfires and oncological diseases can be found, was a major hypothesis of this study.

METHODS

Study area

The Far Eastern Federal District (FEFD) is sparsely populated district (area 6.9 million km^2) with a variety of climatic, vegetation, and topographic features. The majority of the FEFD population lives in large cities in the south of the district. Seven administrative units (AUs) of the FFED with developed medical registration system were taken for this study (Fig. 1).

Definition of spatial regions of analysis and cancer classification used in this study

Spatial regions of analysis, where possibility of statistical relationship between wildfires and oncological diseases was investigated, were designed based on the set of seven AUs of the FFED. Each spatial region of analysis was a combination from one, two, etc., up to the seven AUs. Existence of statistical relationship “wildfires/oncological diseases” was checked for the all 127 spatial regions (C^1_7+ C^2_7 + C^3_7 + C^4_7 + C^5_7 + C^6_7 + C^7_7 = 127), where C^m_7 is a number of possible combinations of m from the seven AUs) for two age groups “children/teenagers up to 14 years” and “the entire population”. Difference in etiology of cancers was not considered for comparison of the two age groups. Analysis of all cancer incidences in this study for young children up to 4 years, children/teenagers up to 14 years and the entire population is done for major cancer types for children for the unity of approach The major cancer types for children in this study mainly followed the international classification of malignant tumors [16]. Five major malignant tumor types (leukemia (LK), Hodgkin lymphomas (HL), non-Hodgkin lymphomas (NHL), central nervous system tumors (CNS), and soft tissue sarcomas (STS)), which constitute major child cancer cases both in highly industrialized countries, like Russia, and in the world (approximately 75%) [16].

Possibility of existence of statistical relationship “wildfires/oncological diseases” was studied in more details for the age cohort of young children (0–4 years) in Khabarovskij Kraj (central AU of the FFED until 2018). The choice of age cohort

Fig. 1. Far Eastern Federal District (FEFD) of Russian Federation in borders till the year 2018 (in yellow) and administrative units used in our study: 1 — Primorskij Kraj; 2 — Khabarovskij Kraj; 3 — Amurskaja Oblast; 4 — Kamchatskij Kraj; 5 — Magadan Oblast; 6 — Sakhalin Oblast. Khabarovsk is the largest city of FEFD (613 thousand inhabitants) and capital of FEFD till the year 2018

of young children (0–4 years) for an additional analysis was done because tumors of young children usually are started to develop already in prenatal period [17], while impact of carcinogens at the level of entire population may take several years or even decades [18]. Three additional embryonal types of cancer (retinoblastoma, neuroblastoma, nefroblastoma) and five major benign tumors (BT) in young children, namely hemangiomas, lymphangiomas, teratomas, soft tissue tumors, and papillomas, were included additionally to the five common cancer types for young children (0–4 years).

Number of fires as a proxy for human exposure to wildfire smoke in FEFD

It was possible to use either annual burnt area in AUs data or annual number of fires in AUs data, because the fine resolution data on spatial and seasonal distribution of fire hotspots were limited by the year 1996 [19] and spatial-temporal CI data are available only at annual time step. Canadian researchers [20] suggested to use annual burnt areas at a distance 30–50 km from settlements for an analysis of relationships "wildfires/oncological diseases. However, it is not possible to use total areas burnt in AU (as a proxy of population exposure to smoke from wildfires in FEFD due to uneven location of settlements in FEFD (all major settlements are situated here to the south of 55 NL). Oppositely, total number of fires in administrative unit in FEFD is a good proxy for long term exposure to carcinogens (mostly PM2.5). Indeed, they highly correlate with areas burnt for five southern populated AUs of FEFD (see Supplementary Analysis of number of total, human and lightning fires in administrative units of Russian Far East against areas burnt in 1990–2014) and number of human ignited fires (situated almost exclusively near the cities) is almost equal to number of total fires in these five AUs. Administrative units with large remote areas (Republic Sakha and Magadan Oblast) have total area burnt mainly correlated with number of lightning fires which are few, while number of human fires (located in proximity of cities) is still correlated to total number of fires in these two remaining AUs. The fires in southern populated areas are mainly understory small fires (92% on average for entire FFED, see Supplementary Analysis of number of total, human and lightning fires in administrative units of Russian Far East against areas burnt in 1990–2014), which are producing major emissions (including particulate) reaching population, while large and long wildfires are going mainly in hardly accessible areas in the North. Thus, this study adopts total number of fires in AUs as a proxy for population long-term exposure to wildfire carcinogens emissions. Annual total number of fires were normalized to an average value for the entire period 28-years period in each of the seven AUs for inter-comparison and weighted to the population numbers in AUs when administrative units were combined together.

Data

Data on CI (persons with cancer for 100 000 persons) for five major cancer types in seven listed oblasts (or AUs) in two age groups (children and teenagers 0–14 years and the entire population) for the 28-year period (1992–2019) were used in this study (see Table 1 in Supplementary Data)). Data consist of the annual number of all cancer cases by type registered for one of the population groups in an AU to hundred thousand persons in this group (e.g., for age population group: children/teens 0–14 year in the year 1992, this is a number of cancer cases by a type for persons of the 1978–1992 birth years in the AU divided by the total number of children/teen 0–14 years old in the year 1992, expressed in 100 000 persons, in this AU). The data were extracted from federal statistical data using the Informational Analytical Data Base Management System (Russian state software registration number 2011617155) in the Russian Center for Information Technology and Epidemiology Studies in Oncology named after Pierre Herzen (author Olga

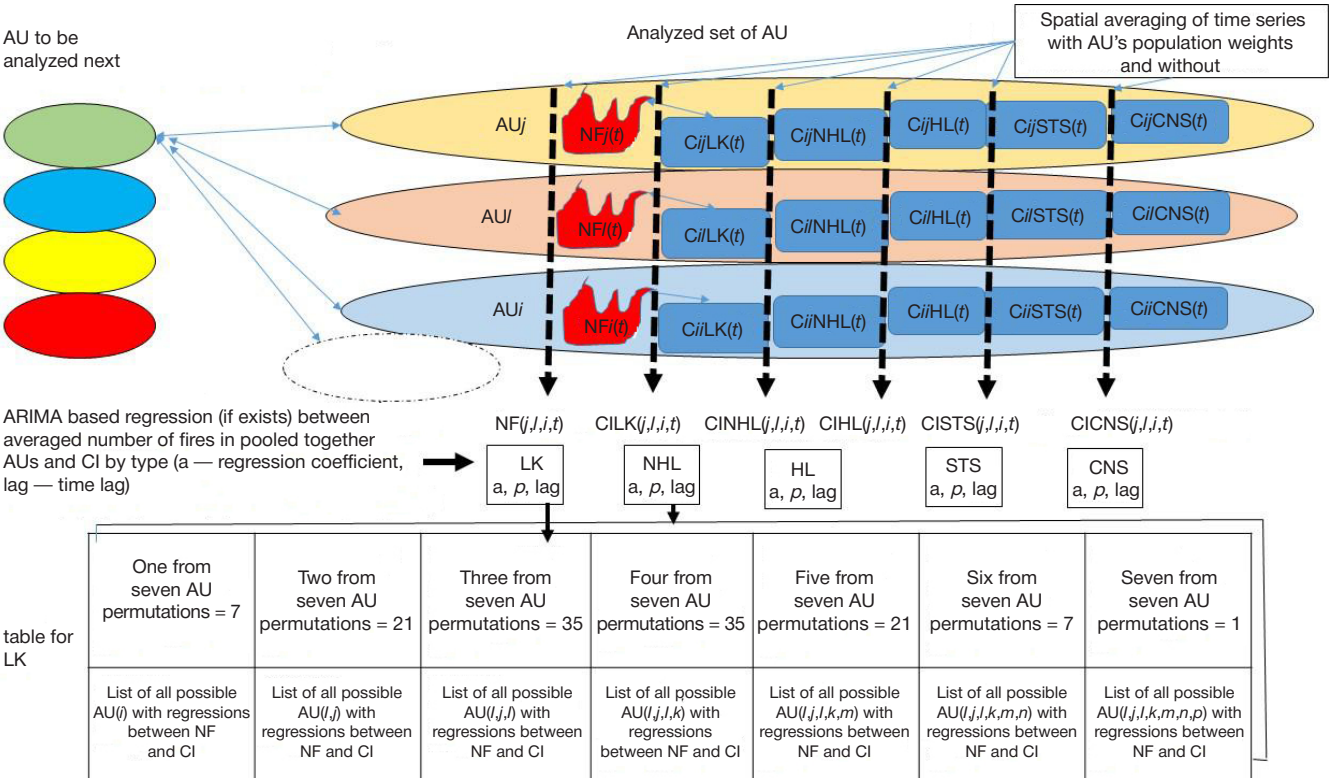

Fig. 2. Analysis diagram for time series analysis, where NF*i* (*t*) — 28 years time series for normalized total number of fires in *i*-th, CI*i*LK(*t*) — 28 years time series for normalized cancer incidence to leukemia in *i*-th AU (similar abbreviation for other four cancer types), NF*jli* (*t*) — 28 years time series for normalized total number of fires in *j*-th AU, *l*-th AU and *i*-th AU pooled together, CI*jli*LK (*t*) — 28 years time series for normalized cancer incidence to leukemia in *j*-th AU, *l*-th AU and *i*-th AU pooled together by one from two pooling algorithms (similar abbreviation for other four cancer types).

P. Gretsova, 2020). Annual cancer incidence values were normalized to a maximum value for the entire period 28-years period for the seven AUs for each of the five cancer types for inter-comparison purposes.

We also analyzed data on tumor incidence in young children 0-4 year. Our data were collected for the largest city of FEFD, Khabarovsk (over 613 thousand inhabitants), the capital of FEFD until 2018, with the most developed medical registration system, and for Khabarovskij Kraj (central AU until 2018). The data were presented for the total number of births for years 1976–1986 in Khabarovsk for benign tumors (see Table 2, Supplementary Data) and for years 1972–1988 for Khabarovskij Kraj for malignant tumors (see Table 3, Supplementary Data).

Number of fires by the seven AUs (Table 4, Supplementary Data) was downloaded from the Russian Ministry of Forestry dataset.

Statistical analysis

Annual values of CI by the five cancer types and NF in the AUs were normalized for their maximum values over the 28-year period for all of the seven AUs. Such a normalization allows comparison of amplitudes, trends, number of cycles and autoregressive features of time series. This approach does not allow to estimate factor dependence of CI by NF (this was not our objective), but allows to minimize influence of different regional co-factors of oncological diseases by statistical analysis.

Firstly, we checked if statistically significant difference of medians for normalized NF and CI by the five cancer types within each of the two population age groups for the seven AUs was observed. This was done using Krsukal–Wallis test with a threshold $\alpha = 0.05$. Similar analysis was conducted after the time series of CI and NF were weighted to a ratio of total number of population in an AU to the total number of population in all seven AUs. Additionally, we checked if statistically significant difference between CIs for the five cancer types (also for the weighted by total number of population time series) was observed within each from the seven AUs using Krsukal–Wallis test with an $\alpha = 0.05$.

The temporal dependence of CI (normalized) on NF (normalized) for a long time series (28 years) was studied using ARIMA models [20], which were applied as for a description of wildfires dynamic characteristics [21], so for description of CIs [22]. An ARIMA model was first applied to the NF (assumed to be a predictor) with a time lag of 0–6 years (upper border of the time lag is approximately twice as the time for complete renewal of organism's cells). Afterwards, the ARIMA model was fit to the CI (by type). The resulting fitted series (predicted against dependent variables) were cross-correlated to identify associations. A statistically significant association between NF with a lag from 0 to 6 years and a CI by type was prescribed to have a p-value less than 0.05 and marginally statistically significant association was prescribed to have a *p*-value between 0.05 and 0.1. The Ljung-Box Q test was applied to statistically significant associations to ensure that the residuals series were white noise, which indicates the goodness of the resulting association. Statistical associations "NF/CI" were studied within two age groups (children/teens 0–14 years and entire population) for the 127 sets of AUs combinations ($C^1_7 + C^2_7 + + C^3_7 + C^4_7 + C^5_7 + C^6_7 + C^7_7 = 127$ see Fig. 2). Cancer incidence time series for each cancer types and NF time series for all AUs within one combination were pooled together making five CIs time series and one NF time series for 28 years in this combination. Pooling in a single time series for CIs from the initial time series was performed in two ways: 1) annual mean

CI for several pooled AUs was calculated for each year and 2) annual CIs were weighted by ratios of population in each from AUs to total population within the combination before summation for each year. The two methods of calculation for pooling together of CI time series produce similar results, but some difference in value exists (not shown). Pooling in a single time series for normalized NF from the initial time series was done with weighting of annual values by ratios of population in each from AUs to total population within the combination before summation for each year. One hundred twenty-seven combinations were divided into seven classes (with one to seven combined AUs in a class) and list of correlated associations "CI/NF" in sense of ARIMA modelling with their regression coefficients, *p*-values and time lags was identified within each class (Fig. 2). Bonferroni-Holm approach was applied to estimate a probability of type I error when conducting multiple ARIMA calculation within each of the two age groups for the five types of cancer.

A short time series of CI by type were studied using linear regression and correlation analyses for an age cohort "children 0–4 years". We considered the possibility of time lags in pollution stress for tumor development and conducted linear regression and correlation analysis of CI against NF with a time lag relatively to the birth year of the children (–3, –2, –1, 0, 1, 2, 3 — in years). Such a linear statistical analysis was applied to analyze the incidence of benign tumors in young children cohorts 0–4 years old born between 1976–1986 against NF in Khabarovsk. A similar analysis was performed for malignant tumors in cohorts born between 1972–1988 for the entire Khabarovskij Kraj.

We generalized our analysis of temporal relationships between CI and NF by making of histograms for number of "CI/NF" statistical associations by the five cancer types within each of the two age groups in the FFED with confidence tresholds $\alpha = 0.1$ and $\alpha = 0.05$. Values of number of "CI/NF" statistical associations were normalized to the maximum value for the five cancer types to get a relative strength (RS) of relationship between NF and CI by the five cancer types within each of the two age groups for the two values of the threshold α.Hystogram for the coefficient of determination of linear regression CI against NF for the all types of cancer and benign tumors for children 0–4 years for the central AU of the FFED was used for generlaziation of the linear statistical analysis.

RESULTS

Comparison of distributions of normalized values of cancer incidence and number of fires for administrative units of Far Eastern federal district

We found that the median values for normalized CI for the five cancer types in each of AU of FEFD had statistically significant differences ($p < 0.05$) as for the age group "children and teenagers 0–14 years", so for "the entire population" group (Fig. 3A–D) both in the case of normalized units and in the case of normalized units, weighted by number of population in an AU to the total population in the AUs. Medians of almost all CIs and NF (elven for the normalized units and twelve (all) for the normalized weighted units) had statistically significant differences for the group of entire seven AUs within the two age groups. An exception was a case of leukemia in the age group "children and teenagers 0–14 years" for the normalized units ($p = 0.0536$ close to the threshold). Weighting by number of population in an AU to the total population in the AUs made better subdivision of both CIs and NF by the AUs and larger statistical significance of differences as for the age group "children and teenagers 0–14 years" (Fig. 3A, C), so for "the entire population" group (Fig. 3B, D). Intervals between low and upper quartiles of CI distributions were (as a rule) larger for the age group "children and teenagers 0–14 years" than for age group "the entire population". Distributions of CIs differed from NF distributions most profoundly as by medians, so by lower and upper quartiles, for Kamchatskij Kraj and Sakhalin Oblast'.

Time series analysis of relationship between number of fires and cancer incidence by cancer types and spatial regions with different administrative units combinations

Statistically significant associations with marginal threshold $\alpha = 0.1$ between normalized NF and normalized CI time series by different cancer types and by two pooling methods with a lag from 0 to 3 years, when controlled for probability of type I error during multiple ARIMA calculations, were found for 27 pooled together combination sets of AUs within the two age groups "children/teens 0–14 years" and "entire population". Statistically significant relationships ($\alpha = 0.05$) were found for eight spatial areas ((see Supplementary List of spatial clusters of ARIMA associations between number of fires and cancer incidence by types with regression coefficients and p-values with statistical significance $\alpha = 0.1$ and $\alpha = 0.05$ after Holms–Bonferroni correction)). Majority (six from eight) statistical relationships NF/CI with $\alpha = 0.05$ where found for pooling together AUs method with weighting to number of population in AUs. Kamchatskij Kraj and Sakhalin Oblast, where distributions of NF and CIs are considerably different (see above) were not met in any from 27 spatial regions with NF/CI relationships. The four most populous AUs pooled together (Primorskij Kraj — Khabarovskij Kraj — Amurskaja Oblast — Respublika Sakha) showed the largest number of ARIMA-based statistical associations between NF and CI (six) with $\alpha = 0.1$ (two from these six had $\alpha < 0.05$). However, adding to a pooled combination of an administrative unit with a smaller population may distort the previously found associations. Negative values of ARIMA-based regression coefficients of annual NF against annual CI were found in some cases (see Supplementary List of spatial clusters of ARIMA associations between number of fires and cancer incidence by types with regression coefficients and *p*-values with statistical significance $\alpha = 0.1$ and $\alpha = 0.05$ after Holms–Bonferroni correction)). These negative regressions coefficients were found for the age group "children/teens 0–14 years" for leukemia (only for time lag 2 years, not for other lags), CNS tumors (lag 3 years) and STS tumors (lag 2 years) and for the age group "entire population" for leukemia (only for lags 2 years and 3 years, not for other lags). We found with ARIMA analysis that time lags for statistical associations between NF and CI are rather independent from geographical area for a taken cancer type. Time lags lay between zero (NHL for children) and 3 years (CNS tumors for children/teens 0–14 years), but mostly they are equal to 2–3 years.

Results of linear analysis of statistical dependencies between number of fires and benign, embryonal, and malignant tumor incidence by type in the age cohort: young children up to 4 years

Positive significant correlations between NF and tumor incidence in the age group: young children 0–4 were found for the period 1972–1986 in Khabarovskij Kraj/Khabarovsk. Correlations were observed for all three groups analyzed: for

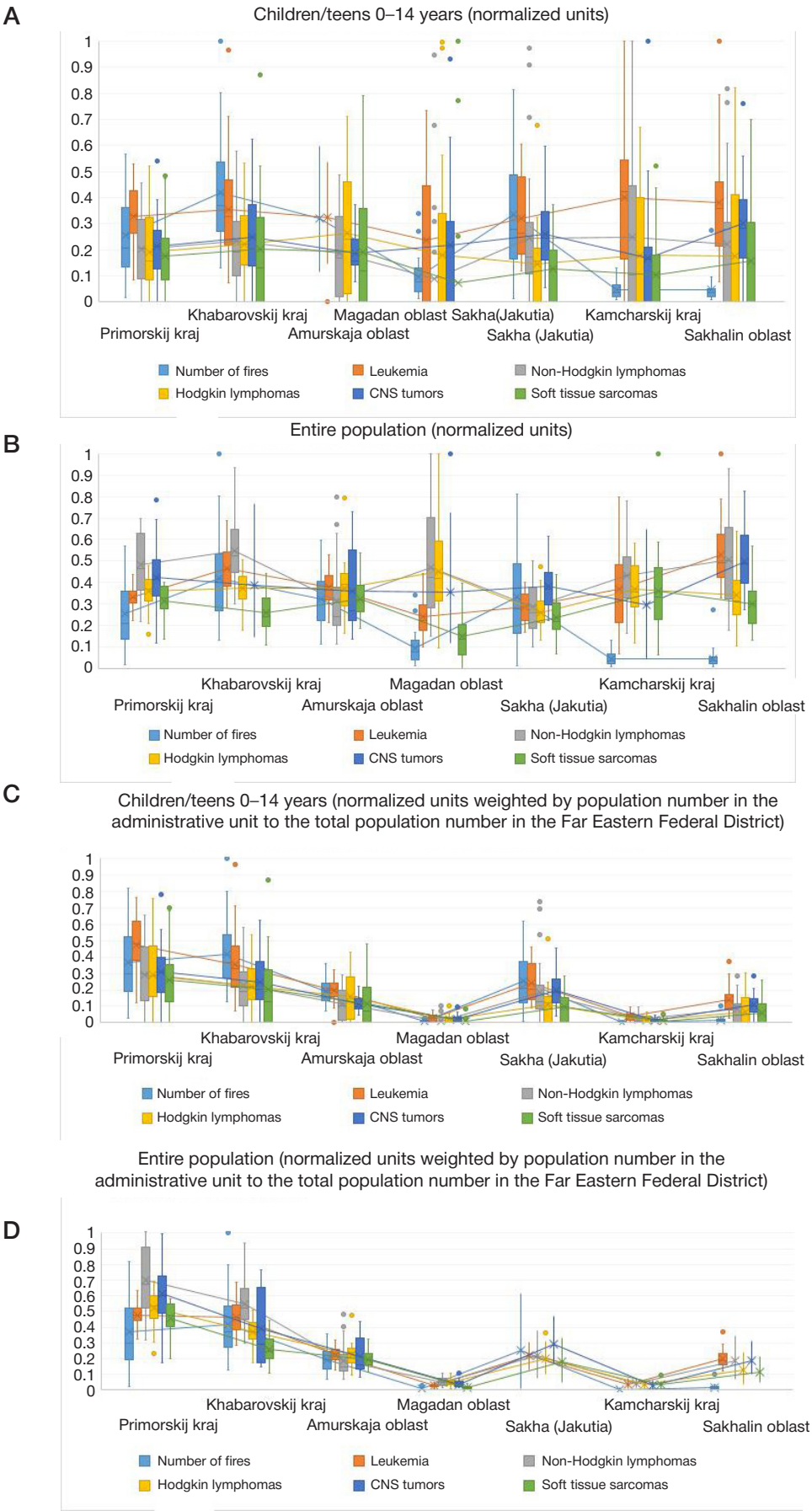

Fig. 3. Comparison of distributions of normalized values of cancer incidence and number of fires for AU of Far Eastern federal district. **A**. Age group "children and teenagers 0–14 years". **B**. Age group "the entire population". **C**. Age group "children and teenagers 0–14 years" with weighting by number of population in AU to the total population in all of the AUs. **D**. Age group "the entire population" with weighting by number of population in AU to the total population in all of the AUs

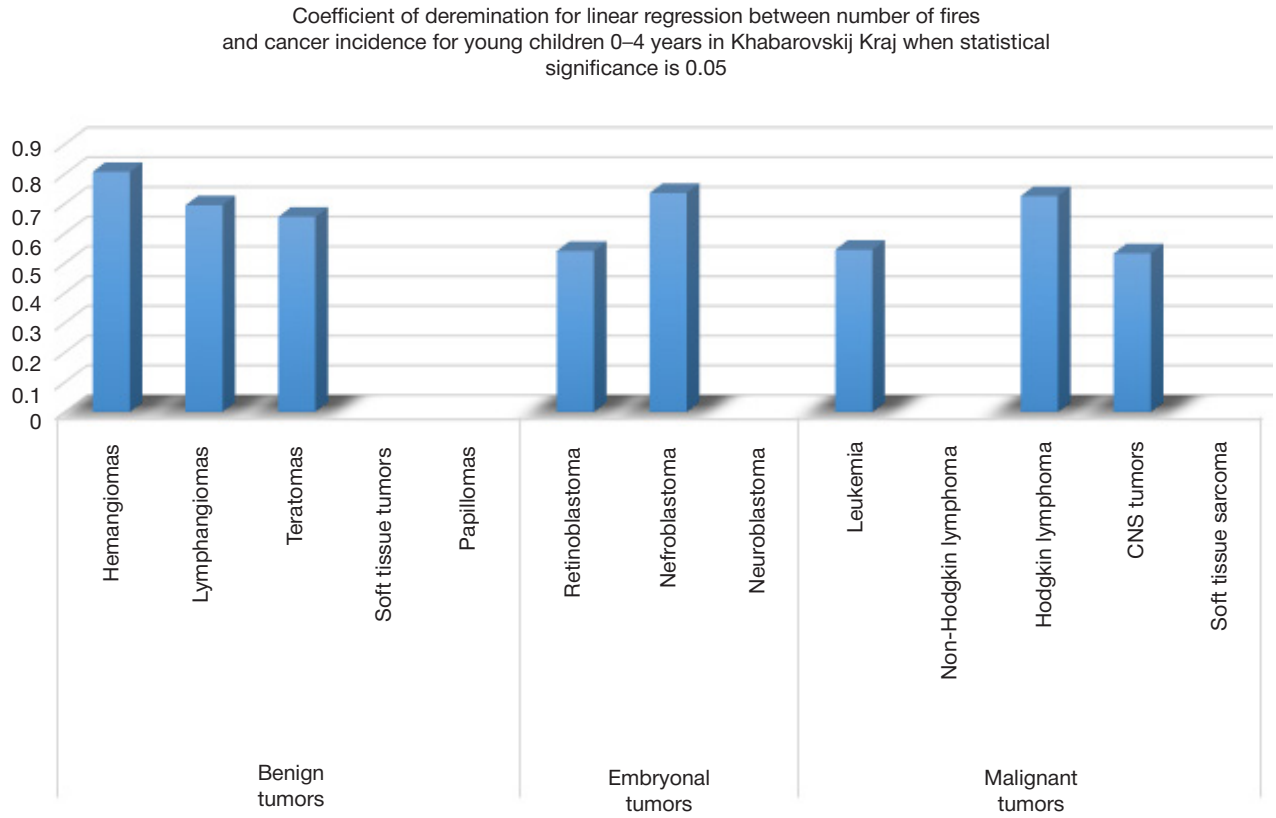

Fig. 4. Coefficient of determination R2 for linear regression between number of fires and tumor incidence for young children up to 4 years in Khabarovskij Kraj

benign tumors (3 from 5 analyzed $0.66 < R^2 < 0.84$; $0.003 < p < 0.014$), embryonal tumors (2 from 3 analyzed $0.54 < R^2 < 0.74$; $0.037 < p < 0.046$), and malignant tumors (3 from 5 analyzed $0.533 < R^2 < 0.73$; $0.009 < p < 0.036$) (Fig. 4).

Hodgkin lymphomas had largest coefficient of determination R^2 for linear regression between NF and CI for young children up to 4 years. Generally, R^2 is higher for benign tumors than for malignant tumors for this age cohort.

Both prenatal and postnatal influences of fires were found for the age cohort: 0–4 years, which is seen from the time lags (see Supplementary Linear Statistical Analysis), which are close to the ones from ARIMA-based analysis for certain cancer types.

Cancer types in relation to wildfires

Relative strength (RS) of relationships (from 0 to 1) between normalized NF and CI, summed over all five types of cancer, was larger for the age group "entire population" as for the threshold $\alpha = 0.1$ (Fig. 5A), so for the threshold $\alpha = 0.05$ (Fig. 5B). Leukemia and non-Hodgkin lymphomas had the largest cumulative input to RS by both thresholds.

DISCUSSION

Statistical analysis of time series of CI by the five cancer types against NF confirms existence of statistical associations CI/NF in spatial regions, consisting from combinations of the five AUs of FEFD, excluding Kamchatskij Kraj and Sakhalin Oblast. We speculate that absence of statistically significant relationships between CI and NF in spatial regions which include Kamchatskij Kraj and Sakhalin Oblast, can be explained by maritime climate in these AUs, which determines smoke pattern from wildfires here. This hypothesis, as well as a hypothesis of existence of other large scale environmental spatial determinants, setting an absence or an existence of statistically significant relationships between CI and NF, should be studied further on.

Spatial regions, consisting from the AUs with largest population numbers, demonstrate the largest number of statistically significant CI/NF relationships. This can be explained a) by bigger size of samples and/or b) by better medical information systems in AUs with larger number of population. Clarification of influence of demographic and logistic spatial reasons for existence/absence of CI/NF relationships is a topic for further studies as well.

It can be assumed that negative ARIMA regression coefficients, observed in some spatial regions of analysis for some cases of cancer, are set by absence of seasonality in CI data. It is known that seasonality of CI data is related to non-sufficient registration of oncological diseases in periods of summer vacations [23]. It may be assumed that oncological diseases develop under carcinogens from smoke of large fires in summer of previous year, but get registered in a cold time of next year (i.e. 0.5 years are added to time lag, which should be rounded by adding 1 year). An example of such a situation presumably can be a result of ARIMA regression for leukemia in the age group "children/teens 0–14 years" in the spatial region, consisting from Primorskij Kraj, Khabarovskij Kraj and Sakha (Yakutia), (see Supplementary List of spatial clusters of ARIMA associations between number of fires and cancer incidence by types with regression coefficients and p-values with statistical significance $\alpha = 0.1$ and $\alpha = 0.05$ after Holms-Bonferroni correction). ARIMA regression coefficient in this case is negative for the time lag 2 years, but positive for the time lag 3 years. It can be explained most likely, by late registration of part of leukemia incidence cases, developed in the summer of year 2, in the beginning of winter of the year 3. This hypothesis, however, requires further investigation.

We found the stronger association of NF with CI for the age population group "entire population" for majority from five

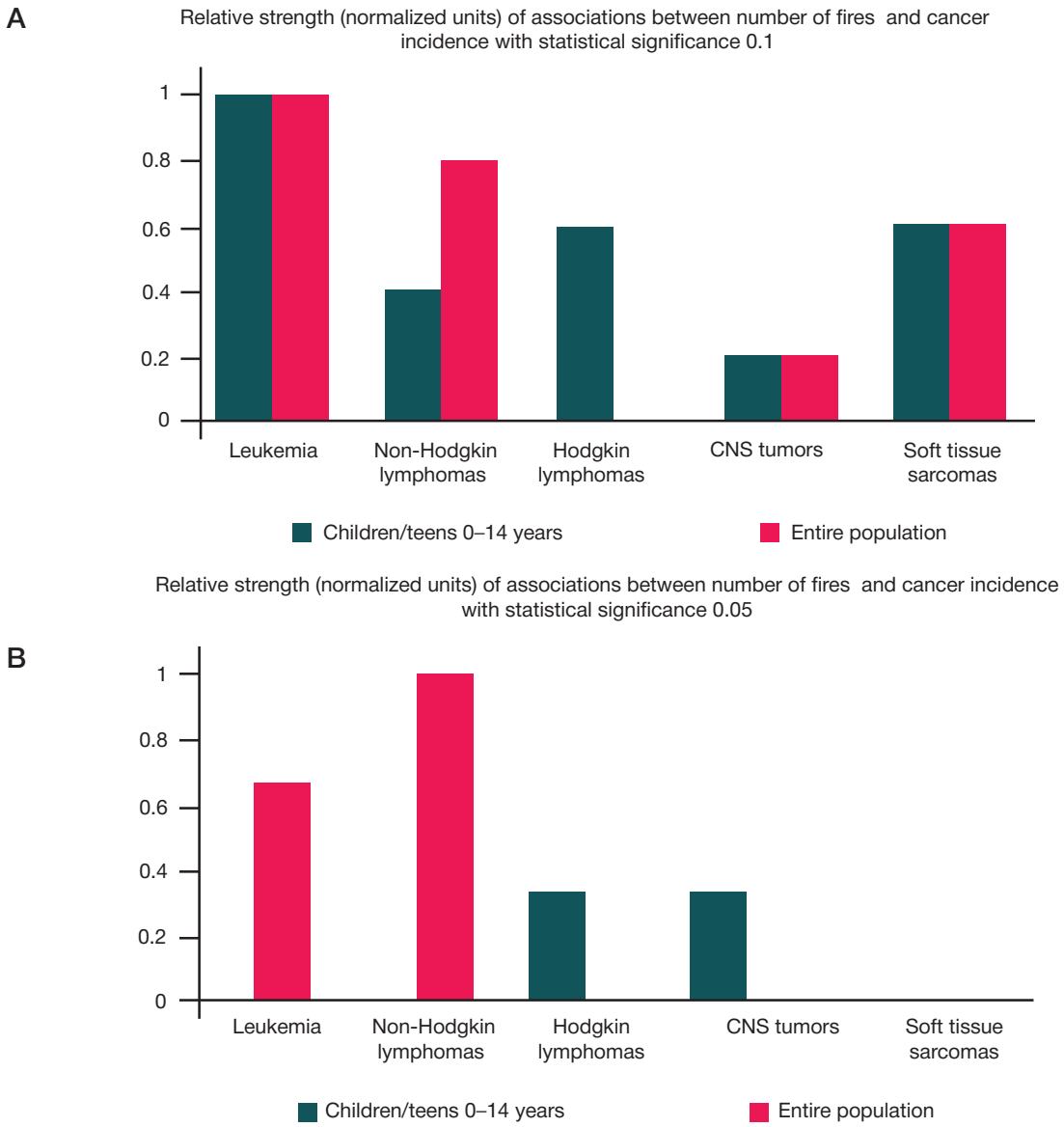

Fig. 5. Relative strength (RS) of relationships (from 0 to 1) between normalized number of fires and cancer incidence for five types of cancer for two age groups with confidence threshold $\alpha = 0.1$ (**A**); with confidence threshold $\alpha = 0.05$ (**B**)

cancers in terms of RS (Fig. 5). There can be several reasons: 1) pure demographic reason, i.e. a result of longer exposure of "entire population" group to smoke carcinogens due to larger age period within the group; 2) gerontological reason, i.e. due to inclusion in this group elderly population prone to many diseases including cancers; 3) socio-economic, i.e. result of influence of cofounding factors, like smoking of cigarettes or long-term exposure to industrial and/or agricultural carcinogens of some part of "entire population". Synergetic impact of cofounding particulate emissions to cancer (e.g. particulate emission from heating in winter in FEFD [24]) and joint impact of heat wave and smoke of wildfires (e.g. example of Moscow fires in 2010 [25]) should be considered in future,

There is wide experimental and observed evidence of the carcinogenic impact of smoke from wildfires on humans (e.g. [7]). Intrusion of carcinogenic chemicals and particles of smoke into the blood leads to oxidative stress, an integrative vector for environmental impacts on organisms, which in turn promotes the hallmarks of benign and malignant tumors, such as inflammation and genetic variation caused by mutations and direct chromosome damage [26]. Three blood cancers (leukemia, non-Hodgkin lymphoma, and Hodgkin lymphoma) most likely had the strongest associations with wildfires, not only because blood is an immediate agent of smoke intrusion, but also because oxidative stress interacts with other negative external impacts on humans. For example, the dependence of non-Hodgkin lymphoma on environmental factors and certain lifestyles has been well studied [27]. It was found that environmental factors that increase viral exposure or reaction to viruses (from all HIV found mostly by the entire population) pose a risk of non-Hodgkin lymphomas. Wildfires most likely affect non-Hodgkin lymphomas by weakening an individual's immune system during inhalation of smoke with further increase in reaction to viruses.

Our results demonstrate statistically significant relationship between incidence to Hodgkin lymphoma and number of fires both in FEFD for the age group "children/teens 0–14 years" and in Khabarovskij Kraj for young children up to 4 years (with the threshold $\alpha < 0.05$). We speculate, that impact of wildfire to development of Hodgkin lymphomas is related to respiratory diseases caused by smoke, which weaken immunity with further activation of new or chronic infection by Epstein–Barr virus (EBV). EBV is a I class carcinogen in the World Health Organization category and pediatric Hodgkin lymphoma (for children up to 10 years) is associated with EBV up to 80% [28].

Leukemia is seen by some authors as “preventable pathology” [29] because observations confirm an increase in leukemia risk with prenatal, in utero, and postnatal exposure to tobacco smoke or automobile gases in young children [30] Our analysis demonstrated a broad range of negative impacts of wildfire smoke on leukemia risk in the prenatal period for young children 0–4 year, so to children/teens 0–14 and entire population leukemia with a variety of time lags.

We found on example of young children up to 4 years in Khabarovsk City/Khabarovskij Kraj that incidence to benign tumors has stronger correlation with number of wildfires in comparison to incidence to malignant tumors. It is known that benign tumors considerably outnumber malignant tumors, but only few of benign tumors got transformed to the malignant ones [31]. It would be useful to extent to the entire territory of FEFD comparison of relationships CI to NF with relationships of incidence to benign tumors to NF in order to study a role of wildfires to evolution of tumors in humans.

CONCLUSIONS

The following conclusions were drawn: 1) Fluctuations in the incidence of hematopoietic, lymphoid, vascular, and soft tissue neoplasms, as well as CNS tumors in young children 0–4 years, children/teens 0-14 years and the entire population of FEFD to some extent are related to wildfires, described by normalized and weighted by population number NF as a proxy. 2) The most sensitive age group to the impact of NF on CI in FEFD is the “entire population” group. 3) Development of different types of neoplasia has different time lags and different relative strengths of statistical dependence from wildfires. Three blood cancers (leukemia, non-Hodgkin lymphoma, and Hodgkin lymphoma) had the strongest associations with wildfires, from the five analyzed types of cancers common for the age cohort and two age population groups. They also have the widest range of time lag, for example, from 2 years of prenatal time lag in the “young children up to 4 years” age cohort to 0–3 years lag for the entire population for “leukemia” type. 4) Statistically significant relationships between NF and CIs were found in spatial regions, which included climatically homogenous AUs of FEFD. Largest number of these relationships are observed for geographical domains with a large number of population. Statistically significant results on relationship of leukemia and non-Hodgkin lymphomas incidence with number of fires for the age group “entire population” and on relationship of Hodgkin lymphomas incidence with number of fires for the age group “children/teens 0–14 years” with time lags 0–3 years can be applied in practice. Influence of fires can be accounted during diagnostic of these diseases as large fire years are well known for the Russian Far East. Further studies should include an analysis of a) environmental, demographic, socio-economic and logistic determinants of spatial and temporal patterns of cancer incidence in FEFD; b) influence of seasonality on statistical relationships between cancer incidence and number of fires; c) influence of number of fires to ratio of benign and malignant tumors. Open is also a question about spatial transferability of our approaches of analysis of relationships between cancer incidence and number of fires to other geographical areas prone to wildfires in Russia (Siberian and Ural Federal districts) and in bordering countries (Kazakhstan and China).

References

1. Sung H, Ferlay J, Siegel RL, Laversanne M, Soerjomataram I, Jemal AD, et al. Global Cancer Statistics 2020: GLOBOCAN Estimates of Incidence and Mortality Worldwide for 36 Cancers in 185 Countries. CA: A Cancer Journal for Clinicians. 2021; 71: 209–49. PubMed PMID: 33538338.
2. Amin RW, Stafford B, Guttmann RP. A spatial study of bladder cancer mortality and incidence in the contiguous US: 2000–2014. Science of The Total Environment 2019; 670: 806–13.
3. Fitzmaurice C, Allen C, Barber RM, Barregard L, Bhutta ZA, Brenner H, et al. Global Burden of Disease Cancer Collaboration; Global, Regional, and National Cancer Incidence, Mortality, Years of Life Lost, Years Lived With Disability, and Disability Adjusted Life-years for 32 Cancer Groups, 1990 to 2015: A Systematic Analysis for the Global Burden of Disease Study. JAMA Oncology. 2017; 3 (4): 524–48. PubMed PMCID: PMC6103527.
4. ONCOLOGY.RU Zlokachestvennye novoobrazovaniya v Rossii. Dostupno po ssylke: http://www.oncology.ru/service/statistics/malignant_tumors/ (dostup: 17.01.2023). Russian.
5. Dobroxleb VG. Starenie naseleniya Rossii: regional'nyj aspekt // Voprosy territorial'nogo razvitiya. 2018; 4 (44). DOI: 10.15838/tdi.2018.4.44.4. Russian.
6. Lupyan EA, Bartalev SA, Balashov IV, Egorov VA, Ershov DV, Kobec DA, i dr. Sputnikovyj monitoring lesnyh pozharov v 21 veke na territorii Rossijskoj Federacii (cifry i fakty po dannym detektirovaniya aktivnogo goreniya). Sovremennye problemy distancionnogo zondirovaniya Zemli iz kosmosa. 2017; 14 (6): 158–75. DOI: 10.21046/2070-7401-2017-14-6-158-175. Russian.
7. Navarroa KM, Kleinmanb MT, Mackayc CE, Reinhardtd TE, Balmese JR, Broylesf GA, et al. Wildland firefighter smoke exposure and risk of lung cancer and cardiovascular disease mortality. Environmental Research. 2019; 173: 462–8. PubMed PMID: 30981117.
8. ROSGIDROMET. Obzor sostoyaniya i zagryazneniya okruzhayushhej sredy v Rossijskoj Federacii. Dostupno po ssylke: https://www.meteorf.gov.ru/product/infomaterials/90/. Russian.
9. Gambaryan MG, Drapkina OM. Rasprostranennost' potrebleniya tabaka v Rossii: dinamika i tendencii. Analiz rezul'tatov global'nyx i nacional'nyh oprosov. Profilakticheskaya medicina. 2018; 21 (5): 45–62. DOI: 10.17116/profmed20182105145. Russian.
10. Reid CE, Brauer M, Johnston FH, Jerrett M, Balmes JR, Elliott CT. Critical review of health impacts of wildfire smoke exposure. Environmental health perspectives. 2016; 124 (9): 1334–43. PubMed PMID: 27082891.
11. Turner MC, Krewski D, Diver WR, Pope III CA, Burnett RT, Jerrett M, et al. Ambient air pollution and cancer mortality in the cancer prevention study II. Environmental health perspectives. 2017; 125 (8): 087013. PubMed PMID: 28886601.
12. Dobrykh VA, Zakharycheva TA. Forest fire smoke and health. Khabarovsk: Publishing House of the Far Eastern State Medical University, 2009. 201 p. ISBN 5-85797-172-1. http://www.fesmu.ru/elib/PdfViewer/default.aspx?id=33&res=1366%2c657.
13. Korsiak J, Pinault L, Christidis T, Burnett RT, Abrahamowicz M, Weichenthal S. Long-term exposure to wildfires and cancer incidence in Canada: a population-based observational cohort study. The Lancet Planetary Health. 2022; 6 (5): e400–e9. PubMed PMID: 35550079.
14. Chizhov AYa, Pinaev SK. Sistemnyj analiz vliyaniya solnechnoj radiacii i dyma lesnyh pozharov na risk lejkoza u detej. Radiaciya i risk. 2018; 27 (4): 87–94. DOI: 10.21870/0131-3878-2018-27-4-87-94. Russian.
15. Pinaev SK, Chizhov AYa, Pinaeva OG. Svyaz' dyma i solnechnoj aktivnosti s novoobrazovaniyami cheloveka. Kazanskij medicinskij zhurnal. 2022; 103 (4): 650–7. DOI: 10.17816/KMJ2022-650. Russian.
16. Steliarova-Foucher E, Stiller C, Lacour B, Kaatsch P. International Classification of Childhood Cancer, third edition.

Cancer. 2005; 103 (7): 1457–67. DOI: 10.1002/cncr.20910. PubMed PMID: 15712273.
17. Bleyer A, Barr R, Ries J, Whelan A, Ferrari, editors. Cancer in Adolescents and Young Adults: Pediatric Oncology: Springer International Publishing AG; 2017. DOI: 10.1007/978-3-319-33679-4.
18. Botsivali M, Kyrtopoulos SA. Transplacental exposure to carcinogens and risks to children: evidence from biomarker studies and the utility of omic profiling. Archives of Toxicology. 2019; 93 (4): 833–57. PubMed PMID: 30859261.
19. Ponomarev EI. Estimation of Direct Fire Emissions from Forests Burning in Siberia. Environmental Sciences Proceedings. 2021; 4 (1): 12. PubMed PMID: DOI: 10.3390/ecas2020-08114. PubMed PMID: 35513193.
20. Box GEP, Jenkins GM, Reinsel GC, Ljung GM. Time series analysis. Forecasting and control. Wiley, 2016; p. 712. DOI: 10.1111/jtsa.12194.
21. Jesus CSLd, Delgado RC, Wanderley HS, Teodoro PE, Pereira MG, Lima M, et al. Fire risk associated with landscape changes, climatic events and remote sensing in the Atlantic Forest using ARIMA model. Remote Sensing Applications: Society and Environment 2022; 26: 100761.
22. Arul E, Sue ME, Fanny S, Jeremy M. Forecasting annual incidence and mortality rate for prostate cancer in Australia until 2022 using autoregressive integrated moving average (ARIMA) models. BMJ Open. 2019; 9: e031331.
23. Wikén I, Andersson TML, Radkiewicz C. Seasonal effects on cancer incidence and prognosis. Acta Oncologica. 2023; 62: 103–9.
24. Lin C, Labzovskii LD, Mak HWL, Fung JC, Lau AK, Kenea ST, et al. Observation of PM2. 5 using a combination of satellite remote sensing and low-cost sensor network in Siberian urban areas with limited reference monitoring. Atmospheric Environment. 2020; 227: 117410. DOI: 10.1016/j.atmosenv.2020.117410.
25. Shaposhnikov D, Revich B, Bellander T, Bedada GB, Bottai M, Kharkova T, et al. Mortality related to air pollution with the Moscow heat wave and wildfire of 2010. Epidemiology (Cambridge, Mass). 2014; 25 (3): 359–64. PubMed PMID: 24598414.
26. Hayes JD, Dinkova-Kostova TA, Tew KD. Oxidative Stress in Cancer. Cancer Cell. 2020; 38 (2): 167–97. PubMed PMID: 32649885.
27. Bassig BA, Lan Q, Rothman N, Zhang Y, Zheng T. Current Understanding of Lifestyle and Environmental Factors and Risk of Non-Hodgkin Lymphoma: An Epidemiological Update. Journal of Cancer Epidemiology. 2012; 2012: 978930. PubMed PMID: 23008714.
28. Naumova AS, Tiganova OA, Kondratchik KL. Rol' virusa Ehpshtejna–Barr v patogeneze limfomy Xodzhkina u detej. Pediatriya. 2019; 98 (1): 178–85. Russian.
29. Greaves M. A causal mechanism for childhood acute lymphoblastic leukaemia. Nature Reviews Cancer. 2018; 18 (8): 471–4. PubMed PMID: 29784935.
30. Cárceles-Álvarez A, Ortega-García JA, López-Hernández FA, Orozco-Llamas M, Espinosa-López B, Tobarra-Sánchez E, et al. Spatial clustering of childhood leukaemia with the integration of the Paediatric Environmental History. Environmental Research. 2017; 156: 605–12. PubMed PMID: 28454012.
31. Marino-Enriquez A, Fletcher CDM. Shouldn't we care about the biology of benign tumours? Nature Reviews Cancer. 2014; 14: 701–2.

Литература

1. Sung H, Ferlay J, Siegel RL, Laversanne M, Soerjomataram I, Jemal AD, et al. Global Cancer Statistics 2020: GLOBOCAN Estimates of Incidence and Mortality Worldwide for 36 Cancers in 185 Countries. CA: A Cancer Journal for Clinicians. 2021; 71: 209–49. PubMed PMID: 33538338.
2. Amin RW, Stafford B, Guttmann RP. A spatial study of bladder cancer mortality and incidence in the contiguous US: 2000–2014. Science of The Total Environment. 2019; 670: 806–13.
3. Fitzmaurice C, Allen C, Barber RM, Barregard L, Bhutta ZA, Brenner H, et al. Global Burden of Disease Cancer Collaboration; Global, Regional, and National Cancer Incidence, Mortality, Years of Life Lost, Years Lived With Disability, and Disability Adjusted Life-years for 32 Cancer Groups, 1990 to 2015: A Systematic Analysis for the Global Burden of Disease Study. JAMA Oncology. 2017; 3 (4): 524–48. PubMed PMCID: PMC6103527.
4. ONCOLOGY.RU Злокачественные новообразования в России. Доступно по ссылке: http://www.oncology.ru/service/statistics/malignant_tumors/ (доступ: 17.01.2023).
5. Доброхлеб В. Г. Старение населения России: региональный аспект // Вопросы территориального развития. 2018; 4 (44). DOI: 10.15838/tdi.2018.4.44.4.
6. Лупян Е. А., Барталев С. А., Балашов И. В., Егоров В. А., Ершов Д. В., Кобец Д. А. и др. Спутниковый мониторинг лесных пожаров в 21 веке на территории Российской Федерации (цифры и факты по данным детектирования активного горения). Современные проблемы дистанционного зондирования Земли из космоса. 2017; 14 (6): 158–75. DOI: 10.21046/2070-7401-2017-14-6-158-175.
7. Navarroa KM, Kleinmanb MT, Mackayc CE, Reinhardtd TE, Balmese JR, Broylesf GA, et al. Wildland firefighter smoke exposure and risk of lung cancer and cardiovascular disease mortality. Environmental Research. 2019; 173: 462–8. PubMed PMID: 30981117.
8. РОСГИДРОМЕТ. Обзор состояния и загрязнения окружающей среды в Российской Федерации. Доступно по ссылке: https://www.meteorf.gov.ru/product/infomaterials/90/.
9. Гамбарян М. Г., Драпкина О. М. Распространенность потребления табака в России: динамика и тенденции. Анализ результатов глобальных и национальных опросов. Профилактическая медицина. 2018; 21 (5): 45–62. DOI: 10.17116/profmed20182105145.
10. Reid CE, Brauer M, Johnston FH, Jerrett M, Balmes JR, Elliott CT. Critical review of health impacts of wildfire smoke exposure. Environmental health perspectives. 2016; 124 (9): 1334–43. PubMed PMID: 27082891.
11. Turner MC, Krewski D, Diver WR, Pope III CA, Burnett RT, Jerrett M, et al. Ambient air pollution and cancer mortality in the cancer prevention study II. Environmental health perspectives. 2017; 125 (8): 087013. PubMed PMID: 28886601.
12. Добрых В. А., Захарычева Т. А. Дым лесных пожаров и здоровье. Хабаровск: изд-во ГОУ ВПО ДВГМУ, 2009; 201 с.
13. Korsiak J, Pinault L, Christidis T, Burnett RT, Abrahamowicz M, Weichenthal S. Long-term exposure to wildfires and cancer incidence in Canada: a population-based observational cohort study. The Lancet Planetary Health. 2022; 6 (5): e400–e9. PubMed PMID: 35550079.
14. Чижов А. Я., Пинаев С. К. Системный анализ влияния солнечной радиации и дыма лесных пожаров на риск лейкоза у детей. Радиация и риск. 2018; 27 (4): 87–94. DOI: 10.21870/0131-3878-2018-27-4-87-94.
15. Пинаев С. К., Чижов А. Я., Пинаева О. Г. Связь дыма и солнечной активности с новообразованиями человека. Казанский медицинский журнал. 2022; 103 (4): 650–7. DOI: 10.17816/KMJ2022-650.
16. Steliarova-Foucher E, Stiller C, Lacour B, Kaatsch P. International Classification of Childhood Cancer, third edition. Cancer. 2005; 103 (7): 1457–67. DOI: 10.1002/cncr.20910. PubMed PMID: 15712273.
17. Bleyer A, Barr R, Ries J, Whelan A, Ferrari, editors. Cancer in Adolescents and Young Adults: Pediatric Oncology: Springer International Publishing AG; 2017. DOI: 10.1007/978-3-319-33679-4.
18. Botsivali M, Kyrtopoulos SA. Transplacental exposure to carcinogens and risks to children: evidence from biomarker studies and the utility of omic profiling. Archives of Toxicology. 2019; 93 (4): 833–57. PubMed PMID: 30859261.
19. Ponomarev EI. Estimation of Direct Fire Emissions from Forests Burning in Siberia. Environmental Sciences Proceedings. 2021; 4

(1): 12. PubMed PMID: DOI: 10.3390/ecas2020-08114. PubMed PMID: 35513193.
20. Box GEP, Jenkins GM, Reinsel GC, Ljung GM. Time series analysis. Forecasting and control. Wiley, 2016; p. 712. DOI: 10.1111/jtsa.12194.
21. Jesus CSLd, Delgado RC, Wanderley HS, Teodoro PE, Pereira MG, Lima M, et al. Fire risk associated with landscape changes, climatic events and remote sensing in the Atlantic Forest using ARIMA model. Remote Sensing Applications: Society and Environment 2022; 26: 100761.
22. Arul E, Sue ME, Fanny S, Jeremy M. Forecasting annual incidence and mortality rate for prostate cancer in Australia until 2022 using autoregressive integrated moving average (ARIMA) models. BMJ Open. 2019; 9: e031331.
23. Wikén I, Andersson TML, Radkiewicz C. Seasonal effects on cancer incidence and prognosis. Acta Oncologica. 2023; 62: 103–9.
24. Lin C, Labzovskii LD, Mak HWL, Fung JC, Lau AK, Kenea ST, et al. Observation of PM2. 5 using a combination of satellite remote sensing and low-cost sensor network in Siberian urban areas with limited reference monitoring. Atmospheric Environment. 2020; 227: 117410. DOI: 10.1016/j.atmosenv.2020.117410.
25. Shaposhnikov D, Revich B, Bellander T, Bedada GB, Bottai M, Kharkova T, et al. Mortality related to air pollution with the Moscow heat wave and wildfire of 2010. Epidemiology (Cambridge, Mass). 2014; 25 (3): 359–64. PubMed PMID: 24598414.
26. Hayes JD, Dinkova-Kostova TA, Tew KD. Oxidative Stress in Cancer. Cancer Cell. 2020; 38 (2): 167–97. PubMed PMID: 32649885.
27. Bassig BA, Lan Q, Rothman N, Zhang Y, Zheng T. Current Understanding of Lifestyle and Environmental Factors and Risk of Non-Hodgkin Lymphoma: An Epidemiological Update. Journal of Cancer Epidemiology. 2012; 2012: 978930. PubMed PMID: 23008714.
28. Наумова А. С., Тиганова О. А., Кондратчик К. Л. Роль вируса Эпштейна–Барр в патогенезе лимфомы Ходжкина у детей. Педиатрия. 2019; 98 (1): 178–85.
29. Greaves M. A causal mechanism for childhood acute lymphoblastic leukaemia. Nature Reviews Cancer. 2018; 18 (8): 471–4. PubMed PMID: 29784935.
30. Cárceles-Álvarez A, Ortega-García JA, López-Hernández FA, Orozco-Llamas M, Espinosa-López B, Tobarra-Sánchez E, et al. Spatial clustering of childhood leukaemia with the integration of the Paediatric Environmental History. Environmental Research. 2017; 156: 605–12. PubMed PMID: 28454012.
31. Marino-Enriquez A, Fletcher CDM. Shouldn't we care about the biology of benign tumours? Nature Reviews Cancer. 2014; 14: 701–2.

NONINVASIVE PREIMPLANTATION GENETIC TESTING FOR ANEUPLOIDY

Lisitsyna OI ✉, Ekimov AN, Atapina EE, Syrkasheva AG, Goryainova EG, Makarova NP, Trofimov DYu, Dolgushina NV

Kulakov National Medical Research Center for Obstetrics, Gynecology and Perinatology, Moscow, Russia

To date the world community is actively working to optimize the approaches to determining chromosomal abnormalities in embryos. The study was aimed to assess the possibility of using noninvasive preimplantation genetic testing for aneuploidy (niPGT-A) through analysis of cell-free DNA in spent culture medium (SCM). We conducted niPGT-A of aneuploid embryos by analysis of cell-free DNA in SCM. All blastocysts were considered to be aneuploid based on the results of previous preimplantation genetic testing for aneuploidy (PGT-A) with trophectoderm (TE) biopsy. The study involved 11 embryos from seven couples. All the embryos were warmed and individually cultured in the 10 μL drops for 9 h. All SCM was collected and analyzed by niPGT-A. The results obtained were tested for concordance with previous PGT-A data. A total of 12 SCM samples were assessed: 11 samples, in which the embryos were cultured, and one control sample. Chaotic niPGT-A results not allowing the karyotype diagnosis were obtained in one case (9.1%) out of 11. Full concordance of the PGT-A and niPGT-A results was revealed in seven cases out of 10 (70%), while clinical concordance was found in nine cases out of 10 (90%). In one case (10%), the blastocyst was considered to have euploid karyotype based on the niPGT-A data. It has been concluded that niPGT-A can be a promising method of preimplantation embryonal chromosomal status diagnosis that requires no biopsy.

Keywords: noninvasive preimplantation genetic testing, noninvasive PGT-A, niPGT-A, PGT-A, spent culture medium, SCM, trophectoderm biopsy, aneuploidy, cell-free DNA

Funding: the study was supported by the Russian Foundation for Basic Research under research project №23-25-00346.

Author contribution: Makarova NP, Lisitsyna OI, Dolgushina NV — study concept and design; Lisitsyna OI, Makarova NP, Dolgushina NV, Syrkasheva AG, Ekimov AN — manuscript writing and editing; Lisitsyna OI — statistical processing of the results; Goryainova EG, Makarova NP — biomaterial collection; Ekimov AN, Atapina EE — laboratory phase; Dolgushina NV, Trofimov DYu — publication approval.

Compliance with ethical standards: the study was approved by the Ethics Committee of the Kulakov National Medical Research Center for Obstetrics, Gynecology and Perinatology (protocol № 10 of 28 October 2021). The patients submitted the informed consent to study participation.

✉ **Correspondence should be addressed:** Olga I. Lisitsyna
Akademika Oparina, 4, Moscow, 117997, Russia; o_yazykova@inbox.ru

Received: 18.06.2023 **Accepted:** 09.08.2023 **Published online:** 30.08.2023

DOI: 10.24075/brsmu.2023.034

НЕИНВАЗИВНОЕ ПРЕИМПЛАНТАЦИОННОЕ ГЕНЕТИЧЕСКОЕ ТЕСТИРОВАНИЕ НА АНЕУПЛОИДИИ

О. И. Лисицына ✉, А. Н. Екимов, Е. Е. Атапина, А. Г. Сыркашева, Е. Г. Горяйнова, Н. П. Макарова, Д. Ю. Трофимов, Н. В. Долгушина

Национальный медицинский исследовательский центр акушерства, гинекологии и перинатологии имени В. И. Кулакова, Москва, Россия

В настоящее время в мире идет активная работа по оптимизации применения подходов к определению хромосомной патологии эмбрионов. Целью исследования было оценить возможность использования неинвазивного преимплантационного генетического тестирования на анеуплоидии (ниПГТ-А) путем анализа внеклеточной ДНК в отработанной культуральной среде (ОКС). Проведено ниПГТ-А анеуплоидных эмбрионов путем анализа внеклеточной ДНК в ОКС. Все бластоцисты были анеуплоидными по результатам предшествующего преимплантационного генетического тестирования на анеуплоидии (ПГТ-А) с биопсией трофэктодермы (ТФЭ). В исследование было включено 11 эмбрионов от семи супружеских пар. Все эмбрионы размораживали и культивировали в каплях по 10 мкл в течение 9 ч. Весь объем ОКС собирали и анализировали путем ниПГТ-А. Полученные результаты сравнивали на соответствие с предшествующими данными по ПГТ-А. Суммарно выполнили анализ 12 образцов ОКС: 11 образцов, в которых были культивированы эмбрионы, и один контрольный образец. В одном случае (9,1%) из 11 были получены хаотичные результаты по данным ниПГТ-А, не позволяющие провести диагностику состояния кариотипа. Полное соответствие результатов ПГТ-А и ниПГТ-А получено в семи случаях из 10 (70%), клиническое соответствие результатов — в девяти случаях из 10 (90%). В одном случае (10%) по данным ниПГТ-А кариотип бластоцисты был диагностирован как эуплоидный. Вывод: ниПГТ-А может быть перспективным, не требующим биопсии, методом диагностики хромосомного статуса преимплантационных эмбрионов.

Ключевые слова: неинвазивное преимплантационное генетическое тестирование, неинвазивное ПГТ-А, ниПГТ-А, ПГТ-А, отработанная культуральная среда, ОКС, биопсия трофэктодермы, анеуплоидия, внеклеточная ДНК

Финансирование: исследование выполнено при финансовой поддержке РНФ в рамках научного проекта №23-25-00346.

Вклад авторов: Н. П. Макарова, О. И. Лисицына, Н. В. Долгушина — концепция и дизайн исследования; О. И. Лисицына, Н. П. Макарова, Н. В. Долгушина, А. Г. Сыркашева, А. Н. Екимов — написание и редактирование текста; О. И. Лисицына — статистическая обработка результатов; Е. Г. Горяйнова, Н. П. Макарова — сбор биологического материала; А. Н. Екимов, Е. Е. Атапина — лабораторный этап; Н. В. Долгушина, Д. Ю. Трофимов — утверждение публикации.

Соблюдение этических стандартов: исследование одобрено этическим комитетом ФГБУ «Национальный медицинский исследовательский центр акушерства, гинекологии и перинатологии имени В. И. Кулакова» (протокол № 10 от 28 октября 2021 г.). Пациенты подписали добровольное информированное согласие на участие в исследовании.

✉ **Для корреспонденции:** Ольга Игоревна Лисицына
ул. Академика Опарина, д. 4, г. Москва, 117997, Россия; o_yazykova@inbox.ru

Статья получена: 18.06.2023 **Статья принята к печати:** 09.08.2023 **Опубликована онлайн:** 30.08.2023

DOI: 10.24075/vrgmu.2023.034

Preimplantation genetic testing (PGT) was introduced into clinical practice in the late 1980s (it was previously referred to as preimplantation genetic diagnosis (PGD) or preimplantation genetic screening). The first PGD programs were aimed to avoid the X-linked inheritance. The range of detecting possible genetic disorders expanded significantly with subsequent development of the embryological and laboratory phase technologies, and the new goals of the methods were both preventing genetic disorders and improving the chances of giving birth to a healthy child in difficult categories of the assisted reproductive technology (ART) patients [1].

Currently, preimplantation genetic testing for aneuploidy (PGT-A) by next generation sequencing (NGS) with trophectoderm (TE) biopsy has become the most effective method that is more and more widely used with the development of the capabilities of embryological and genetic laboratories. Numerous studies demonstrate high sensitivity and specificity of this approach, however, the need for invasive interventions still represents one of its drawbacks [1, 2].

Embryonic mosaicism and concordance between the embryo's TE chromosomal pattern and its inner cell mass (ICM) are the other issues that attract the researchers' attention [3, 4]. Despite the fact that biopsy of several cells makes it possible to partially overcome the above shortage, it is impossible to completely eliminate the risk of rejection of the embryo, the transfer of which into the uterine cavity can result in giving birth to a healthy baby.

Noninvasive analysis of cell-free DNA in spent culture medium (SCM), in which the embryo has developed, is a new promising PGT-A technology. Certain conditions of the embryo culture and medium sample collection are required to obtain adequate results (to increase the DNA concentration and reduce possible contamination), however, no invasive intervention is needed [5–7]. A number of researchers believe that noninvasive preimplantation genetic testing for aneuploidy (niPGT-A) is a more helpful PGT-A method, particularly because of the fact that, according to the literature, cell-free DNA contained in SCM originates not only from the TE cells, but also from the ICM [8, 9]. Other authors, on the contrary, argue that it is unrepresentative, since the issue of the true origin of cell-free DNA contained in SCM is yet to be resolved [10, 11]. Anyway, this approach is extensively studied by the researchers and can probably be used in clinical practice.

The study was aimed to assess the efficiency of niPGT-A. For that we conducted re-analysis of blastocysts, that were considered to be aneuploid based on PGT-A with TE biopsy, by niPGT-A.

METHODS

Embryological phase was implemented at the B.V. Leonov Department of Assisted Technologies in Infertility Treatment; PGT-A and niPGT-A were performed in the Institute of Reproductive Genetics.

The study involved 11 embryos from seven couples. All blastocysts were considered to be aneuploid based on previous PGT-A with TE biopsy. The embryos were obtained in ART cycles with PGT-A by NGS in April–September 2020.

Embryo culture, TE biopsy and PGT–A

Fertilization of oocytes was performed by intracytoplasmic sperm injection (ICSI), after that the fertilized cells were transferred to the Continuous Single Culture Complete (CSCM) medium (IrvineScientific; USA). All embryo culture steps and morphological assessment of blastocysts were performed in accordance with the previously reported method [12]. On day 5–6 after fertilization, TE cell biopsy was performed in embryos, the quality of which was considered to be excellent or good according to morphological criteria. Borosilicate glass needles were used for biopsy. After biopsy the embryos were subjected to cryopreservation by vitrification in accordance with the instructions of the culture media manufacturer. The cells obtained were transported to the laboratory in the Eppendorf tubes containing the lysis buffer and stored at a temperature of –20 °C until subjected to further analysis. PGT-A was performed by next generation sequencing (NGS) using the Illumina platform (Illumina; USA) in accordance with the manufacturer's protocol. The results obtained were processed using the SeqVario software (DNA-Technology; Russia).

Embryo thawing and culture, spent culture medium collection

The donated embryos were thawed in the Kitazato media (Kitazato; Japan) in accordance with the manufacturer's protocol. After that blastocysts were individually cultured in 10 μL microdroplets of the CSCM medium for 9 h. A drop of the culture medium (1 sample) kept in the same culture conditions, but containing no embryo, was used as a negative control. All spent culture medium was collected in the Eppendorf tubes and transferred to the laboratory, where the tubes were stored at a temperature of –20 °C for 14 days until used for further analysis.

Noninvasive preimplantation genetic testing for aneuploidy

NiPGT-A was performed using the NICSInst kits (Yicon Genomics; China) in accordance with the manufacturer's instructions. The next generation sequencing was carried out in the NextSeq unit (Illumina; USA). The results obtained were analyzed using the original algorithms and software tools developed by the Center for PGT-A by SeqVario NGS.

Analysis of the results

Statistical analysis was performed using the Jamovi software package (freely distributed statistical software package). The results obtained were tested for concordance with the earlier reported PGT-A data. The full chromosome ploidy concordance rate (based on the PGT-A and niPGT-A data) was considered to be a primary endpoint of the study. The diagnostic concordance rate (euploid/aneuploid) of the embryos based on the PGT-A and niPGT-A data was a secondary endpoint. Binary categorical data were specified as absolute numbers N and the percentage of the total value for group P in the N format (P%). Binomial test was used to determine statistical significance of full and clinical concordance of the results. The significance level (p) was set at 0.05.

RESULTS

A total of 12 SCM samples were analyzed: 11 samples, in which the embryos were cultures, and one control sample. All samples of the study group successfully went through whole-genome amplification and analysis by NGS. No DNA was detected in the control sample. The PGT-A and niPGT-A results along with the concordance of these results for the studied embryos are provided in Table 1.

Table 1. Results of the studied embryos' PGT–A and niPGT–A

№	PGT-A results	niPGT-A results	Full concordance (+/–)	Diagnostic concordance (+/–)	Sex concordance
1	(11)x3 Sex – XX	(11)x3 Sex – XX	+	+	+
2	(20)x3, (21)x1 Sex – XX	(20)x3, (21)x1 Sex – XX	+	+	+
3	(17)x1, (22)x1 Sex – XY	(17)x1, (22)x1 Sex – XY	+	+	+
4	(8)x3, (21)x1	"heteroploid"			
5	(22)x3 Sex – XY	(22)x3 Sex – XY	+	+	+
6	(8)x1, (18)x3, (22)x1 Sex – XX	(8)x1, (18)x3, (22)x1 Sex – XX	+	+	+
7	(15)x3, (17)x3 Sex – XY	(15)x3, (17)x3 Sex – XY	+	+	+
8	(21)x3 Sex – XY	(15)x1,(21)x3 Sex – XY	–	+	+
9	(22)x3 Sex – XY	Del 5(p) Sex – XX	–	+	–
10	(21)x2,5 Sex – XY	N, XY	–	–	+
11	(16)x3 Sex – XY	(16)x3 Sex – XY	+	+	+

It is noteworthy that chaotic niPGT-A results not allowing the karyotype diagnosis were obtained in one case (9.1%) out of 11 (Fig. 1).

We failed to detect aneuploidy in an embryo based on the niPGT-A data in one case out of 10 (10%) due to high noise level, that is why the result was considered to be "euploid" (Fig. 2).

Full concordance of the results was obtained in seven cases out of 10 (70%) (Fig. 3). Concordance of the results based on sex chromosomes was determined in nine cases out of 10 (90%). Clinical concordance of the results was found in nine cases out of 10 (90%).

Comparison of full and clinical concordance between the PGT-A and niPGT-A results is provided in Table 2. Binomial test revealed no significant differences in the rate of full concordance between the PGT-A and niPGT-A results ($p = 0.344$), however, a significant result was obtained for diagnostic concordance between the PGT-A and niPGT-A data ($p = 0.021$).

When assessing the results in accordance with the intention to study, i.e. when assessing all 11 embryos that were included in the study in practical terms, the results obtained meant that in 81.8% of cases the clinical decision about the possibility of embryo transfer in the uterine cavity would remain unchanged. In 9.1% of cases, the clinical decision about the possibility of embryo transfer made based on the niPGT-A data only would be different (an euploid embryo was recommended for transfer). It was impossible to make a clinical decision about the possibility of embryo transfer in 9.1% of cases.

DISCUSSION

The study planned as a pilot project was limited by small sample size, availability of aneuploid embryos only (based on the PGT-A data), no analysis of the ICM chromosomal composition in the studied blastocysts. Nevertheless, the study results showed that cell-free DNA (cfDNA) was detected in SCM in 100% of cases, a high proportion of results appropriate for clinical interpretation (90.9%) was also reported.

In the majority of studies conducted so far the data of PGT-A with TE biopsy have been considered as reference data and compared with the niPGT-A results. The concordance rate of the results in these studies is 33.3–89.1% [5, 8, 13–17]. However, it should be noted that the above papers more often described the protocol for niPGT-A in a fresh cycle. Our study involved the protocol for thawed embryos, and the concordance rate was consistent with the data of the above studies (full concordance in 70% of cases, diagnostic concordance in 90% of cases).

In other studies the whole embryo was considered as a reference, and SCM was collected after the post-thawing embryo culture. The concordance rate of the niPGT-A and PGT-A results for the whole embryo in such studies varied between 32.2–89.9%. Xu et al. assessed SCM of the thawed D3 embryos after culturing to 5 days. Among 42 embryos, assessment of 66.7% showed full concordance of the results [18]. Yin et al. assessed SCM of 75 thawed D5–D6 blastocysts after culturing for 24 h. The diagnostic concordance rate of the results was 89.8%, while full concordance rate was 32.2% [19]. Huang et al. managed to get information about SCM of 48 D5–D6 embryos out of 52 after thawing and culturing for 24 h. Full concordance rate of the results was 85.4% [9]. Shitara et al. reported full concordance rate of 56.3% when assessing SCM after thawing and culturing 5D embryos for 24 h and 6D embryos for 3 h [20]. Xu et al. assessed 35 thawed 3D and 5D embryos. The minimum incubation time was 24 h.

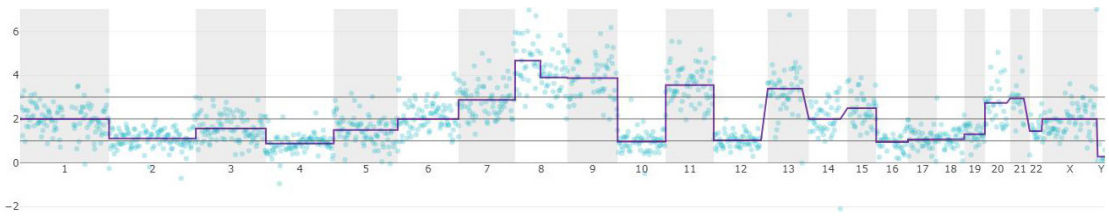

Fig. 1. An example of "heteroploid" niPGT-A result

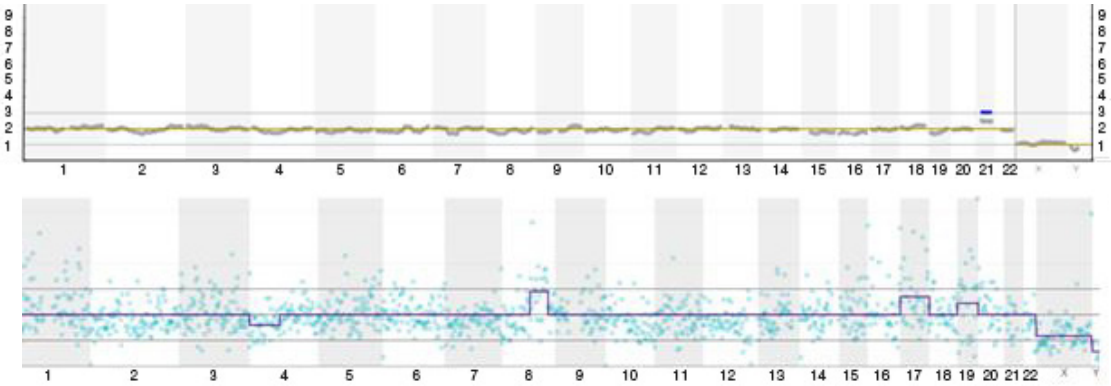

Fig. 2. Results of the embryo PGT–A and niPGT–A showing discordance between the PGT–A and niPGT–A data: the upper curve shows aneuploidy based on the PGT-A data, the lower curve shows euploidy based on the niPGT-A data.

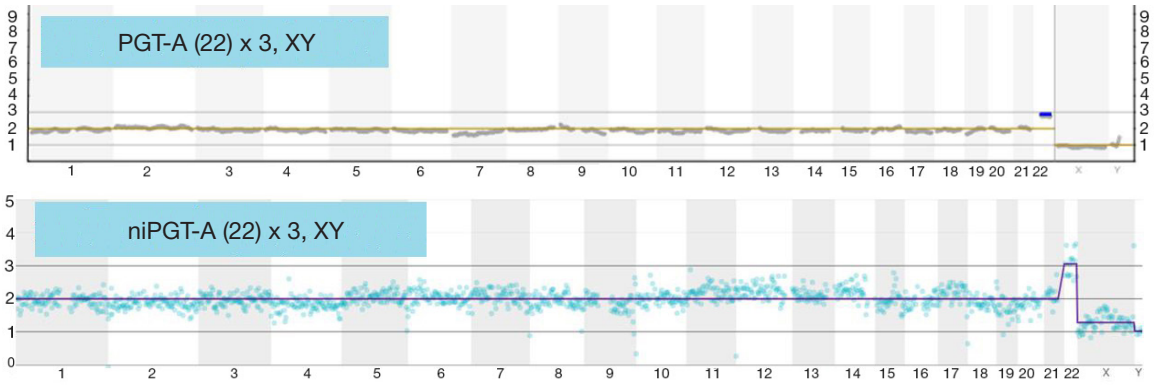

Fig. 3. An example of full concordance of the results based on the PGT-A and niPGT-A data

A total of 88.6% SCM samples successfully went through whole-genome amplification. Full concordance rate of the ICM niPGT-A and PGT-A results was 58.3% (14/24) [21].

It should be noted that the culture medium drop volume in these studies involving culturing thawed embryos varied between 10–30 μL, while the test sample volume was 3.5–25 μL. Incubation time was at least 24 h in the majority of cases. Our study demonstrated successful detection and analysis of cfDNA in SCM when culturing thawed blastocysts for 9 h in the 10 μL drops, thereby showing the possibility of obtaining adequate results after culturing thawed embryos within a shorter time period.

Of particular interest is the study of additional options to use niPGT-A in clinical practice. Noteworthy is the paper, the authors of which performed niPGT-A for mosaic embryos based on the results of previous PGT-A with TE biopsy. They thawed and re-cultured 41 mosaic embryos for 14–18 h, then performed PGT-A with TE biopsy of the whole embryo and SCM niPGT-A. The results of ICM assessment showed that 84.4% of embryos (35/41) had normal chromosome pattern. The niPGT-A data were concordant with the results of PGT-A based on the whole embryo biopsy in 74.4% of cases [22]. In the paper published the authors reported retrospective data on the transfer of mosaic embryos in 60 couples having no euploid embryos. Clinical pregnancy was later diagnosed in 30 patients. Thus, the researchers assumed that additional use of niPGT-A in such clinical cases had some possible benefits.

In our study we also obtained one “euploid” niPGT-A result for aneuploid embryo (karyotype (21) × 1.5) based on the data of previous PGT-A with TE biopsy. Furthermore, no abnormality of the 21st pair of chromosomes was detected (Fig. 2). Given the above, it is reasonable to collect SCM in the cycles with PGT-A in order to explore the possibility of additional niPGT-A use for more correct diagnosis in complicated or questionable cases (if necessary).

Also of interest is the paper published in 2022 focused on assessing the chances of the clinical use of niPGT-A in the thawed embryo transfer ART cycles [23]. The embryos were thawed and cultured in the 20 μL drops for 6 h in all cases until transferred into the uterine cavity. The authors retrospectively assessed the outcomes of thawed embryo transfer in 210 patients based on the niPGT-A results. The rates of clinical pregnancy, ongoing pregnancy and live birth were significantly higher in embryos that were considered to be euploid based on niPGT-A compared to aneuploid embryos (56.2% vs. 29.4%). However, no differences in the above reproductive outcomes between “euploid” and “chaotic” embryos were revealed based on the niPGT-A data (56.2% vs. 60.4%). The percentage of aneuploid embryos was significantly higher among the embryos that were considered to be of low or medium quality based on morphological features compared to the good quality embryos (46%, 34.6% and 21.5%, respectively; $p = 0.013$). The researchers noted a possible advantage of using a combination

Table 2. Comparison of the rates of full and clinical concordance between the PGT-A and niPGT-A results based on the binomial test data

Concordance	Yes/No	Share	Total	Proportion	*p*
Full	Yes	7	10	0.7	$p = 0.344$
	No	3		0.3	
Diagnostic	Yes	9	10	0.9	$p = 0.021$
	No	1		0.1	

approach (morphological assessment in combination with niPGT-A) to selection of the most promising embryo in terms of transfer into the uterine cavity. Furthermore, the authors proposed to rank the embryos in order of decreasing priority for embryo transfer in the following way: 1) good quality euploid embryos; 2) good quality "chaotic" embryos; 3) euploid embryos of medium quality based on morphological features; 4) "chaotic" embryos of medium quality based on morphological features.

It should be emphasized that other researchers also recommend to interpret chaotic niPGT-A results with caution, since such results are more likely to reflect the biomaterial storage conditions and DNA degradation processes than the embryos' chromosomal patterns [8, 24]. In our study we have also obtained chaotic niPGT-A results in one case (9.1%) (Fig. 1).

Thus, it should be noted that dealing with cfDNA and niPGT-A has some features that should be taken into account when interpreting the results and selecting the most promising embryos for transfer into the uterine cavity. However, the non-invasive nature of the method should be noted as its chief feature. Considering the fact that a number of scientific papers report the data indicative of possible adverse effects of TE biopsy on the course of pregnancy (hypertensive disorders, premature birth, placental disorders) and the health of newborns, it is the study of niPGT-A that seems to be the most relevant [25–27]. However, it should be noted that no such correlations have been revealed in a large number of other studies [28–30].

CONCLUSIONS

Noninvasive preimplantation genetic testing for aneuploidy is a promising new method to assess the embryo's chromosomal status that does not require biopsy. Further research is necessary to further develop and improve the method, as well as to determine the possibility and indications for the use of method in clinical practice.

References

1. Sciorio R, Tramontano L, Catt J. Preimplantation genetic diagnosis (PGD) and genetic testing for aneuploidy (PGT-A): status and future challenges. Gynecol. Endocrinol. 2020; 36 (1): 6–11.
2. Malysheva OV, Pendina AA, Efimova OA, Chiryaeva OG. Predymplantacionnoe geneticheskoe testirovanie. V knige: Kogan I. Yu., redaktor. Ehkstrakorporal'noe oplodotvorenie: prakticheskoe rukovodstvo dlya vrachej. M.: GEhOTAR-Media, 2021; s. 357–67. Russian.
3. Zhigalina DI, Skryabin NA, Kanbekova OR, Artyukhova VG, Svetlakov AV, Lebedev IN. Comparative cytogenetics of embryoblast, trophectoderm and blastocoele fluid of human blastocyst. Medical Genetics. 2018; 17 (2): 46–52. Russian.
4. Makarova NP, Ekimov AN, Kulakova EV, Drapkina YuS, Sysoeva AP, Krasnova NA, et. al. Characteristics of embryonic mosaicism in infertility treatment with assisted reproductive technologies. Obstetrics and gynecology. 2021; (7): 144–51. Russian.
5. Navarro-Sánchez L, García-Pascual C, Rubio C, Simón C. Non-invasive preimplantation genetic testing for aneuploidies: an update. Reprod. Biomed. Online. 2022; 44 (5): 817–28.
6. Brouillet S, Martinez G, Coutton C, Hamamah S. Is cell-free DNA in spent embryo culture medium an alternative to embryo biopsy for preimplantation genetic testing? A systematic review. Reprod. Biomed. Online. 2020; 40 (6): 779–6.
7. Lisitsyna OI, Makarova NP, Dolgushina NV. Evaluation of extracellular DNA as a method for non-invasive preimplantation genetic testing of embryos in infertility treatment programs using assisted reproductive technologies. Obstetrics and gynecology. 2022; (6): 13–19. Russian.
8. Rubio C, Navarro-Sánchez L, García-Pascual CM, Ocali O, Cimadomo D, Venier W, et al. Multicenter prospective study of concordance between embryonic cell-free DNA and trophectoderm biopsies from 1301 human blastocysts. Am J Obstet Gynecol. 2020; 223 (5): 751.e1–13.
9. Huang L, Bogale B, Tang Y, Lu S, Xie XS, Racowsky C. Noninvasive preimplantation genetic testing for aneuploidy in spent medium may be more reliable than trophectoderm biopsy. Proc Natl Acad Sci USA. 2019; 116 (28): 14105–12.
10. Rubio C, Racowsky C, Barad DH, Scott RT, Simon C. Noninvasive preimplantation genetic testing for aneuploidy in spent culture medium as a substitute for trophectoderm biopsy. Fertil Steril. 2021; 115 (4): 841–9.
11. Tomic M, Vrtacnik Bokal E, Stimpfel M. Non-invasive preimplantation genetic testing for aneuploidy and the mystery of genetic material: a review article. Int J Mol Sci. 2022; 23 (7): 3568.
12. Makarova NP, Lisitsyna OI, Nepsha OS, Krasnyi AM, Sadekova AA, Nezlina AL, et al. Mitichondrial DNA expression profile in embryo culture medium in assisted reproductive technology. Obstetrics and gynecology. 2022; (3): 89–96. Russian.
13. Chen L, Sun Q, Xu J, Fu H, Liu Y, Yao Y, et al. A Non-invasive Chromosome Screening Strategy for Prioritizing in vitro Fertilization Embryos for Implantation. Front Cell Dev Biol. 2021; 9: 708322.
14. Ho JR, Arrach N, Rhodes-Long K, Ahmady A, Ingles S, Chung K, et al. Pushing the limits of detection: investigation of cell-free DNA for aneuploidy screening in embryos. Fertil Steril. 2018; 110 (3): 467–475.e2.
15. Rubio C, Rienzi L, Navarro-Sánchez L, Cimadomo D, García-Pascual CM, Albricci L, et al. Embryonic cell-free DNA versus trophectoderm biopsy for aneuploidy testing: concordance rate and clinical implications. Fertil Steril. 2019; 112 (3): 510–19.
16. Vera-Rodriguez M, Diez-Juan A, Jimenez-Almazan J, Martinez S, Navarro R., Peinado V, et al. Origin and composition of cell-free DNA in spent medium from human embryo culture during preimplantation development. Hum Reprod. 2018; 33 (4): 745–56.
17. Yeung QSY, Zhang YX, Chung JPW, Lui WT, Kwok YKY, Gui B, et al. A prospective study of non-invasive preimplantation genetic testing for aneuploidies (NiPGT-A) using next-generation sequencing (NGS) on spent culture media (SCM). J Assist Reprod Genet. 2019; 36 (8): 1609–21.
18. Xu J, Fang R, Chen L, Chen D, Xiao JP, Yang W, et al. Noninvasive chromosome screening of human embryos by genome sequencing of embryo culture medium for in vitro fertilization. Proc Natl Acad Sci USA. 2016; 113 (42): 11907–12.
19. Yin B, Zhang H, Xie J, Wei Y, Zhang C, Meng L. Validation of preimplantation genetic tests for aneuploidy (PGT-A) with DNA from spent culture media (SCM): concordance assessment and implication. Reprod Biol Endocrinol. 2021; 19 (1): 41.
20. Shitara A, Takahashi K, Goto M, Takahashi H, Iwasawa T, Onodera Y, et al. Cell-free DNA in spent culture medium effectively reflects the chromosomal status of embryos following culturing beyond implantation compared to trophectoderm biopsy. PLoS One. 2021; 16 (2): e0246438.
21. Xu CL, Wei YQ, Tan QY, Huang Y, Wu JJ, Li CY, et al. Concordance of PGT for aneuploidies between blastocyst biopsies and spent blastocyst culture medium. Reprod Biomed. 2023; 46 (3): 483–90.
22. Li X, Hao Y, Chen D, Ji D, Zhu W, Zhu X, et al. Non-invasive preimplantation genetic testing for putative mosaic blastocysts: a pilot study. Hum Reprod. 2021; 36 (7): 2020–34.
23. Chen R, Tang N, Du H, Yao Y, Zou Y, Wang J, et al. Clinical application of noninvasive chromosomal screening for elective single-blastocyst transfer in frozen-thawed cycles. J Transl Med. 2022; 20 (1): 553.
24. Rubio C, Simón C. Noninvasive preimplantation genetic testing for aneuploidy: Is the glass half-empty or half-full? Fertil. Steril.

2021; 115 (6): 1426–7.
25. Kakourou G, Mamas T, Vrettou C, Traeger-Synodinos J. An Update on Non-invasive Approaches for Genetic Testing of the Preimplantation Embryo. Curr Genomics. 2022; 23 (5): 337–52.
26. Alteri A, Cermisoni GC, Pozzoni M, Gaeta G, Cavoretto PI, Viganò P. Obstetric, neonatal, and child health outcomes following embryo biopsy for preimplantation genetic testing. Hum Reprod Updat. 2023; 29 (3): 291–306.
27. Makhijani R, Bartels CB, Godiwala P, Bartolucci A, DiLuigi A, Nulsen J, et al. Impact of trophectoderm biopsy on obstetric and perinatal outcomes following frozen-thawed embryo transfer cycles. Hum Reprod. 2021; 36 (2): 340–8.
28. Awadalla MS, Park KE, Latack KR, McGinnis LK, Ahmady A, Paulson RJ. Influence of Trophectoderm Biopsy Prior to Frozen Blastocyst Transfer on Obstetrical Outcomes. Reprod Sci. 2021; 28 (12): 3459–65.
29. He H, Jing S, Lu CF, Tan YQ, Luo KL, Zhang SP, et al. Neonatal outcomes of live births after blastocyst biopsy in preimplantation genetic testing cycles: a follow-up of 1,721 children. Fertil Steril. 2019; 112 (2): 82–88.
30. Swanson K, Huang D, Kaing A, Blat C, Rosenstein MG, Mok-Lin E, et al. Is Preimplantation Genetic Testing Associated with Increased Risk of Abnormal Placentation After Frozen Embryo Transfer? Am J Perinatol. 2021; 38 (2): 105–10.

Литература

1. Sciorio R, Tramontano L, Catt J. Preimplantation genetic diagnosis (PGD) and genetic testing for aneuploidy (PGT-A): status and future challenges. Gynecol. Endocrinol. 2020; 36 (1): 6–11.
2. Малышева О. В., Пендина А. А., Ефимова О. А., Чиряева О. Г. Предымплантационное генетическое тестирование. В книге: Коган И. Ю., редактор. Экстракорпоральное оплодотворение: практическое руководство для врачей. М.: ГЭОТАР-Медиа, 2021; с. 357–67.
3. Жигалина Д. И., Скрябин Н. А., Канбекова О. Р., Артюхова В. Г., Светлаков А. В., Лебедев И. Н. Сравнительная цитогенетика эмбриобласта, трофэктодермы и внутриполостной жидкости бластоцисты человека. Медицинская генетика. 2018; 17 (2): 46–52.
4. Макарова Н. П., Екимов А. Н., Кулакова Е. В., Драпкина Ю. С., Сысоева А. П., Краснова Н. А. и др. Особенности мозаицизма у эмбрионов человека в программах лечения бесплодия методами вспомогательных репродуктивных технологий. Акушерство и гинекология. 2021; (7): 144–51.
5. Navarro-Sánchez L, García-Pascual C, Rubio C, Simón C. Non-invasive preimplantation genetic testing for aneuploidies: an update. Reprod. Biomed. Online. 2022; 44 (5): 817–28.
6. Brouillet S, Martinez G, Coutton C, Hamamah S. Is cell-free DNA in spent embryo culture medium an alternative to embryo biopsy for preimplantation genetic testing? A systematic review. Reprod. Biomed. Online. 2020; 40 (6): 779–6.
7. Лисицына О. И., Макарова Н. П., Долгушина Н. В. Оценка внеклеточной ДНК как метод неинвазивного преимплантационного генетического тестирования эмбрионов в программах лечения бесплодия методами вспомогательных репродуктивных технологий. Акушерство и гинекология. 2022; 6: 13–19.
8. Rubio C, Navarro-Sánchez L, García-Pascual CM, Ocali O, Cimadomo D, Venier W, et al. Multicenter prospective study of concordance between embryonic cell-free DNA and trophectoderm biopsies from 1301 human blastocysts. Am J Obstet Gynecol. 2020; 223 (5): 751.e1–13.
9. Huang L, Bogale B, Tang Y, Lu S, Xie XS, Racowsky C. Noninvasive preimplantation genetic testing for aneuploidy in spent medium may be more reliable than trophectoderm biopsy. Proc Natl Acad Sci USA. 2019; 116 (28): 14105–12.
10. Rubio C, Racowsky C, Barad DH, Scott RT, Simon C. Noninvasive preimplantation genetic testing for aneuploidy in spent culture medium as a substitute for trophectoderm biopsy. Fertil Steril. 2021; 115 (4): 841–9.
11. Tomic M, Vrtacnik Bokal E, Stimpfel M. Non-invasive preimplantation genetic testing for aneuploidy and the mystery of genetic material: a review article. Int J Mol Sci. 2022; 23 (7): 3568.
12. Макарова Н. П., Лисицына О. И., Непша О. С., Красный А. М., Садекова А. А., Незлина Е. А. и др. Особенности профиля экспрессии митохондриальной ДНК в среде культивирования эмбрионов в программах вспомогательных репродуктивных технологий. Акушерство и гинекология. 2022; (3): 89–96.
13. Chen L, Sun Q, Xu J, Fu H, Liu Y, Yao Y, et al. A Non-invasive Chromosome Screening Strategy for Prioritizing in vitro Fertilization Embryos for Implantation. Front Cell Dev Biol. 2021; 9: 708322.
14. Ho JR, Arrach N, Rhodes-Long K, Ahmady A, Ingles S, Chung K, et al. Pushing the limits of detection: investigation of cell-free DNA for aneuploidy screening in embryos. Fertil Steril. 2018; 110 (3): 467–475.e2.
15. Rubio C, Rienzi L, Navarro-Sánchez L, Cimadomo D, García-Pascual CM, Albricci L, et al. Embryonic cell-free DNA versus trophectoderm biopsy for aneuploidy testing: concordance rate and clinical implications. Fertil Steril. 2019; 112 (3): 510–19.
16. Vera-Rodriguez M, Diez-Juan A, Jimenez-Almazan J, Martinez S, Navarro R, Peinado V, et al. Origin and composition of cell-free DNA in spent medium from human embryo culture during preimplantation development. Hum Reprod. 2018; 33 (4): 745–56.
17. Yeung QSY, Zhang YX, Chung JPW, Lui WT, Kwok YKY, Gui B, et al. A prospective study of non-invasive preimplantation genetic testing for aneuploidies (NiPGT-A) using next-generation sequencing (NGS) on spent culture media (SCM). J Assist Reprod Genet. 2019; 36 (8): 1609–21.
18. Xu J, Fang R, Chen L, Chen D, Xiao JP, Yang W, et al. Noninvasive chromosome screening of human embryos by genome sequencing of embryo culture medium for in vitro fertilization. Proc Natl Acad Sci USA. 2016; 113 (42): 11907–12.
19. Yin B, Zhang H, Xie J, Wei Y, Zhang C, Meng L. Validation of preimplantation genetic tests for aneuploidy (PGT-A) with DNA from spent culture media (SCM): concordance assessment and implication. Reprod Biol Endocrinol. 2021; 19 (1): 41.
20. Shitara A, Takahashi K, Goto M, Takahashi H, Iwasawa T, Onodera Y, et al. Cell-free DNA in spent culture medium effectively reflects the chromosomal status of embryos following culturing beyond implantation compared to trophectoderm biopsy. PLoS One. 2021; 16 (2): e0246438.
21. Xu CL, Wei YQ, Tan QY, Huang Y, Wu JJ, Li CY, et al. Concordance of PGT for aneuploidies between blastocyst biopsies and spent blastocyst culture medium. Reprod Biomed. 2023; 46 (3): 483–90.
22. Li X, Hao Y, Chen D, Ji D, Zhu W, Zhu X, et al. Non-invasive preimplantation genetic testing for putative mosaic blastocysts: a pilot study. Hum Reprod. 2021; 36 (7): 2020–34.
23. Chen R, Tang N, Du H, Yao Y, Zou Y, Wang J, et al. Clinical application of noninvasive chromosomal screening for elective single-blastocyst transfer in frozen-thawed cycles. J Transl Med. 2022; 20 (1): 553.
24. Rubio C, Simón C. Noninvasive preimplantation genetic testing for aneuploidy: Is the glass half-empty or half-full? Fertil Steril. 2021; 115 (6): 1426–7.
25. Kakourou G, Mamas T, Vrettou C, Traeger-Synodinos J. An Update on Non-invasive Approaches for Genetic Testing of the Preimplantation Embryo. Curr Genomics. 2022; 23 (5): 337–52.
26. Alteri A, Cermisoni GC, Pozzoni M, Gaeta G, Cavoretto PI, Viganò P. Obstetric, neonatal, and child health outcomes following embryo biopsy for preimplantation genetic testing. Hum Reprod Updat. 2023; 29 (3): 291–306.
27. Makhijani R, Bartels CB, Godiwala P, Bartolucci A, DiLuigi A, Nulsen J, et al. Impact of trophectoderm biopsy on obstetric and perinatal outcomes following frozen-thawed embryo transfer cycles. Hum Reprod. 2021; 36 (2): 340–8.
28. Awadalla MS, Park KE, Latack KR, McGinnis LK, Ahmady A, Paulson RJ. Influence of Trophectoderm Biopsy Prior to Frozen Blastocyst Transfer on Obstetrical Outcomes. Reprod Sci. 2021; 28 (12): 3459–65.

29. He H, Jing S, Lu CF, Tan YQ, Luo KL, Zhang SP, et al. Neonatal outcomes of live births after blastocyst biopsy in preimplantation genetic testing cycles: a follow-up of 1,721 children. Fertil Steril. 2019; 112 (2): 82–88.

30. Swanson K, Huang D, Kaing A, Blat C, Rosenstein MG, Mok-Lin E, et al. Is Preimplantation Genetic Testing Associated with Increased Risk of Abnormal Placentation After Frozen Embryo Transfer? Am J Perinatol. 2021; 38 (2): 105–10.

TRYPTOPHAN CATABOLITES AND PREDICTED GUT FLORA ENZYME-ENCODING GENE

Shatova OP[1,2] ✉, Gaponov AM[3], Grigoryeva TV[4], Vasiliev IYu[4], Stoletova LS[5], Makarov VV[6], Yudin SM[6], Roumiantsev SA[1,3,7], Shestopalov AV[1,5,7]

[1] Pirogov Russian National Research Medical University, Moscow, Russia
[2] Peoples' Friendship University of Russia, Moscow, Russia
[3] Center for Digital and Translational Biomedicine, Center for Molecular Health, Moscow, Russia
[4] Kazan (Volga Region) Federal University, Kazan, Russia
[5] Dmitry Rogachev National Research Center of Pediatric Hematology, Oncology and Immunology, Moscow, Russia
[6] Centre for Strategic Planning and Management of Biomedical Health Risks of the Federal Medical Biological Agency, Moscow, Russia
[7] National Medical Research Center of Endocrinology, Moscow, Russia

The signaling role of tryptophan and its catabolites is well known. However, their effects on the potential microbiota metabolic activity is still poorly understood. The study was aimed to assess concordance between changes in the predicted gut microbiome enzyme-encoding gene abundance and the tryptophan catabolites. The study involved 109 healthy volunteers and 114 obese patients. Quantification of tryptophan catabolites in the feces was performed by HPLC. Bacterial DNA was extracted from fecal samples, and the 16S rRNA gene V3-V4 region was sequenced. Primary processing of the sequencing data was performed using the QIIME v.1.9.1 tool. The alleged metabolic role of microbiota members was explored via reconstruction of unobservable states using PICRUSt. The maximum number of significant correlations between the unobservable states and the predicted gut microbiome enzyme-encoding gene abundance in obese individuals was reported for indole-3-lactate. A significant correlation between indole-3-lactate and the abundance of genes encoding the enzymes involved in metabolism of fructose, amino sugars, nucleotides, amino acids, polyamines, and sulfosaccharides was revealed. It has been found that obese patients show a threefold increase in the indole-3-lactate-producing microbiota. It has been shown that in obese individuals microbial population of the intestine is represented by the totally different genera and species of microorganisms. It is concluded that indole-3-lactate has a significant effect on the predicted gut microbiome enzyme-encoding gene abundance in obese patients.

Keywords: gut microbiome, tryptophan metabolites, indole-3-lactate, indole, microbial tryptophan catabolites (MICT)

Funding: the study was performed as part of the Assignment № 0373100122119000041 for the project "Creation of a bank of blood serum and fecal samples from healthy donors and patients with obesity, metabolic syndrome, type 2 diabetes mellitus, impaired mucosal barrier of the gastrointestinal tract with the aim of identifying candidate species-specific mediators of the quorum sensing human microbiota systems modulating the endocrine and metabolic function of adipose tissue".

Author contribution: Shatova OP — primary data acquisition, statistical processing, manuscript writing and preparation of figures; Gaponov AM — manuscript writing; Grigoryeva TV — microbiome assessment; Vasiliev IYu — microbiome assessment and statistical data processing; Stoletova LS — data analysis; Makarov VV, Yudin SM — writing parts of the manuscript; Roumiantsev SA — study concept, manuscript editing; Shestopalov AV — study concept, data analysis, manuscript writing and editing.

Compliance with ethical standards: the study was approved by the Ethics Committee of the Pirogov Russian National Research Medical University (protocol No. 186 of 26 June 2019). All patients submitted the informed consent to the use of biomaterial for scientific purposes.

✉ **Correspondence should be addressed:** Olga P. Shatova
Ostrovityanova, 1, Moscow, 117997, Russia; shatova.op@gmail.com

Received: 21.06.2023 **Accepted:** 20.07.2023 **Published online:** 07.08.2023

DOI: 10.24075/brsmu.2023.027

КАТАБОЛИТЫ ТРИПТОФАНА И ГЕНЫ ФЕРМЕНТОВ МИКРОБИОМА КИШЕЧНИКА

О. П. Шатова[1,2] ✉, А. М. Гапонов[3], Т. В. Григорьева[4], И. Ю. Васильев[4], Л. С. Столетова[5], В. В. Макаров[6], С. М. Юдин[6], С. А. Румянцев[1,3,7], А. В. Шестопалов[1,5,7]

[1] Российский национальный исследовательский медицинский университет имени Н. И. Пирогова, Москва, Россия
[2] Российский университет дружбы народов имени Патриса Лумумбы, Москва, Россия
[3] Центр цифровой и трансляционной биомедицины ООО «Центр молекулярного здоровья», Москва
[4] Институт фундаментальной медицины и биологии Казанского (Приволжского) федерального университета, Казань, Россия
[5] Национальный медицинский исследовательский центр Детской гематологии, онкологии и иммунологии имени Дмитрия Рогачева, Москва, Россия
[6] Центр стратегического планирования и управления медико-биологическими рисками здоровью Федерального медико-биологического агентства, Москва, Россия
[7] Национальный медицинский исследовательский центр эндокринологии, Москва, Россия

Общеизвестна сигнальная роль триптофана и его катаболитов. Однако до сих пор не изучено их влияние на потенциальную метаболическую активность микробиоты. Целью исследования было провести анализ согласованности изменений прогностической представленности генов ферментов микробиома кишечника и катаболитов триптофана. В исследовании приняли участие 109 здоровых добровольцев и 114 больных с ожирением. Количественный анализ катаболитов обмена триптофана в кале проводили методом ВЭЖХ. Из образцов фекалий выделяли бактериальную ДНК и проводили секвенирование (V3-V4 региона) гена 16S рРНК. Первичную обработку данных секвенирования осуществляли в программе «QIIME v.1.9.1». Анализ предположительной метаболической роли участников микробиоты проводили путем реконструкции ненаблюдаемых состояний при помощи PICRUSt. Максимальное количество статистически значимых взаимосвязей между катаболитами триптофана и прогностической представленностью генов ферментов микробиома у лиц с ожирением было установлено для индол-3-лактата. Показана статистически значимая взаимосвязь индол-3-лактата и представленности генов ферментов обмена фруктозы, аминосахаров, нуклеотидов, аминокислот, полиаминов и сульфосахаров. Установлено, что у больных ожирением происходит трехкратное увеличение индол-3-лактат-продуцирующей микробиоты. Показано, что микробиотическая популяция кишечника представлена совершенно другими родами и видами микроорганизмов у лиц, имеющих ожирение. Сделан вывод, что при ожирении индол-3-лактат значимо влияет на прогностическую представленность генов ферментов микробиома кишечника.

Ключевые слова: микробиом кишечника, метаболиты обмена триптофана, индол-3-лактат, индол, микробные катаболиты триптофана (MICT).

Финансирование: работа выполнена в рамках договора № 0373100122119000041 по проекту «Создание банка биообразцов сыворотки крови и фекалий от здоровых доноров и пациентов с ожирением, метаболическим синдромом, сахарным диабетом II типа, нарушением мукозального барьера желудочно-кишечного тракта с целью выявления кандидатных видонеспецифических медиаторов систем quorum sensing микробиоты человека, модулирующих эндокринную и метаболическую функцию жировой ткани».

Вклад авторов: О. П. Шатова — сбор первичного материала, статистическая обработка, подготовка текста статьи и рисунков; А. М. Гапонов — подготовка текста статьи; Т. В. Григорьева — исследование микробиома; И. Ю. Васильев — исследование микробиома и статистическая обработка данных; Л. С. Столетова — анализ материала; В. В. Макаров, С. М. Юдин — написание разделов статьи; С. А. Румянцев — идея исследования, редактирование статьи; А. В. Шестопалов — идея исследования, анализ материала, написание и редактирование статьи.

Соблюдение этических стандартов: исследование одобрено этическим комитетом РНИМУ имени Н. И. Пирогова (протокол № 186 от 26 июня 2019 г.). Все пациенты подписали добровольное информированное согласие на использование биологического материала в научных целях.

✉ **Для корреспонденции:** Ольга Петровна Шатова
ул. Островитянова, д. 1, г. Москва, Россия; 117997; shatova.op@gmail.com

Статья получена: 21.06.2023 **Статья принята к печати:** 20.07.2023 **Опубликована онлайн:** 07.08.2023

DOI: 10.24075/vrgmu.2023.027

In the last decade, the research aimed at understanding hologenome has reached a new level due to advances in high-throughput next generation sequencing (NGS) allowing one to accurately identify microbial species and related metabolic pathways. A hologenome is a sum of the host genes and symbiotic/mutualistic microbial genes [1]. There are numerous reports of the studies focused on assessing the taxonomic gut microbiota composition associated with various physiological states and disorders. Many researchers pay close attention to studying the role of dysbiosis in obesity and diabetes mellitus [2], non-specific ulcerative colitis [3] and other gastrointestinal tract disorders [4–6]. There is no doubt, that gut microbiota is a major player in metabolic disorders and the so-called "metabolic inflammation" [7]. It is well known that metabolites produced by microbiota act as signaling molecules [8]. It has been found that indole-3-ethanol, indole-3-pyruvate, and indole-3-aldehyde regulate the apical junctional complex integrity and ensure normal intestinal barrier permeability via the aryl hydrocarbon receptors (AhR) of enterocytes [9, 10]. Thus, microbial tryptophan catabolites (MICT) modulate both intestinal barrier function and resistance to intestinal pathogens [11]. However, there is still little data on regulation of gut microbiota enzymes by tryptophan derivatives. That is why one of the objectives of our study was to explore the relationship between the predicted gut microbiome enzyme-encoding gene abundance and the levels of tryptophan catabolites.

Many researchers analyze the features of gut microbiota taxonomic composition in healthy individuals and individuals with various disorders [12, 13], such as obesity, or assess fecal levels of tryptophan catabolites that are more likely to be produced by microbiota only [8]. However, all this has yet to be proven, since microbiota composition in obese patients is still poorly understood [12]. Some authors believe that indole-3-acetate is the entirely microbiota-derived metabolite [13], however, an enzyme is expressed in humans that is potentially capable of producing this metabolite. This enzyme, aldehyde dehydrogenase (EC: 1.2.1.3), converts indole-3-acetaldehyde to indole-3-acetate [14]. That is why the second objective of our study was to estimate concordance between changes in the levels of tryptophan metabolites and enzymes that could potentially be involved in tryptophan metabolite production. Today, it is believed that MICT include indole, tryptamine, skatole, indole-3-pyruvate, indole-3-lactate, indole-3-acrylate, indole-3-propionate, indole-3-acetamide, indole-3-ethanol, indole-3-aldehyde, and indole-3-acetaldehyde [8]. It should be noted that among all MICT the highest intestinal levels have been reported for indole, which represents both quorum sensing (QS) microbiota molecule and signaling molecule in the human body [15]. It is generally accepted that the main MICT also include indole-3-acetate and indole-3-lactate [16]. Tryptophan acquired from food can be metabolized into indole-3-acetate by gut microbiota via the indole-3-acetamide pathway catalyzed by tryptophan monooxygenase (EC: 1.13.12.3) and indole-3-acetamide hydrolase (EC: 3.5.1.4). Indole-3-lactate is derived from indole-3-pyruvate as a result of the reduction reaction catalyzed by aromatic 2-oxoacid reductase (EC: 1.1.1.110), while indole-3-pyruvate is formed due to three enzymes: tryptophan transaminase (EC: 2.6.1.27), L-tryptophan-pyruvate aminotransferase (EC: 2.6.1.99), and L-amino acid oxidase (EC: 1.4.2.2). Indole-3-lactate can be further converted to indole-3-acrylate by 3-(aryl)acryloyl-CoA:(R)-3-(aryl)lactate CoA-transferase (EC: 2.8.3.17) [17]. It should be noted that metabolite derived from indole-3-lactate (indole-3-acrylate) activates indole pyruvate decarboxylase (EC: 4.1.1.74) involved in indole-3-pyruvate conversion via the indole-3-acetate pathway [17] (Fig. 1).

The studies focused on exploring obesity have revealed elevated blood levels of indole-3-acetate, indole-3-lactate, and indole in affected individuals [8, 18]. At the same time many authors report impoverishment of microbiota taxonomic composition in obese patients [19, 20]. The role of indole-3-acetate and indole-3-propionate in suppression of inflammation contributing to adipose tissue remodeling and insulin resistance has been proven [21]. There is no doubt that correction of the diet results in significant changes of the gut microbiota taxonomic composition. However, it is difficult to say whether these changes will be persistent and how long it will take to return to the dysbiosis phenotype typical for obesity. These indicators will often be specific for each particular patient [22].

Thus, this leaves open the question of the composition of certain tryptophan metabolite producers, homeostatic stability of this composition in healthy and obese individuals, as well as the place these metabolites occupy in the overall metabolic profile of the gut microbial community and their impact on the gut microbiome enzymatic landscape. The "enzymatic landscape" (abundance of enzyme-encoding genes) is the presence and content (in arbitrary units) of genes encoding various enzymes, i.e. the possible presence of enzymes corresponding to the abundance of microbial DNAs potentially capable of expressing certain enzymes.

The study was aimed to assess the levels of tryptophan metabolites in fecal extracts and their correlation with the predicted gut microbiome enzyme-encoding gene abundance in obese patients.

METHODS

Trial arm

A total of 223 patients with an average age of 39.9 ± 4.2 years were surveyed. Two clinical groups were formed. Group 1 (n = 109): control group of healthy volunteers with no obesity and/or metabolic syndrome, average body mass index (BMI) of 19.8 [18.5–22.0] kg/m^2 and waist circumference (WC) of 73.0 [68.0–74.5] cm. Inclusion criteria for group 1: age 30–50 years, BMI < 25 kg/m^2, WC < 80 cm for females and < 94 cm for males; taking no antibiotics, prebiotics or probiotics within three months before enrollment; submitted informed consent to study participation. Exclusion criteria for group 1: pregnancy and lactation, decompensated chronic disease, cancer, history of congenital tryptophan metabolism disorder, acute viral respiratory infection; any gastrointestinal tract disorder (including non-specific ulcerative colitis, Crohn's disease, irritable bowel syndrome); depression; alcoholism, and no obesity and/or metabolic syndrome. Group 2 (n = 114): study group with obesity and/or metabolic syndrome, average BMI of 33.0 [31.0–36.0] kg/m^2 and WC of 90.0 [96.0–105.0] cm. Inclusion criteria for group 2: age 30–50 years, BMI 30–34.9 kg/m^2, WC > 80 cm for females and > 94 cm for males; taking no antibiotics, prebiotics or probiotics within three months before enrollment; submitted informed consent to study participation. Exclusion criteria for group 2: pregnancy and lactation, decompensated chronic disease, cancer, history of congenital tryptophan metabolism disorder, acute viral respiratory infection; any gastrointestinal tract disorder (including non-specific ulcerative colitis, Crohn's disease, irritable bowel syndrome); depression; alcoholism. Patients of the study groups did not follow any diet. A stool (feces) sample was obtained from each study participant. Individuals living in the same area (Rostov

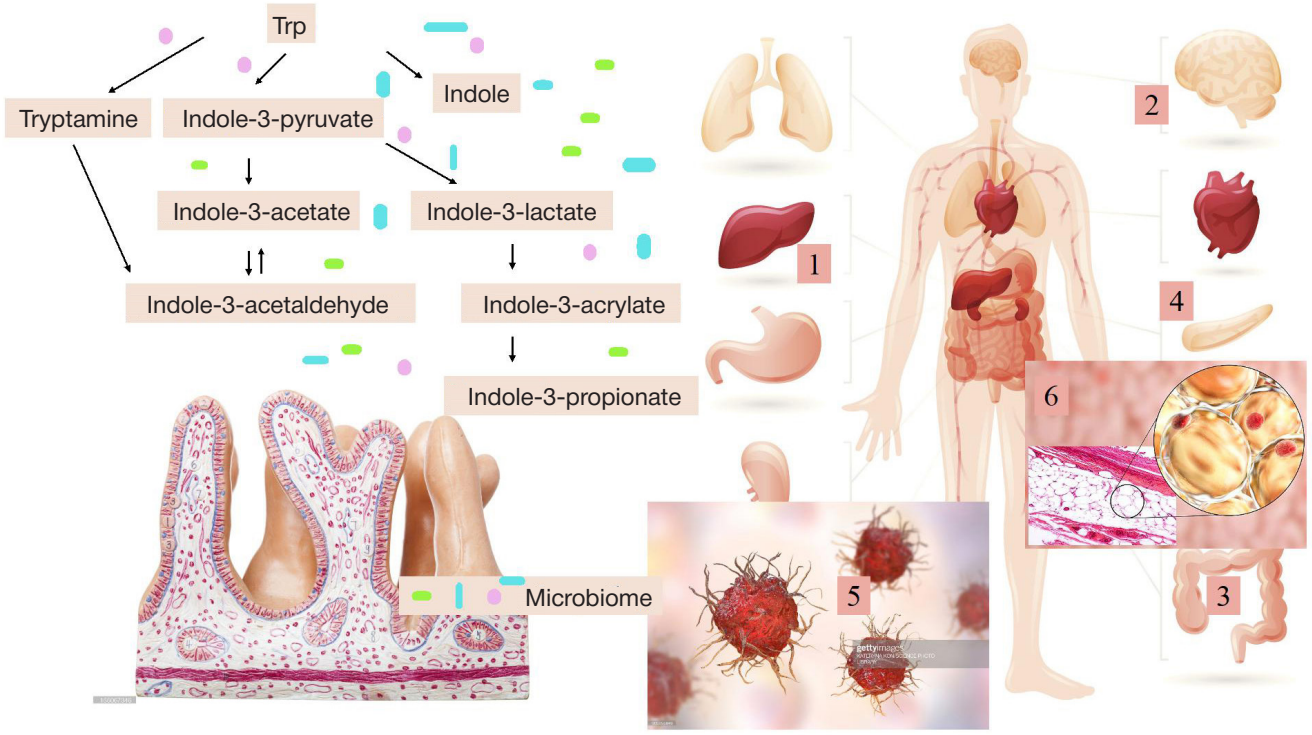

Fig. 1. MICT formation and role in human organism: indole-3-acetate and indole-3-propionate regulate hepatic lipogenesis and prevent fatty degeneration of the liver (**1**); indole-3-propionate has a neuroprotective effect; indole-3-lactate is responsible for axonal growth and cognitive ability (**2**); indole-3-propionate regulates permeability of the mucosal barrier, it increases the synthesis of tight junction proteins, reduces production of tumor necrosis factor-α (TNF-α) and possesses antioxidant activity (**3**); in the pancreas, MICT suppress autoimmune inflammation and prevent type 1 diabetes mellitus; furthermore, it has been shown that indole-3-acetate suppresses tumor cell proliferation in the pancreas (**4**); indole-3-acetate reduces production of pro-inflammatory cytokines by macrophages; indole-3-acetaldehyde increases production of interleukin 22 (IL-22) in immune cells, including intestinal cells (**5**); in adipose tissue, indole-3-acetate and indole-3-propionate have an anti-inflammatory effect, thereby preventing insulin resistance (**6**)

Region and the city of Rostov-on-Don) in summer and autumn were enrolled in order to minimize the effects of climate, diet and ethnic factors on the gut microbiome.

Chromatographic analysis

Stool samples were obtained from all study participants in accordance with the study protocol. The samples were transported and stored in accordance with the cold chain protocol at a temperature not exceeding –40 °C.

The tryptophan metabolites were quantified in the feces by high-performance liquid chromatography-mass spectrometry (HPLC-MS/MS). Analysis was performed using the Agilent 1290 LC system (Agilent Inc.; USA) equipped with autosampler, thermostatted column compartment, and degasser. During fecal sample preparation, the sample was lyophilized to dryness, then a portion with the weight of about 5 mg was subjected to extraction in 50% aqueous methanol solution supplemented with internal standard and ascorbic acid. After centrifugation the sample was analyzed by HPLC-MS/MS.

Chromatographic separation was performed using the Discovery PFP HS F5 column (2.1 × 150 mm; 3 µm, Supelco Inc, St. Louis, Missouri, USA). Detection was carried out in the Agilent 6470 triple quadrupole mass spectrometer (Agilent Inc.; USA) coupled to MRM and electrospray ionisation. The parent and daughter ions that were characteristic of each compound in the MRM mode, as well as ionization and dissociation parameters were optimized using standards for the studied metabolites. The signal received was processed using the Masshunter software (Agilent Inc.; USA).

The column temperature and flow rate were set at 40 °C and 0.4 mL/min, respectively. The mobile phases consisted of 0.1% aqueous formic acid solution (phase A) and acetonitrile (phase B). The gradient program was as follows: 0 min — 1% B; 4 min — 10% B; 9 min — 90% B; 10 min — 90% B; 10.1 — 1% B; 12 min — 1% B. The positive ion electrospray ionization was used. The main MS parameters were as following: gas temperature — 300 °C; gas consumption — 8 L/min; nebulizer gas — 20 pounds per square inch; inert gas heater — 300; inert gas consumption — 10 L/min; capillary voltage — 3500 kV.

Metabolite concentrations were calculated by the internal standard (2-hydroxynicotinic acid) method. The standards for analytes were prepared using artificial matrix containing bovine serum albumin and sodium chloride. The studied metabolites were added to the matrix, and preparation was performed in accordance with the assessment method.

The method was validated based on selectivity, linearity, accuracy, reproducibility, matrix effect, and analyte stability. Validation was performed in accordance with the FDA guidelines on validation of bioanalytical techniques. Fecal samples were lyophilized to dryness, them the sample with the weight of about 5 mg was subjected to extraction in 50% aqueous methanol solution supplemented with internal standard and ascorbic acid. Sample preparation was performed as follows: 100 µL of methanolic fecal extracts (calibrators or QC) were mixed with the internal standard solution, 10 µL of the source solution, 10 µg/mL of the 2-hydroxynicotinic acid solution, and 400 µL of acetonitrile. Then the mixture was shaken, centrifuged for 10 min at 13,000 rpm, and evaporated to dryness in the vacuum centrifugal evaporator at 37 °C. After that the residue was retrieved with 100 µL of 0.02% ascorbic acid solution in 10% methanol, centrifuged, and transferred to the tube for LC-MS. The extract (5 µL) was introduced into the liquid chromatography system for further analysis by HPLC-MS/MS.

Table 1. Fecal levels of tryptophan metabolites in adults, nmol/g

Metabolite	Healthy adults (n = 109)	Obese adults (n = 114)
Indole	464 ± 462	389 ± 361
Indole-3-lactate	454 ± 18.6	101 ± 218*
Indole-3-acetate	21.9 ± 40.6	21.9 ± 42.9
Indole-3-propionate	21.51 ± 29.9	8.28 ± 11.3*
Kynurenic acid	7.68 ± 9.15	5.59 ± 9.71
Indole-3-carboxaldehyde	5.14 ± 4.31	2.60 ± 2.24*
Quinolinic acid	5.13 ± 4.71	2.23 ± 2.26*
Tryptamine	2.59 ± 7.42	2.11 ± 8.52
Xanthurenic acid	2.36 ± 4.18	1.06 ± 2.22*
3-hydroxyindole-acetoacetic acid	2.35 ± 4.28	1.45 ± 2.13*
Kynurenine	0.651 ± 0.961	0.551 ± 0.571
Anthranilic acid	0.321 ± 0.231	0.191 ± 0.261*
Indole-3-acrylate	0.161 ± 0.211	0.051 ± 0.081*

Note: * — the difference is significant at $p < 0.05$.

16S rRNA gene V3-V4 region sequencing

Bacterial DNA was extracted from fecal samples using the QIAamp Fast DNA Stool Mini Kit (QIAGEN GmbH; Germany). The resulting microbial DNA was amplified using primers specific for the 16S rRNA gene V3-V4 variable region. After the AMPure XP (Beckman Coulter; USA) paramagnetic beads purification of the mixture, the PCR products were indexed using the Nextera XT Index Kit (Illumina, Inc.; USA). The mixture was purified using paramagnetic beads again, and the resulting libraries were sequenced using the MiSeq plarform (Illumina, Inc.; USA) in accordance with the manufacturer's protocol.

Technical processing of sequencing results

Quality control of the resulting reads was performed using the fastQC tool in accordance with the following criteria: 1) base quality distribution — at least 90% with the quality > 25; 2) base length distribution — at least 90% of reads reach a length of 300 nucleotides; 3) maximum percentage of undefined bases — 1.

The gene sequences obtained were assessed using the QIIME v.1.9.1 tool and the Greengenes v.13.8 reference database with the 97% similarity threshold. The data on the bacterial taxa abundance in the overall pool of reads were obtained as proportions (0–1) calculated based on the number of mapped reads per taxon. The total number of observed operational taxonomic units (Observed OTUs) was calculated in order to characterize the gut microbiome alpha diversity. An operational taxonomic unit is a surrogate taxonomic level, the result of bacterial 16s RNA gene sequencing data clustering.

Bioinformatics analysis

Primary processing of the sequencing results and compilation of the list of OTUs was performed in QIIME v.1.9.1 [23]. The second phase involved analysis of the microbiota members' probable metabolic role by reconstructing unobservable states with PICRUSt [24].

The predicted enzyme-encoding gene abundance was assessed using bioinformatics analysis involving matching of metagenomic sequencing data with the KEGG Enzyme database using PICRUSt [24]. The resulting predicted enzyme-encoding gene abundance data specified in relative units could be compared between samples and cohorts of the studied groups within a project.

Statistical analysis of the study results was performed using the STATISTICA 12.0 software package (StatSoft Inc; USA). All the data sets obtained were tested for normality using the Shapiro–Wilk test. The distribution was normal, and the data were presented as mean and standard deviation.

Spearman's rank correlation coefficients are provided in tables. The correlation analysis involved assessment of the correlation coefficient significance. The differences were considered significant at $p < 0.05$.

RESULTS

Fecal levels of tryptophan catabolites

Assessment of the tryptophan catabolite fecal levels has shown that indole and indole-3-lactate are dominant MICT (Table 1).

The fecal levels of eight tryptophan metabolites were significantly lower in adult obese patients than in healthy donors: indole-3-lactate, quinolinic acid, 3-hydroxyindole-acetoacetic acid, anthranilic acid, xanthurenic acid, indole-3-carboxaldehyde, indole-3-acrylate, and indole-3-propionate. It should be noted that obese patients have dramatically reduced fecal levels of indole-3-lactate: the average level of this tryptophan metabolite is 78% lower compared to normal (Table 1).

Correlation of the fecal tryptophan catabolite levels with the predicted abundance of the gut microbiome enzyme-encoding genes

We used PICRUSt analysis of the microbiome taxonomic diversity to quantify the predicted abundance of various enzyme-encoding genes based on the abundance of DNA of various intestinal microorganisms in healthy and obese individuals, then we performed the correlation analysis of the predicted gut microbiome enzyme abundance and the fecal levels of tryptophan catabolites.

It was found that obese individuals had a stronger link between the abundance of the gut microbiota enzyme-encoding genes and the tryptophan metabolites. Thus, we have found 251 significant correlations (significance level = 3, $p \leq 0.001$) in healthy subjects, while among obese individuals there are 479 significant correlations with the same significance level (Fig. 2).

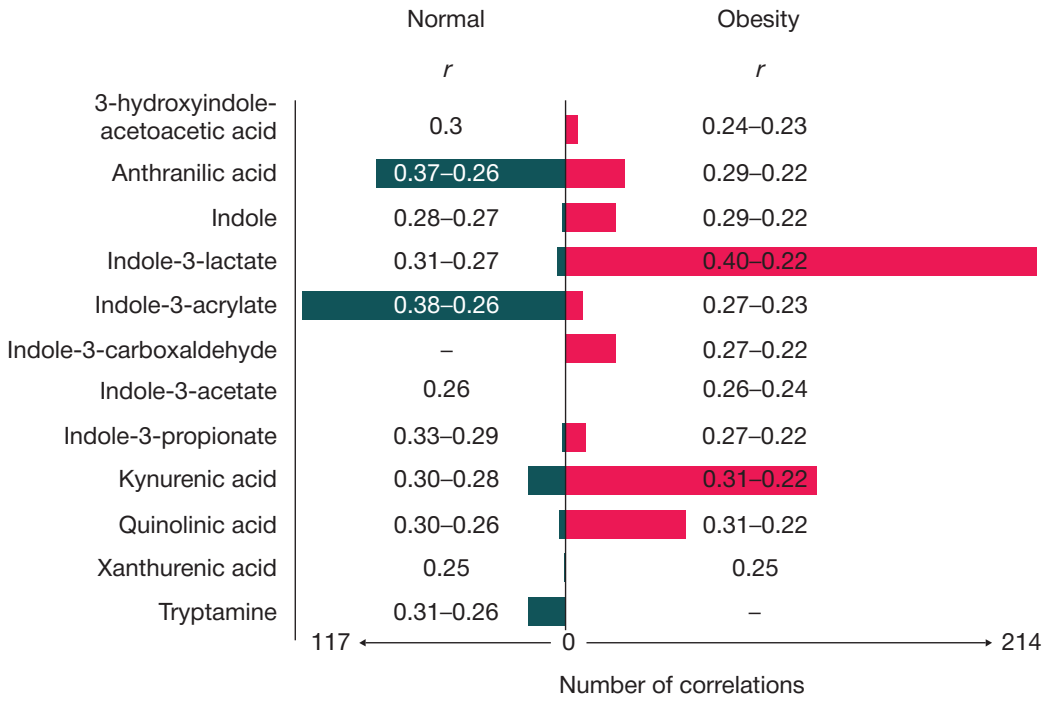

Fig. 2. Quantitative analysis of the correlations "tryptophan catabolite — predicted gut microbiome enzyme-encoding gene abundance". In healthy individuals, anthranilic acid and indole-3-acrylate are the key catabolites that are closely linked to the predicted gut microbiome enzyme-encoding gene abundance. In obese individuals, indole, indole-3-lactate, kynurenic and quinolinic acids are correlated to the predicted gut microbiome enzyme-encoding gene abundance

It was found that there were no significant changes in the fecal indole levels of obese individuals (Table 1), while the predicted gut microbiome enzyme-encoding gene abundance correlated to the indole levels increased tenfold (Fig. 2).

A significant decrease in fecal levels associated with obesity was found for the second dominant intestinal tryptophan catabolite, indole-3-lactate (Table 1). However, the number of significant correlation pairs for indole-3-lactate and the predicted abundance of genes encoding various gut microbiome enzymes increased from five pairs we had found in healthy individuals to 214 pairs in obese individuals (Fig. 2).

In was found that in obese patients the potential key signaling tryptophan metabolites correlated to the predicted gut microbiome enzyme-encoding gene abundance were as follows: indole, indole-3-lactate, kynurenic and quinolinic acids. In non-obese individuals, these key signaling molecules included indole-3-acrylate and anthranilic acid (Fig. 2).

Further analysis revealed enzymes, the predicted abundance of genes encoding which was more strongly correlated (Spearman's rank correlation coefficient 0.407–0.340) to the fecal levels of indole-3-lactate (Table 2).

Among microbiome enzymes, the predicted abundance of genes which is correlated to the intestinal levels of indole-3-lactate in obese patients, the enzymes involved in metabolism of carbohydrates, amino acids, polyamines, nucleotides and sulfosaccharides were identified (Table 2). It was also found that fecal levels of indole-3-lactate correlated with the predicted abundance of genes encoding enzymes involved in metabolism of amino acids: arginine, glutamate and glutamine.

Correlation of the gut microorganism taxonomic abundance with the fecal levels of indole-3-lactate

Analysis of the bacterial and archaeal abundance at the family (f), genus (g) and species (s) levels in healthy subjects showed that there was a significant correlation between the fecal levels of indole-3-lactate and the abundance of the following families of microorganisms: *Ruminococcaceae*, *Lachnospiraceae*, *Akkermansiaceae*, *Barnesiellaceae* (Appendix 1).

At the same time it was found that in obese patients other members of gut microbiota, such as Enterobacteriaceae and Pseudomonadaceae, were significantly correlated to fecal levels of indole-3-lactate (Appendix 2). It is important to note that in obese individuals microorganisms, the content of which was correlated to intestinal levels of indole-3-lactate, were different from normal. Whereas in healthy individuals a total of 54 significant correlations between various microbial species in the intestine and indole-3-lactate were found, there were three times more significant correlations in obese patients (154 pairs).

Our analysis revealed no significant correlations between indole-3-lactate and the abundance of Klebsiella, Pseudomonas, Escherichia-Shigella in the intestine of individuals with normal weight. It is obvious that in obese individuals indole-3-lactate is produced mainly by the family Enterobacteriaceae. It is important to note that, according to the literature, obesity results in the gut microbiota taxonomic composition impoverishment [19]. However, our study has shown that obesity instead results in enrichment of taxonomic abundance of the gut microbiota being a potential producer of indole-3-lactate.

DISCUSSION

It is interesting to note, that obese individuals show a decrease in the fecal levels of tryptophan catabolites, and the maximum decrease has been determined for indole-3-lactate. Meanwhile, this specific metabolite is a dominant in both healthy and obese individuals. However, we have found that indole-3-lactate plays a key role as a potential regulator of the predicted gut microbiome enzyme-encoding gene abundance only in obese individuals. We have identified 214 various enzymes, the predicted abundance of which is potentially dependent on indole-3-lactate.

We believe that the predicted abundances we have determined for the enzymes involved in polyamine metabolism

Table 2. Correlation "fecal levels of indole-3-lactate – predicted gut microbiome enzyme-encoding gene abundance" in obese patients

Enzymes	Spearman's rank correlation coefficient	Metabolic pathways
Allosakinase EC: 2.7.1.55	0.407	Fructose and monose metabolism
UDP-4-amino-4-deoxy-L-arabinose formyltransferase EC: 2.1.2.13	0.372	Amino sugar and nucleotide sugar metabolism
UDP-glucuronic acid dehydrogenase EC: 1.1.1.305	0.372	Amino sugar and nucleotide sugar metabolism
UDP-4-amino-4-deoxy-L-arabinose aminotransferase EC: 2.6.1.87	0.371	Amino sugar and nucleotide sugar metabolism
Sulfoquinovose isomerase EC: 5.3.1.31	0.370	Sulfoquinovose breakdown (sulfoglycolysis)
Oxalyl-CoA decarboxylase EC: 4.1.1.8	0.363	Glyoxylate and dicarboxylate metabolism
Glucose-1-phosphatase EC: 3.1.3.10	0.358	Gluconeogenesis
1,4-dihydroxy-2-naphthoyl-CoA hydrolase EC: 3.1.2.28	0.351	Vitamin K metabolism. Biosynthesis of secondary metabolites
N-hydroxyarylamine O-acetyltransferase EC: 2.3.1.118	0.351	N-acetylation of arylamines and acetylation of aryl hydroxamates
Dodecenoyl-CoA isomerase EC: 5.3.3.8	0.350	Lipid metabolism
Sulfofructose kinase EC: 2.7.1.184	0.349	Sulfoquinovose breakdown (sulfoglycolysis)
Formate dehydrogenase EC: 1.1.5.6	0.347	Sulfoquinovose breakdown (sulfoglycolysis)
Succinylornithine transaminase EC: 2.6.1.81	0.347	Arginine and polyamine metabolism
Enterobacter ribonuclease EC: 3.1.27.6	0.346	Two-step endonucleolytic cleavage producing 3'-nucleotides
Sulfofructosephosphate aldolase EC: 4.1.2.57	0.346	Sulfoquinovose breakdown (sulfoglycolysis)
Ferric-chelate reductase (NADPH) EC: 1.16.1.9	0.345	Reduction of ferric iron bound to a variety of iron chelators (siderophores)
Succinic semialdehyde dehydrogenase (NAD(+) EC: 1.2.1.24	0.344	Glutamine glutamate metabolism
(d)CTP diphosphatase EC: 3.6.1.65	0.343	Pyrimidine nucleotide metabolism
dTDP-4-amino-4,6-dideoxy-D-galactose acyltransferase EC: 2.3.1.210	0.343	Biosynthesis of nucleotide sugars
Inosine kinase EC: 2.7.1.73	0.343	Purine nucleotide metabolism
TDP-N-acetylfucosamine: lipid II N-acetylfucosaminyltransferase EC: 2.4.1.325	0.343	Enterobacterial common antigen biosynthesis
Kdo2-lipid IVA palmitoleoyltransferase EC: 2.3.1.242	0.342	Lipid A, lipopolysaccharide biosynthesis
Gluconate 2-dehydrogenase EC: 1.1.1.215	0.342	Ketogluconate metabolism, pentose phosphate pathway
Sulfolactaldehyde 3-reductase EC: 1.1.1.373	0.341	Sulfoquinovose breakdown (sulfoglycolysis)
alpha-D-ribose 1-methylphosphonate 5-triphosphate synthase EC: 2.7.8.37	0.340	Phosphonate and phosphinate metabolism

constitute an important target of indole-3-lactate in the pathogenesis of obesity. It is well known that gut microbiota synthesizes polyamines from arginine and its product, ornithine [20]. Polyamine metabolism plays a pivotal role in regulation of the systemic and mucosal adaptive immunity. Arginine, for its part, is an important modulator of the macrophage and T cell metabolism capable of affecting the effector functions of these cells. Furthermore, polyamines inhibit production of pro-inflammatory cytokines and possess antioxidant effect [25]. In the intestine, polyamines can reduce the cytokine release, thereby promoting reparation of damaged epithelium and restoration of normal barrier function. Spermine (polyamine) inhibits activation of inflammasome, which is a protein complex expressed by epithelial cells that is capable of regulating the IL18 secretion [25]. It has been also shown that the presence of the Bifidobacterium animalis probiotic strain can induce resistance to oxidative stress and contribute to the increase in life expectancy depending on the increased microbial synthesis of polyamines [26]. According to the literature, the elevated polyamine levels in white adipose tissue, liver or skeletal muscles can stimulate energy metabolism and protection from alimentary obesity [27]. It is also known that polyamine metabolites are involved in adipogenesis [28]. It has been shown that treatment with exogenic spermine effectively reduces body weight and fasting glucose levels, it also improves glucose tolerance in mice with obesity caused by diet [29]. Furthermore, spermine affects insulin receptors and insulin sensitivity [30]. Thus, immunological and metabolic effects of polyamines are largely congruent with the effects of the indole AhR signaling. The correlations we have identified may be indicative of the involvement of both indole-3-lactate and polyamines in the mechanisms underlying tolerogenicity (or their impairment) in obese patients; a simultaneous decrease in these two tolerogenicity mechanisms associated with obesity might cause the increase in the intestinal barrier permeability.

The relationship between the fecal levels of indole-3-lactate and the predicted abundance of genes encoding the gut microbiome enzymes involved in sulfoglycolysis is poorly understood. The sulfoquinose (SQ) sulfosaccharide is produced by almost all photosynthetic organisms on the Earth and is metabolized by bacteria via sulfoglycolysis. The Embden–Meyerhof–Parnas sulfoglycolytic pathway metabolizes SQ to produce dihydroxyacetone phosphate and sulpholactate aldehyde, it is similar to conventional glycolysis pathway [31, 32]. The literature reports studies focused on identification of microorganisms involved in sulfoglycolysis [33]. However, there are no studies aimed at assessing the relationship between the sulfoglycolysis metabolites and the levels of indole tryptophan metabolites. We have found significant correlations between the predicted abundance of genes encoding the gut microbiome enzymes involved in sulfoglycolysis and the fecal levels of indole-3-lactate in obese individuals (Fig. 3). It should be noted that sulfosaccharides represent a reservoir of sulfate that can potentially be used for synthesis of glycosaminoglycans and

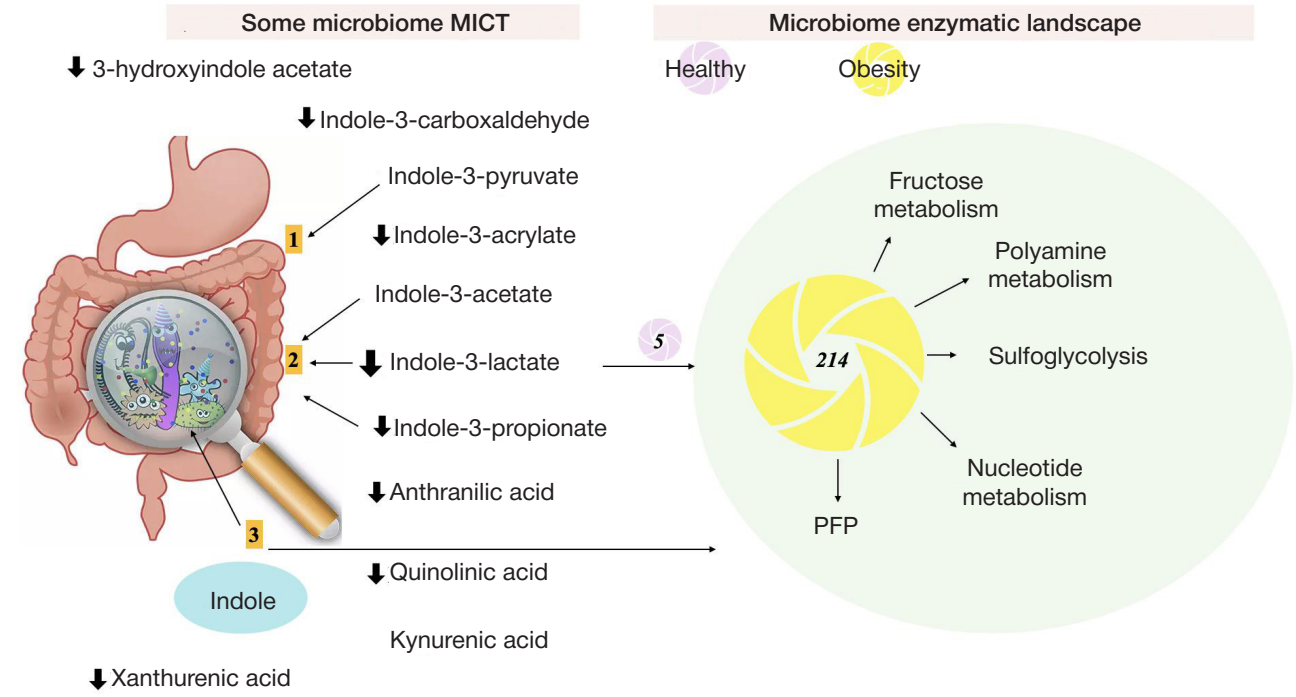

Fig. 3. Obesity is associated with significant deviations of the link between the indole-3-lactate levels and the predicted gut microbiome enzyme-encoding gene abundance. In healthy donors, a total of five significant correlation pairs between indole-3-lactate and the predicted gut microbiome enzyme-encoding gene abundance were identified, while obese individuals showed a significant microbiome enrichment having significant correlation pairs for the fecal levels of indole-3-lactate and the predicted abundance of genes encoding the enzymes involved in various metabolic pathways. ⬇ — decrease in the concentration of MICT in fecal samples; **1** — indole-3-pyruvate affects cells of the intestine (via AhR) and determines the tight junction integrity; **2** — indole-3-acetate, indole-3-propionate, and indole-3-lactate affect immune cells of the intestine (via AhR), increase the pathogen resistance and decrease the intestinal barrier permeability; **3** — interspecies-specific molecule QS — indole having a constant concentration

remodeling of extracellular matrix, which is important for both development of chronic sluggish inflammation associated with obesity and formation of pro-tumorigenic phenotype typical for obese individuals [21].

It is important to note that we have found no significant correlations between the fecal levels of tryptophan catabolites and the abundance of genes encoding the gut microbiome enzymes involved in their production.

Obesity is associated with alteration of the gut microbiota genotype and possibly phenotype: the number of taxa that might supply indole-3-lactate increases three times. Meanwhile, a significant increase in fecal levels of indole-3-lactate can be indicative of severe bacterial colonization of the intestine and increased uptake of this tryptophan catabolite by appropriate microbiota, the taxa typical for obese patients. It is fecal levels of indole-3-lactate for which the number of significant correlations with the predicted abundance of genes encoding the enzymes involved in carbohydrate, lipid, nucleotide and amino acid metabolism, as well as sulfoglycolysis, is increased. Microbiota, including gut microbiota, is believed to be stable and evolutionarily selected at the population level. However, commensal microbiota can be qualitatively and quantitatively modulated [19] by the diet, various signaling molecules and cytokines. Perhaps, enrichment of the indole-3-lactate-producing taxa is of a compensatory nature and occurs to suppress production of pro-inflammatory cytokines that is usually found in obese patients. Thus, it is well known that indole-3-lactate has a profound anti-inflammatory effect: it is involved in induction of immunoregulatory T cells and suppression of inflammatory T cells [34]. The recent research has shown that indole-3-lactate is a dominant tryptophan catabolite for Bifidobacterium (B. longum subsp. infantis). Furthermore, rather high levels of indole-3-lactate are found in human breast milk [34]. We have shown that fecal levels of indole-3-lactate in obese patients might depend on the family Enterobacteriaceae taxonomic abundance. Reduction of the share of this family in gut microbiota is correlated to the decrease in indole-3-lactate levels of obese individuals. However, taking into account the increase in serum levels of indole-3-lactate in obese individuals we have revealed earlier [18], it is likely that production of this MICT in the intestine is stable or even increased, while transport of indole-3-lactate from the intestine into blood in obese patients can be intensified. The answer remains to be seen, since not only gut microbiota can be the source of indole-3-lactate, but also microbiota occupying other ecological niches in the human body.

CONCLUSIONS

Indole and indole-3-lactate are dominant tryptophan catabolites in both healthy and obese individuals. Obese patients show a significant decrease in fecal levels of indole-3-lactate, quinolinic acid, 3-hydroxyindole-acetoacetic acid, anthranilic acid, xanthurenic acid, indole-3-carboxaldehyde, indole-3-acrylate, and indole-3-propionate. The maximum decrease is reported specifically for indole-3-lactate. Obese individuals show a stronger link between the predicted gut microbiome enzyme-encoding gene abundance and MICT. In the group of healthy subjects, the abundance of gut microbiome enzyme-encoding genes is correlated to the levels of indole-3-acrylate and anthranilic acid, while in obese individuals other MICT (indole and indole-3-lactate) together with quinolinic and kynurenic acids define the gut microbiome “enzymatic landscape”. The more close correlations between the predicted gut microbiome enzyme-encoding gene abundance and MICT have been revealed specifically for indole-3-lactate. It has been found that the fecal levels of indole-3-lactate are correlated to the predicted abundance of genes encoding the gut

microbiome enzymes, including those involved in metabolism of carbohydrates, nucleotides, amino acids, polyamines, and sulfosaccharides. No significant correlations between the levels of tryptophan catabolites and the predicted abundance of genes encoding the enzymes involved in tryptophan catabolite production have been revealed. Obese patients of the studied population show the increase in taxonomic diversity of potential indole-3-lactate producers. Potential adjustment of the gut microbiota metabolic activity with tryptophan catabolites can be of preventive and therapeutic significance for obese patients.

References

1. Bharti K, Grimm DJ. Current challenges and best-practice protocols for microbiome analysis Briefings. in Bioinformatics. 2021; 22 (1): 178–93. PubMed PMID: 31848574.
2. Singer-Englar T, Barlow G, Mathur R. Obesity, diabetes, and the gut microbiome: an updated review. Expert Rev Gastroenterol Hepatol. 2019; 13 (1): 3–15. PubMed PMID: 30791839.
3. Franzosa EA, Sirota-Madi A, Avila-Pacheco J, Fornelos N, Haiser HJ, Reinker S, et al. Gut microbiome structure and metabolic activity in inflammatory bowel disease. Nat Microbiol. 2019; 4 (2): 293–305. PubMed PMID: 30531976.
4. Halfvarson J, Brislawn CJ, Lamendella R, Vázquez-Baeza Y, Walters WA, Bramer LM, et al. Dynamics of the human gut microbiome in inflammatory bowel disease. Nat Microbiol. 2017; 13 (2): 17004. PubMed PMID: 28741610.
5. Kiyohara H, Sujino T, Teratani T, Miyamoto K, Arai MM, Nomura E, et al. Toll-like receptor 7 agonist-induced dermatitis causes severe dextran sulfate sodium colitis by altering the gut microbiome and immune cells. Cell Mol Gastroenterol Hepatol. 2018; 25 (7): 135–56. PubMed PMID: 30510995.
6. Desai SN, Landay AL. HIV and aging: role of the microbiome. Curr Opin HIV AIDS. 2018; 13 (1): 22–27. PubMed PMID: 29035948.
7. Burcelin R. HIV and aging: role of the microbiome. Biol Aujourdhui. 2017; 211 (1): 1-18. PubMed PMID: 28682223. French.
8. Roager HM, Licht TR. Microbial tryptophan catabolites in health and disease. Nat Commun. 2018; 9 (1): 3294. PubMed PMID: 30120222.
9. Scott SA, Fu J, Chang PV. Microbial tryptophan metabolites regulate gut barrier function via the aryl hydrocarbon receptor. Proc Natl Acad Sci USA. 2020; 117 (32): 19376–87. PubMed PMID: 32719140.
10. Wong CB, Tanaka A, Kuhara T, Xiao JZ. Microbial tryptophan metabolites regulate gut barrier function via the aryl hydrocarbon receptor. Microorganisms. 2020; 8 (3): 398. PubMed PMID: 32178456.
11. Aust AC, Benesova E, Vidova V, Coufalikova K, Smetanova S, Borek I, et al. Profiling tryptophan catabolites of human gut microbiota and acute-phase protein levels in neonatal dried blood specimens. Front Microbiol. 2021; 12: 665743. PubMed PMID: 34777268.
12. Thursby E, Juge N. Introduction to the human gut microbiota. Biochem J. 2017; 474: 1823–36. PubMed PMID: 34777268.
13. Vyhlídalová B, Krasulová K, Pečinková P, Vyhlídalová B, Krasulová K, Pečinková P, et al. Gut microbial catabolites of tryptophan are ligands and agonists of the aryl hydrocarbon receptor: a detailed characterization. Int J Mol Sci. 2020; 21 (7): 2614. PubMed PMID: 32283770.
14. Yoval-Sánchez B, Pardo JP, Rodríguez-Zavala JS. New insights into the half-of-the-sites reactivity of human aldehyde dehydrogenase 1A1. Proteins. 2013; 81 (8): 1330–9. DOI: 10.1002/prot.24274.
15. Qu Y, Dai C, Zhang X, Ma Q. A new interspecies and interkingdom signaling molecule-Indole. Sheng Wu Gong Cheng Xue Bao. 2019; 35 (11): 2177–88. PubMed PMID: 31814363. Chinese.
16. Ji Y, Gao Y, Chen H, Yin Y, Zhang W. Indole-3-acetic acid alleviates nonalcoholic fatty liver disease in mice via attenuation of hepatic lipogenesis, and oxidative and inflammatory stress. Nutrients. 2019; 11 (9): 2062. PubMed PMID: 31484323.
17. Available from: https://www.genome.jp/pathway/map00380+C00954
18. Shestopalov AV, Shatova OP, Karbyshev MS, Gaponov AM, Moskaleva NE, Appolonova SA, et al. «Kynurenine switch» and obesity. Bulletin of Siberian Medicine. 2021; 20: 103–11. DOI: 10.20538/1682-0363-2021-4-103-111].
19. Mosca A, Leclerc M, Hugot JP. Gut microbiota diversity and human diseases: should we reintroduce key predators in our ecosystem? Front Microbiol. 2016; 7: 455. PubMed PMID: 27065999.
20. Ramos-Molina B, Queipo-Ortuño MI, Lambertos A, Tinahones FJ, Peñafiel R. Dietary and gut microbiota polyamines in obesity- and age-related diseases. Front Nutr. 2019; 6: 24. PubMed PMID: 30923709.
21. Silveira EA, da Silva Filho RR, Spexoto MC, Haghighatdoost F, Sarrafzadegan N, de Oliveira C. The role of sarcopenic obesity in cancer and cardiovascular disease: a synthesis of the evidence on pathophysiological aspects and clinical implications. Int J Mol Sci. 2012; 22 (9): 4339. PubMed PMID: 33919368.
22. Zhang C, Yin A, Li H, Wang R, Wu G, Shen J, et al. Dietary modulation of gut microbiota contributes to alleviation of both genetic and simple obesity in children. EBioMedicine. 2015; 2 (8): 968–84. PubMed PMID: 26425705.
23. Available from: http://qiime.org/
24. Available from: https://picrust.github.io/picrust/
25. Levy M, Thaiss CA, Elinav E. Metabolites: messengers between the microbiota and the immune system. Genes Dev. 2016; 30 (14): 1589–97. PubMed PMID: 27474437.
26. Matsumoto M, Kurihara S, Kibe R, Ashida H, Benno Y. Longevity in mice is promoted by probiotic-induced suppression of colonic senescence dependent on upregulation of gut bacterial polyamine production. PLoS One. 2011; 6 (8): e23652. PubMed PMID: 21858192.
27. Bonhoure N, Byrnes A, Moir RD, Hodroj W, Preitner F, Praz V, et al. Loss of the RNA polymerase III repressor MAF1 confers obesity resistance. Genes Dev. 2015; 29 (9): 934–47. PubMed PMID: 25934505.
28. Ishii I, Ikeguchi Y, Mano H, Wada M, Pegg AE, Shirahata A. Polyamine metabolism is involved in adipogenesis of 3T3-L1 cells. Amino Acids. 2012; 42 (2-3): 619–26. PubMed PMID: 21809076.
29. Sadasivan SK, Vasamsetti B, Singh J, Marikunte VV, Oommen AM, Jagannath MR, et al. Exogenous administration of spermine improves glucose utilization and decreases bodyweight in mice. Eur J Pharmacol. 2014; 729: 94–99. PubMed PMID: 24530553.
30. Pedersen SB, Hougaard DM, Richelsen B. Polyamines in rat adipocytes: their localization and their effects on the insulin receptor binding. Mol Cell Endocrinol. 1989; 62 (2): 1661–6. PubMed PMID: 2663568.
31. Sharma M, Abayakoon P, Epa R, Jin Y, Lingford JP, Shimada T, et al. Molecular basis of sulfosugar selectivity in sulfoglycolysis. ACS Cent Sci. 2021; 7 (3): 476–87. PubMed PMID: 33791429.
32. Frommeyer B, Fiedler AW, Oehler SR, Hanson B, Loy A, Franchini P, et al. Environmental and intestinal phylum firmicutes bacteria metabolize the plant sugar sulfoquinovose via a 6-deoxy-6-sulfofructose transaldolase pathway. iScience. 2020; 23 (9): 101510. PubMed PMID: 32919372.
33. Haange SB, Groeger N, Froment J. Multiplexed quantitative assessment of the fate of taurine and sulfoquinovose in the intestinal microbiome. Metabolites. 2020; 10 (11): 430. PubMed PMID: 33114761.
34. Huang W, Cho KY, Meng D, Walker WA. The impact of indole-3-lactic acid on immature intestinal innate immunity and development: a transcriptomic analysis. Sci Rep. 2021; 11 (1): 8088. PubMed PMID: 33850185.

Литература

1. Bharti K, Grimm DJ. Current challenges and best-practice protocols for microbiome analysis Briefings. in Bioinformatics. 2021; 22 (1): 178–93. PubMed PMID: 31848574.
2. Singer-Englar T, Barlow G, Mathur R. Obesity, diabetes, and the gut microbiome: an updated review. Expert Rev Gastroenterol Hepatol. 2019; 13 (1): 3–15. PubMed PMID: 30791839.
3. Franzosa EA, Sirota-Madi A, Avila-Pacheco J, Fornelos N, Haiser HJ, Reinker S, et al. Gut microbiome structure and metabolic activity in inflammatory bowel disease. Nat Microbiol. 2019; 4 (2): 293–305. PubMed PMID: 30531976.
4. Halfvarson J, Brislawn CJ, Lamendella R, Vázquez-Baeza Y, Walters WA, Bramer LM, et al. Dynamics of the human gut microbiome in inflammatory bowel disease. Nat Microbiol. 2017; 13 (2): 17004. PubMed PMID: 28741610.
5. Kiyohara H, Sujino T, Teratani T, Miyamoto K, Arai MM, Nomura E, et al. Toll-like receptor 7 agonist-induced dermatitis causes severe dextran sulfate sodium colitis by altering the gut microbiome and immune cells. Cell Mol Gastroenterol Hepatol. 2018; 25 (7): 135–56. PubMed PMID: 30510995.
6. Desai SN, Landay AL. HIV and aging: role of the microbiome. Curr Opin HIV AIDS. 2018; 13 (1): 22–27. PubMed PMID: 29035948.
7. Burcelin R. HIV and aging: role of the microbiome. Biol Aujourdhui. 2017; 211 (1): 1-18. PubMed PMID: 28682223. French.
8. Roager HM, Licht TR. Microbial tryptophan catabolites in health and disease. Nat Commun. 2018; 9 (1): 3294. PubMed PMID: 30120222.
9. Scott SA, Fu J, Chang PV. Microbial tryptophan metabolites regulate gut barrier function via the aryl hydrocarbon receptor. Proc Natl Acad Sci USA. 2020; 117 (32): 19376–87. PubMed PMID: 32719140.
10. Wong CB, Tanaka A, Kuhara T, Xiao JZ. Microbial tryptophan metabolites regulate gut barrier function via the aryl hydrocarbon receptor. Microorganisms. 2020; 8 (3): 398. PubMed PMID: 32178456.
11. Aust AC, Benesova E, Vidova V, Coufalikova K, Smetanova S, Borek I, et al. Profiling tryptophan catabolites of human gut microbiota and acute-phase protein levels in neonatal dried blood specimens. Front Microbiol. 2021; 12: 665743. PubMed PMID: 34777268.
12. Thursby E, Juge N. Introduction to the human gut microbiota. Biochem J. 2017; 474: 1823–36. PubMed PMID: 34777268.
13. Vyhlídalová B, Krasulová K, Pečinková P, Vyhlídalová B, Krasulová K, Pečinková P, et al. Gut microbial catabolites of tryptophan are ligands and agonists of the aryl hydrocarbon receptor: a detailed characterization. Int J Mol Sci. 2020; 21 (7): 2614. PubMed PMID: 32283770.
14. Yoval-Sánchez B, Pardo JP, Rodríguez-Zavala JS. New insights into the half-of-the-sites reactivity of human aldehyde dehydrogenase 1A1. Proteins. 2013; 81 (8): 1330–9. DOI: 10.1002/prot.24274.
15. Qu Y, Dai C, Zhang X, Ma Q. A new interspecies and interkingdom signaling molecule-Indole. Sheng Wu Gong Cheng Xue Bao. 2019; 35 (11): 2177–88. PubMed PMID: 31814363. Chinese.
16. Ji Y, Gao Y, Chen H, Yin Y, Zhang W. Indole-3-acetic acid alleviates nonalcoholic fatty liver disease in mice via attenuation of hepatic lipogenesis, and oxidative and inflammatory stress. Nutrients. 2019; 11 (9): 2062. PubMed PMID: 31484323.
17. Available from: https://www.genome.jp/pathway/map00380+C00954
18. Shestopalov AV, Shatova OP, Karbyshev MS, Gaponov AM, Moskaleva NE, Appolonova SA, et al. «Kynurenine switch» and obesity. Bulletin of Siberian Medicine. 2021; 20: 103–11. DOI: 10.20538/1682-0363-2021-4-103-111].
19. Mosca A, Leclerc M, Hugot JP. Gut microbiota diversity and human diseases: should we reintroduce key predators in our ecosystem? Front Microbiol. 2016; 7: 455. PubMed PMID: 27065999.
20. Ramos-Molina B, Queipo-Ortuño MI, Lambertos A, Tinahones FJ, Peñafiel R. Dietary and gut microbiota polyamines in obesity- and age-related diseases. Front Nutr. 2019; 6: 24. PubMed PMID: 30923709.
21. Silveira EA, da Silva Filho RR, Spexoto MC, Haghighatdoost F, Sarrafzadegan N, de Oliveira C. The role of sarcopenic obesity in cancer and cardiovascular disease: a synthesis of the evidence on pathophysiological aspects and clinical implications. Int J Mol Sci. 2012; 22 (9): 4339. PubMed PMID: 33919368.
22. Zhang C, Yin A, Li H, Wang R, Wu G, Shen J, et al. Dietary modulation of gut microbiota contributes to alleviation of both genetic and simple obesity in children. EBioMedicine. 2015; 2 (8): 968–84. PubMed PMID: 26425705.
23. Available from: http://qiime.org/
24. Available from: https://picrust.github.io/picrust/
25. Levy M, Thaiss CA, Elinav E. Metabolites: messengers between the microbiota and the immune system. Genes Dev. 2016; 30 (14): 1589–97. PubMed PMID: 27474437.
26. Matsumoto M, Kurihara S, Kibe R, Ashida H, Benno Y. Longevity in mice is promoted by probiotic-induced suppression of colonic senescence dependent on upregulation of gut bacterial polyamine production. PLoS One. 2011; 6 (8): e23652. PubMed PMID: 21858192.
27. Bonhoure N, Byrnes A, Moir RD, Hodroj W, Preitner F, Praz V, et al. Loss of the RNA polymerase III repressor MAF1 confers obesity resistance. Genes Dev. 2015; 29 (9): 934–47. PubMed PMID: 25934505.
28. Ishii I, Ikeguchi Y, Mano H, Wada M, Pegg AE, Shirahata A. Polyamine metabolism is involved in adipogenesis of 3T3-L1 cells. Amino Acids. 2012; 42 (2-3): 619–26. PubMed PMID: 21809076.
29. Sadasivan SK, Vasamsetti B, Singh J, Marikunte VV, Oommen AM, Jagannath MR, et al. Exogenous administration of spermine improves glucose utilization and decreases bodyweight in mice. Eur J Pharmacol. 2014; 729: 94–99. PubMed PMID: 24530553.
30. Pedersen SB, Hougaard DM, Richelsen B. Polyamines in rat adipocytes: their localization and their effects on the insulin receptor binding. Mol Cell Endocrinol. 1989; 62 (2): 1661–6. PubMed PMID: 2663568.
31. Sharma M, Abayakoon P, Epa R, Jin Y, Lingford JP, Shimada T, et al. Molecular basis of sulfosugar selectivity in sulfoglycolysis. ACS Cent Sci. 2021; 7 (3): 476–87. PubMed PMID: 33791429.
32. Frommeyer B, Fiedler AW, Oehler SR, Hanson B, Loy A, Franchini P, et al. Environmental and intestinal phylum firmicutes bacteria metabolize the plant sugar sulfoquinovose via a 6-deoxy-6-sulfofructose transaldolase pathway. iScience. 2020; 23 (9): 101510. PubMed PMID: 32919372.
33. Haange SB, Groeger N, Froment J. Multiplexed quantitative assessment of the fate of taurine and sulfoquinovose in the intestinal microbiome. Metabolites. 2020; 10 (11): 430. PubMed PMID: 33114761.
34. Huang W, Cho KY, Meng D, Walker WA. The impact of indole-3-lactic acid on immature intestinal innate immunity and development: a transcriptomic analysis. Sci Rep. 2021; 11 (1): 8088. PubMed PMID: 33850185.

CLINICAL SIGNIFICANCE OF CYTOKINE COUNTING IN PATIENTS WITH MULTIPLE SCLEROSIS AND ITS RELATIONSHIP WITH HERPES INFECTION

Baranova NS[1] ✉, Gris MS[1], Baranov AA[1], Spirin NN[1], Artyuhov AS[2], Shakirova KM[2], Nasonov EL[3,4]

[1] Yaroslavl State Medical University, Yaroslavl, Russia

[2] Pirogov Russian National Research Medical University, Moscow, Russia

[3] Nasonova Research Institute of Rheumatology, Moscow, Russia

[4] Sechenov First Moscow State Medical University (Sechenov University), Moscow, Russia

There are persistent infections that contribute to the emergence and development of multiple sclerosis (MS) exacerbations; they are triggered by the Epstein–Barr, herpes type 6, herpes simplex types 1 and 2, varicella-zoster viruses. Cytokines are crucial to arresting the spread of a herpes infection in a body. If their production is out of balance, MS can progress faster. This study aimed at determining the level of cytokines in the blood serum of MS patients, assessing their clinical significance and how they affect reactivation of herpes infection. We examined 36 patients (12 male and 24 female) with confirmed MS (McDonald criteria) in remission. In 18 of them, we diagnosed reactivation of peripheral herpes virus. Serum levels of 15 cytokines (IL1ß, IL4, IL6, TNF-a, INF-γ, IL10, IL17A, IL17F, IL21, IL22, IL23, IL25, IL31, IL33, sCD40L) were determined with the help of xMAP multiplexing. Compared to the control group, MS patients had increased levels of IL10, IL33 ($p < 0.001$), with high IL33 identified most often (20 patients; 52.8%). During exacerbations, the average level of IL10 grew up ($p < 0.01$), as did that of IL31, the high levels of which were detected significantly more often (42.8 and 6.9%, respectively; $p = 0.04$). In addition, a prevailing scenario was the increased levels of IL33 and other cytokines (IL17A, IL17F, IL21, IL31) (57.1 and 6.9% of cases, respectively; $p = 0.008$). Reactivation of herpes translated into higher levels of IL1ß, IL23 and IL33 compared to cases without reactivation ($p < 0.05$ and $p < 0.01$, respectively). High levels of IL33 were significantly more frequently recorded in this group of patients (77.7 and 33.3%; $p = 0.008$). We discuss involvement of IL10, IL31, IL33 and other cytokines in the pathogenesis of herpes-associated MS.

Keywords: multiple sclerosis, herpes, cytokines, interleukin 10, interleukin 31, interleukin 33

Funding: the work was supported by the Innovations Assistance Fund within the framework of the UMNIK program: Participant of the youth scientific and innovative competition (contracts № 3560GU1/2014 of 23.09.2014, № 8815GU2/2015 of 17.12.2015).

Author contribution: NS Baranova, MC Gris — study planning and design, data analysis, manuscript authoring; MC Gris, AS Artyukhov, KM Shakirova — data collection and research; AA Baranov — data analysis; all autors — manuscript editing.

Compliance with ethical standards: the study was approved by the Ethics Committee of the Yaroslavl State Medical University (Minutes № 1 of October 1, 2013). All patients signed a voluntary informed consent.

✉ **Correspondence should be addressed:** Natalia S. Baranova
Revolutsionnaya, 5, Yaroslavl, 150000, Russia; baranova_ns@mail.ru

Received: 24.07.2023 **Accepted:** 20.08.2023 **Published online:** 31.08.2023

DOI: 10.24075/brsmu.2023.032

КЛИНИЧЕСКОЕ ЗНАЧЕНИЕ ОПРЕДЕЛЕНИЯ ЦИТОКИНОВ У ПАЦИЕНТОВ С РАССЕЯННЫМ СКЛЕРОЗОМ И ВЗАИМОСВЯЗЬ С ГЕРПЕТИЧЕСКОЙ ИНФЕКЦИЕЙ

Н. С. Баранова[1] ✉, М. С. Грись[1], А. А. Баранов[1], Н. Н. Спирин[1], А. С. Артюхов[2], К. М. Шакирова[2], Е. Л. Насонов[3,4]

[1] Ярославский государственный медицинский университет, Ярославль, Россия

[2] Российский национальный исследовательский медицинский университет имени Н. И. Пирогова, Москва, Россия

[3] Научно-исследовательский институт ревматологии имени В. А. Насоновой, Москва, Россия

[4] Первый Московский государственный медицинский университет имени И. М. Сеченова, Москва, Россия

В возникновении и развитии обострений рассеянного склероза (РС) участвуют персистирующие инфекции: вирусы Эпштейна–Барр, герпеса 6-го типа, простого герпеса 1-го и 2-го типов, варицелла-зостер-вирус. Выработка цитокинов имеет ключевое значение в ограничении распространения герпетической инфекции в организме человека, а дисбаланс их продукции является фактором прогрессирования РС. Целью исследования было определить уровень цитокинов в сыворотке крови у пациентов РС, оценить их клиническое значение и взаимосвязь с реактивацией герпетической инфекции. Обследовано 36 пациентов (12 мужчин и 24 женщины), с достоверным РС (критерии McDonald) и ремитирующим течением. У 18 человек выявлена реактивация периферической герпес-вирусной инфекции. Сывороточный уровень 15 цитокинов: IL1β, IL4, IL6, ФНО-а, ИНФ-γ, IL10, IL17A, IL17F, IL21, IL22, IL23, IL25, IL31, IL33, sCD40L исследовали с помощью мультиплексной технологии xMAP. При РС, в сравнении с контролем, выявлено увеличение IL10, IL33 ($p < 0{,}001$). Наиболее часто выявляли высокие значения IL33 — у 20 (52,8%) пациентов. При обострении заболевания средний уровень IL10 был выше ($p < 0{,}01$), достоверно чаще встречались высокие значения IL31 (соответственно 42,8 и 6,9%; $p = 0{,}04$) и превалировало сочетанное повышение IL33 с другими цитокинами (IL17A, IL17F, IL21, IL31) (соответственно в 57,1 и 6,9% случаев; $p = 0{,}008$). При реактивации герпес-вирусной инфекции уровень IL1β, IL23 и IL33 был выше, чем без нее ($p < 0{,}05$ и $p < 0{,}01$ соответственно). Высокие значения IL33 значимо чаще регистрировали в этой группе пациентов (77,7 и 33,3%; $p = 0{,}008$). Обсуждается участие IL10, IL31, IL33 и других цитокинов в патогенезе ассоциированного с вирусами герпеса РС.

Ключевые слова: рассеянный склероз, герпес, цитокины, интерлейкин 10, интерлейкин 31, интерлейкин 33

Финансирование: работа выполнена при финансовой поддержке Федерального государственного бюджетного учреждения «Фонд содействия развитию малых форм предприятий в научно-технической сфере» (Фонд содействия инновациям) в рамках программы УМНИК: Участник молодежного научно-инновационного конкурса (договоры №3560ГУ1/2014 от 23.09.2014, № 8815ГУ2/2015 от 17.12.2015).

Вклад авторов: Н. С. Баранова, М. С. Грись — планирование, дизайн исследования, анализ данных, подготовка рукописи; М. С. Грись, А. С. Артюхов, К. М. Шакирова — сбор данных, проведение исследования; А. А. Баранов — анализ данных; все авторы — редактирование рукописи.

Соблюдение этических стандартов: исследование одобрено этическим комитетом ФГБОУ ВО ЯГМУ Минздрава РФ (протокол № 1 от 1 октября 2013 г). Все пациенты подписали добровольное информированное согласие.

✉ **Для корреспонденции:** Наталия Сергеевна Баранова
ул. Революционная, д. 5, г. Ярославль, 150000, Россия; baranova_ns@mail.ru

Статья получена: 24.07.2023 **Статья принята к печати:** 20.08.2023 **Опубликована онлайн:** 31.08.2023

DOI: 10.24075/vrgmu.2023.032

Multiple sclerosis (MS) is a chronic disease of the central nervous system with autoimmune inflammatory and neurodegenerative mechanisms of development [1]. The processes important for immunopathogenesis of the disease are penetration of activated T cells (type 1 T helper cells (Th1), Th17 cells) and macrophages through the blood-brain barrier into the brain tissue, local activation of astrocytes and microglia, production of anti-inflammatory cytokines by them [2, 3] and subsequent demyelination and neuron degeneration. The etiology of MS remains unknown. It is believed that, in addition to genetic factors, various persistent infections contribute to its development [4]. Herpes simplex virus type 1 and 2 (HSV-1 and HSV-2) [5], varicella zoster virus (VZV) [6], human herpesvirus 6 (HHV6) [7] and Epstein–Barr virus (EBV) play a major role in the occurrence of MS, development of exacerbations and progression of the pathological process [8–11].

Production of cytokines as part of the innate immune response is crucial for arrest of spread of herpes infection in a body [11, 12]. In MS cases, lack of balance between production of pro- and anti-inflammatory cytokines is also considered the key factor in the development of the disease's exacerbations and progression of the inflammatory immune response. Interleukins (IL) IL1-β, IL2, IL4, IL6, IL10, IL17, IL23, tumor necrosis factor — (TNF-α) and interferon-γ (INF-γ) are the best studied response agents [2, 3, 13–15]. The role played by other cytokines, IL31 and IL33 in particular, in the pathogenesis of MS has not been investigated sufficiently; the data available originate from foreign sources exclusively [16–21]. Moreover, neither in Russia nor abroad have researchers sought to determine cytokines in blood serum during reactivation of herpes infection in MS patients, and subsequently assess their clinical significance. This gap in data presented in the published works substantiated this study, which aimed at determining the level of cytokines in the blood serum of MS patients, assessing their clinical significance and how they affect reactivation of herpes infection.

METHODS

The work was conducted at the premises of the Research and Educational Center for Demyelinating Diseases of the Yaroslavl State Medical University and Center for Multiple Sclerosis of Yaroslavl Clinical Hospital № 2 (Russia).

The study included 36 patients, 12 male and 24 female, with MS confirmed under McDonald criteria [22] (Table 1). The mean age of the patients at the time of the study was 38.5 (28.0; 48.5) years, the age of onset of the disease — 27.00 (21.5; 38.0) years, and duration of the disease — 9.50 (3.5; 12.5) years. Multiple sclerosis was relapsing-remitting (RRMS) in all patients, with 29 (80.6%) of them in remission and 7 (19.4%) suffering exacerbation of the disease.

Thirty (83.3%) patients were undergoing a course of MS disease modifying drugs (DMDs), with 14 taking glatiramer acetate (GA), 16 — high-dose interferons (INF); the mean duration of the course was 30.0 (9.0; 67.0) months. Six (16.7%) patients were out of DMDs therapy at the time of examination.

For clinical assessment of the patients' neurological status, we relied on the J.F Kurtzke's assessment system [23] that includes the Functional Status Scale (FSS) and the Expanded Disability Status Scale (EDSS). The average score on the EDSS scale was 3.25 (2.00; 4.50), and the sum of neurological impairment — 6.50 (3.00; 9.00) points. Using the F. Lublin's classification [24], we divided the RRMS patients into active MS (*n* = 17, 47.2%) and inactive MS (*n* = 19, 52.8%) groups. In the active MS group, we also marked patients with highly active MS (*n* = 6, 35.3%), i.e., two or more exacerbations a year.

The key indicators of the course of the disease taken into account were first symptoms, duration of the first remission, patient's age at the time of onset, total neurological impairment score on Kurtzke's scale (TNIS), number and severity of exacerbations. We distinguished between mild MS exacerbations (TNIS growing by 0.5–1 point on EDSS scale), moderate exacerbations (growth by 1–2 points) and severe

Table 1. Clinical characteristics of the MS patients (Me (25^{th}, 75^{th} percentile), *n* = 36)

Characteristic	Value
Gender, m/f, *n* (%)	12/24 (33.3/66.7)
Age (years)	38.50 (28.0; 48.5)
Age of onset (years)	27.00 (21.5; 38.0)
Duration of the disease (years)	9.50 (3.5; 12.5)
MRI+ exacerbations (activity in RRMS), *n* (%)	17 (47.2)
Highly active, *n* (%)	6 (35.3)
Active exacerbation, *n* (%)	7/29 (19.4/80.6)
EDSS at the time of examination (points)	3.25 (2.00; 4.50)
Total number of exacerbations	4.00 (3.00; 6.00)
Average annual frequency of exacerbations	0.58 (0.33; 1.00)
Rate of progression (point/year)	0.40 (0.21; 0.75)
Duration of the 1^{st} remission (months)	12.00 (6.00; 24.00)
Progression index	0.78 (0.35; 1.50)
Time to disability level 3 by EDSS (years)	2.25 (0.00; 7.00)
Severity of flu-like syndrome (points)	6.00 (2.00; 11.00)
Neurological impairment by FS scale (points)	6.50 (3.00; 9.00)
Active course of MS disease modifying drugs (DMDs) at the time of the study, *n* (%)	30 (83.3)
Duration of DMDs course (months)	30.00 (9.00; 67.00)
DMDS (*n* = 30): INF/GA, *n* (%)	16/14 (53.3/46.7)

Table 2. Clinical characteristics of MS patients with and without clinical signs of PHVI reactivation (Me; 25th, 75th percentile)

Characteristic	MS with clinical signs of PHVI (*n* = 18)	MS without clinical signs of PHVI (*n* = 18)
Gender, male, *n* (%)	4 (22.2)	8 (44.4)
Female, *n* (%)	14 (77.8)	10 (55.6)
Age at the time of examination (years)	36.50 (28.00; 43.00)	39.00 (28.00; 57.00)
Age of onset (years)	24.00* (19.00; 30.00)	33.00 (23.00; 41.00)
Duration of the disease (years)	8.50 (3.00; 20.00)	10.50 (4.00; 12.00)
MRI+ exacerbations (activity in RRMS), *n* (%)	8 (44.4)	9 (50.0)
Highly active, *n* (%)	3 (16.7)	3 (16.7)
Active exacerbations, *n* (%)	5 (27.8)	2 (11.1)
Number of exacerbations	4.50 (3.00; 6.00)	4.00 (3.00; 5.00)
Average annual frequency of exacerbations	0.67 (0.32; 1.00)	0.42 (0.33; 1.00)
EDSS at the time of examination (points)	3.25 (2.00; 4.00)	3.25 (2.00; 4.50)
Rate of progression (point/year)	0.44 (0.19; 0.75)	0.40 (0.23; 0.65)
Duration of the 1st remission (months)	12.50 (8.00; 36.00)	12.00 (6.00; 20.00)
RND (points)	0.65 (0.25; 1.50)	0.91 (0.36; 1.50)
Time to disability level 3 by EDSS (years)	3.00 (0.00; 8.00)	1.00 (0.00; 7.00)
TNIS on Kurtzke's scale (points)	6.50 (3.00; 9.00)	6.50 (4.00; 8.00)
Active course of DMDs at the time of the study, *n* (%)	16 (88.9)	14 (77.8)
Duration of DMDs course (months)	29.50 (5.00; 69.00)	34.50 (14.00; 63.00)
DMDs: INF, *n* (%)	10 (62.5)	6 (42.9)
DMDs: GA, *n* (%)	6 (37.5)	8 (57.1)
Flu-like syndrome as response to MSMT (points)	8.00 (1.00; 12.00)	5.00 (2.00; 6.00)
Presence of serological markers of HSV-1 and HSV-2, VZV infections, *n* (%)	18 (100)	18 (100)
Presence of serological markers of a recent EBV infection, *n* (%)	18 (100)	18 (100)
Presence of serological markers of a recent CMV infection, *n* (%)	14 (77.8)	17 (94.4)
Presence of serological markers of a recent mixed infection with two viruses HSV-1, HSV-2/VZV and EBV, *n* (%)	3 (16.7)	0
Presence of serological markers of a recent mixed infection with three viruses HSV-1, HSV-2/VZV, EBV and CMV, *n* (%)	4 (22.2)	8 (44.4)
Presence of serological markers of a recent mixed infection with four viruses HSV-1, HSV-2, VZV, EBV, CMV, *n* (%)	11 (61.1)	10 (55.6)

Note: * — $p < 0.05$ between groups.

exacerbations (growth by more than 2 points) [25]. The mean annual frequency of exacerbations was taken as a ratio of the number of exacerbations to the duration of the acute period in years. The rate of disease progression was taken as a ratio of the level of disability (as per EDSS, in points) to the duration of the disease in years (point/year).

The progression index, which reflects the rate of neurological decline (RND), was calculated as the ratio of FSS score (TNIS) to the duration of the disease in years. Prognosis of the MS course was based on the calculated period of time before the patient became persistently disabled (3 EDSS points), duration of the first remission, and time before onset of secondary progression.

In the anamnesis, we paid special attention to herpesvirus diseases. In order to refine the MS development and aggravation risk factors, we designed a special questionnaire with which the patients reported if they suffered manifestations of labial and genital herpes often, had virus-associated exacerbations of MS, lived with chronic stress, subfebrility, chronic foci of infection, frequently contracted respiratory viral diseases and saw links between them and exacerbations of MS. We also examined patients for herpes rashes.

Based on the data obtained, the patients were divided into two groups. The first group included 18 patients (50%) with confirmed MS and reactivation of peripheral herpes virus infection (PHVI). The inclusion criteria for this group were confirmed MS combined with signs of PHVI, i.e., presence of both clinical (typical vesicular rashes, subfebrility, lymphadenopathy, arthralgia, myalgia, etc.) and serological signs of an active herpes virus infection; presence of only clinical signs of HSV at the time of exacerbation or within two weeks before and after it. Serological sign: low type-specific IgG antibodies avidity index (less than 50%) and IgG positivity coefficient (PC) three or more times greater than the reference range or specific IgM antibodies in the blood. The second group comprised 18 patients (50%) with confirmed MS with no signs of reactivation of PHVI registered by clinical and serological studies and/or recorded in the medical history. Table 2 presents clinical characteristics of these groups.

In cases of PHVI, the onset occurred at an earlier age ($p < 0.05$, significant difference), the disease affected mainly women and had a shorter duration. The flu-like response to MS DMDs was more apparent, and exacerbations happened virtually twice as often (27.8%) as in the control group (11.1%). No differences were noted in other considered characteristics of patients between the compared groups, including age at the time of examination, disease severity, level of disability,

Table 3. Concentration (Me; 25th, 75th percentile) of cytokines in blood serum of participants from the MS and control groups

Indicator (pg/ml)	Control (n = 18)	MS patients (n = 36)	MS, exacerbation (n = 7)	MS, no exacerbation (n = 29)
IL1β	1.45 (0.16; 2.18)	0.04 (0.00; 0.08)*	0.06 (0.00; 0.12)	0.04 (0.00; 0.05)
IL4	0.01 (0.73; 3.24)	4.43 (2.22; 10.95)	12.33 (2.89; 16.36)	5.51 (2.22; 5.75)
IL6	1.36 (0.27; 3.68)	0.59 (0.30; 1.07)	0.81 (0.15; 1.48)	0.59 (0.30; 0.96)
IL10	0.01 (0.00; 0.01)	2.03 (0.90; 2.73)*	3.67 (1.80; 5.25)°	1.80 (0.90; 2.73)
IL17A	0.58 (0.00; 1.74)	0.57 (0.28; 0.89)	0.92 (0.42; 1.56)	0.57 (0.28; 0.78)
IL17 F	6.76 (4.02; 10.6)	0.01 (0.00; 0.78)*	0.01 (0.01; 5.10)	0.01 (0.01; 0.62)
IL21	0.01 (0.00; 0.49)	0.01 (0.00; 0.01)	0.01 (0.00; 0.01)	0.01 (0.00; 0.01)
IL22	47.43 (38.42; 72.64)	0.01 (0.00; 0.32)*	0.63 (0.00; 2.21)	0.01 (0.00; 0.32)
IL23	80.11 (0.00; 114.44)	2.94 (0.00; 8.81)	10.26 (0.00; 19.74)	2.94 (0.00; 7.34)
IL25	13.73 (6.1; 28.99)	0.11 (0.00; 0.32)*	0.32 (0.11; 0.84)	0.11 (0.00; 0.32)
IL31	6.28 (2.87; 8.62)	6.33 (3.85; 10.37)	8.81 (6.33; 15.73)	6.33 (3.00; 9.43)
IL33	0.52 (0.17; 0.78)	4.32 (1.40; 7.49)*	6.67 (2.79; 11.60)	4.18 (1.12; 6.67)
INF-γ	0.45 (0.00; 5.33)	0.49 (0.49; 1.36)	0.49 (0.49; 1.48)	0.49 (0.49; 0.99)
TNF-α	17.38 (13.65; 31.61)	0.53 (0.45; 1.04)*	1.01 (0.49; 1.39)	0.51 (0.44; 0.68)
sCD40L	110.81 (83.58; 122.55)	76.77 (36.82; 115.04)	115.00 (69.49; 158.01)	69.02 (34.36; 110.35)

Note: * — $p < 0.001$ compared to the control group, ° — $p < 0.01$ compared to the MS group's no exacerbation subgroup.

MS DMDs therapy status. In both groups, patients had mixed HSV infection in most cases, but only those with PHVI exhibited serological markers of two infections (HSV-1, HSV-2/VZV and EBV).

The control group included 18 practically healthy donors without clinical, historical and serological signs of PHVI. These participants had no chronic neurological diseases and somatic pathology in the acute stage. Seeking to detect diseases that could affect results of the study, we examined everyone (standard neurological examination) and collected medical histories thoroughly. This group was comparable to the MS group in terms of gender and age: 7 (38.9%) male and 11 (61.1%) female participants, mean age of 39.10 (29.00; 49.60).

Using the EIA method and standard kits (Vector-Best; Russia), we examined blood serum of all participants (both MS group and control group) with the aim to establish the levels of type-specific IgM and IgG antibodies to HSV-1 and HSV-2, IgM and IgG to VZV, IgM and IgG to capsid antigen VCA EBV, IgG to early EA antigens and nuclear antigen NA EBV, IgM and IgG to CMV. The examination followed manufacturer's instructions and was carried out in the clinical and diagnostic laboratory of Set LLC (Yaroslavl). The PI taken as reference for the determined level of antibodies to HSV-1 and HSV-2 was >1 u/ml, that for the level of IgG to CMV — 0.25 RU/ml. The result was considered positive if the level of immunoglobulins G (IgG) exceeded the PI by 3 or more times, the IgG avidity index was low (less than 50%), or the blood contained immunoglobulins M (IgM) and we clinically registered activation of a latent herpes infection.

The concentration of 15 cytokines in blood serum (IL1ß, IL4, IL6, IL10, IL17A, IL17F, IL21, IL22, IL23, IL25, IL31, IL33, INF-γ, TNF-α, sCD40L) was determined with the help of a Bio-PlexTM 200 System analyzer (Bio-Rad; USA) utilizing xMAP multiplexing technology. The tests were carried out with manufacturer's reagents in the laboratory of the Translational Medicine Research Institute of Pirogov Russian National Research Medical University. We analyzed both the mean level of each cytokine and the frequency of its increase (peaks beyond the upper limit of normal M+3 σ in the control group).

For statistical processing, we used Statistica 10.0 software package (StatSoft; USA) and generally accepted methods of parametric and nonparametric analysis. Mann–Whitney test enabled comparison of two groups for parameters with abnormal distribution, and for 3 or more groups in such cases, we used the Kruskal–Wallis test. The results are presented as a median (Me) with interquartile range [25th, 75th percentile]. To compare samples by qualitative attribute and to assess the proportion of occurrence of a characteristic/sign, we used the Fisher's exact test. Spearman's rank correlation coefficient was used for the correlation analysis. The differences were considered statistically significant at $p < 0.05$.

RESULTS

Cytokine study of the MS group patients (acute stage and remission)

No gender-related differences were registered in the average cytokine levels among participants from the MS group. We detected significant positive associations between age of the patients at the time of examination and concentration of IL6 (r= 0.36; $p < 0.05$), TNF-α (r = 0.35; $p < 0.05$) and sCD40L (r = 0.42, $p < 0.05$); duration of the disease did not correlate with cytokine level.

Compared to the control group, MS patients exhibited significantly increased mean levels of IL10 and IL33 ($p < 0.001$) upward trend of IL4 ($p > 0.05$) (Table 3). Concentrations of IL1-β, IL17F, IL22, IL25 and TNF-α against the background of MS were significantly lower ($p < 0.001$) than in participants from the control group, and the level of IL23 was lower, but the difference did not reach significance ($p > 0.05$). The levels of IL6, IL17A, IL21, IL31, INF-γ and sCD40L did not differ in the compared groups.

The most common phenomenon registered was hyperproduction of IL33 (n = 20, 52.8%). Significantly less frequently, we registered peaking levels of IL17A, IL17F, IL21, IL31 (in 2.8, 5.6, 5.6 and 13.8% of cases, respectively). No other cytokine level exceeded the upper limit of the reference range. The level of IL17A, IL17F, IL21 has always been combined with an increase of that of IL33. Hyperproduction of IL31 was isolated only in one patient; in other participants, it was coupled with hyperproduction of IL33. Isolated growth of concentration

Table 4. Concentration (Me; 25th, 75th percentile) of cytokines in blood serum of MS patients exhibiting clinical signs of reactivation of PHVI and not

Indicator (pg/ml)	MS with clinical signs of PHVI (n = 18)	MS without clinical signs of PHVI (n = 18)
IL1β	0.05 (0.01;0.08) *	0.01 (0.00;0.05)
IL4	4.88 (2.35;0.05)	2.66 (1.75;6.04)
IL6	0.78 (0.30;1.55)	0.44 (0.30;0.74)
IL10	2.73 (1.80;2.73)	1.50 (0.60;2.26)
IL17A	0.75 (0.42;0.99)	0.50 (0.14;0.57)
IL17 F	0.16 (0.00;0.93)	0.01 (0.00;0.01)
IL21	0.01 (0.00;2.37)	0.01 (0.00;0.01)
IL22	0.32 (0.00;0.63)	0.01 (0.00;0.32)
IL23	8.80 (0.00;11.72)*	1.10 (0.00;5.87)
IL25	0.27 (0.11;0.53)	0.11 (0.00;0.21)
IL31	6.95 (5.09;9.43)	6.33 (3.00;13.78)
IL33	6.26 (3.63;9.96) **	2.37 (1.12;5.02)
INF-γ	0.74 (0.49;1.48)	0.49 (0.49;0.99)
TNF-α	0.56 (0.44;1.06)	0.52 (0.45;0.74)
sCD40L	76.77 (34.36;110.35)	74.66 (39.5;127.72)

Note: * — $p < 0.05$; ** — $p < 0.01$ between groups.

of IL33, on the contrary, was detected in most (14 (70%) of 20) patients, and in 6 it grew together with other cytokines, most often — four cases — with IL31. High levels of IL33 were significantly associated with increased concentration of IL17A (r = 0.38; $p < 0.05$), IL17F (r = 0.38; $p < 0.05$), IL21 (r = 0.54; $p < 0.001$) and IL31 (r = 0.68; $p < 0.001$).

During exacerbation of MS, the average level of IL10 was significantly higher than outside of this period ($p < 0.01$), and, the levels of IL4, IL23, IL31, IL33 and sCD40L tended to grow ($p > 0.05$). The mean values of IL1ß, IL6, IL17A, IL17F, IL21, IL22, IL25, TNF-α and INF-γ did not differ between the compared groups.

High levels of IL31 were registered significantly more often during exacerbations (in 42.8% and 6.9% of cases, respectively; p = 0.04), with IL33 production simultaneously on the rise (71.4 and 51.7%; $p > 0.05$). The level of IL33 was predominantly growing with other cytokines (IL17A, IL17F, IL21, IL31) (in 57.1 and 6.9% of cases, respectively; p = 0.008). We have also identified positive associations between MS exacerbations and high values of IL17A (r = 0.34; $p < 0,05$), IL17F (r = 0.34; $p < 0.05$) and IL31 (r = 0.41; $p < 0,01$). The combined hyperproduction of IL33 correlated significantly exacerbations of the disease (r = 0.53; p = 0.001).

Cytokine levels in MS patients depending on the clinical manifestations of reactivation of PHVI

In MS patients with clinical manifestations of PHVI, the average level of IL1ß, IL23 and IL33 was significantly higher than in those who did no have the infection reactivated ($p < 0.05$ and $p < 0.01$, respectively); we have also noted the upward trend for mean values of IL4 ($p > 0.05$; Table 4). Concentrations of IL6, IL10, IL17A, IL17F, IL21, IL22, IL25, IL31, INF-γ, TNFa and sCD40L did not differ between the compared groups.

The frequency of growth of IL31 was similar in both groups of patients (16.7 and 11.1%; $p > 0.05$). As for IL33, its level was significantly more often (77.7%) higher against the background of reactivated PHVI than outside of this condition (33.3%; p = 0.008). Clinical signs of PHVI were detected somewhat more often when IL33 was growing together with other cytokines than alone (in 83.3 and 64.3% of cases, respectively); with IL 33 concentration at the normal level, PHVI manifested itself only in 25% of cases (p = 0.02). Hyperproduction of IL33 was significantly associated with reactivation of PHVI (r = 0.45; p = 0.006); we established no similar pattern for IL17A, IL17F, IL21 and IL31 (r = 0.17, r = 0.17, r = 0.24 and r = 0.08, respectively; $p > 0.05$ in all cases).

Isolated or combined increase of level of IL33 was significantly associated with frequent (more than once a year) manifestations of Herpes labialis (r = 0.42 and r = 0.38, $p < 0.01$ in both cases), and simultaneous growth of IL33 and other cytokines pointed to repeated episodes of herpes zoster in adulthood (r = 0.55; $p < 0.001$).

The amount of antibodies to the EBV IgG capsid protein significantly positively correlated only with concentration of IL1ß (r = 0.34; $p < 0.05$). We identified no correlations between the level of other cytokines and laboratory markers of herpetic infection.

DISCUSSION

The clinical significance of cytokine counting in MS patients is ambiguous. Some authors point to gender as a factor affecting their levels: IL31 and sCD40L was found increased in male MS patients [26], IL33 — in female MS patients [18]. Other researchers state that gender and age of the patients have no effect on serum concentration of IL33 [27], or report its increase mainly in elderly patients [28]. IL31 and sCD40L typically grow during the early (up to 5 years) period of the disease [19], which was established by other authors, too [21]: they discovered significant negative correlations between duration of the disease and levels of IL1ß, IL17, IL21, IL23, IL31 and IL33. In our study, we identified no differences in cytokine concentrations between men and women, there was no relationship with the duration of the disease found, and age of the patients positively correlated only with the values of IL6, TNFa and sCD40L.

Compared to the control group, MS patients had significantly higher concentrations of IL10, IL33, IL4 tending to grow, and simultaneously falling levels of IL1β, IL17F, IL22, IL25 and TNF-α. These results are somewhat consistent with data reported by other authors. In a controlled study that analyzed 15 cytokines (multiplexing), MS patients had increased blood plasma concentrations of IL4, IL33, sCD40L and decreased level of TNF-α, as well as high counts of IL1ß, IL10, IL33 and low level of sCD40L in the cerebrospinal fluid [17].

Low level of proinflammatory cytokines in MS patients is associated with the effect of MS DMDs [26, 29]. The majority of participants of our study (83.3%) were also taking MS DMDs. However, there is a study that involved RRMS patients that did not take such drugs [17]. In addition, another study reports high concentration of IL33 in 32 RRMS patients registered before they started therapy with glucocorticoids or MS DMDs [16]. A multiplex analysis of concentration of 41 cytokines in 56 naive MS patients revealed that the levels of IL2, IL4, IL7, IL8, IL17A, TNF-α and sCD40L drop compared to healthy donors [15].

During exacerbation of MS, levels of IL1ß, IL2, IL6, IL17, IL23, TNF-α, INF-γ typically grow and those of IL4 and IL10 drop [2, 3, 30]. However, some papers report that during this phase of the disease, the level of IL17 goes down while counts of TNF-α and IL10 remain on par with values registered in the control group [31], while RRMS patients in remission enjoy a significant decrease in the concentration of IL10 [32]. Participants of our study had the level of IL10 significantly higher during exacerbations, which also triggered hyperproduction of IL31 and growth of IL33 and other cytokines (IL17A, IL17F, IL21, IL31).

One of the main objectives of this study was to assess the effect of herpetic infection on cytokine levels in MS patients. In the literature available to us, we found no studies investigating the the relationship between production of cytokines and reactivation of herpes infection. The best researched connection is that between γ-herpesviruses, EBV [10, 33] and HHV-6 [7] in particular, and chronic latent infection in B cells and T cells of MS patients [12]. In adolescent patients predisposed to MS, these viruses cause development of the disease [11, 12, 33]. Relapses of MS may be associated with faults in control of EBV reactivation by $CD8^+$T cells [34]. β-herpes CMV infection, on the contrary, can protect against MS and reduce the risk of its occurrence [35].

However, α-herpes viruses (HSV-1, HSV-2 and VZV) are partake in pathogenesis of MS. The viruses of this group can persists in neurons for a long time, periodically reactivate and replicate (lytic pattern), which triggers relapses with a short reproductive cycle and rapid destruction of the infected host cells [36]. In a case-control study, HSV-1 DNA was detected in peripheral blood monocytes of 45.1% of RRMS patients, while in healthy people this indicator was at 3.4% [37]. HSV-1 is more often found in the brain tissue of MS patients than in that of individuals without this disease [38].

In MS patients, monoinfection of herpesvirus is less common than the mixed variety. The most frequently diagnosed combination includes four herpesviruses: HSV-1 and 2 + VZV + EBV + CMV [39]. Development of clinical exacerbations of RRMS was established to be accompanied by reactivation of HSV-1 in peripheral blood monocytes [40]. HSV-1 seropositivity is associated with an increased risk of MS in individuals who have no DRB1*15 allele [41]. These data confirm the possible involvement of HSV-1 and HSV-2 and VZV in the development of MS and its exacerbations in patients specifically predisposed genetically.

Analyzing the clinical signs peculiar to the reactivated PHVI group, we identified a number of characteristic features that sum up to an earlier disease onset age and frequent exacerbations. This is consistent with the data reported by other researchers [42] and the results of our earlier work [39]. We detected significantly higher mean levels of IL1ß, IL23, IL33, and prevailing production of IL4 in the RRMS patients with clinical manifestations of PHVI that participated in this study. At the same time, IL1ß and IL23 did not rise in other groups. High values of IL33 were significantly more common in PHVI patients; the level of this protein was growing both alone and in combinations with IL17A, IL17F, IL21 or IL31. There was also a significant association between high levels of IL33 and clinical manifestations of recurrent infection that are typical for α-herpes viruses HSV-1 and HSV-2, and VZV.

Our results allow discussing the special character of the role played by cytokines in the pathogenesis of MS associated with herpes viruses, which is obviously linked to the realization of their biological functions. For example, IL10 has a powerful anti-inflammatory effect and affects the innate and acquired immune response. It curtails production of IL1ß, IL6, IL8, IL12, IL23 and TNFa, which also possesses neuroprotective action effect [43]. Traditionally, increased level of IL10 in MS patients is linked to the early stages of remission of the disease, with production of IL17, IL23 and IL25 suppressed in the background [2]. Our data indicate that RRMS exacerbations may be accompanied by simultaneous growth of IL10 and proinflammatory cytokines.

The encountered differences may stem from our use of multiplexing technology to count the cytokines. Unlike uniplexing analysis technology, common earlier, multiplexing enables simultaneous assessment of a complex of molecules and not just individual indicators. For example, multiplexing allowed detecting growth of IL10, IL17 and IL23 in RRMS in remission [21].

At the same time, viral infections can trigger excessive synthesis of IL10, which is of particular importance if the patient has MS. In the active phase of inflammation, this protein is produced to limit the undesirable consequences of hyperactive innate immunity response to the pathogen [44]. However, evolving, viruses have learned to use the immunoregulatory function of IL10 to evade the host's immune system and thus up their chances of survival. With inflammation in the active phase, antiviral CD4 and CD8 T cells become the main sources of IL10 [45], but the protein, which suppresses the function of Th1 cells, reduces their ability to present the antigen. Increased synthesis of IL10 with prolonged activity of the antigen can deplete the stock of antiviral T cells, switch their phenotype and thus make them cells predominantly producing IL10 that are unable to activate upon repeated presentation of the antigen [44].

In addition, EBV encodes synthesis of the protein that is a homologue of human IL10 (viral homologue IL10 (EBV IL10), as well as synthesis of conventional IL10 (cIL10) [46]. EBV IL10, a late lytic phase protein encoded by the BCRF-1 gene, is approximately 80% homologous to human IL10. IL10 homologues allow the virus to escape immune response of the host or limit its action. Compared to IL10, EBV IL10 induces a much weaker STAT3 phosphorylation in the peripheral blood monocytes; it is less effective in suppressing inflammatory genes [47]. EBV IL10 degrades expression of CD163 on monocytes, which translates in inhibition of their polarization in M2 cells possessing antiinflammatory properties. Moreover, the process disrupts participation of monocytes in clearance of apoptotic cells, which, accumulated, promote secondary necrosis. It is believed that, with EBV infection in the background, IL10 synthesized by cells and EBV IL10 act simultaneously and in a functionally coordinated manner, helping the virus to stay in B lymphocytes for a long time and neutralize the antiviral potential of T cells [46]. EBV IL10 can activate B cells [48]. Both of these cytokines are found in CNS; they support the pool of B-cells with latent EBV infection, which locally stimulate pathogenic T cells. Given the presence of serological markers of EBV infection in all RRMS patients involved in this study, it is possible that these mechanisms shaped production of IL10 in our case, too.

IL17 is known to be one of the key cytokines in the pathogenesis of MS [2]. It also plays an important role in

the immune response to viral infections [12]. Stimulated by HSV, Th17 cells produce IL17 [49]. The expression of KIR2DL2 receptor on NK cells in MS patients makes them more susceptible to HSV-1 infection [50]. The bulk of IL17A is released by KIR2DL2+NK cells [51]. In this study, we did not register differences in concentrations of IL17A and IL17F between RRMS and control groups; the levels did not differ during exacerbations and remissions and were not dependent on PHVI reaction or lack thereof.

IL23 also participates in pathogenesis of MS. Compared to healthy donors, RRMS patients have more serum IL23 [52]. Moreover, IL23 plays an important role in HSV infection cases. It induces proliferation of memory T cells [53] and can be detected as early as on the 3rd day of infection in the nerve ganglia of mice infected with HSV [54]. IL23 stimulates production of IL17 by NK cells, attracts neutrophils to the infection locus and supports local synthesis of antiinflammatory cytokines IL1β, IL6 and TNFα. We have registered a significant growth of IL23 in the reactivated HSV group, which was not the case for IL17.

IL31 belongs to the IL family; it is mainly synthesized by Th2 cells, and it is dependent on IL4 [55, 56]. IL31 acts through a heterodimeric receptor that comprises an IL31RA chain and a — chain of the oncostatin M receptor. The protein targets mast cells found in peripheral tissues innervated with minor nerve fibers, as well as in endoneural part of peripheral nerves, brain's tunic and blood vessels [57]. Various subpopulations of leukocytes, epithelial and stromal cells, spinal ganglia, keratinocytes and fibroblasts were found to express IL31RA [20, 58]. IL31 and its receptor play an important part in regulation of neuroinflammation. IL31 promotes tissue remodeling and inflammation through induction of IL6, chemokines and matrix metalloproteinases [59, 60]. Compared to healthy donors, RRMS patients had high level of IL31 in serum, which decreased during remissions [19, 52]. The patients involved in this study also had IL31 hyperproduced during exacerbations, but it was not related to PHVI reactivation.

IL33 is a member of the IL1 family, which includes IL1β and IL18. It plays an important role in pathogenesis of various diseases, including MS [55]. Compared to healthy donors, RRMS patients were found to have significantly higher level of blood serum IL33 [52]. The action of IL33 is realized through binding to its receptor, ST2, which can be soluble (pST2) and membrane-bound (ST2). The first form of the receptor is a decoy, it isolates free IL33 and thus locally restricts the activity of extracellular IL33, which allows avoiding undesirable consequences of inflammatory reactions [62]. IL33 affects various types of cells bearing ST2 receptors on their surfaces. The list includes eosinophiles and basophiles, mast cells, Th1 and Th2 lymphocytes, cytotoxic T lymphocytes, natural killers and Type 2 innate lymphocytes [63]. Membrane-bound ST2 activates the MyD88/NF-kB signal pathway reinforcing function of mast cells, Th2 cells, regulatory T cells and Type 2 innate lymphocytes [62].

It is believed that polymorphism of IL33 and ST2 play an important part in the development of MS. There are data suggesting connection between single nucleotide polymorphism rs1929992 in the gene of IL33 and various courses of MS [64]. Another controlled study reports no significant differences in the frequency of detection of three single nucleotide polymorphisms, IL4 (rs2070874), IL17A (rs2275913) and IL33 (rs7044343) [65]. Only the genetic polymorphism rs10204137 of IL33 receptor's gene was shown to have associations with MS against the background of high levels of this protein [66].

While IL33 is one of the best studied cytokines in the context of neural system pathologies and MS, its participation in neuroinflammation and neurodegeneration is ambiguous. It is expressed not only on astrocytes and oligodendrocytes but also on neurons and microglia cells [67]. ST2, the receptor of IL33, is mainly found on neurons and oligodendrocytes. The cross-expression of IL33 and ST2 on various CNS cells indicates the complexity of autocrine and paracrine mechanisms of IL33/ST2 signaling in CNS, in addition to the protein's immunomodulating action in cases of inflammation [67].

IL33 boosts invasion of CNS by immune cells from the blood flow and activation of the resident immune cells [55]. IL33 directly affects oligodendrocytes and activates astrocytes [67–69].

In MS patients, peripheral leukocytes and astrocytes are the important sources of IL33, which activates the microglia cells [16, 70]. IL33 released by the glia forces neighboring cells to produce inflammatory molecules that are detrimental to neurons [71, 72]. The glial maturation factor also makes astrocytes produce IL33 faster, and the protein acts synergistically with it and promotes synthesis of TNF-α by these cells [73]. Incubation of the mixes of astrocytes and neurons or only neurons with IL33 decreases their amount, rids neurons of their processes, destroys their network and shapes neurite-like changes of the cells' exterior [73].

IL33 also participates in damaging and disruption of reparation of myelin. Experiments on the co-cultures of myelinated cells of rat's CNS have shown that IL33, while not influencing the density of axons, can suppress their myelination significantly [67]. In MS patients, the levels of IL33 mRNA and IL33 itself are very high in the lesions [16]. Foci of inflammation were also found to host high local expression of ST2 in axons and damaged myelin, as opposed to its diffused distribution in the normal human brain cortex [67].

At the same time, there is an ongoing discussion about the neuroprotective effects of IL33. The plasma levels of IL33 were revealed to be increased in patients with mild MS, and blood concentration of this cytokine shown to correlate negatively with the amount of T2 hyperintensive lesions seen on MRI scans [21]. The growth of IL17A and IL33 in the blood serum of MS patients is not connected to EDSS [65]. Macrophages are known to actively participate in inflammatory processes with MS in the background [74]. IL33 modulates polarization of microglia into the M2 phenotype and promotes neuroprotection [75].

Administration of recombinant IL33 to mice with experimental autoimmune encephalomyelitis (EAE) after onset of the disease switches the immune response from proinflammatory, mediated by Th1 and Th17 cells, to antiinflammatory, dependent on Th2. M2 polarized macrophages produce less IL17 and INF-γ and more IL5 and IL13 [76]. In EAE cases, high levels of circulating IL33 are considered to constitute the mechanism self-limiting chronic inflammation. With low concentration, the effect produced by IL33 may be insufficient, which is compensated for by production of other cytokines, such as IL1. It seems like these mechanisms are universally important; they also play a part in prevention of generalized encephalitis with a herpes infection in the background, which is confirmed by the increased levels of IL1β and IL33 in the reactivated PHVI group.

Gender is also a factor. Experiments on SJL mice infected with EAE have shown that male subjects had the concentration of testosterone growing when they were immunized with myelin peptide (PLP139-151), which stimulates production of IL33 by mast cells with androgen receptor on their surface [77]. IL33 activates Type 2 innate lymphocytes producing IL13, which accumulate in lymph glands, brain tunics and CNS, and promote Th2 dependent protective response. In male specimen, ST2+ maste cells and basophils sensitive to IL33 boost polarization of Th2 cells through production of IL4 and IL13.

With testosterone level low, mast cells in female specimen express molecules of IL1β and TNF-α instead of IL33; moreover, its insufficient amount disallows activation of Type 2 innate lymphocytes. These lymphocytes, in turn, are known to help restore tissues, they actively express IL33's receptor on its surface and can produce IL4, IL5, IL9, IL13 [63, 78]. Without the suppressive effect of IL33, the encephalitogenic Th17 dependent immune response prevails in females. This response can be inhibited by administration of exogenous IL33.

Through activation of Type 2 innate lymphocytes, IL33 controls accumulation of regulatory T cells in the foci of inflammation, as well as their effector function and macrophage polarization [79]. IL33 also stimulates regulatory B cells that are important for maintaining peripheral tolerance and suppression of inflammatory autoimmune reactions. Administration of IL33 to mice increases the amount of B cells producing IL10 [80, 81].

IL33 participates in the innate immune response to tissue damage peculiar to infections. However, this cytokine appears in circulation and functions differently from IL1β and IL18 [79]. Typically, IL33 is released from cells as a biologically active full-sized molecule during necrosis or necroptosis, but not cell apoptosis [82, 83]. As opposed to IL1β and IL18, formation of a biologically active form of IL33 does not require preconditioning with caspase 1 and participation of inflammasome. On the contrary, its molecule can undergo apoptosis-associated scission by caspases 3 and 7, which makes half-life of IL33 shorter and decreases its biological activity [84]. Inactivation of IL33 via caspases suppresses the immune response, not enhances it. IL33 is also contained in the cell nucleus as a chromatin-associated factor, which is rapidly released during their necrosis [85, 86]. Interacting directly with NF-kB, nuclear IL33 isolates it and prevents signal transmission, acting as a nuclear transcription suppressor and thereby reducing the pro-inflammatory activity of cells [87].

Other enzymes, such as neutrophil serine proteases, cathepsin G and elastase, are capable of sciccioning IL33 and, unlike caspases, increase the biological activity of cut forms by 10–30 times compared to the full-size form [88, 89]. Mast cell-specific chymase and tryptase generate a form of IL33 with enhanced ability to activate Type 2 innate lymphocytes [90], which, unlike Type 1 and Type 3 innate lymphocytes, are not present in active lesions in MS patients [12] but participate in HSV-IL2-induced demyelination of the CNS, as shown in a mice model of MS [91].

Necroptosis was found to develop against the background of MS [92]. Cortical lesion samples from a patient with caspase 8 activation defect contained mediators RIPK1, RIPK3, MLKL characteristic of it. The mechanisms of necroptosis induced by TNF-a lead to degeneration of oligodendrocytes, and inhibition of receptor of protein kinase 1 (RIPK1) prevents their death [92].

Necrosis and necroptosis of cells are also peculiar to an HSV infection [93]. Such an infection makes various molecules, including the viral DNA genome, RNA types obtained by transcription, non-coding cellular RNAs, activate transmembrane (toll-like) and cytosolic pattern recognition receptors associated with pathogens, and they transmit signals through individual adapter proteins to initiate innate antiviral immunity. This leads to the production of cytokines, cell necroptosis through mechanisms similar to those in MS, which are linked with protein kinase-3 by its receptor (RIPK3), and activation of the NF-kB pathway [94].

Programmed necrotic cell death limits virus replication and virion propagation [95]. In such situations, IL33 appear in the circulation and acts as an alarm signal. It initiates biological effects aimed at elimination of threats to the body, including through the of production of pro-inflammatory cytokines [55]. Activation of NF-kB via toll-like receptor signaling pathways leads to secretion of TNF-α and IL1-β, which mediate the transcription of IL33 [96, 97]. IL33 itself also induces mRNA expression in TNF-α and IL1-β microglia.

In many cases, the combined increase of IL33 and IL31 correlates with the severity of signs of inflammation [55]. It is believed that IL33 secreted as a result of cell damage promotes IL4-dependent release of IL31 by Th2 cells [98]. These data may explain the association of IL33 and IL31 we have registered during MS exacerbations, as well as the joint production of IL33 and IL1β, IL4, IL23 in the reactivated herpes infection group.

There is a delicate balance between direct damage (necrosis) to cells in an HSV infection case and an immune response to it [99]. In infection recurrence, excessive cytokine production can not only limit the spread of the virus but also activate mechanisms of cell necroptosis with organ dysfunction, which is especially important for the CNS, where tissue regeneration capabilities are limited [12, 99, 100].

The reflection of these processes, apparently, is the increase in the concentration of IL33 detected by us mainly during reactivation of HSV. It is possible that α-herpes viruses, HSV-1 and HSV-2, as well as VZV, should not be considered an etiological cause of MS in most cases; rather, they may be viewed as a factor contributing to excessive activation of the immune system in genetically predisposed individuals, which is crucial for progression of demyelinating diseases. Processes such as molecular mimicry, regulation of endogenous retroviruses, or impaired remyelination can be mediated by this pathogen [101], and frequent relapses of this infection create conditions for the progression of neurodegeneration and transition of RRMS into SPMS.

Our data are consistent with the opinion of other researchers about the importance of the IL31/IL33/ST2 axis in the development of MS, which is possibly based on its participation in demyelination in the CNS, in contrast to the protective antiinflammatory function of the injected recombinant IL33. Moreover, they expand our understanding of the involvement of herpetic infections in immuno-inflammatory reactions and processes of demyelination or remyelination disorders characteristic of MS. Further investigation of functioning of IL10, IL31 and IL33/ST2 systems, which are an important link between immune cells, the nervous system and the epithelial tissues, under herpes viral load, will be crucial for the development of new approaches to treatment of MS [102].

CONCLUSION

The results of this work indicate the important involvement of IL10, IL31 and IL33 in the pathogenesis of MS, but their role is ambiguous. We believe that the increase of level of IL10 in MS patients, during exacerbations and otherwise, largely depends on the realization of its biological role in inflammation caused by an EBV infection. On the contrary, the combined growth of the levels of IL1ß, IL23 and especially IL33, registered during reactivation of PHVI, is apparently triggered by HSV and VZV.

Our study was exploratory in nature, we did not formally assess the sample size and adjusted for multiple comparisons, therefore, the results/trends learned should be confirmed in future works. Nevertheless, this study reflects the data of real clinical practice of managing patients with RRMS, which brings us closer to deciphering the mechanisms involved in exacerbation of MS and progression of the disease.

References

1. Бойко А. Н., Хачанова Н. В., Мельников М. В., Сиверцева С. А., Евдошенко Е. П., Спирин Н. Н. и др. Новые направления иммунокоррекции при рассеянном склерозе. Журнал неврологии и психиатрии им. С. С. Корсакова. 2020; 120 (2): 103–9. DOI: 10.17116/jnevro2020120021103.
2. Göbel K, Ruck T, Meuth SG. Cytokine signaling in multiple sclerosis: Lost in translation. Mult Scler J. 2018; 24 (4): 432–9. DOI: 10.1177/ 1352458518763094.
3. D'Angelo C, Reale M, Costantini E, Di Nicola M, Porfilio I, de Andrés C, et al. Profiling of Canonical and Non-Traditional Cytokine Levels in Interferon-β-Treated Relapsing–Remitting-Multiple Sclerosis Patients. Front Immunol. 2018, 9: 1240. DOI: 10.3389/fimmu.2018.01240.
4. Бойко А. Н., Смирнова Н. Ф., Золотова С. Н., Гусев Е. И. Эпидемиология и этиология рассеянного склероза. Consilium Medicum. 2008; 10 (7): 5–8.
5. Pietropaolo V, Fioriti D, Mischitelli M, Anzivino E, Santini M, Millefiorini E, et al. Detection of human herpesviruses and polyomaviruses DNA in a group of patients with relapsing-remitting multiple sclerosis. New Microbiol. 2005; 28 (3): 199–203.
6. Sotelo J, Ordonez G, Pineda B, Flores J. The participation of varicella zoster virus in relapses of multiple sclerosis. Clin Neurol Neurosurg. 2014; 119: 44–8. DOI: 10.1016/j.clineuro.2013.12.020.
7. Engdahl E, Gustafsson R, Huang J, Biström M, Lima Bomfim I, Stridh P, et al. Increased Serological Response Against Human Herpesvirus 6A Is Associated With Risk for Multiple Sclerosis. Front Immunol. 2019; 10: 2715. DOI: 10.3389/fimmu.2019.02715.23.
8. Попова Е. В., Бойко А. Н., Хачанова Н. В., Шаранова С. Н. Вирус Эпштейна–Барр в патогенезе рассеянного склероза (обзор). Журнал неврологии и психиатрии им. С.С. Корсакова. Спецвыпуски. 2014; 114 (2–2): 29–34.
9. Attfield KE, Jensen LT, Kaufmann M, Friese MA, Fugger L. The immunology of multiple sclerosis. Nat Rev Immunol. 2022; 22: 734–50. DOI: 10.1038/s41577-022-00718-z.
10. Bjornevik K, Cortese M, Healy BC, Kuhle J, Mina MJ, Leng Y, et al. Longitudinal analysis reveals high prevalence of Epstein–Barr virus associated with multiple sclerosis. Science. 2022; 375 (6578): 296–301. DOI: 10.1126/science.abj8222.
11. Bjornevik K, Münz C, Cohen JI, Ascherio A. Epstein–Barr virus as a leading cause of multiple sclerosis: mechanisms and implications. Nat Rev Neurol. 2023; 19 (3): 160–171. DOI: 10.1038/s41582-023-00775-5.
12. Aghbash PS, Hemmat N, Nahand JS, Shamekh A, Memar MY, Babaei A, et al. The role of Th17 cells in viral infections. Int Immunopharmacol. 2021; 91: 107331. DOI: 10.1016/j.intimp.2020.107331.
13. Воробьева А. А., Иванова М. В., Фоминых В. В., Захарова М. Н., Зигангирова Н. А., Гуляева Н. В. Биомаркеры рассеянного склероза (обзор и собственные данные). Журнал неврологии и психиатрии им. С.С. Корсакова. Спецвыпуски. 2013; 113 (10–2): 23–31.
14. D'Ambrosio A, Pontecorvo S, Colasanti T, Zamboni S, Francia A, Margutti P. Peripheral blood biomarkers in multiple sclerosis. Autoimmun. Rev. 2015; 14: 1097–110. DOI: 10.1016/j.autrev.2015.07.014 1568-9972.
15. Melamud MM, Ermakov EA, Boiko AS, Kamaeva DA, Sizikov AE, Ivanova SA, et al. Multiplex Analysis of Serum Cytokine Profiles in Systemic Lupus Erythematosus and Multiple Sclerosis. Int J Mol Sci. 2022; 23: 13829. DOI: 10.3390/ijms232213829.
16. Christophi GP, Gruber RC, Panos M, Christophi RL, Jubelt B, Massa PT. Interleukin-33 upregulation in peripheral leukocytes and CNS of multiple sclerosis patients. Clin Immunol. 2012; 142 (3): 308–19. DOI: 10.1016/j.clim.2011.11.007.
17. Sosvorova L, Kanceva R, Vcelak J, Kancheva L, Mohapl M, Starka L, et al. The comparison of selected cerebrospinal fluid and serum cytokine levels in patients with multiple sclerosis and normal pressure hydrocephalus. Neuro Endocrinol Lett. 2015; 36 (6): 564–71. PMID: 26812299.
18. Alsahebfosoul F, Rahimmanesh I, Shajarian M, Etemadifar M, Sedaghat N, Hejazi Z, et al. Interleukin-33 plasma levels in patients with relapsing-remitting multiple sclerosis. BioMol Concepts. 2017; 8 (1): 55–60. DOI: 10.1515/bmc-2016-0026.
19. de J Guerrero-García J, Rojas-Mayorquín AE, Valle Y, Padilla-Gutiérrez JR, Castañeda-Moreno VA, Mireles-Ramírez MA, et al. Decreased serum levels of sCD40L and IL-31 correlate in treated patients with Relapsing-Remitting Multiple Sclerosis. Immunobiology. 2018; 223: 135–41. DOI: 10.1016/j.imbio.2017.10.001.
20. Franzoi AEA, Gonçalves MVM, Nascimento O, Becker J. Interleukin 31 and Mast Cells: A New Piece in the Puzzle of the Pathophysiology of Multiple Sclerosis? Int J Brain Disord Treat. 2018; 4: 026. DOI: 10.23937/2469-5866/1410026.
21. Maier S, Motataianu A, Barcutean L, Balint A, Hutanu A, Zoltan B, et al. A Interferon-β 1a, an immunomodulatory in relapsing remitting multiple sclerosis patients. The effect on pro-inflammatory cytokines. Farmacia. 2020; 68 (1): 65–75. DOI: 10.31925/farmacia.2020.1.10.
22. Polman CH, Reingold SC, Banwell B, Clanet M, Cohen JA, Filippi M, et al. Diagnostic criteria for multiple sclerosis: 2010 revisions to the McDonald criteria. Ann Neurol. 2011; 69 (2): 292–302. DOI: 10.1002/ana.22366.
23. Kurtzke JF. Rating neurologic impairment in multiple sclerosis: An expanded disability status scale (EDSS). Neurology. 1983; 33: 1444–52. DOI: 10.1212/WNL.33.11.1444.
24. Lublin FD, Reingold SC, Cohen JA, Cutter GR, Sørensen PS, Thompson AJ, et al. Defining the clinical course of multiple sclerosis: the 2013 revisions. Neurology. 2014; 83 (3): 278–286. DOI: 10.1212/WNL.0000000000000560.
25. Бойко А. Н., Гусева М. Р., Хачанова Н. В., Гусев Е. И. Вопросы современной терминологии при рассеянном склерозе. Журнал неврологии и психиатрии им. С. С. Корсакова. Спецвыпуски. 2018; 118 (8–2): 121–7. DOI: 10.17116/jnevro2018118082121.
26. Bărcuţean LI, Romaniuc A, Maier S, Bajko Z, Moţăţăianu A, Adina H, et al. Clinical and serological biomarkers of treatment's response in multiple sclerosis patients treated continuously with interferonβ-1b for more than a decade. CNS Neurol Disord Drug Targets. 2018; 17 (10): 780–92. DOI: 10.2174/1871527317666180917095256.
27. Ad'hiah AH, Salman ED. Predictive Significance of Interleukins 17A and 33 in Risk of Relapsing–Remitting Multiple Sclerosis. Baghdad Science J. 2022; 1191–200. DOI: 10.21123/bsj.2022.6431.
28. Mado H, Adamczyk-Sowa M, Bartman W, Wierzbicki K, Tadeusiak B, Sowa P. Plasma Interleukin-33 level in relapsing-remitting multiple sclerosis. Is it negatively correlated with central nervous system lesions in patients with mild disability? Clin Neurol Neurosurg. 2021; 206: 106700. DOI: 10.1016/j.clineuro.2021.106700.
29. Мельников М. В., Шаранова С. Н., Коновалова О. Е., Смирнова Н. Ф., Пащенков М. В., Бойко А. Н. Влияние глатирамера ацетата на функционирование Th1- и Th17-клеток у больных рассеянным склерозом. Журнал неврологии и психиатрии им. С. С. Корсакова. 2018; 8 (2): 151. DOI: 10.17116/jnevro2018118082121.
30. Оспельникова Т. П., Морозова О. В., Исаева Е. И., Лиждвой В. Ю., Колодяжная Л. В., Андреева С. А. и др. Мониторинг цитокинов у больных рассеянным склерозом в процессе лечения препаратом IFNβ-1a. Журнал неврологии и психиатрии им. С. С. Корсакова. Спецвыпуски. 2015; 115 (8–2): 71–71.
31. Якушина Т. И., Лиждвой В. Ю., Василенко И. А., Андрюхина О. М., Котов С. В. Дополнительные показатели для оценки эффективности терапии рассеянного склероза (предварительные данные). Журнал неврологии и психиатрии им. С. С. Корсакова. Спецвыпуски. 2013; 113 (2–2): 61–65.
32. Сурсякова Н. В., Байдина Т. В., Куклина Е. М., Трушникова Т. Н., Ожгибесова Т. В. Факторы, регулирующие активность В-лимфоцитов, как потенциальные биомаркеры рассеянного склероза. Журнал неврологии и психиатрии им. С. С. Корсакова. Спецвыпуски. 2019; 119 (2–2): 24–27. DOI: 10.17116/jnevro20191192224.

33. Soldan SS, Lieberman PM. Epstein–Barr virus and multiple sclerosis. Nat Rev Microbiol. 2023; 21 (1): 51–64. DOI: 10.1038/s41579-022-00770-5;
34. Pender MP, Csurhes PA, Burrows JM, Burrows SR. Defective T-cell control of Epstein–Barr virus infection in multiple sclerosis. Clin Transl Immunology. 2017; 6 (1): e126. DOI: 10.1038/cti.2016.87.
35. Grut V, Biström M, Salzer J, Stridh P, Jons D, Gustafsson R, et al. Cytomegalovirus seropositivity is associated with reduced risk of multiple sclerosis-a presymptomatic case-control study. Eur J Neurol. 2021; 28 (9): 3072–9. DOI: 10.1111/ene.14961.
36. Zhao J, Qin C, Liu Y, Rao Y, Feng P. Herpes simplex virus and pattern recognition receptors: an arms race. Front Immunol. 2021; 11: 613799. DOI: 10.3389/fimmu.2020.613799.
37. Najafi S, Ghane M, Poortahmasebi V, Jazayeri S, Yousefzadeh-Chabok, S. Prevalence of herpes simplex virus in patients with relapsing-remitting multiple sclerosis: a case-control study in the North of Iran. Arch Clin Infect Dis. 2016; 11: e36576. DOI: 10.5812/archcid.36576.
38. Duarte LF, Farıas MA, A´lvarez DM, Bueno SM, Riedel CA, Gonzálex PA. Herpes simplex virus type 1 infection of the central nervous system: insights into proposed interrelationships with neurodegenerative disorders. Front Cell Neurosci. 2019; 13: 46. DOI: 10.3389/fncel.2019.00046.
39. Грись М. С., Баранова Н. С., Спирин Н. Н., Касаткин Д. С., Киселев Д. В., Шипова Е. Г. Рассеянный склероз у пациентов с герпесвирусной инфекцией: особенности клинической картины и течения. Неврология, нейропсихиатрия, психосоматика. 2021; 13 (Прил. 1): 21–26. DOI: 10.14412/2074-2711-2021-1S-21-26.
40. Ferrante P, Mancuso R, Pagani E, Guerini FR, Calvo MG, Saresella M, et al. Molecular evidences for a role of HSV-1 in multiple sclerosis clinical acute attack. J Neurovirol. 2000; 6 (2): 109–14. PMID: 10871797.
41. Waubant E, Mowry EM, Krupp L, Chitnis T, Yeh EA, Kuntz N, Common viruses associated with lower pediatric multiple sclerosis risk. Neurology. 2011; 76 (23): 1989–95. DOI: 10.1212/WNL.0b013e31821e552a.
42. Гончарова З. А., Беловолова Р. А., Мегерян В. А. Клинико-иммунологические особенности рассеянного склероза на фоне реактивации персистирующей герпесвирусной инфекции. Саратовский научно-медицинский журнал. 2018; 14 (1): 126–32.
43. Kwilasz AJ, Grace PM, Serbedzija P, Maier SF, Watkins LR. The therapeutic potential of interleukin-10 in neuroimmune diseases. Neuropharmacology. 2015; 96: 55–57. DOI: 10.1016/j.neuropharm.2014.10.020.
44. Rojas JM, Avia M, Martín V, Sevilla N. IL-10: A Multifunctional Cytokine in Viral Infections. J Immunol Res. 2017; 2017: 6104054. DOI: 10.1155/2017/6104054.
45. Zhang L, Yuan S, Cheng G, Guo B. Type I IFN promotes IL10 production from T cells to suppress Th17 cells and Th17-associated autoimmune inflammation. PLoS One. 2011; 6 (12): 1–11. DOI: 10.1371/journal.pone.0028432.
46. Schönrich G, Abdelaziz MO, Raftery MJ. Epstein–Barr virus, interleukin-10 and multiple sclerosis: A me´nage à trois. Front. Immunol. 2022; 13: 1028972. DOI: 10.3389/fimmu.2022.1028972.
47. Jog NR, Chakravarty EF, Guthridge JM, James JA. Epstein Barr Virus Interleukin 10 Suppresses Anti-inflammatory Phenotype in Human Monocytes. Front Immunol. 2018; 9: 2198. DOI: 10.3389/fimmu.2018.02198.
48. Kang MS, Kieff E. Epstein–Barr virus latent genes. Exp Mol Med. 2015; 47 (1): e131. DOI: 10.1038/emm.2014.84.
49. Maertzdorf J, Osterhaus AD, Verjans GM. IL-17 expression in human herpetic stromal keratitis: modulatory effects on chemokine production by corneal fibroblasts. J Immunol. 2002; 169 (10): 5897–903. DOI: 10.4049/jimmunol.169.10.5897.
50. Fredj NB, Rizzo R, Bortolotti D, Nefzi F, Chebel S, Rotola A, et al., Evaluation of the implication of KIR2DL2 receptor in multiple sclerosis and herpesvirus susceptibility. J Neuroimmunol. 2014; 271 (1–2): 30–35. DOI: 10.1016/j.jneuroim.2014.03.017.
51. Rizzo R, Bortolotti D, Fainardi E, Gentili V, Bolzani S, Baldi E, et al. KIR2DL2 inhibitory pathway enhances Th17 cytokine secretion by NK cells in response to herpesvirus infection in multiple sclerosis patients. J Neuroimmunol. 2016; 294: 1–5. DOI: 10.1016/j.jneuroim.2016.03.007.
52. Maier S, Simu M, Hutanu A, Barcutean L, Voidazan S, Bajko Z, et al. Clinical immunological correlations in patients with multiple sclerosis treated with natalizumab. Brain Sci. 2020; 10 (11): 802. DOI: 10.3390/brainsci10110802.
53. Watford WT, Moriguchi M, Morinobu A, O'Shea JJ. The biology of IL-12: coordinating innate and adaptive immune responses. Cytokine Growth Factor Rev. 2003; 14: 361–68. DOI: 10.1016/S1359-6101(03)00043-1.
54. Broberg EK, Setala N, Eralinna JP, Salmi AA, Roytta M, Hukkanen V. Herpes simplex virus type 1 infection induces upregulation of interleukin-23 (p19) mRNA expression in trigeminal ganglia of BALB/c mice. J Interferon Cytokine Res. 2004; 22: 641–51. DOI: 10.1089/10799900260100123.
55. Di Salvo E, Ventura-Spagnolo E, Casciaro M, Navarra M, Gangemi S. IL-33/IL-31 axis: a potential inflammatory pathway. Mediator. Inflammat. 2018: 3858032. DOI: 10.1155/2018/3858032.
56. Maier E, Werner D, Duschl A, Bohle B, Horejs-Hoeck J. Human Th2 but not Th9 cells release IL-31 in a STAT6/ NF-κB–dependent way. J Immunol. 2014; 193 (2): 645–54. DOI: 10.4049/jimmunol.1301836.
57. Dong H, Zhang X, Qian Y. Mast cells and neuroinflammation. Med Sci Monit Basic Res. 2014; 20: 200–6. DOI: 10.12659/MSMBR.893093.
58. Nemmer JM, Kuchner M, Datsi A, Oláh P, Julia V, Raap U, et al. Interleukin-31 signaling bridges the gap between immune cells, the nervous system and epithelial tissues. Front Med. 2021; 8: 639097. DOI: 10.3389/fmed.2021.639097.
59. Singh B, Jegga AG, Shanmukhappa KS, Edukulla R, Khurana Hershey GH, Medvedovic M, et al. IL-31-driven skin remodeling involves epidermal cell proliferation and thickening that lead to impaired skin-barrier function. PLoS One. 2016; 11 (8): e0161877. DOI: 10.1371/journal.pone.0161877.
60. Yagi Y, Andoh A, Nishida A, Shioya M, Nishimura T, et al. Interleukin-31 stimulates production of inflammatory mediators from human colonic subepithelial myofibroblasts. Int J Mol Med. 2007; 19: 941–6. DOI: 10.3892/ijmm.19.6.941.
61. Jafarzadeh A, Mahdavi R, Jamali M, Hajghani H, Nemati M, Ebrahimi HA. Increased concentrations of Interleukin-33 in the serum and cerebrospinal fluid of patients with multiple sclerosis. Oman Med J. 2016; 31 (1): 40–45. DOI: 10.5001/omj.2016.08.
62. Griesenauer B, Paczesny S. The ST2/IL-33 axis in immune cells during inflammatory diseases. Front Immunol. 2017; 8: 475. DOI: 10.3389/fimmu.2017.00475.
63. Peine M, Marek RM, Löhning M. IL-33 in T Cell Differentiation, Function, and Immune Homeostasis. Trends Immunol. 2016; 37 (5): 321–33. DOI: 10.1016/j.it.2016.03.007.
64. Jamali M, Rostami M, Gholamreza R, Sarab A, Mahdavi R. IL-33 polymorphism rs1929992 and its association with susceptibility to different pattern of multiple sclerosis. Tehran Univ Med J. 2018; 76 (7): 446–51.
65. Al-Naseri MAS, Salman ED, Ad'hiah AH. Genetic analysis of IL4 (rs2070874), IL17A (rs2275913), and IL33 (rs7044343) polymorphisms in Iraqi multiple sclerosis patients by using T-plex real-time PCR method. Meta Gene. 2022; 31: 100986. DOI: 10.1016/j.mgene.2021.100986.
66. Ahmadi M, Fathi F, Fouladi S, Alsahebfosul F, Manian M, Eskandari N. Serum IL-33 level and IL-33, IL1RL1 gene polymorphisms in asthma and multiple sclerosis patients. Curr Mol Med. 2019; 19 (5): 357–63. DOI: 10.2174/1566524019666190405120137.
67. Allan D, Fairlie-Clarke KJ, Elliott CD, Schuh C, Barnett SC, Lassmann H, et al. Role of IL-33 and ST2 signalling pathway in multiple sclerosis: expression by oligodendrocytes and inhibition of myelination in central nervous system. Acta Neuropathol. Commun. 2016; 4 (1): 75. DOI: 10.1186/s40478-016-0344-1.
68. Pei C, Barbour M, Fairlie-Clarke KJ, Allan D, Mu R, Jiang HR. Emerging role of interleukin-33 in autoimmune diseases. Immunology. 2014; 141: 9–1. DOI: 10.1111/imm.12174.
69. Hudson CA, Christophi GP, Gruber RC, Wilmore JR, Lawrence DA, Massa PT. Induction of IL-33 expression and activity in central

nervous system glia. J Leukocyte Biol. 2008; 84: 631–43. DOI: 10.1189/jlb.1207830.
70. Zhang F, Tossberg JT, Spurlock CF, Yao SY, Aune TM, Sriram S. Expression of IL-33 and its epigenetic regulation in multiple sclerosis. Ann Clin Transl Neurol. 2014; 1: 307–18. DOI: 10.1002/acn3.47.
71. Gadani SP, Walsh JT, Smirnov I, Zheng J, Kipnis J. The glia-derived alarmin IL-33 orchestrates the immune response and promotes recovery following CNS injury. Neuron. 2015; 85: 703–9. DOI: 10.1016/j.neuron.2015.01.013.
72. Yasuoka S, Kawanokuchi J, Parajuli B, Jin S, Doi Y, Noda M, et al. Production and functions of IL-33 in the central nervous system. Brain Res. 2011; 1385: 8–17. DOI: 10.1016/j.brainres.2011.02.045.
73. Kempuraj D, Khan MM, Thangavel R, Xiong Z, Yang E, Zaheer A. Glia maturation factor induces interleukin-33 release from astrocytes: implications for neurodegenerative diseases. J Neuroimmune Pharmacol. 2013; 8: 643–50. DOI: 10.1007/s11481-013-9439-7.
74. Мельников М. В., Свиридова А. А., Роговский В. С., Бойко А. Н., Пащенков М. В. Роль макрофагов в развитии нейровоспаления при рассеянном склерозе. Журнал неврологии и психиатрии им. С. С. Корсакова. 2022; 122 (5): 51–56. DOI: 10.17116/jnevro202212205151.
75. Franco R, Fernández-Suárez D. Alternatively activated microglia and macrophages in the central nervous system. Prog Neurobiol. 2015; 131: 65–86. DOI: 10.1016/j.pneurobio.2015.05.003.
76. Jiang HR, Milovanović M, Allan D, Niedbala W, Besnard AG, Fukada SY, et al. IL-33 attenuates EAE by suppressing IL-17 and IFN-γ production and inducing alternatively activated macrophages. Eur J Immunol. 2012; 42: 1804–14. DOI: 10.1002/eji.20114194718.
77. Russi AE, Ebel ME, Yang Y, Brown MA. Male-specific IL-33 expression regulates sex-dimorphic EAE susceptibility. PNAS. 2018; 115 (7): E1520–E1529. DOI: 10.1073/pnas.1710401115.
78. Klose CS, Artis D. Innate lymphoid cells as regulators of immunity, inflammation and tissue homeostasis. Nat Immunol. 2016; 17 (7): 765–774. DOI: 10.1038/ni.3489.
79. Braun H, Afonina IS, Mueller C, Beyaert R. Dichotomous function of IL-33 in health and disease: From biology to clinical implications. Biochemical Pharmacology. 2018; 148: 238–52. DOI: 10.1016/j.bcp.2018.01.0100006-2952.
80. Komai-Koma M, Gilchrist DS, McKenzie AN, Goodyear CS, Xu D, Liew FY. IL-33 activates B1 cells and exacerbates contact sensitivity. J Immunol. 2011; 186 (4): 2584–91. DOI: 10.4049/jimmunol.1002103.
81. Sattler S, Ling GS, Xu D, Hussaarts L, Romaine A, Zhao H, et al. IL-10- producing regulatory B cells induced by IL-33 (Breg(IL-33)) effectively attenuate mucosal inflammatory responses in the gut. J Autoimmun. 2014; 50: 107–22. DOI: 10.1016/j.jaut.2014.01.032.
82. Cayrol C, Girard J-Ph. Interleukin-33 (IL-33): a nuclear cytokine from the IL-1 family. Immunol Rev. 2018; 281: 154–168. DOI: 10.1111/imr.12619.
83. Bertheloot D, Latz E, Franklin BS. Necroptosis, pyroptosis and apoptosis: an intricate game of cell death. Cell Mol Immunol. 2021; 18: 1106–21. DOI: 10.1038/s41423-020-00630-3.
84. Lüthi AU, Cullen SP, McNeela EA, Duriez PJ, Afonina IS, Sheridan C, et al. Suppression of interleukin-33 bioactivity through proteolysis by apoptotic caspases. Immunity. 2009; 31: 84–98. DOI: 10.1016/j.immuni.2009.05.007.
85. Carriere V, Roussel L, Ortega N, Lacorre DA, Americh L, Aguilar L, et al. IL-33, the IL-1-like cytokine ligand for ST2 receptor, is a chromatin-associated nuclear factor in vivo. Proc Natl Acad Sci USA. 2007; 104 (1): 282–7. DOI: 10.1073/pnas.0606854104.
86. Cayrol C, Girard JP. IL-33: an alarmin cytokine with crucial roles in innate immunity, inflammation and allergy. Curr Opin Immunol. 2014; 31: 31–7. DOI: 10.1016/j.coi.2014.09.004.
87. Ali S, Mohs A, Thomas M, Klare J, Ross R, Schmitz ML, et al. The dual function cytokine IL-33 interacts with the transcription factor NF-kappaB to dampen NF-kappaB-stimulated gene transcription. J Immunol. 2011; 187 (4): 1609–16. DOI: 10.4049/jimmunol.1003080.
88. Lefrancais E, Roga S, Gautier V, Gonzalez-de-Peredo A, Monsarrat B, Girard JP, et al. IL-33 is processed into mature bioactive forms by neutrophil elastase and cathepsin G. Proc Natl Acad Sci USA. 2012; 109 (5): 1673–8. DOI: 10.1073/pnas.1115884109.
89. Waern I, Lundequist A, Pejler G, Wernersson S. Mast cell chymase modulates IL-33 levels and controls allergic sensitization in dust-mite induced airway inflammation. Mucosal Immunol. 2013; 6 (5): 911–20. DOI: 10.1038/ mi.2012.129.
90. Lefrancais E, Duval A, Mirey E, Roga S, Espinosa E, Cayrol C, et al. Central domain of IL-33 is cleaved by mast cell proteases for potent activation of group-2 innate lymphoid cells. Proc Natl Acad Sci U S A. 2014; 111 (43): 15502–7. DOI: 10.1073/pnas.1410700111.
91. Hirose S, Jahani PS, Wang S, Jaggi U, Tormanen K, Yu J, et al. Type 2 innate lymphoid cells induce CNS demyelination in an HSV-IL-2 mouse model of multiple sclerosis. iScience. 2020; 23 (10): 101549. DOI: 10.1016/j.isci.2020.101549.
92. Ofengeim D, Ito Y, Najafov A, Zhang Y, Shan B, DeWitt JP, et al. Activation of necroptosis in multiple sclerosis. Cell Rep. 2015; 10: 1836–49. DOI: 10.1016/j.celrep.2015.02.051.
93. Verzosa AL, McGeever LA, Bhark SJ, Delgado T, Salazar N, Sanchez EL. Herpes simplex virus 1 infection of neuronal and nonneuronal cells elicits specific innate immune responses and immune evasion mechanisms. Front Immunol. 2021; 12: 644664. DOI: 10.3389/fimmu.2021.644664.
94. Zhao J, Qin C, Liu Y, Rao Y, Feng P. Herpes simplex virus and pattern recognition receptors: an arms race. Front Immunol. 2021; 11: 613799. DOI: 10.3389/fimmu.2020.613799.
95. Kaiser WJ, Upton JW, Mocarski ES. Receptor-interacting protein homotypic interaction motif-dependent control of NF-kappa B activation via the DNA dependent activator of IFN regulatory factors. J Immunol. 2008; 181: 6427–34. DOI: 10.4049/jimmunol.181.9.6427 104.
96. Nile CJ, Barksby E, Jitprasertwong P, Preshaw PM, Taylor JJ. Expression and regulation of interleukin-33 in human monocytes. Immunology. 2010; 130 (2): 172–80. DOI: 10.1111/j.1365-2567.2009.03221.x.
97. Zhang L, Lu R, Zhao G, Pflugfelder SC, Li DQ. TLR-mediated induction of pro-allergic cytokine IL-33 in ocular mucosal epithelium. Int J Biochem Cell Biol. 2011; 43: 1383–91. DOI: 10.1016/j.biocel.2011.06.003.
98. Furue M, Yamamura K, Kido-Nakahara M, Nakahara T, Fukui Y. Emerging role of interleukin-31 and interleukin-31 receptor in pruritus in atopic dermatitis. Allergy. 2018; 73 (1): 29–36. DOI: 10.1111/all.13239.
99. Ellermann-Eriksen S. Macrophages and cytokines in the early defence against herpes simplex virus. Virology J. 2005; 2: 59. DOI: 10.1186/1743-422X-2-59.
100. Roychoudhury P, Swan DA, Duke E, Corey L, Zhu J, Davé V, et al. Tissue-resident T cell–derived cytokines eliminate herpes simplex virus-2–infected cells. J Clin Invest. 2020; 130 (6): 2903–19. DOI: 10.1172/JCI132583.
101. Bello-Morales R, Andreu S, López-Guerrero JA. The role of herpes simplex virus type 1 infection in demyelination of the central nervous system. Int J Mol Sci. 2020; 21 (14): 5026. DOI: 10.3390/ijms21145026.
102. Sun Y, Wen Y, Wang L, Wen L, You W, Wei S, et al. Therapeutic opportunities of interleukin-33 in the central nervous system. Front Immunol. 2021; 12: 654626. DOI: 10.3389/fimmu.2021.654626.

Литература

1. Бойко А. Н., Хачанова Н. В., Мельников М. В., Сиверцева С. А., Евдошенко Е. П., Спирин Н. Н. и др. Новые направления иммунокоррекции при рассеянном склерозе. Журнал неврологии и психиатрии им. С. С. Корсакова. 2020; 120 (2): 103–9. DOI: 10.17116/jnevro2020120021103.
2. Göbel K, Ruck T, Meuth SG. Cytokine signaling in multiple sclerosis: Lost in translation. Mult Scler J. 2018; 24 (4): 432–9. DOI: 10.1177/ 1352458518763094.

3. D'Angelo C, Reale M, Costantini E, Di Nicola M, Porfilio I, de Andrés C, et al. Profiling of Canonical and Non-Traditional Cytokine Levels in Interferon-β-Treated Relapsing–Remitting-Multiple Sclerosis Patients. Front Immunol. 2018, 9: 1240. DOI: 10.3389/fimmu.2018.01240.
4. Бойко А. Н., Смирнова Н. Ф., Золотова С. Н., Гусев Е. И. Эпидемиология и этиология рассеянного склероза. Consilium Medicum. 2008; 10 (7): 5–8.
5. Pietropaolo V, Fioriti D, Mischitelli M, Anzivino E, Santini M, Millefiorini E, et al. Detection of human herpesviruses and polyomaviruses DNA in a group of patients with relapsing-remitting multiple sclerosis. New Microbiol. 2005; 28 (3): 199–203.
6. Sotelo J, Ordonez G, Pineda B, Flores J. The participation of varicella zoster virus in relapses of multiple sclerosis. Clin Neurol Neurosurg. 2014; 119: 44–8. DOI: 10.1016/j.clineuro.2013.12.020.
7. Engdahl E, Gustafsson R, Huang J, Biström M, Lima Bomfim I, Stridh P, et al. Increased Serological Response Against Human Herpesvirus 6A Is Associated With Risk for Multiple Sclerosis. Front Immunol. 2019; 10: 2715. DOI: 10.3389/fimmu.2019.02715.23.
8. Попова Е. В., Бойко А. Н., Хачанова Н. В., Шаранова С. Н. Вирус Эпштейна–Барр в патогенезе рассеянного склероза (обзор). Журнал неврологии и психиатрии им. С.С. Корсакова. Спецвыпуски. 2014; 114 (2–2): 29–34.
9. Attfield KE, Jensen LT, Kaufmann M, Friese MA, Fugger L. The immunology of multiple sclerosis. Nat Rev Immunol. 2022; 22: 734–50. DOI: 10.1038/s41577-022-00718-z.
10. Bjornevik K, Cortese M, Healy BC, Kuhle J, Mina MJ, Leng Y, et al. Longitudinal analysis reveals high prevalence of Epstein–Barr virus associated with multiple sclerosis. Science. 2022; 375 (6578): 296–301. DOI: 10.1126/science.abj8222.
11. Bjornevik K, Münz C, Cohen JI, Ascherio A. Epstein–Barr virus as a leading cause of multiple sclerosis: mechanisms and implications. Nat Rev Neurol. 2023; 19 (3): 160–171. DOI: 10.1038/s41582-023-00775-5.
12. Aghbash PS, Hemmat N, Nahand JS, Shamekh A, Memar MY, Babaei A, et al. The role of Th17 cells in viral infections. Int Immunopharmacol. 2021; 91: 107331. DOI: 10.1016/j.intimp.2020.107331.
13. Воробьева А. А., Иванова М. В., Фоминых В. В., Захарова М. Н., Зигангирова Н. А., Гуляева Н. В. Биомаркеры рассеянного склероза (обзор и собственные данные). Журнал неврологии и психиатрии им. С.С. Корсакова. Спецвыпуски. 2013; 113 (10–2): 23–31.
14. D'Ambrosio A, Pontecorvo S, Colasanti T, Zamboni S, Francia A, Margutti P. Peripheral blood biomarkers in multiple sclerosis. Autoimmun. Rev. 2015; 14: 1097–110. DOI: 10.1016/j.autrev.2015.07.014 1568-9972.
15. Melamud MM, Ermakov EA, Boiko AS, Kamaeva DA, Sizikov AE, Ivanova SA, et al. Multiplex Analysis of Serum Cytokine Profiles in Systemic Lupus Erythematosus and Multiple Sclerosis. Int J Mol Sci. 2022; 23: 13829. DOI: 10.3390/ijms232213829.
16. Christophi GP, Gruber RC, Panos M, Christophi RL, Jubelt B, Massa PT. Interleukin-33 upregulation in peripheral leukocytes and CNS of multiple sclerosis patients. Clin Immunol. 2012; 142 (3): 308–19. DOI: 10.1016/j.clim.2011.11.007.
17. Sosvorova L, Kanceva R, Vcelak J, Kancheva L, Mohapl M, Starka L, et al. The comparison of selected cerebrospinal fluid and serum cytokine levels in patients with multiple sclerosis and normal pressure hydrocephalus. Neuro Endocrinol Lett. 2015; 36 (6): 564–71. PMID: 26812299.
18. Alsahebfosoul F, Rahimmanesh I, Shajarian M, Etemadifar M, Sedaghat N, Hejazi Z, et al. Interleukin-33 plasma levels in patients with relapsing-remitting multiple sclerosis. BioMol Concepts. 2017; 8 (1): 55–60. DOI: 10.1515/bmc-2016-0026.
19. de J Guerrero-García J, Rojas-Mayorquín AE, Valle Y, Padilla-Gutiérrez JR, Castañeda-Moreno VA, Mireles-Ramírez MA, et al. Decreased serum levels of sCD40L and IL-31 correlate in treated patients with Relapsing-Remitting Multiple Sclerosis. Immunobiology. 2018; 223: 135–41. DOI: 10.1016/j.imbio.2017.10.001.
20. Franzoi AEA, Gonçalves MVM, Nascimento O, Becker J. Interleukin 31 and Mast Cells: A New Piece in the Puzzle of the Pathophysiology of Multiple Sclerosis? Int J Brain Disord Treat. 2018; 4: 026. DOI: 10.23937/2469-5866/1410026.
21. Maier S, Motataianu A, Barcutean L, Balint A, Hutanu A, Zoltan B, et al. A Interferon-β 1a, an immunomodulatory in relapsing remitting multiple sclerosis patients. The effect on pro-inflammatory cytokines. Farmacia. 2020; 68 (1): 65–75. DOI: 10.31925/farmacia.2020.1.10.
22. Polman CH, Reingold SC, Banwell B, Clanet M, Cohen JA, Filippi M, et al. Diagnostic criteria for multiple sclerosis: 2010 revisions to the McDonald criteria. Ann Neurol. 2011; 69 (2): 292–302. DOI: 10.1002/ana.22366.
23. Kurtzke JF. Rating neurologic impairment in multiple sclerosis: An expanded disability status scale (EDSS). Neurology. 1983; 33: 1444–52. DOI: 10.1212/WNL.33.11.1444.
24. Lublin FD, Reingold SC, Cohen JA, Cutter GR, Sørensen PS, Thompson AJ, et al. Defining the clinical course of multiple sclerosis: the 2013 revisions. Neurology. 2014; 83 (3): 278–286. DOI: 10.1212/WNL.0000000000000560.
25. Бойко А. Н., Гусева М. Р., Хачанова Н. В., Гусев Е. И. Вопросы современной терминологии при рассеянном склерозе. Журнал неврологии и психиатрии им. С. С. Корсакова. Спецвыпуски. 2018; 118 (8–2): 121–7. DOI: 10.17116/jnevro2018118082121.
26. Bărcuţean LI, Romaniuc A, Maier S, Bajko Z, Moţăţăianu A, Adina H, et al. Clinical and serological biomarkers of treatment's response in multiple sclerosis patients treated continuously with interferonβ-1b for more than a decade. CNS Neurol Disord Drug Targets. 2018; 17 (10): 780–92. DOI: 10.2174/1871527317666180917095256.
27. Ad'hiah AH, Salman ED. Predictive Significance of Interleukins 17A and 33 in Risk of Relapsing–Remitting Multiple Sclerosis. Baghdad Science J. 2022; 1191–200. DOI: 10.21123/bsj.2022.6431.
28. Mado H, Adamczyk-Sowa M, Bartman W, Wierzbicki K, Tadeusiak B, Sowa P. Plasma Interleukin-33 level in relapsing-remitting multiple sclerosis. Is it negatively correlated with central nervous system lesions in patients with mild disability? Clin Neurol Neurosurg. 2021; 206: 106700. DOI: 10.1016/j.clineuro.2021.106700.
29. Мельников М. В., Шаранова С. Н., Коновалова О. Е., Смирнова Н. Ф., Пащенков М. В., Бойко А. Н. Влияние глатирамера ацетата на функционирование Th1- и Th17-клеток у больных рассеянным склерозом. Журнал неврологии и психиатрии им. С. С. Корсакова. 2018; 8 (2): 151. DOI: 10.17116/jnevro2018118082121.
30. Оспельникова Т. П., Морозова О. В., Исаева Е. И., Лиждвой В. Ю., Колодяжная Л. В., Андреева С. А. и др. Мониторинг цитокинов у больных рассеянным склерозом в процессе лечения препаратом IFNβ-1a. Журнал неврологии и психиатрии им. С. С. Корсакова. Спецвыпуски. 2015; 115 (8–2): 71–71.
31. Якушина Т. И., Лиждвой В. Ю., Василенко И. А., Андрюхина О. М., Котов С. В. Дополнительные показатели для оценки эффективности терапии рассеянного склероза (предварительные данные). Журнал неврологии и психиатрии им. С. С. Корсакова. Спецвыпуски. 2013; 113 (2–2): 61–65.
32. Сурсякова Н. В., Байдина Т. В., Куклина Е. М., Трушникова Т. Н., Ожгибесова Т. В. Факторы, регулирующие активность В-лимфоцитов, как потенциальные биомаркеры рассеянного склероза. Журнал неврологии и психиатрии им. С. С. Корсакова. Спецвыпуски. 2019; 119 (2–2): 24–27. DOI: 10.17116/jnevro20191192224.
33. Soldan SS, Lieberman PM. Epstein–Barr virus and multiple sclerosis. Nat Rev Microbiol. 2023; 21 (1): 51–64. DOI: 10.1038/s41579-022-00770-5;
34. Pender MP, Csurhes PA, Burrows JM, Burrows SR. Defective T-cell control of Epstein–Barr virus infection in multiple sclerosis. Clin Transl Immunology. 2017; 6 (1): e126. DOI: 10.1038/cti.2016.87.
35. Grut V, Biström M, Salzer J, Stridh P, Jons D, Gustafsson R, et al. Cytomegalovirus seropositivity is associated with reduced risk of multiple sclerosis-a presymptomatic case-control study. Eur J Neurol. 2021; 28 (9): 3072–9. DOI: 10.1111/ene.14961.
36. Zhao J, Qin C, Liu Y, Rao Y, Feng P. Herpes simplex virus and

pattern recognition receptors: an arms race. Front Immunol. 2021; 11: 613799. DOI: 10.3389/fimmu.2020.613799.
37. Najafi S, Ghane M, Poortahmasebi V, Jazayeri S, Yousefzadeh-Chabok, S. Prevalence of herpes simplex virus in patients with relapsing-remitting multiple sclerosis: a case-control study in the North of Iran. Arch Clin Infect Dis. 2016; 11: e36576. DOI: 10.5812/archcid.36576.
38. Duarte LF, Farıas MA, A´lvarez DM, Bueno SM, Riedel CA, González PA. Herpes simplex virus type 1 infection of the central nervous system: insights into proposed interrelationships with neurodegenerative disorders. Front Cell Neurosci. 2019; 13: 46. DOI: 10.3389/fncel.2019.00046.
39. Грись М. С., Баранова Н. С., Спирин Н. Н., Касаткин Д. С., Киселев Д. В., Шипова Е. Г. Рассеянный склероз у пациентов с герпесвирусной инфекцией: особенности клинической картины и течения. Неврология, нейропсихиатрия, психосоматика. 2021; 13 (Прил. 1): 21–26. DOI: 10.14412/2074-2711-2021-1S-21-26.
40. Ferrante P, Mancuso R, Pagani E, Guerini FR, Calvo MG, Saresella M, et al. Molecular evidences for a role of HSV-1 in multiple sclerosis clinical acute attack. J Neurovirol. 2000; 6 (2): 109–14. PMID: 10871797.
41. Waubant E, Mowry EM, Krupp L, Chitnis T, Yeh EA, Kuntz N, Common viruses associated with lower pediatric multiple sclerosis risk. Neurology. 2011; 76 (23): 1989–95. DOI: 10.1212/WNL.0b013e31821e552a.
42. Гончарова З. А., Беловолова Р. А., Мегерян В. А. Клинико-иммунологические особенности рассеянного склероза на фоне реактивации персистирующей герпесвирусной инфекции. Саратовский научно-медицинский журнал. 2018; 14 (1): 126–32.
43. Kwilasz AJ, Grace PM, Serbedzija P, Maier SF, Watkins LR. The therapeutic potential of interleukin-10 in neuroimmune diseases. Neuropharmacology. 2015; 96: 55–57. DOI: 10.1016/j.neuropharm.2014.10.020.
44. Rojas JM, Avia M, Martín V, Sevilla N. IL-10: A Multifunctional Cytokine in Viral Infections. J Immunol Res. 2017; 2017: 6104054. DOI: 10.1155/2017/6104054.
45. Zhang L, Yuan S, Cheng G, Guo B. Type I IFN promotes IL10 production from T cells to suppress Th17 cells and Th17-associated autoimmune inflammation. PLoS One. 2011; 6 (12): 1–11. DOI: 10.1371/journal.pone.0028432.
46. Schönrich G, Abdelaziz MO, Raftery MJ. Epstein–Barr virus, interleukin-10 and multiple sclerosis: A me´nage à trois. Front. Immunol. 2022; 13: 1028972. DOI: 10.3389/fimmu.2022.1028972.
47. Jog NR, Chakravarty EF, Guthridge JM, James JA. Epstein Barr Virus Interleukin 10 Suppresses Anti-inflammatory Phenotype in Human Monocytes. Front Immunol. 2018; 9: 2198. DOI: 10.3389/fimmu.2018.02198.
48. Kang MS, Kieff E. Epstein–Barr virus latent genes. Exp Mol Med. 2015; 47 (1): e131. DOI: 10.1038/emm.2014.84.
49. Maertzdorf J, Osterhaus AD, Verjans GM. IL-17 expression in human herpetic stromal keratitis: modulatory effects on chemokine production by corneal fibroblasts. J Immunol. 2002; 169 (10): 5897–903. DOI: 10.4049/jimmunol.169.10.5897.
50. Fredj NB, Rizzo R, Bortolotti D, Nefzi F, Chebel S, Rotola A, et al., Evaluation of the implication of KIR2DL2 receptor in multiple sclerosis and herpesvirus susceptibility. J Neuroimmunol. 2014; 271 (1–2): 30–35. DOI: 10.1016/j.jneuroim.2014.03.017.
51. Rizzo R, Bortolotti D, Fainardi E, Gentili V, Bolzani S, Baldi E, et al. KIR2DL2 inhibitory pathway enhances Th17 cytokine secretion by NK cells in response to herpesvirus infection in multiple sclerosis patients. J Neuroimmunol. 2016; 294: 1–5. DOI: 10.1016/j.jneuroim.2016.03.007.
52. Maier S, Simu M, Hutanu A, Barcutean L, Voidazan S, Bajko Z, et al. Clinical immunological correlations in patients with multiple sclerosis treated with natalizumab. Brain Sci. 2020; 10 (11): 802. DOI: 10.3390/brainsci10110802.
53. Watford WT, Moriguchi M, Morinobu A, O'Shea JJ. The biology of IL-12: coordinating innate and adaptive immune responses. Cytokine Growth Factor Rev. 2003; 14: 361–68. DOI: 10.1016/S1359-6101(03)00043-1.
54. Broberg EK, Setala N, Eralinna JP, Salmi AA, Roytta M, Hukkanen V. Herpes simplex virus type 1 infection induces upregulation of interleukin-23 (p19) mRNA expression in trigeminal ganglia of BALB/c mice. J Interferon Cytokine Res. 2004; 22: 641–51. DOI: 10.1089/10799900260100123.
55. Di Salvo E, Ventura-Spagnolo E, Casciaro M, Navarra M, Gangemi S. IL-33/IL-31 axis: a potential inflammatory pathway. Mediator. Inflammat. 2018: 3858032. DOI: 10.1155/2018/3858032.
56. Maier E, Werner D, Duschl A, Bohle B, Horejs-Hoeck J. Human Th2 but not Th9 cells release IL-31 in a STAT6/ NF-κB–dependent way. J Immunol. 2014; 193 (2): 645–54. DOI: 10.4049/jimmunol.1301836.
57. Dong H, Zhang X, Qian Y. Mast cells and neuroinflammation. Med Sci Monit Basic Res. 2014; 20: 200–6. DOI: 10.12659/MSMBR.893093.
58. Nemmer JM, Kuchner M, Datsi A, Oláh P, Julia V, Raap U, et al. Interleukin-31 signaling bridges the gap between immune cells, the nervous system and epithelial tissues. Front Med. 2021; 8: 639097. DOI: 10.3389/fmed.2021.639097.
59. Singh B, Jegga AG, Shanmukhappa KS, Edukulla R, Khurana Hershey GH, Medvedovic M, et al. IL-31-driven skin remodeling involves epidermal cell proliferation and thickening that lead to impaired skin-barrier function. PLoS One. 2016; 11 (8): e0161877. DOI: 10.1371/journal.pone.0161877.
60. Yagi Y, Andoh A, Nishida A, Shioya M, Nishimura T, et al. Interleukin-31 stimulates production of inflammatory mediators from human colonic subepithelial myofibroblasts. Int J Mol Med. 2007; 19: 941–6. DOI: 10.3892/ijmm.19.6.941.
61. Jafarzadeh A, Mahdavi R, Jamali M, Hajghani H, Nemati M, Ebrahimi HA. Increased concentrations of Interleukin-33 in the serum and cerebrospinal fluid of patients with multiple sclerosis. Oman Med J. 2016; 31 (1): 40–45. DOI: 10.5001/omj.2016.08.
62. Griesenauer B, Paczesny S. The ST2/IL-33 axis in immune cells during inflammatory diseases. Front Immunol. 2017; 8: 475. DOI: 10.3389/fimmu.2017.00475.
63. Peine M, Marek RM, Löhning M. IL-33 in T Cell Differentiation, Function, and Immune Homeostasis. Trends Immunol. 2016; 37 (5): 321–33. DOI: 10.1016/j.it.2016.03.007.
64. Jamali M, Rostami M, Gholamreza R, Sarab A, Mahdavi R. IL-33 polymorphism rs1929992 and its association with susceptibility to different pattern of multiple sclerosis. Tehran Univ Med J. 2018; 76 (7): 446–51.
65. Al-Naseri MAS, Salman ED, Ad'hiah AH. Genetic analysis of IL4 (rs2070874), IL17A (rs2275913), and IL33 (rs7044343) polymorphisms in Iraqi multiple sclerosis patients by using T-plex real-time PCR method. Meta Gene. 2022; 31: 100986. DOI: 10.1016/j.mgene.2021.100986.
66. Ahmadi M, Fathi F, Fouladi S, Alsahebfosul F, Manian M, Eskandari N. Serum IL-33 level and IL-33, IL1RL1 gene polymorphisms in asthma and multiple sclerosis patients. Curr Mol Med. 2019; 19 (5): 357–63. DOI: 10.2174/1566524019666190405120137.
67. Allan D, Fairlie-Clarke KJ, Elliott CD, Schuh C, Barnett SC, Lassmann H, et al. Role of IL-33 and ST2 signalling pathway in multiple sclerosis: expression by oligodendrocytes and inhibition of myelination in central nervous system. Acta Neuropathol. Commun. 2016; 4 (1): 75. DOI: 10.1186/s40478-016-0344-1.
68. Pei C, Barbour M, Fairlie-Clarke KJ, Allan D, Mu R, Jiang HR. Emerging role of interleukin-33 in autoimmune diseases. Immunology. 2014; 141: 9–1. DOI: 10.1111/imm.12174.
69. Hudson CA, Christophi GP, Gruber RC, Wilmore JR, Lawrence DA, Massa PT. Induction of IL-33 expression and activity in central nervous system glia. J Leukocyte Biol. 2008; 84: 631–43. DOI: 10.1189/jlb.1207830.
70. Zhang F, Tossberg JT, Spurlock CF, Yao SY, Aune TM, Sriram S. Expression of IL-33 and its epigenetic regulation in multiple sclerosis. Ann Clin Transl Neurol. 2014; 1: 307–18. DOI: 10.1002/acn3.47.
71. Gadani SP, Walsh JT, Smirnov I, Zheng J, Kipnis J. The glia-derived alarmin IL-33 orchestrates the immune response and promotes recovery following CNS injury. Neuron. 2015; 85: 703–9. DOI: 10.1016/j.neuron.2015.01.013.
72. Yasuoka S, Kawanokuchi J, Parajuli B, Jin S, Doi Y, Noda M, et al. Production and functions of IL-33 in the central nervous

system. Brain Res. 2011; 1385: 8–17. DOI: 10.1016/j.brainres.2011.02.045.
73. Kempuraj D, Khan MM, Thangavel R, Xiong Z, Yang E, Zaheer A. Glia maturation factor induces interleukin-33 release from astrocytes: implications for neurodegenerative diseases. J Neuroimmune Pharmacol. 2013; 8: 643–50. DOI: 10.1007/s11481-013-9439-7.
74. Мельников М. В., Свиридова А. А., Роговский В. С., Бойко А. Н., Пащенков М. В. Роль макрофагов в развитии нейровоспаления при рассеянном склерозе. Журнал неврологии и психиатрии им. С. С. Корсакова. 2022; 122 (5): 51–56. DOI: 10.17116/jnevro202212205151.
75. Franco R, Fernández-Suárez D. Alternatively activated microglia and macrophages in the central nervous system. Prog Neurobiol. 2015; 131: 65–86. DOI: 10.1016/j.pneurobio.2015.05.003.
76. Jiang HR, Milovanović M, Allan D, Niedbala W, Besnard AG, Fukada SY, et al. IL-33 attenuates EAE by suppressing IL-17 and IFN-γ production and inducing alternatively activated macrophages. Eur J Immunol. 2012; 42: 1804–14. DOI: 10.1002/eji.20114194718.
77. Russi AE, Ebel ME, Yang Y, Brown MA. Male-specific IL-33 expression regulates sex-dimorphic EAE susceptibility. PNAS. 2018; 115 (7): E1520–E1529. DOI: 10.1073/pnas.1710401115.
78. Klose CS, Artis D. Innate lymphoid cells as regulators of immunity, inflammation and tissue homeostasis. Nat Immunol. 2016; 17 (7): 765–774. DOI: 10.1038/ni.3489.
79. Braun H, Afonina IS, Mueller C, Beyaert R. Dichotomous function of IL-33 in health and disease: From biology to clinical implications. Biochemical Pharmacology. 2018; 148: 238–52. DOI: 10.1016/j.bcp.2018.01.0100006-2952.
80. Komai-Koma M, Gilchrist DS, McKenzie AN, Goodyear CS, Xu D, Liew FY. IL-33 activates B1 cells and exacerbates contact sensitivity. J Immunol. 2011; 186 (4): 2584–91. DOI: 10.4049/jimmunol.1002103.
81. Sattler S, Ling GS, Xu D, Hussaarts L, Romaine A, Zhao H, et al. IL-10- producing regulatory B cells induced by IL-33 (Breg(IL-33)) effectively attenuate mucosal inflammatory responses in the gut. J Autoimmun. 2014; 50: 107–22. DOI: 10.1016/j.jaut.2014.01.032.
82. Cayrol C, Girard J-Ph. Interleukin-33 (IL-33): a nuclear cytokine from the IL-1 family. Immunol Rev. 2018; 281: 154–168. DOI: 10.1111/imr.12619.
83. Bertheloot D, Latz E, Franklin BS. Necroptosis, pyroptosis and apoptosis: an intricate game of cell death. Cell Mol Immunol. 2021; 18: 1106–21. DOI: 10.1038/s41423-020-00630-3.
84. Lüthi AU, Cullen SP, McNeela EA, Duriez PJ, Afonina IS, Sheridan C, et al. Suppression of interleukin-33 bioactivity through proteolysis by apoptotic caspases. Immunity. 2009; 31: 84–98. DOI: 10.1016/j.immuni.2009.05.007.
85. Carriere V, Roussel L, Ortega N, Lacorre DA, Americh L, Aguilar L, et al. IL-33, the IL-1-like cytokine ligand for ST2 receptor, is a chromatin-associated nuclear factor in vivo. Proc Natl Acad Sci USA. 2007; 104 (1): 282–7. DOI: 10.1073/pnas.0606854104.
86. Cayrol C, Girard JP. IL-33: an alarmin cytokine with crucial roles in innate immunity, inflammation and allergy. Curr Opin Immunol. 2014; 31: 31–7. DOI: 10.1016/j.coi.2014.09.004.
87. Ali S, Mohs A, Thomas M, Klare J, Ross R, Schmitz ML, et al. The dual function cytokine IL-33 interacts with the transcription factor NF-kappaB to dampen NF-kappaB-stimulated gene transcription. J Immunol. 2011; 187 (4): 1609–16. DOI: 10.4049/jimmunol.1003080.
88. Lefrancais E, Roga S, Gautier V, Gonzalez-de-Peredo A, Monsarrat B, Girard JP, et al. IL-33 is processed into mature bioactive forms by neutrophil elastase and cathepsin G. Proc Natl Acad Sci USA. 2012; 109 (5): 1673–8. DOI: 10.1073/pnas.1115884109.
89. Waern I, Lundequist A, Pejler G, Wernersson S. Mast cell chymase modulates IL-33 levels and controls allergic sensitization in dust-mite induced airway inflammation. Mucosal Immunol. 2013; 6 (5): 911–20. DOI: 10.1038/ mi.2012.129.
90. Lefrancais E, Duval A, Mirey E, Roga S, Espinosa E, Cayrol C, et al. Central domain of IL-33 is cleaved by mast cell proteases for potent activation of group-2 innate lymphoid cells. Proc Natl Acad Sci U S A. 2014; 111 (43): 15502–7. DOI: 10.1073/pnas.1410700111.
91. Hirose S, Jahani PS, Wang S, Jaggi U, Tormanen K, Yu J, et al. Type 2 innate lymphoid cells induce CNS demyelination in an HSV-IL-2 mouse model of multiple sclerosis. iScience. 2020; 23 (10): 101549. DOI: 10.1016/j.isci.2020.101549.
92. Ofengeim D, Ito Y, Najafov A, Zhang Y, Shan B, DeWitt JP, et al. Activation of necroptosis in multiple sclerosis. Cell Rep. 2015; 10: 1836–49. DOI: 10.1016/j.celrep.2015.02.051.
93. Verzosa AL, McGeever LA, Bhark SJ, Delgado T, Salazar N, Sanchez EL. Herpes simplex virus 1 infection of neuronal and nonneuronal cells elicits specific innate immune responses and immune evasion mechanisms. Front Immunol. 2021; 12: 644664. DOI: 10.3389/fimmu.2021.644664.
94. Zhao J, Qin C, Liu Y, Rao Y, Feng P. Herpes simplex virus and pattern recognition receptors: an arms race. Front Immunol. 2021; 11: 613799. DOI: 10.3389/fimmu.2020.613799.
95. Kaiser WJ, Upton JW, Mocarski ES. Receptor-interacting protein homotypic interaction motif-dependent control of NF-kappa B activation via the DNA dependent activator of IFN regulatory factors. J Immunol. 2008; 181: 6427–34. DOI: 10.4049/jimmunol.181.9.6427 104.
96. Nile CJ, Barksby E, Jitprasertwong P, Preshaw PM, Taylor JJ. Expression and regulation of interleukin-33 in human monocytes. Immunology. 2010; 130 (2): 172–80. DOI: 10.1111/j.1365-2567.2009.03221.x.
97. Zhang L, Lu R, Zhao G, Pflugfelder SC, Li DQ. TLR-mediated induction of pro-allergic cytokine IL-33 in ocular mucosal epithelium. Int J Biochem Cell Biol. 2011; 43: 1383–91. DOI: 10.1016/j.biocel.2011.06.003.
98. Furue M, Yamamura K, Kido-Nakahara M, Nakahara T, Fukui Y. Emerging role of interleukin-31 and interleukin-31 receptor in pruritus in atopic dermatitis. Allergy. 2018; 73 (1): 29–36. DOI: 10.1111/all.13239.
99. Ellermann-Eriksen S. Macrophages and cytokines in the early defence against herpes simplex virus. Virology J. 2005; 2: 59. DOI: 10.1186/1743-422X-2-59.
100. Roychoudhury P, Swan DA, Duke E, Corey L, Zhu J, Davé V, et al. Tissue-resident T cell–derived cytokines eliminate herpes simplex virus-2–infected cells. J Clin Invest. 2020; 130 (6): 2903–19. DOI: 10.1172/JCI132583.
101. Bello-Morales R, Andreu S, López-Guerrero JA. The role of herpes simplex virus type 1 infection in demyelination of the central nervous system. Int J Mol Sci. 2020; 21 (14): 5026. DOI: 10.3390/ijms21145026.
102. Sun Y, Wen Y, Wang L, Wen L, You W, Wei S, et al. Therapeutic opportunities of interleukin-33 in the central nervous system. Front Immunol. 2021; 12: 654626. DOI: 10.3389/fimmu.2021.654626.

SPEECH IMPROVEMENT IN CHILDREN WITH CEREBRAL PALSY BY "BRAIN–COMPUTER–HAND EXOSKELETON" NEUROINTERFACE REHABILITATION

Pavlenko VB ✉, Vlasenko SV, Orekhova LS, Biryukova EA

Vernadsky Crimean Federal University, Simferopol, Russia

As explained earlier, neurorehabilitation sessions involving the use of the non-invasive “brain – computer – hand exoskeleton” interface reduce hand muscle spasticity and improve motor skills in children with cerebral palsy (CP). However, the changes in the patients’ speech functions and their relationship with the upper limb mobility have not been analyzed. The study was aimed to assess the correlation between the motor and speech functions of children with CP, as well as to detect the changes in motor realization of speech production following complex treatment of patients including sessions of neurorehabilitation. The study involved children with CP aged 6–15. The index group (n = 40, 16 girls, 24 boys) received complex resort treatment with the course of neurorehabilitation, while the comparison group (n = 20, 10 girls, 10 boys) received standard resort treatment. A significant (p < 0.001) correlation between the total ABILHAND-Kids score and the indicators of speech production motor realization was revealed. In patients of the index group, complex treatment with the course of neurorehabilitation resulted in the significant (p < 0.001) decrease in hand spasticity and the increase in the total ABILHAND-Kids score and speech scores. No significant changes of these indicators were revealed in children of the comparison group. Beneficial effects of neurorehabilitation may be based on the enhanced plasticity of the neural circuits responsible for planning and execution of complex hand movements, as well as speech processes. The findings can be used to develop new methods for correction of motor and cognitive spheres in children with CP.

Keywords: children, cerebral palsy, speech, brain–computer interface

Funding: the study was supported by the Russian Science Foundation and the Republic of Crimea, grant No. 22-15-20035, https://rscf.ru/en/project/22-15-20035/.

Author contribution: Pavlenko VB, Vlasenko SV — study planning, data analysis and interpretation, manuscript writing; Orekhova LS, Biryukova EA — data acquisition and analysis, manuscript writing.

Compliance with ethical standards: the study was approved by the Ethics Committee of the V.I. Vernadsky Crimean Federal University (protocol № 1 of 25 January 2022). The informed consent to the children’s enrollment was obtained from their parents.

✉ **Correspondence should be addressed:** Vladimir B. Pavlenko
Vernadsky pr., 4, Simferopol, 295007, Russia; vpav55@gmail.com

Received: 17.06.2023 **Accepted:** 14.07.2023 **Published online:** 28.07.2023

DOI: 10.24075/brsmu.2023.026

УЛУЧШЕНИЕ РЕЧИ У ДЕТЕЙ С ДЦП НА ФОНЕ РЕАБИЛИТАЦИИ С ПРИМЕНЕНИЕМ НЕЙРОИНТЕРФЕЙСА "МОЗГ–КОМПЬЮТЕР–ЭКЗОСКЕЛЕТ КИСТИ"

В. Б. Павленко ✉, С. В. Власенко, Л. С. Орехова, Е. А. Бирюкова

Крымский федеральный университет имени В. И. Вернадского, Симферополь, Россия

Как было показано ранее, сеансы нейрореабилитации с применением неинвазивного интерфейса «мозг–компьютер–экзоскелет кисти» снижают у детей с детским церебральным параличом (ДЦП) спастичность мышц кисти и улучшают двигательные навыки. Однако изменение речевых функций пациентов и их связь с подвижностью верхних конечностей не анализировали. Целью исследования было проанализировать связь между двигательными и речевыми функциями детей с ДЦП, а также выявить изменения моторной реализации высказывания у пациентов в результате комплексного лечения, включающего сеансы нейрореабилитации. В исследовании приняли участие дети с ДЦП в возрасте 6–15 лет. Основная группа (n = 40, 16 девочек, 24 мальчика) проходила комплексное санаторно-курортное лечение с курсом нейрореабилитации, а группа сравнения (n = 20, 10 девочек, 10 мальчиков) — стандартное санаторно-курортное лечение. Выявлена статистически значимая (p < 0,001) взаимосвязь между величиной суммарного показателя шкалы «Возможности кисти — дети» («ABILHANDKids») и показателями моторной реализации высказывания. Комплексная терапия с курсом нейрореабилитации привела у пациентов основной группы к статистически значимым изменениям (p < 0,001): снижению спастичности кистей рук, росту суммарного показателя «ABILHANDKids» и показателей речи. У детей группы сравнения статистически значимых изменений данных показателей не выявлено. Основой позитивных эффектов нейрореабилитации может быть усиление пластичности нейронных цепей, контролирующих выполнение сложных движений рук, а также речевые процессы. Полученные данные могут быть использованы при разработке новых методов коррекции двигательной и когнитивной сферы детей с ДЦП.

Ключевые слова: дети, церебральный паралич, речь, интерфейс мозг–компьютер

Финансирование: исследование выполнено за счет гранта Российского научного фонда и Республики Крым № 22-15-20035, https://rscf.ru/project/22-15-20035/

Вклад авторов: В. Б. Павленко, С. В. Власенко — планирование исследований, анализ и интерпретация данных, подготовка рукописи; Л. С. Орехова, Е. А. Бирюкова — сбор и анализ данных, подготовка рукописи.

Соблюдение этических стандартов: исследование одобрено этическим комитетом ФГАОУ ВО «Крымский федеральный университет им. В. И. Вернадского» (протокол № 1 от 25 января 2022 г.). Получено информированное согласие от родителей на участие детей в исследовании.

✉ **Для корреспонденции:** Владимир Борисович Павленко
пр. Вернадского, д. 4, г. Симферополь, 295007; vpav55@gmail.com

Статья получена: 17.06.2023 **Статья принята к печати:** 14.07.2023 **Опубликована онлайн:** 28.07.2023

DOI: 10.24075/vrgmu.2023.026

Today it is acknowledged that cerebral palsy (CP) is much more than “postural and motor impairment”, it is often associated with a broad spectrum of dysfunctions that includes cognitive, language, and sensory perception disorders [1]. As stated in the recently published review, 30–87% of patients with CP have speech disorders [2]. A more severe motor impairment is associated with the more severe speech disorders [1, 3–5]. The correlation analysis has made it possible to reveal the relationship between the severity of motor impairment and the severity of speech disorder in patients with CP aged 10–12 [6].

Similarity of motor and speech disorders associated with CP is explained by anatomical proximity of the cortical speech and motor regions, as well as their pathways. Functional similarity of the speech and motor systems has been also noted: organization of each speech act and movement requires preserved explicit kinesthetic perception that goes along with any movement of articulation and other muscles [2]. That is why the exercises designed to overcome motor deficits (especially in hands) are recommended to develop speech functions in children.

Currently, of particular relevance are methods for rehabilitation of the limb motor functions in patients with CP based on the use of non-invasive brain-computer interfaces (BCI) and the principles of biofeedback. Such methods make it possible to reinforce innate physiological resources of the child’s brain [7]. Originally, the number of studies showed the potential for using BCI in children with CP in order to detect when the patient imagines limb movement or movement intention based on the analysis of EEG dynamics [8–10]. The children used BCI to control the cursor movement or various game objects on the computer screen. The researchers from South Korea, who used the results of these and some other studies, utilized a BCI integrated with the electrical stimulator of the wrist extensor muscles [11]. Electrical stimulation was launched based on the on-line analysis of EEG parameters when the patient imagined hand extension. Children with CP showed improvement of the parameters of hand movement execution and focus after a series of sessions.

Later the non-invasive “brain–computer–hand exoskeleton” interfaces that identified typical EEG patterns associated with kinesthetic motor imagery and triggered movement of the exoskeleton “gloves” were used for rehabilitation of children with CP [12, 13]. It has been found that the neurorehabilitation sessions involving the use of such non-invasive BCIs improve the effectiveness of rehabilitation measures applied during the resort phase of treatment. As a result, hand spasticity is reduced, muscle strength and the range of hand motion are improved, and the range of everyday skills is expanded. This promotes socialization of patients with CP. However, the changes in speech functions of patients have not been analyzed in the above studies. That is why our study was aimed to assess the relationship between the motor and speech functions of children with CP and to detect the changes in the patients’ motor realization of speech production after the complex resort treatment including sessions of neurorehabilitation.

METHODS

Sample characteristics

The study was performed at the Health and Rehabilitation Technology Centre (V.I. Vernadsky Crimean Federal University) and the Gelilovitch “Chaika” Sanatorium for Children and their Parents for children with neurological disorders (Republic of Crimea). The study involved 60 children aged 6–15, who underwent health resort rehabilitation. Inclusion criteria: the diagnosis of CP according to ICD-10; hemiparesis with the motor activity level not exceeding III according to the Gross Motor Function Classification System for Cerebral Palsy (GMFCS) in the patient’s structure of neurological disorder. Exclusion criteria: refusal to participate in the study obtained from the patient, his/her parent or legal representative; motor activity level exceeding III according to GMFCS; aphasia; epilepsy not responding to medication; vision problems not allowing the patient to see the instructions on the screen; moderate, severe or profound mental retardation (F71–73 according to ICD-10).

The index group included 40 individuals (16 girls, 24 boys) aged 6–15, who underwent complex resort treatment including the course of neurorehabilitation with the use of the Exohand-2 “brain–computer–hand exoskeleton” interface. The comparison (control) group included 20 children (10 girls, 10 boys) aged 7–13, who underwent complex resort treatment involving the use of standard methods. It should be noted that parents more often registered their children for the course of neurorehabilitation when the children had more severe motor function impairment. Thus, no randomization when forming the groups of patients is a limitation of our study. The complex resort treatment received by both groups of patients included the following: exercise therapy, paretic muscle massage, pelotherapy, hydrokinesitherapy in thermal mineral water, electrical stimulation of muscles that were antagonists of paretic ones.

Assessment of motor and speech function parameters

The following scales were used to assess the upper limb motion range:

1. Modified Ashworth Scale (MAS) allowing the neurologist to estimate spasticity by assessing the resistance experienced during passive range of motion using the 5-point scale (0–4).

2. ABILHAND-Kids, the questionnaire allowing the parents to assess the child’s upper limb motor function when performing daily activities (3 levels of the ability to use the skill: "Impossible", "Difficult" or "Easy"). This scale showed responsiveness and high sensitivity when used to detect changes after the intense training of children with CP. It was recommended for monitoring of the patients’ functional state in clinical trials [14]. In addition to standard action performance indicators (impossible to perform – X0, difficult to perform – X1, easy to perform – X2), a cumulative indicator (X) ranging between 0 and 42, which was calculated according to the formula X = X1+ 2X2, was used to assess functions in general [12].

Neuropsychological diagnosis of speech disorder in children was performed in accordance with the guidelines [15]. The level of motor realization of speech production was assessed by three methods.

1. Assessment of oral praxis and articulatory motility (evaluation of lip and tongue movement, pouting stretch according to the instructions or following the model). The maximum score was 30.

2. Assessment of pronunciation of sounds (repeating words). The maximum score was 30.

3. Making sentences based on the pictures (the child was presented a series of pictures, such as “a boy washes his hands”, which he/she had to describe using one sentence). Correctness of word order, agrammatism and paragrammatic errors were taken into account during the test. The maximum score was 45.

Table 1. Hand spasticity scores according to the Ashworth scale in patients of the index and comparison groups before and after treatment (Me [Q_1; Q_3])

Spasticity (score)	Before treatment	After treatment	*p*
Index group, *n* = 40			
Left hand	2,0 [1,5; 2,0]	1,0 [1,0; 2,0]	*p* < 0,001
Right hand	2,0 [2,0; 3,0]	2,0 [1,0; 2,0]	*p* < 0,001
Comparison group, *n* = 20			
Left hand	2,0 [1,0; 3,0]	1,0 [1,0; 2,0]	*p* = 0,028
Right hand	2,5 [1,0; 3,0]	2,0 [1,0; 2,5]	*p* = 0,018

Rehabilitation procedures

Each child in the index group had 10 sessions of rehabilitation procedures involving the use of the complex consisting of non-invasive BCI and Exohand-2 hand exoskeleton (manufactured by Exoplast LLC, Moscow, in accordance with RU No. RZN 2018/7681). The non-invasive BCI operation is based on the analysis of EEG patterns emerging when an individual imagines hand extension. The program ensures detection of kinesthetic motor imagery based on the EEG pattern analysis, generates the visual feedback signal and issues commands to control the hand exoskeleton.

During neurorehabilitation training the patient was seated in a chair in front of the computer monitor, on which visual instructions were displayed. Hands were housed inside the exoskeleton "gloves". There was a white round mark for gaze fixation in the center of the screen with three arrows around it, which changed color to mark the instructions. The patient executed the following commands: to relax, to kinesthetically imagine the left or right hand extension. To produce a particular kinesthetic image when imagining movement, the children were instructed as follows: "Imagine you have a small ball in your hand, you open your hand and drop it. Feel this movement". When the patient executed the task precisely, the mark for gaze fixation changed its color to green (the color intensity was dependent on EEG parameters), the exoskeleton executed the appropriate movement, and the hand was passively extended. Thus, the combined visual and kinesthetic feedback signal was generated.

Initial assessment of the upper limb motion range and speech function parameters in children of the index and control groups was performed on day two after admission to the sanatorium. The index group patients took a course of neurorehabilitation consisting of 10 sessions (every day except Sunday) starting from day three of resort treatment according to the same scheme: three times per session of 8 min with a rest break of at least 5 min. The motor imagery task for each hand was repeated 24 times during the session. The percentage of correct answers of the classifier (which triggered the exoskeleton and ensured passive extension of the hand) during the first and second session was about 60%, while after the patient's training, by the end of the course, it reached 75–80%. On the next day after the end of the course (day 14–15 of stay in the sanatorium) the data on motor and speech activity of the index group patients were acquired again. Parameters of controls were also assessed on day 14–15 of resort treatment.

Other details of the method have been reported earlier [12, 16].

Statistical analysis

Statistical data processing was performed using the Statistica 12 software (StatSoft Inc.; USA). The distribution of the studied indicators was assessed using the Shapiro–Wilk test. When the distribution was normal, the data were presented as mean and standard error of the mean; the Student's t-test was used to assess intergroup differences. When the distribution was non-normal, statistical data were presented as median and interquartile range (Me [Q_1; Q_3]); the Mann–Whitney *U* test was used to assess the intergroup differences, while the intragroup differences were assessed using the Wilcoxon signed rank test. Sperman's rank correlation was used to calculate the correlation coefficients. The differences and correlation coefficients were considered significant at $p < 0.05$.

RESULTS

Characteristics of motor and speech functions before rehabilitation procedures

The average age of children in the index and control groups was 10.2 ± 0.4 and 10.1 ± 0.3 years, respectively, there were no significant differences ($p = 0.92$). Among patients of the index group, left-sided hemiparesis was revealed in 11 individuals, and right-sided hemiparesis was found in 29 study

Table 2. Everyday activity management scores according to the ABILHAND-Kids scale in patients of the index and comparison groups before and after treatment (Me [Q_1; Q_3])

Everyday activity management (score)	Before treatment	After treatment	*p*
Index group, *n* = 40			
Impossible	1,5 [0,0; 7,0]	0,0 [0,0; 6,0]	*p* = 0,001
Difficult	8,0 [3,5; 14,0]	7,0 [3,0; 13,0]	*p* = 0,055
Easy	6,0 [0,0; 12,0]	7,0 [0,0; 16,0]	*p* < 0,001
Total score	23,0 [14,0; 33,0]	27,0 [16,0; 37,0]	*p* < 0,001
Control group, *n* = 20			
Impossible	2,0 [0,5; 4,5]	2,0 [0,0; 3,0]	*p* = 0,068
Difficult	9,0 [6,0; 13,0]	8,0 [6,0; 13,5]	*p* = 0,593
Easy	7,0 [4,0; 12,0]	7,0 [4,0; 12,0]	*p* = 0,593
Total score	27,5 [13,5; 33,0]	27,5 [15,5; 32,5]	*p* = 0,593

Table 3. Motor realization of speech production in patients of the index and comparison groups before and after treatment (Me [Q_1; Q_3])

Spasticity (score)	Before treatment	After treatment	*p*
Index group, *n* = 40			
Oral praxis and articulation	20,0 [13,0; 25,0]	24,0 [16,0; 27,0]	*p* < 0,001
Pronunciation of sounds	18,0 [12,0; 26,0]	20,0 [12,0; 28,0]	*p* < 0,001
Sentence making	22,0 [5,0; 35,0]	25,0 [6,0; 40,0]	*p* < 0,001
Comparison group, n = 20			
Oral praxis and articulation	23,0 [14,0; 27,0]	23,0 [15,5; 26,0]	*p* = 0,800
Pronunciation of sounds	21,5 [12,0; 25,0]	21,5 [13,0; 25,0]	*p* = 0,109
Sentence making	24,0 [18,5; 36,0]	25,5 [19,0; 37,0]	*p* = 0,237

participants. In the comparison group (controls), left-sided hemiparesis was revealed in seven children, and 13 children had right-sided hemiparesis. Among patients with left-sided hemiparesis the total ABILHAND-Kids score was 27 [19; 34], while children with right-sided hemiparesis had a slightly lower score, 23 [12; 32]. However, the differences in this parameter between patients with left-sided and right-sided hemiparesis were non-significant (p = 0.27). The patients with right-sided hemiparesis also had lower scores for pronunciation of sounds, oral praxis and sentence making than children with left-sided motor impairment, however, the differences were non-significant (p = 0.18–0.93).

The hand spasticity scores of patients of the index and comparison groups are provided in Table 1, the ABILHAND-Kids scores for daily activity management are presented in Table 2, and the characteristics of motor realization of speech production are provided in Table 3. There were no significant differences between the scores of the groups before treatment.

Calculation of the Spearman's rank correlation coefficients showed that the left hand spasticity scores determined in all the surveyed children (n = 60) before treatment negatively correlated with the scores for oral praxis, articulatory motility, pronunciation of sounds, making sentences from pictures (r = –0.37, –0.36, –0.30 at p = 0.004, 0.005 and 0.019, respectively). The right hand spasticity scores correlated significantly with the scores for pronunciation of sounds (r = –0.49 at p < 0.001), i.e. the higher the level of hand spasticity, the lower the level of speech production motor realization. The total ABILHAND-Kids score and the scores for oral praxis, pronunciation of sounds and making sentences from pictures shows a significant (p < 0.001 in all cases) positive correlation (r = 0.69, 0.62, 0.62, respectively), i.e. the better preserved the upper limb function, the higher the level of speech production motor realization. An example of such correlation between the score for hand function and the ability to adequately pronounce sounds is provided in Fig.

Characteristics of motor and speech functions after rehabilitation procedures

A significant decrease in the left and right hand spasticity after both standard resort treatment and complex treatment including the course of neurorehabilitation was revealed in both groups of children (Table 1). However, the analysis of daily activity management based on the parent-reported data (total ABILHAND-Kids score) made it possible to reveal a significant improvement in the index group only (Table 2). The significant improvement of the speech production motor realization level

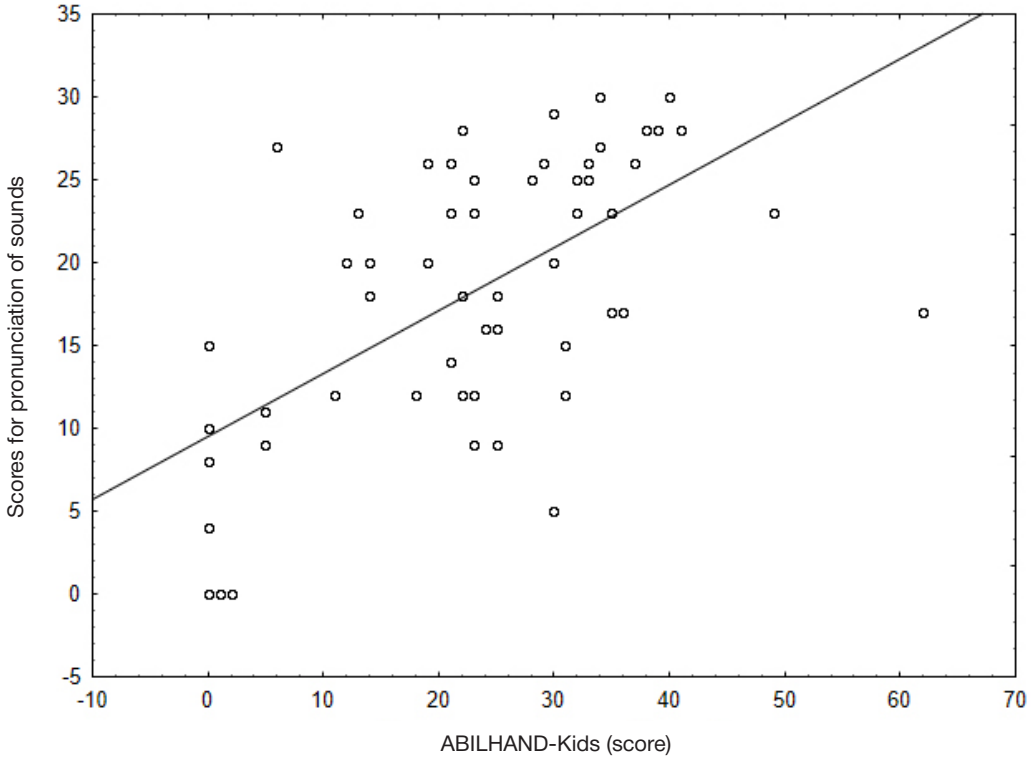

Fig. Correlation between the ABILHAND-Kids scores and scores for pronunciation of sounds in 60 children with CP

was also found only in the index group children (Table 3). Oral praxis, pronunciation of sounds and making sentences from pictures are the components of speech ability and can be considered as the repeated measurements requiring the use of Bonferroni correction for four comparisons. However, significance of differences is retained after applying the correction (as can be seen from p-values).

It should be noted that no significant differences in the studied indicators have been found after treatment. This may be due to the fact that children with the slightly lower scores for everyday skills and motor realization of speech production were included in the index group, where the more complex treatment including the course of neurorehabilitation was used, because of their parents' desire. Their scores did not significantly exceed that of the comparison group even after treatment.

Meanwhile, the following facts further indicate the efficiency of complex resort treatment that involves rehabilitation procedures including the course of neurorehabilitation. In the index group consisting of 40 children, oral praxis and articulation improved in 33 individuals (83%), pronunciation of sounds improved in 24 (60 %), and sentence making improved in 31 patients (78%). Among 20 children of the comparison group who received standard resort treatment only, improvement of scores for oral praxis and articulation associated with pronunciation of sounds was found only in three individuals (15%), while the sentence making improvement was revealed in four patients (20%).

DISCUSSION

We have gathered evidence suggestive of the correlation between the upper limb function parameters and the level of speech production motor realization. The findings confirm the theory that actions including the sequence of fine motor skill components and actions that ensure speech production involve the same cognitive and motor neural network [3]. It has been shown that hand function improvement following a series of neurorehabilitation sessions in children with CP is associated with the increase of scores for oral praxis, articulation, pronunciation of sounds and making sentences from pictures. Such combination of changes may me based on the plasticity processes enhancement not only in the neural circuits of motor and sensorimotor areas of the neocortex responsible for planning and execution of complex hand movements, but also in adjacent conventional speech areas (for example, Broca's area) showing increased activity during execution of sequential upper limb movements [17]. It is interesting to note that improvement of fine motor skills in healthy subjects reported in the recent experiments on teaching stone-tool making also resulted in the development of neural centers and paths involved in generation of speech [18, 19].

One of the factors of enhanced nervous tissue plasticity can be rearrangement of the synthesis and binding of neurotrophic factors secreted mainly by neurons and glia. It has been shown that successful rehabilitation of children with CP involving the use of the "brain–computer–hand exoskeleton" interface is strongly associated with the decrease in the concentration of brain-derived neurotrophic factor (BDNF) in peripheral blood after the end of rehabilitation treatment [16]. In the above study, the decrease in the BDNF levels can be considered as a result of neurorehabilitation session. It is believed that such a decrease is indicative of active binding and internalization of this factor specifically in the nervous tissue resulting in multiple effects: axonal growth, dendrite maturation and increased synaptic plasticity.

CONCLUSIONS

The study has confirmed that children with CP show a significant ($p < 0.001$) correlation between the total ABILHAND-Kids score and the indicators of motor realization of speech production (oral praxis, pronunciation of sounds and making sentences from pictures). The complex treatment of patients with CP involving the use of the "brain–computer–hand exoskeleton" interface has resulted in the significant ($p < 0.001$) decrease in hand spasticity, the increase in the total ABILHAND-Kids score and the indicators of speech production motor realization. Such a combination of changes may be based on the plasticity processes enhancement in the neural circuits of the neocortex responsible for planning and execution of complex hand movements, as well as speech processes. The findings can be used to develop new methods for correction of motor and cognitive spheres in children with CP.

References

1. Fluss J, Lidzba K. Cognitive and academic profiles in children with cerebral palsy: A narrative review. Ann Phys Rehabil Med. 2020; 63 (5): 447–56. DOI: 10.1016/j.rehab.2020.01.005.
2. Nemkova SA. Rechevye narusheniya pri detskom cerebral'nom paraliche: diagnostika i korrekciya. Zhurnal nevrologii i psihiatrii im. S.S. Korsakova. 2019; 119 (5): 112–9. DOI: 10.17116/jnevro2019119051112. Russian.
3. Pirila S, van der Meere J, Pentikainen T, Ruusu-Niemi P, Korpela R, Kilpinen J, et al. Language and motor speech skills in children with cerebral palsy. J Commun Disord. 2007; 40 (2): 116–28. DOI: 10.1016/j.jcomdis.2006.06.002.
4. Koopmans C, Sakash A, Soriano J, Long HL, Hustad KC. Functional communication abilities in youth with cerebral palsy: association with impairment profiles and school-based therapy goals. Lang Speech Hear Serv Sch. 2022; 53 (1): 88–103. DOI: 10.1044/2021_LSHSS-21-00064.
5. Vaillant E, Geytenbeek JJM, Oostrom KJ, Beckerman H, Vermeulen RJ, Buizer AI. Determinants of spoken language comprehension in children with cerebral palsy. Disabil Rehabil. 2023; 45 (10): 1667–79. DOI: 10.1080/09638288.2022.2072960.
6. Soriano JU, Hustad KC. Speech-language profile groups in school aged children with cerebral palsy: nonverbal cognition, receptive language, speech intelligibility, and motor function. Dev Neurorehabil. 2021; 24 (2): 118–29. DOI: 10.1080/17518423.2020.1858360.
7. Fedotova IR, Bobrov PD. Predposylki i osobennosti ispol'zovaniya voobrazheniya dvizheniya i interfejsa mozg-komp'yuter v reabilitacii pri detskom cerebral'nom paraliche. Zhurnal vysshej nervnoj deyatel'nosti im. I. P. Pavlova. 2022; 72 (1): 87–99. DOI: 10.31857/S004446772201004X. Russian.
8. Daly I, Billinger M, Laparra-Hernández J, Aloise F, Lloria García M, Faller J, Scherer R, Müller-Putz G. On the control of brain-computer interfaces by users with cerebral palsy. Clin Neurophysiol. 2013; 124 (9): 1787–97. DOI: 10.1016/j.clinph.2013.02.118.
9. Jochumsen M, Shafique M, Hassan A, Niazi IK. Movement intention detection in adolescents with cerebral palsy from single-trial EEG. J Neural Eng. 2018; 15(6): 066030. DOI: 10.1088/1741-2552/aae4b8.
10. Jadavji Z, Zhang J, Paffrath B, Zewdie E, Kirton A. Can Children With Perinatal Stroke Use a Simple Brain Computer Interface? Stroke. 2021; 52 (7): 2363–70. DOI: 10.1161/STROKEAHA.120.030596.
11. Kim T-W, Lee B-H. Clinical usefulness of brain-computer

interface-controlled functional electrical stimulation for improving brain activity in children with spastic cerebral palsy: a pilot randomized controlled trial. J Phys Ther Sci. 2016; 28: 2491–94. DOI: 10.1589/jpts.28.2491.
12. Larina NV, Korsunskaya LL, Vlasenko SV. Kompleks «Ekzokist'-2» v reabilitacii verhnej konechnosti pri detskom cerebral'nom paraliche s ispol'zovaniem neinvazivnogo interfejsa «mozg-komp'yuter». Nervno-myshechnye bolezni. 2019; 11 (4): 12–20. DOI: DOI: 10.17650/2222-8721-2019-9-4-44-50. Russian.
13. Bobrov PD, Biryukova EV, Polyaev BA, Lajsheva OA, Usachjova EL, Sokolova AV, et al. Rehabilitation of patients with cerebral palsy using hand exoskeleton controlled by brain-computer interface. Bulletin of RSMU. 2020; (4): 33–40. DOI: 10.24075/brsmu.2020.047.
14. Bleyenheuft Y, Gordon AM, Rameckers E, Thonnard JL, Arnould C. Measuring changes of manual ability with ABILHAND-Kids following intensive training for children with unilateral cerebral palsy. Dev Med Child Neurol. 2017; 59 (5): 505–11. DOI: 10.1111/dmcn.13338.
15. Fotekova TA, Ahutina TV. Nejropsihologicheskaya diagnostika rechevoj patologii u detej. Shkol'nyj psiholog. 2001; (37): 3–14. Russian.
16. Larina NV, Gordienko AI, Vlasenko SV, Himich NV, Korsunskaya LL, Pavlenko VB. Dinamika koncentracii nejrotroficheskogo faktora mozga v krovi kak prediktor dolgosrochnoj effektivnosti primeneniya programmno-apparatnogo kompleksa v reabilitacii detej s detskim cerebral'nym paralichom. Medicinskij vestnik Severnogo Kavkaza. 2020; 15 (4): 496–9. DOI: 10.14300/mnnc.2020.15116. Russian.
17. Hodgson JC, Hirst RJ, Hudson JM. Hemispheric speech lateralisation in the developing brain is related to motor praxis ability. Dev Cogn Neurosci. 2016; 22: 9–17. DOI: 10.1016/j.dcn.2016.09.005.
18. Stankova EP, Kruchinina OV, Shepovalnikov AN, Galperina EI. Evolyuciya central'nyh mekhanizmov ustnoj rechi. Zhurnal evolyucionnoj biohimii i fiziologii. 2020; 56 (3): 171–184. DOI: 10.31857/S0044452920030079. Russian.
19. Hecht EE, Pargeter J, Khreisheh N, Stout D. Neuroplasticity enables bio-cultural feedback in Paleolithic stone-tool making. Sci Rep. 2023; 13 (1): 2877. DOI: 10.1038/s41598-023-29994-y.

Литература

1. Fluss J, Lidzba K. Cognitive and academic profiles in children with cerebral palsy: A narrative review. Ann Phys Rehabil Med. 2020; 63 (5): 447–56. DOI: 10.1016/j.rehab.2020.01.005.
2. Немкова С. А. Речевые нарушения при детском церебральном параличе: диагностика и коррекция. Журнал неврологии и психиатрии им. С. С. Корсакова. 2019; 119 (5): 112–9. DOI: 10.17116/jnevro2019119051112.
3. Pirila S, van der Meere J, Pentikainen T, Ruusu-Niemi P, Korpela R, Kilpinen J, et al. Language and motor speech skills in children with cerebral palsy. J Commun Disord. 2007; 40 (2): 116–28. DOI: 10.1016/j.jcomdis.2006.06.002.
4. Koopmans C, Sakash A, Soriano J, Long HL, Hustad KC. Functional communication abilities in youth with cerebral palsy: association with impairment profiles and school-based therapy goals. Lang Speech Hear Serv Sch. 2022; 53 (1): 88–103. DOI: 10.1044/2021_LSHSS-21-00064.
5. Vaillant E, Geytenbeek JJM, Oostrom KJ, Beckerman H, Vermeulen RJ, Buizer AI. Determinants of spoken language comprehension in children with cerebral palsy. Disabil Rehabil. 2023; 45 (10): 1667–79. DOI: 10.1080/09638288.2022.2072960.
6. Soriano JU, Hustad KC. Speech-language profile groups in school aged children with cerebral palsy: nonverbal cognition, receptive language, speech intelligibility, and motor function. Dev Neurorehabil. 2021; 24 (2): 118–29. DOI: 10.1080/17518423.2020.1858360.
7. Федотова И. Р., Бобров П. Д. Предпосылки и особенности использования воображения движения и интерфейса мозг–компьютер в реабилитации при детском церебральном параличе. Журнал высшей нервной деятельности им. И. П. Павлова. 2022; 72 (1): 87–99. DOI: 10.31857/S004446772201004X.
8. Daly I, Billinger M, Laparra-Hernández J, Aloise F, Lloria García M, Faller J, Scherer R, Müller-Putz G. On the control of brain-computer interfaces by users with cerebral palsy. Clin Neurophysiol. 2013; 124 (9): 1787–97. DOI: 10.1016/j.clinph.2013.02.118.
9. Jochumsen M, Shafique M, Hassan A, Niazi IK. Movement intention detection in adolescents with cerebral palsy from single-trial EEG. J Neural Eng. 2018; 15(6): 066030. DOI: 10.1088/1741-2552/aae4b8.
10. Jadavji Z, Zhang J, Paffrath B, Zewdie E, Kirton A. Can Children With Perinatal Stroke Use a Simple Brain Computer Interface? Stroke. 2021; 52 (7): 2363–70. DOI: 10.1161/STROKEAHA.120.030596.
11. Kim T-W, Lee B-H. Clinical usefulness of brain-computer interface-controlled functional electrical stimulation for improving brain activity in children with spastic cerebral palsy: a pilot randomized controlled trial. J Phys Ther Sci. 2016; 28: 2491–94. DOI: 10.1589/jpts.28.2491.
12. Ларина Н. В., Корсунская Л. Л., Власенко С. В. Комплекс «Экзокисть-2» в реабилитации верхней конечности при детском церебральном параличе с использованием неинвазивного интерфейса «мозг–компьютер». Нервно-мышечные болезни. 2019; 11 (4): 12–20. DOI: 10.17650/2222-8721-2019-9-4-44-50..
13. Бобров П. Д., Бирюкова Е. В., Поляев Б. А., Лайшева О. А., Усачёва Е. Л., Соколова А. В. и др. Реабилитация больных с детским церебральным параличом с помощью экзоскелета кисти, управляемого интерфейсом «мозг–компьютер». Вестник РГМУ. 2020; (4): 34–41. DOI: 10.24075/vrgmu.2020.047.
14. Bleyenheuft Y, Gordon AM, Rameckers E, Thonnard JL, Arnould C. Measuring changes of manual ability with ABILHAND-Kids following intensive training for children with unilateral cerebral palsy. Dev Med Child Neurol. 2017; 59 (5): 505–11. DOI: 10.1111/dmcn.13338.
15. Фотекова Т. А., Ахутина Т. В. Нейропсихологическая диагностика речевой патологии у детей. Школьный психолог. 2001; 37: 3–14.
16. Ларина Н. В., Гордиенко А. И., Власенко С. В., Химич Н. В., Корсунская Л. Л., Павленко В. Б. Динамика концентрации нейротрофического фактора мозга в крови как предиктор долгосрочной эффективности применения программно-аппаратного комплекса в реабилитации детей с детским церебральным параличом. Медицинский вестник Северного Кавказа. 2020; 15 (4): 496–9. DOI: 10.14300/mnnc.2020.15116.
17. Hodgson JC, Hirst RJ, Hudson JM. Hemispheric speech lateralisation in the developing brain is related to motor praxis ability. Dev Cogn Neurosci. 2016; 22: 9–17. DOI: 10.1016/j.dcn.2016.09.005.
18. Станкова Е. П., Кручинина О. В., Шеповальников А. Н., Гальперина Е. И. Эволюция центральных механизмов устной речи. Журнал эволюционной биохимии и физиологии. 2020; 56 (3): 171–84. DOI: 10.31857/S0044452920030079.
19. Hecht EE, Pargeter J, Khreisheh N, Stout D. Neuroplasticity enables bio-cultural feedback in Paleolithic stone-tool making. Sci Rep. 2023; 13 (1): 2877. DOI: 10.1038/s41598-023-29994-y.

PROMISING BIOCEMICAL MARKERS OF PARKINSON'S DISEASE

Gusyakova OA, Smirnov SV ✉, Kuznetsova OYu, Apergenova AR, Albikova AR

Samara State Medical University, Samara, Russia

Parkinson's disease (PD) is a chronic neurodegenerative disease associated with specific neurological deficits in patients, it mainly affects dopaminergic neurons in the substantia nigra causing accumulation of the neurotoxic amounts of aggregated α-synuclein protein in the neuronal cell bodies. The paper reports the authors' view of certain pathochemical and biochemical aspects of the Parkinson's disease development in terms of interplay between the metabolic pathways of catecholamines and pigments, particularly the possible pathway of neuromelanin synthesis in the neuronal cell bodies and its importance in the life of cells. Assessment of the use of certain neurodegenerative disorder biomarkers, which are of direct pathognomonic value, in the laboratory diagnosis of the disease is provided. It is suggested to use the results in the field of deeper understanding of biochemical patterns underlying neuronal death for early diagnosis of PD in individuals of different age groups, as well as for further study of pathogenesis based on fundamental biochemistry and pathobiochemistry of intracellular processes.

Keywords: Parkinson's disease, dopamine, dopamine receptors, key aspects of pathochemistry and pathogenesis, biomarkers

Acknowledgments: we would like to thank staff members of the Department of Fundamental and Clinical Biochemistry with Laboratory Diagnosis at the Samara State Medical University, specifically Professor F.N. Gilmiyarova, D. Sc. (Medicine), and Associate Professor A.V. Zhdanova, Cand. Sc. (Pharmacy), for their help in manuscript drafting and design.

Author contribution: Gusyakova OA — literature analysis; Smirnov SV — data acquisition in the field of fundamental biochemistry; Kuznetsova OYu — research data analysis and interpretation; Apergenova AR, Albikova AR — manuscript writing.

✉ **Correspondence should be addressed:** Sergey V. Smirnov
Arcybushevskaya, 171, 443001, Samara, Russia; s.v.smirnov@samsmu.ru

Received: 24.07.2023 **Accepted:** 14.08.2023 **Published online:** 29.08.2023

DOI: 10.24075/brsmu.2023.030

ПЕРСПЕКТИВНЫЕ БИОХИМИЧЕСКИЕ МАРКЕРЫ БОЛЕЗНИ ПАРКИНСОНА

О. А. Гусякова, С. В. Смирнов ✉, О. Ю. Кузнецова, А. Р. Апергенова, А. Р. Альбикова

Самарский государственный медицинский университет, Самара, Россия

Болезнь Паркинсона (БП) — хроническое нейродегенеративное заболевание с характерными неврологическими расстройствами у пациентов, поражающее преимущественно дофаминергические нейроны черной субстанции с накоплением в телах нейронов нейротоксичных доз агрегатов белка α-синуклеина. В статье представлен взгляд авторов на отдельные патохимические и биохимические аспекты развития болезни Паркинсона во взаимосвязи путей обмена катехоламинов и пигментов, в частности возможного пути синтеза нейромеланина в телах нейронов и его значение в жизни клетки. Дана оценка определенным, имеющим прямое патогномоничное значение, биомаркерам нейродегенеративной патологии в лабораторной диагностике этого заболевания. Предложено использовать полученные результаты в сфере глубокого понимания биохимических процессов, лежащих в основе нейрональной смерти, для ранней диагностики БП в разных возрастных группах и дальнейшего изучения патогенеза на основе фундаментальной биохимии и патобиохимии процессов, протекающих в клетке.

Ключевые слова: болезнь Паркинсона, дофамин, дофаминовые рецепторы, ключевые аспекты патохимии и патогенеза, биомаркеры

Благодарности: выражаем благодарность за помощь сотрудникам кафедры фундаментальной и клинической биохимии с лабораторной диагностикой ФГБОУ ВО СамГМУ Минздрава России, в частности профессору, д.м.н. Ф. Н. Гильмияровой, доценту, к.ф.н. А. В. Ждановой в подготовке материалов и дизайна рукописи.

Вклад авторов: О. А. Гусякова — анализ литературы; С. В. Смирнов — сбор данных в сфере фундаментальной биохимии; О. Ю. Кузнецова — анализ и интерпретация научных данных; А. Р. Апергенова, А. Р. Альбикова — подготовка рукописи.

✉ **Для корреспонденции:** Сергей Вячеславович Смирнов
ул. Арцыбушевская, д. 171, 443001, г. Самара, Россия; s.v.smirnov@samsmu.ru

Статья получена: 24.07.2023 **Статья принята к печати:** 14.08.2023 **Опубликована онлайн:** 29.08.2023

DOI: 10.24075/vrgmu.2023.030

Parkinson's disease (PD) is a chronic neurodegenerative and neuroinflammatory disease associated with the development of motor and non-motor impairments. The disease mainly affects dopaminergic neurons in the substantia nigra causing accumulation of α-synuclein protein and Lewy bodies in the cells. Individuals over the age of 65 are more likely to develop PD; the prevalence is about 140 cases per 100,000 population. The incidence of PD among males is 1.5 times higher, which can be due to exposure to toxic substances, traumatic brain injury, X-linked genetic defects. However, the researchers pay maximum attention to the neuroprotective role of estrogens. Taking into account the low pace of studying the mechanisms underlying this disorder, no description of the key aspects of pathobiochemistry and in-depth studies of particular processes, no understanding of the chemical essence of the behavior of certain substances that are of diagnostic value, this disorder can be considered to be an urgent medical and social issue, especially for individuals of older age groups [1–11]. The study was aimed to familiarize the reader with our opinion about certain pathochemical aspects of Parkinson's disease and laboratory value of some biomarkers.

Interrelationship between the dopamine and melanin biosynthesis pathways

Neuromelanin is synthesized directly from catecholamines. L-DOPA (L-dihydroxyphenylalanine) is subjected to hydroxylation and decarboxylation in natural conditions as a dopamine precursor. An alternative pathway of the mediator and its precursor metabolism is represented by endosomal accumulation of the mediator that moves to mitochondria by means of specific transporter (VMAT2) to be further biotransformed by monoamine

oxidase (MAO). The over-ac cumulated dopamine and DOPA are oxidized by iron-containing enzymes to quinones and semiquinones and are stored in the form of neuromelanin [12, 13]. The neuromelanin exact structure and functions are still poorly understood. We are going to try to model the cyclic structure of possible neuromelanin polymer formation and suggest the reader to discuss this structure. The structure of dioxyindole is provided below (Fig. 1). This fused heterocycle has rather interesting properties allowing us to shed some light on its biochemical behavior in the cell bodies of the CNS neurons and its role of possible neuromelanin monomer.

In particular, we believe that the side chain hydroxyl group being mainly an ortho-director enables aggregation through lateral cross-linking of the benzene rings of the benzpyrrole bicyclic system of indole involving attachment to the linear structure of neuromelanin in ortho position. However, considering the properties of the pyrrole part of the indole molecule, different pattern of interaction should be expected. It is pyrrole rings that enable formation of the product of intermolecular cyclization, similar to unsubstituted porphyrins, yielding tetra-dioxyindole. The +M effect of eight OH groups in the cyclic structure contributes to better stabilization of the delocalized π-conjugated system and enhancement of its chelating properties towards the center (as in heme), however, enhancement of acidic properties by the type of phenol in lateral OH groups of the molecule benzene nucleus should be also taken into account (Fig. 2).

Considering the fact that iron ions (Fe^{3+}) accumulate in the cells as part of the ferritin micelles after passing through apoferritin that can be rich with tryptophan amino acid residues, iron ions (Fe^{2+}) oxidize and stay in the micelle core in the form of complex complexone with the following biochemical composition: $[(FeO^{*}\mathbf{OH})_{8}(FeO^{*}OPO_{3}H_{2})]$. We can see similar stoichiometric ratio of OH groups (highlighted in bold) that can be involved in retention of the +3 oxydation state iron ions. Furthermore, the chelating part apparently can reduce Fe^{3+} ions to Fe^{2+} is addition to pericyclic adsorption of eight Fe^{3+} ions by the cyclic variant of neuromelanin. This presents a certain danger to the cell's life and underlies neuronal death. The reason is that the iron ions contained in such structure (despite the fact that it is similar to porphyrin structure) cannot have the same function as that contained in the heme transport substances with constant +2 oxydation state or in cytochromes, in which iron is in fact represented by the Fe^{3+}/Fe^{2+} redox couple. This is how the +2 oxidation state iron ions being powerful reducing

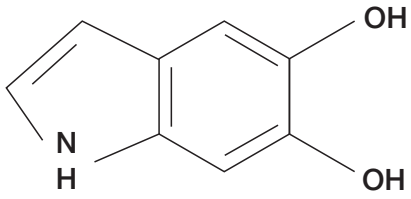

Fig. 1. Chemical structure of dioxyindole being the neuromelanin monomer involved in the eumelanin metabolic pathway of tyrosine

agents are accumulated, thereby provoking oxidative stress and eventually cell death.

Dopamine biochemical properties and functions

Dopamine, a mediator of neuroendocrine and paracrine regulation of the peripheral organs, does not cross the blood-brain barrier. Dopamine receptors belong to the family of the transmembrane metabotropic type G protein-coupled receptors. Five dopamine receptor subtypes were revealed when the gene cloning technique was introduced: D_1, D_2, D_3, D_4, D_5. Dopaminergic receptors are considered to be "slow" G (from the word "guanine) protein-coupled receptors using secondary intracellular mediators (3',5'-cyclic adenosine monophosphate or cAMP in this case), in contrast to "fast" receptors (such as GABA receptors) that bind directly to the ligand-gated channels. Receptors are divided into two main groups: 1) D_1-like receptors (D_1, D_5) activate adenylate cyclase, activation of such receptors causes muscle relaxation and vasodilation; 2) D_2-like receptors (D_2, D_3, D_4), presynaptic in sympathetic nerves, inhibit adenylate cyclase, activation of such receptors enchances the effects of catecholamines. In the central nervous system (CNS) these receptors play an important role in regulation of motion and cognitive function realization. Receptors of the D_{1A} and D_{2A} subgroups regulate the cardiovascular system functions. Disruption of the substantia nigra and abnormalities of the D_1-like receptors can be observed in individuals with Parkinson's disease; dopamine production and the effect on the receptors are reduced [8, 9].

PD laboratory signs

In blood serum and oral fluid

Presynaptic α-synuclein protein is involved in the synaptic vesicle transpot and subsequent neurotransmitter release. There are three

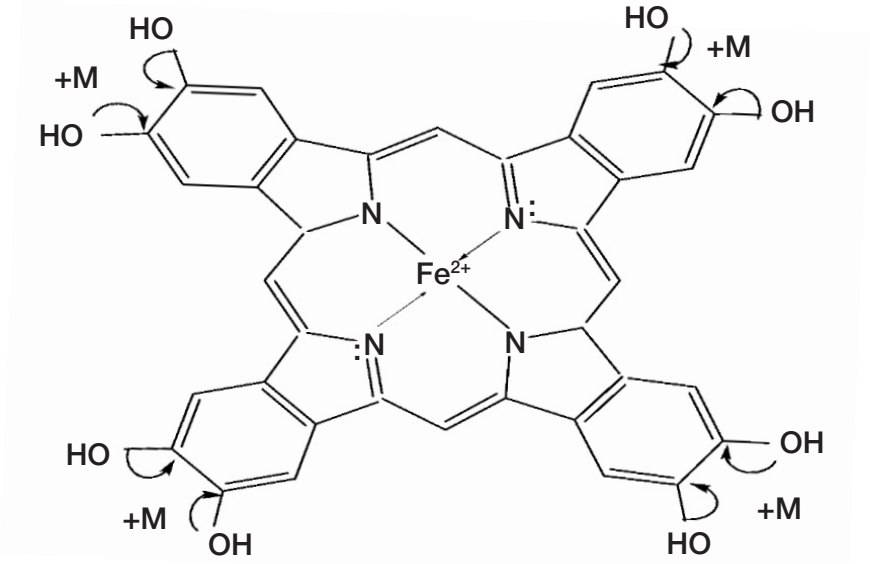

Fig. 2. Possible product of intermolecular cyclization: dioxyindole tetramer as a basis of the neuromelain cyclic tructure

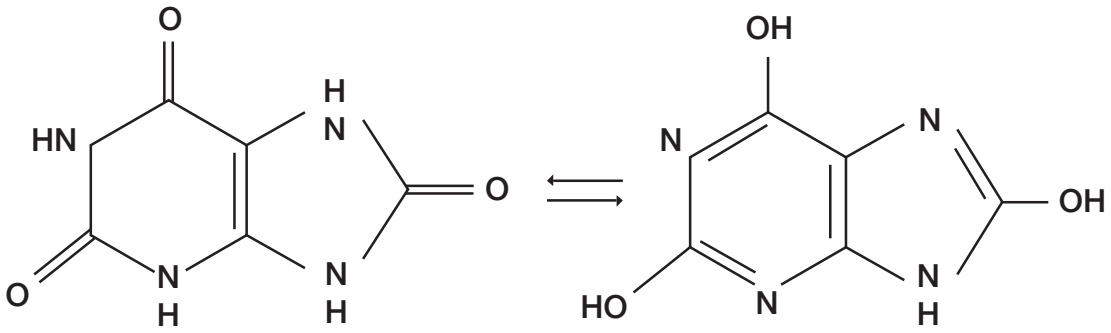

Fig. 3. Chemical structure of uric acid in the form of two possible native tautomers

α-synuclein isoforms produced by alternative splicing: 140 amino acids (base form), 126 amino acids and 112 amino acids. The base form of α-synuclein consists of the hydrophobic central region (non-amyloid component), amino-terminal region containing recurring amino acid sequences, and the negatively charged C-terminal region containing several phosphorylation sites and the domain responsible for α-synuclein chaperone activity. The N- terminal region is similar to the lipid-binding domain of apolipoproteins, which indicates the α-synuclein ability to interact with the membrane lipids. There is an assumption that two forms of this protein exist in the cells: native and membrane-binding. The α-synuclein native form is an unfolded protein with the disordered spiral structure. It is the increase in neurotoxic aggregates of this small protein that is important for the disease pathochemistry [3].

The Parkinson disease protein 7 (DJ-1 protein) is involved in cell functions, including transcription regulation and the response to oxidative stress, the processes that are directly related to neurodegeneration. Mutations of the gene encoding this protein are a rare cause of autosomal recessive parkinsonism; such mutations are associated with impaired DJ-1 capability of dimerization, its stability and folding. The DJ-1 protein functions include antioxidant, transcription co-activator and molecular chaperone activity. This protein has different catalytic and non-catalytic functions in different compartments of the cell: the DJ-1 protein acts as a co-activator of various signaling pathway in the cell nucleus, thereby preventing cell death; in mitochondria, it is contained in syntasomes, in which it interacts with the ATP synthase β-subunit. The decrease in the levels of normal protein results in the decrease in its function in oxidative stress [6, 14].

Uric acid: the risk of PD is inversely related to plasma levels of uric acid. Thanks to its double bonds, uric acid can possess antioxidant activity as an unsaturated, electron-deficient heterocyclic structure [7, 8, 10–12]. This property of the compound can underlie total antioxidant capacity of blood plasma and cerebrospinal fluid, thereby protecting the human body against reactive oxygen species and nitrogen (singlet oxygen, hydroxyl radicals, hydrogen peroxide and peroxynitrite).

In blood plasma

The emergence of autoantibodies in blood plasma of individuals with PD is associated with chronic neuronal damage and degeneration. Neuropeptides, nucleofactor 200, S100, etc. are products of neuronal degradation (this triggers autoimmune component of the disease pathogenesis resulting in synthesis of specific antibodies (cell adhesion molecule 4, myotilin, fibronectin, elongation factor 1-alpha 1).

In cerebrospinal fluid

High interleukin 6 (Il6) levels are associated with the 3.5-fold increase in the risk of PD, which is a neuroinflammation biomarker. Interleukin 6 belongs to the family of Il6 cytokines, the other members of which include Il11, Il27, Il31, etc. The Il6 biological activity is related to its ability to activate the target genes involved in cell differentiation, survival, apoptosis, and proliferation. Il6 is involved in intracellular signal transmission, thereby causing activation of tyrosine kinase triggering phosphorylation of transcription factors involved in regulation of the Il6 synthesis. Stimulation of the acute phase inflammatory response, associated with the expression of the Il-encoding gene in the liver and manifesting itself in the increase in the concentration of the acute phase inflammatory proteins (primarily C-reactive protein and haptoglobin), represents the Il6 pro-inflammatory effect. We believe that one of its pathochemical mechanisms can underlie its pro-inflammatory effect on glial cells in case of high levels in cerebrospinal fluid, as well as the decrease in biosynthesis of neurotrophic peptides (belonging to the group of peptide NTF biomolecules, which, like IL6, implement signaling pathways through gp130 in the neuronal membrane apparatus) that contribute to survival of the cerebral neurons in oxidative stress in healthy body. In inflammation, this group of cytokines is likely to play a role of intracellular anti-inflammatory factors similar to anti-inflammatory myokines of the muscle tissue belonging to the same family of biomolecules based on biochemistry [15].

Uric acid

In our opinion, biochemical potential of uric acid in neurodegenerative disorders is of interest. As is known, there are two tautomeric forms of this organic acid: lactim and lactam. In the body it obviously can exist in both forms playing a certain role in pathochemistry of some disorders, including PD (Fig. 3). Thus, a well-known fact in the PD pathogenesis is the loss of catecholamine neurons by the patient's body that eventually results in progression of clinical manifestations. This means that the effects of substances capable of increasing the effects of biogenic amines have a certain positive influence on the disease course and the patients' condition improvement. It has been found that the patients' health improvement correlates with the increase in the levels of this metabolite in cerebrospinal fluid. The logical question is: what is the possible mechanism of action of the acid itself? Apparently, there are at least two such mechanisms. According to pharmacological biochemistry, tri- and dimethylxanthines are inhibitors of certain phosphodiesterases. The enzymes of this class are divided into two types based on their localization in the cell: membrane-bound and cytosole. It is possible that the lactim form of this acid that has a certain dipole moment and a polarized OH group (besides, not only one) has strong acidic properties and is unable to cross the cell membrane. However, by analogy with the "mobile" OH group and aromatic nature of the chroman core of tocopherols, it can be retained in the membrane apparatus of

certain cells, including neurons. Furthermore, on the one hand it functions as a local antioxidant, and on the other hand as a phosphodiesterase inhibitor (as a xanthine derivative), thereby prolonging the effects of catecholamines (while biogenic amines have a membrane-mediated mechanism of action). Meanwhile, it is the membrane-bound form of mostly type I phosphodiesterase that is inhibited: it targets cAMP activated by Ca^{2+} cations, $4Ca^{2+}$-calmodulin complex + cGMP in healthy body.

CONCLUSION

Thus, we have systematized and characterized in terms of biochemistry the following laboratory signs of Parkinson's disease: 1) α-synuclein accumulation; 2) mutations of the gene encoding the DJ-1 protein; 3) changes in a number of blood plasma antibodies; 4) presence of potential biomarkers: Il6, uric acid. A number of processes play an important role in pathochemistry of Parkinson's disease: the decrease in the levels of dopamine and the number of neurons in the substantia nigra; accumulation of neuromelanin with certain chemical structure in neurons; the decrease in tyrosine hydroxylase activity; the final link of the PD pathochemistry is represented by α-synuclein degradation in the CNS and peripheral ANS neurons; it is possible that the decrease in the levels of the uric acid lactim form in the membrane apparatus of the cell bodies of neurons is of some importance. The reported details of the neuromelanin production pathochemistry and biochemistry of the uric acid behavior in native conditions can be biomarkers or biosensors of oxidative stress experienced by the neuronal cell bodies of individuals with this disorder. These details can be of some diagnostic value even in the pre-clinical phase of the disease (before manifestation). We believe that further research is required for better understanding of biochemistry of various intracellular processes and the behavior of substances that are of some pathogenetic and diagnostic value to enable early diagnosis and timely detection of the new disease cases in the population not only in the groups at risk, but also in other age groups.

References

1. Kucheryanu VG, Bocharov EV, Voronina NA, Bocharova OA. Ispol'zovanie nejroprotektorov pri parkinsonizme. Acta Naturae (russkoyazychnaya versiya). 2019; 11 (S1): 35. Russian.
2. Chuxlovin BA, Guzeva VI, Chuxlovina ML, Shabalov NP. Vozrastnye aspekty sindroma parkinsonizma. Pediatriya. Zhurnal im. G.N. Speranskogo. 2008; 87 (6): 118–20. Russian.
3. Yakshimbetova AI, Karyagina NT. Rol' a-sinukleina v patoximii bolezni Parkinsona. Vestnik Bashkirskogo gosudarstvennogo medicinskogo universiteta. 2022; S5: 110–5. Russian.
4. Palyulin VA. Dizajn novyx veshhestv dlya korrekcii narushenij funkcij centraln'oj nervnoj sistemy. NIR: grant # 20-15-18009. Rossijskij nauchnyj fond. 2020. Russian.
5. Buchachenko AL. Razrabotka novyx idej i metodov v ximii bioantiaksidantov kak sredstva protiv okislitel'nogo stressa. NIR: grant # 20-13-00148. Rossijskij nauchnyj fond. 2020. Russian.
6. Buneeva OA, Medvedev AE. Belok DJ-1 i ego rol' v razvitii bolezni Parkinsona: issledovaniya na ehksperimental'nyx modelyax. Bioximiya. 2021; 86 (6): 771–86. DOI: 10.31857/S0320972521060026. Russian.
7. Illarioshkin SN, Levin OS. Rukovodstvo dlya vrachej. V sbornike: Materialy IV nacional'nogo kongressa po bolezni Parkinsona i rasstrojstvam dvizhenij (s mezhdunarodnym uchastiem). M., 2017; 381 s. Russian.
8. Sokolov AV, Miliukhina IV, Belsky YP, et al. Potential role of lactoferrin in early diagnostics and treatment of Parkinson disease. Medical Academic Journal. 2020; 20 (1): 37–44. DOI: 10.17816/MAJ33848.
9. Zaripov NA. Bemorii Parkinson, me"yorњoi tashxis va tashxisim tafriќavї. Avdzhi Zuxal. 2021; 1: 136–41. Russian.
10. Daminova XM. Modern view to optimization of the diagnosis of the course of Parkinson's disease. New Day in Medicine. 2022; 1 (39): 115–8.
11. Vishniakou UA. Yiwei X. IT Diagnostics of Parkinson's Disease Based on the Analysis of Voice Markers and Machine Learning. V sbornike: Doklady Belorusskogo gosudarstvennogo universiteta informatiki i radioehlektroniki. 2023; 21 (3): 102–10. DOI: 10.35596/1729-7648-2023-21-3-102-110.
12. Katunina EA, Ilina EP, Sadekova GI, Gajsenyuk EI. Podxody k rannej diagnostike bolezni Parkinsona. Zhurnal nevrologii i psixiatrii im. C.C. Korsakova. 2019; 119 (6): 119–27. DOI: 10.17116/jnevro2019119061119. Russian.
13. Available from (aktivna na 08.08.2023): https://wiki2.org/ru/nejromelanin.
14. Available from (aktivna na 11.08.2023): http://elib.fesmu.ru/eLib/Article.aspx?id=414239.
15. Available from (aktivna na 11.08.2023) https/en.wikipedia.org/wiki/Ciliary_neurotrophic_factor.

Литература

1. Кучеряну В. Г., Бочаров Е. В., Воронина Н. А., Бочарова О. А. Использование нейропротекторов при паркинсонизме. Acta Naturae (русскоязычная версия). 2019; 11 (S1): 35.
2. Чухловин Б. А., Гузева В. И., Чухловина М. Л., Шабалов Н. П. Возрастные аспекты синдрома паркинсонизма. Педиатрия. Журнал им. Г.Н. Сперанского. 2008; 87 (6): 118–20.
3. Якшимбетова А. И., Карягина Н. Т. Роль а-синуклеина в патохимии болезни Паркинсона. Вестник Башкирского государственного медицинского университета. 2022; S5: 110–5.
4. Палюлин В. А. Дизайн новых веществ для коррекции нарушений функций центральной нервной системы. НИР: грант № 20-15-18009. Российский научный фонд. 2020.
5. Бучаченко А. Л. Разработка новых идей и методов в химии биоантиаксидантов как средства против окислительного стресса. НИР: грант № 20-13-00148. Российский научный фонд. 2020.
6. Бунеева О. А., Медведев А. Е. Белок DJ-1 и его роль в развитии болезни Паркинсона: исследования на экспериментальных моделях. Биохимия. 2021; 86 (6): 771–86. DOI: 10.31857/S0320972521060026.
7. Иллариошкин С. Н., Левин О. С. Руководство для врачей. В сборнике: Материалы IV национального конгресса по болезни Паркинсона и расстройствам движений (с международным участием). М., 2017; 381 с.
8. Sokolov AV, Miliukhina IV, Belsky YP, et al. Potential role of lactoferrin in early diagnostics and treatment of Parkinson disease. Medical Academic Journal. 2020; 20 (1): 37–44. DOI: 10.17816/MAJ33848.
9. Зарипов Н. А. Бемории Паркинсон, меъёрњои ташхис ва ташхисим тафриќавї. Авджи Зухал. 2021; 1: 136–41.
10. Daminova XM. Modern view to optimization of the diagnosis of the course of Parkinson's disease. New Day in Medicine. 2022; 1 (39): 115–8.
11. Vishniakou UA. Yiwei X. IT Diagnostics of Parkinson's Disease Based on the Analysis of Voice Markers and Machine Learning. В сборнике: Доклады Белорусского государственного

университета информатики и радиоэлектроники. 2023; 21 (3): 102–10. DOI: 10.35596/1729-7648-2023-21-3-102-110.
12. Катунина Е. А., Ильина Е. П., Садекова Г. И., Гайсенюк Е. И. Подходы к ранней диагностике болезни Паркинсона. Журнал неврологии и психиатрии им. С.С. Корсакова. 2019; 119 (6): 119–27. DOI: 10.17116/jnevro2019119061119.
13. Доступно по ссылке (активна на 08.08.2023): https://wiki2.org/ru /нейромеланин.
14. Доступно по ссылке (активна на 11.08.2023): http://elib.fesmu.ru/eLib/Article.aspx?id=414239.
15. Доступно по ссылке (активна на 11.08.2023) https/en.wikipedia.org/wiki/Ciliary_neurotrophic_factor.

BIOCHEMICAL AND MORPHOLOGICAL SUBSTANTIATION OF THE CONNECTIVE TISSUE HYPOTHESIS OF MANDIBULAR THIRD MOLAR ERUPTION

Korshunov AS[1,4] ✉, Vagner VD[2], Belskaya LV[3], Kuryatnikov KN[1,4], Serov DO[4], Krasnov VA[4], Tigranyan GO[1], Bondar IA[1]

[1] Omsk State Medical University, Omsk, Russia

[2] Central Research Institute of Dentistry and Maxillofacial Surgery, Moscow, Russia

[3] Omsk State Pedagogical University, Omsk, Russia

[4] City Clinical Dental Polyclinic № 1, Omsk, Russia

Studying the mechanism underlying tooth eruption is an important and promising area due to the increased incidence of the diseases associated with tooth eruption abnormalities or difficulties that can result in purulent and septic complications. The study was aimed to explore variability and structural features of the hard tissue mineral component and organic matrix in mandibular third molars being at different stages of tooth eruption. Microscopic examination and biochemical testing of the enamel, dentin, and dentin–enamel junction of the study participants' (n = 67; females aged 14–36) mandibular third molars were performed by scanning electron microscopy and Fourier transform infrared (FT-IR) spectroscopy. The association of the tooth eruption stage with the hard tissue structural features, such as the degree of mineralization and the size of dentinal tubules, orientation and size of the enamel prisms, was revealed. There were significant differences in the mandibular third molar hard tissue water content, which was demonstrated by metabolic processes and maturation rate ($p < 0.05$). According to the IR spectroscopy data, intensity of the collagen absorption bands in the enamel increases with age, while in dentin it decreases (1202, 1249, and 1342 cm^{-1}). Furthermore the combination of the reduced intensity of the 1202 cm^{-1} band with the increase in the 1342 cm^{-1} dentin–enamel junction band confirms the important role it plays as a link between the enamel and dentin due to its metabolic, shock-absorbing, protective, and nutritional functions. The findings demonstrate significant changes in the wrapping and orientation of the collagen fibrils and fibers in the hard tissue, which affect primary spatial orientation and mandibular dental topography.

Keywords: IR spectroscopy, connective tissue dysplasia, biochemistry, eruption, enamel, dentin, dentin–enamel junction

Author contribution: Korshunov AS — study planning, literature analysis, data interpretation, clinical data acquisition, manuscript writing; Vagner VD — study planning, literature analysis, data interpretation; Belskaya LV — study planning, biochemical investigations, manuscript writing; Kuryatnikov KN — clinical data acquisition, literature analysis, data interpretation, manuscript writing; Serov DO — clinical data acquisition, data interpretation, literature analysis; Krasnov VA — clinical data acquisition, sample preparation for assessment; Tigranyan GO, Bondar IA — sample preparation for assessment, data analysis.

Compliance with ethical standards: the study was approved by the Ethics Committee of the Omsk State Medical University (extract from the protocol № 113 of 26 November 2019); the informed consent was submitted by all study participants or their legal representatives.

✉ **Correspondence should be addressed:** Andrey S. Korshunov
Kosareva, 34, Omsk, 644043, Russia; andrey_k_180588@mail.ru

Received: 31.07.2023 **Accepted:** 23.08.2023 **Published online:** 31.08.2023

DOI: 10.24075/brsmu.2023.035

БИОХИМИЧЕСКОЕ И МОРФОЛОГИЧЕСКОЕ ОБОСНОВАНИЕ СОЕДИНИТЕЛЬНОТКАННОЙ ГИПОТЕЗЫ ПРОРЕЗЫВАНИЯ НИЖНИХ ТРЕТЬИХ МОЛЯРОВ

А. С. Коршунов[1,4] ✉, В. Д. Вагнер[2], Л. В. Бельская[3], К. Н. Курятников[1,4], Д. О. Серов[4], В. А. Краснов[4], Г. О. Тигранян[1], И. А. Бондарь[1]

[1] Омский государственный медицинский университет, Омск, Россия

[2] Центральный научно-исследовательский институт стоматологии и челюстно-лицевой хирургии, Москва, Россия

[3] Омский государственный педагогический университет, Омск, Россия

[4] Городская клиническая стоматологическая поликлиника № 1, Омск, Россия

Изучение механизма прорезывания зубов является важным и перспективным направлением ввиду увеличения частоты случаев возникновения болезней, связанных с нарушением или затрудненным прорезыванием, которые могут приводить к гнойно-септическим осложнениям. Целью исследования было изучить вариабельность и структурные особенности минерального компонента и органического матрикса в твердых тканях нижних третьих моляров, находящихся на разных стадиях прорезывания. У участников исследования (n = 67; женщины, возраст от 14 до 36 лет) проводили микроскопическое и биохимическое исследование эмали, дентина и эмалево-дентинного соединения нижних третьих моляров методами растровой электронной микроскопии и ИК-Фурье-спектроскопии. Продемонстрирована связь стадии прорезывания со структурными особенностями твердых тканей: уровнем минерализации и размерами дентинных канальцев, ориентацией и размерами эмалевых призм. Содержание воды в твердых тканях нижних третьих моляров значимо различается, что характеризуют обменные процессы и скорость созревания ($p < 0,05$). По данным ИК-спектроскопии интенсивность полос поглощения коллагена с возрастом в эмали увеличивается, а в дентине уменьшается (1202, 1249 и 1342 $см^{-1}$), при этом сочетание снижения интенсивности полосы 1202 $см^{-1}$ с увеличением полосы 1342 $см^{-1}$ у эмалево-дентинного соединения подтверждает его важную роль связующего звена между эмалью и дентином за счет обменной, амортизирующей, защитной, питательной функций. Полученные данные указывают на значительные изменения упаковки и ориентации коллагеновых фибрилл и волокон в твердых тканях, что влияет на первичную пространственную ориентацию и топографическое расположение зубов в нижней челюсти.

Ключевые слова: ИК-спектроскопия, дисплазия соединительной ткани, биохимия, прорезывание, эмаль, дентин, эмалево-дентинное соединение

Вклад авторов: А. С. Коршунов — планирование исследования, анализ литературы, интерпретация данных, набор клинического материала, подготовка рукописи; В. Д. Вагнер — планирование исследования, анализ литературы, интерпретация данных; Л. В. Бельская — планирование исследования, проведение биохимических исследований, подготовка рукописи; К. Н. Курятников — набор клинического материала, анализ литературы, интерпретация данных, подготовка рукописи; Д. О. Серов — набор клинического материала, интерпретация данных, анализ литературы; В. А. Краснов — набор клинического материала, подготовка образцов для исследования; Г. О. Тигранян, И. А. Бондарь — подготовка образцов для исследования, анализ данных.

Соблюдение этических стандартов: исследование одобрено этическим комитетом ФГБОУ ВО ОмГМУ Министерства здравоохранения РФ (выписка из протокола № 113 от 26 ноября 2019 г.); все участники исследования или их представители подписали добровольное информированное согласие.

✉ **Для корреспонденции:** Андрей Сергеевич Коршунов
ул. Косарева, д. 34, г. Омск, 644043, Россия; andrey_k_180588@mail.ru

Статья получена: 31.07.2023 **Статья принята к печати:** 23.08.2023 **Опубликована онлайн:** 31.08.2023

DOI: 10.24075/vrgmu.2023.035

Tooth eruption is a unique natural process with multifactorial reproducibility mechanism that makes it possible to judge about the development of not only oral, but also the whole body's organs and tissues [1]. Eruption is a complex biological event involving dynamic changes at the tissue and cellular levels [2]. It is guided by anatomical structures, biological and molecular factors that make the tooth move to its final functional position in the oral cavity [3].

During eruption the teeth move in three directions and gradually increase in size within the alveolar part of the mandible before active eruption. The tooth demonstrates minor circular movements when the coronal part is formed [4, 5].

Some tooth eruption theories were proposed centuries ago, many of these theories were revised, amended or disproved [6]. The best known and well substantiated ones are as follows: the tooth theory (Hunter, 1870), alveolar theory (L.J. Baume, 1890), pulp theory (G.V. Yasvoin, 1929), bone tissue rearrangement theory (J. Tandler, 1928; A.Ya. Katz, 1940; B. Orban, 1953; J. Reichborn-Kjennerud, 1959; M.Ya. Berry, 1968). Many authors accept the theory that the connective tissue embracing the erupting mandibular third molar is the most probable source of eruptive forces [7]. According to other data, the coronal and basal cells of tooth enamel and tooth follicle can send a signal that induces differentiation of the relatively nearby mesenchymal or progenitor cells, transforms these into cells having specific functions, i.e. osteoblasts and osteoclasts [8].

According to another hypothesis, vascular and tissue pressure can affect the eruption rate. The experiment involving dental alveoli of rats has shown that pressure increases after removal of interstitial fluid, eventually causing the eruption rate reduction [9].

The researchers believe that a major role is played by differentiation of the tooth germ tissues, when the volume increases and certain pressure (tension) is generated in it under the force during eruption [10].

The developing mandibular third molar must be through the cascade of mineralized and non-mineralized connective tissues, and the enamel provides an insulating barrier that protects the tooth against physical, chemical, and thermal exposures under favorable conditions. In some cases the dental enamel structure insufficiency can make the course of dental disease more severe. There is an opinion that dental enamel contains no collagen, however, there are sporadic reports that provide evidence of the presence of collagen in this unique biological tissue [11, 12].

The complex epithelial-mesenchymal interactions and crosstalk within hard tissues take place at the early stages of tooth formation [13]. Recent observations make it possible to challenge conventional scientific evidence and assume that the enamel crystal growth is initiated by the mineralized collagen fibrils from dentin. Then these crystals cross the dentin–enamel junction to reach the ameloblast membrane and spread across the enamel surface. Such structure makes it possible to build the connective complexes, in which secretory ameloblasts form a semi-permeable barrier for intercellular transport of minerals and ions that circulate freely in the enamel matrix. Intercellular transport of fluids that neutralize pH of the enamel matrix can be realized through the above connective complexes [14].

The presence of collagen fibrils in the dental hard tissues is of significant scientific and practical value for dentistry. It has been found that in humans, amelogenins and enamelins interact with the collagen family members during intraosseous eruption [13]. Collagens are produced by odontoblasts and are found in the dentin, while amelogenins are produced by ameloblasts and are contained in the enamel. It has been shown that type IV collagen is expressed within the dentin–enamel junction, type I and VII collagens come from dentin and cross the dentin–enamel junction to reach the enamel. The role of the amelogenin–collagen and enamelin–collagen interactions or expansion of dentinal collagens into the enamel inner matrix will help explain the importance and unusual structural and biochemical features of the dentin–enamel junction [15].

Thanks to the development of dentistry, biochemistry, nanotechnology, new protein, dentin, and bone species have been reported that possess unique capabilities of affecting the hard tissue mineral structure. Microscopy results are indicative of the complex relationship between the apatite crystals; the issues of intermolecular and intramolecular interactions between protein matrices and the maxillofacial region mineralized tissue inorganic phase are the most pressing [16].

It is well known that inorganic phase of the dental enamel and dentin is represented by hydroxyapatite crystals showing more stable vibrations in the mid-IR region [12].

The literature reports studies of proteins contained in human fetal tooth germs and mature enamel of permanent teeth. Such studies cover just a few frequencies or IR spectra of proteins, while interpretation of the studies can be found in sporadic reports. More recent studies show that dental enamel of the fetal tooth germ is not similar to the erupted tooth enamel. The tooth germ enamel contains thousands of times less protein than the permanent tooth enamel, it differs little from soft tissues of the body in terms of density and protein content [17].

It has been found that the components of organix matrix originate from the dentin–enamel junction, where it partially intertwines with the dentin collagen fibrils along the whole length. The organic matrix that is above the dentin–enamel junction is represented by the layer of intertwined fine fibers forming something like an inhomogeneous wide-loop mesh along the whole length of the dentin–enamel junction separating enamel from dentin. Such a complex structure allows many researchers to affirm that the dentin collagen fibrils intertwine with the enamel organix matrix [18]. This, in turn, results to the emergence of collagen among specific enamel proteins, amelogenins and enamelins, while the organic matrix diffraction pattern is determined by the diffusely blurred rings.

The other studies demonstrate the decrease of the organic phosphate levels in the fetal dental enamel and mature enamel with age, which is reflected in the decrease in the IR spectra absorption bands. IR spectra of fetal dental enamel differ considerably from the collagen and keratin spectra, which makes it possible to consider the majority of enamel proteins to be collagen or keratin type proteins [19].

During enamel formation, intensity of the protein bands that are within the absorbance region of carboxyl groups is reduced in the IR spectra due to binding of mineral components. The content of orthophosphate groups in the fetal tooth germ enamel increases during formation of the apatite structure, while in mature enamel, the content of orthophosphate groups almost does not change with age. Intensity of vibrations of pyrophosphate groups contained in apatite of the enamel increases during pre- and postnatal ontogenesis [20].

Based on the reviewed literature, we believe that it is relevant and desirable to describe new ideas about the mandibular third molar eruption on the basis of biochemical and morphological rearrangements in these teeth.

The study was aimed to explore variability of the hard tissue organic matrix and mineral component in mandibular third molars being at different stages of tooth eruption using microscopy and biochemical methods.

Table 1. Size of the dentin layer and dentinal tubules of mandibular third molars of the surveyed patients during various eruption phases

Age group / Parameter		14–17 years	18–21 years	22–26 years	27–31 years	32–36 years
Dentin layer thickness, mm	1	–	–	–	–	–
	2	2.9	2.8	3.3	3.5	3.4
		[2.7; 3.0]	[2.6; 3.0]	[3.1; 3.5]	[3.3; 3.8]	[3.3; 3.6]
	3	3.2*	3.3*	3.7*	3.9*	3.4
		[3.0; 3.5]	[3.1; 3.5]	[3.6; 3.9]**	[3.8;4.0]	[3.2; 3.6]
		(p = 0.002)	(p = 0.01)	(p = 0.002)	(p = 0.02)	(p = 1.90)
	4	3.7	3.8	4.1*	4.3*	3.2
		[3.6; 3.8]	[3.6; 3.9]	[4.0; 4.3]**	[4.2; 4.5]	[3.1; 3.5]**
		(p = 0.002)	(p = 0.001)	(p = 0.02)	(p = 0.001)	(p = 1.99)
Width of dentinal tubules near the pulp, nm	1	–	–	–	–	–
	2	2.33	2.35	2.41	2.41	2.41
		[2.31; 2.34]	[2.33; 2.36]	[2.39; 2.43]**	[2.40; 2.43]	[2.40; 2.43]
	3	2.39*	2.39*	2.46*	2.45*	2.34*
		[2.37; 2.43]	[2.37; 2.42]	[2.45; 2.48]**	[2.44; 2.47]	[2.32; 2.35]**
		(p = 0.001)	(p = 0.02)	(p = 0.02)	(p = 0.02)	(p = 0.0001)
	4	2.45*	2.43	2.49*	2.48	2.31
		[2.44; 2.47]	[2.42; 2.44]	[2.48; 2.51]**	[2.47; 2.49]	[2.29; 2.32]
		(p = 0.02)	(p = 0.91)	(p = 0.001)	(p = 0.22)	(p = 0.34)
Width of dentinal tubules near the dentin–enamel layer, nm	1	1.21	1.23	1.25	1.24	1.21
		[1.19; 1.26]	[1.19; 1.28]	[1.22; 1.28]	[1.22; 1.27]	[1.18; 1.25]
	2	3.24*	3.26*	3.41*	3.39*	3.13
		[3.21; 3.28]	[3.23; 3.29]	[3.39; 2.44]**	[3.35; 3.45]	[3.09; 3.17]**
		(p = 0.0001)	(p = 0.0001)	(p = 0.0001)	(p = 0.0001)	(p = 0.001)
	3	3.31*	3.33*	3.45	3.45	3.12
		[3.29; 3.31]	[3.32; 3.35]**	[3.43; 3.48]**	[3.44; 3.46]	[3.07; 3.17**]
		(p = 0.02)	(p = 0.01)	(p = 0.56)	(p = 0.19)	(p = 0.88)
	4	3.35*	3.36	3.51	3.52*	3.15
		[3.32; 3.39]	[3.33; 3.39]	[3.46; 3.55]**	[3.48; 3.55]	[3.11; 3.19]**
		(p = 0.02)	(p = 0.17)	(p = 1.05)	(p = 0.02)	(p = 1.98)

Note: * — differences between tooth eruption phases; ** — significant differences between age groups (Mann–Whitney U test, Wilcoxon signed-rank test, Bonferroni corrected at $p < 0.02$). No significant differences in/between age groups have been revealed ($p > 0.05$). 1 — tooth germ phase; 2 — tooth grown to the level of the gum; 3 — tooth grown to the mid-crown of the second molar; 4 — fully erupted tooth.

METHODS

Clinical trial

The study involved 67 women aged 14–17, 18–21, 22–26, 27–31, 32–36, who were followed up and treated by orthodontist and oral surgeon at the General Practice Dental Department of the City Clinical Dental Polyclinic №1, Center for Diagnosis and Treatment of Connective Tissue Dysplasia of the Omsk State Medical University (Omsk, Russian Federation). All study participants underwent extraction of teeth 38, 48 (due to orthodontic indications or tooth eruption difficulties) in 2021–2022. IR spectroscopy was performed in the Laboratory of Biochemistry Research of the Omsk State Pedagogical University.

Inclusion criteria for the study group: women, who underwent extraction of intact teeth (38, 48), with the confirmed diagnosis (according to ICD-10) of K05.22 (aggressive periodontitis), K05.32 (chronic periodontitis), K00.6 (disturbances in tooth eruption), K01.0 (embedded teeth); age 14–36 years; Slavic appearance (Caucasian race); connective tissue dysplasia; total score of +17 (severe degree). The comparison group included normosthenic women.

Exclusion criteria: male patients, women under the age of 14 and over the age of 36; mandibular third molars with chronic foci of infection in periapical tissues affected by caries; subcompensated or decompensated chronic disorder; individuals addicted to alcohol or drugs, those who had earlier used ulcerogenic drugs (non-steroidal anti-inflammatory drugs, glucocorticosteroids, etc.); hypersthenic body habitus; Asian or Negroid appearance; connective tissue dysplasia; total score of less than 17 (mild-to-moderate degree); the diagnosis not mentioned as an inclusion criterion (according to ICD-10).

The mandibular third molar eruption stages were assessed based on the computed tomography images and divided into four groups: tooth germ, tooth grown to the level of the gum, tooth grown to the mid-crown of the second molar, fully erupted tooth.

Connective tissue dysplasia was diagnosed, and dental hard tissues were collected for biochemical tests in accordance with the previously reported methods [21, 22].

Method to collect enamel, dentin–enamel junction, dentin for microscopy

During the first phase the extracted tooth was fixed with a woodworking clamp and separated in a mesiodistal direction

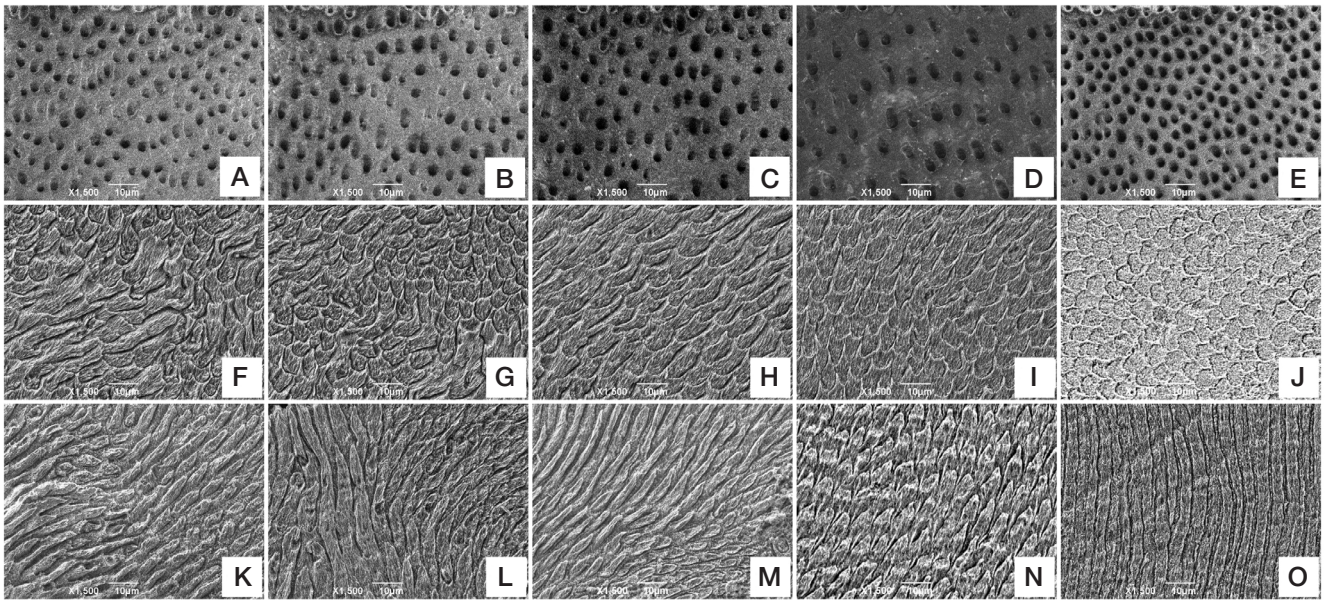

Fig. 1. Structure of dentinal tubules, packaging of enamel prisms in the surface and deep layers (scanning electron microscopy; 1500× magnification). Structure of dentinal tubules: 14–17 years (**A**); 18–21 years (**B**); 22–26 years (**C**); 27–31 years (**D**); 32–36 years (**E**). Packaging of enamel prisms in the surface layer: 14–17 years (**F**); 18–21 years (**G**); 22–26 years (**H**); 27–31 years (**I**); 32–36 years (**J**). Packaging of enamel prisms in the deep layer: 14–17 years (**K**); 18–21 years (**L**); 22–26 years (**M**); 27–31 years (**N**); 32–36 years (**O**)

with a diamond disc to provide a longitudinal section. The tooth fragment prepared was placed in the PVC tube chuck with the cut turned down and poured with the two part epoxy resin for 24 h.

During the second phase the resulting specimen was processed using the MP-1B Grinder/Polisher (MRC; UK) and the 800, 1500, 2000, 2500 grit dexter grinding wheels (Leroy Merlin; France). Final polishing was performed using the felt polishing wheel with the GOI polishing paste for plastics. The specimen surface was pickled with the 37% phosphoric acid (H_3PO_4) for 20 s in the enamel area and for 15 s in the dentin area. The specimen was dried with the cellulose napkin. The specimen was placed on the stage of the Jeol JCM – 5700 scanning electron microscope (JEOL Ltd.; Japan) for examination. The use of the described method makes it possible to study the enamel, dentin, and dentin–enamel junction morphology on the longitudinal section using a scanning electron microscope.

Method of IR spectra acquisition and pre-processing

The enamel, dentin, and dentin–enamel junction samples were dried to the constant weight at a temperature of 105 °C for 6 h, then the mass fraction of moisture was determined. Powders were tested in tablets pressed in a mixture with potassium bromide (ratio 1 : 100; diameter 3.5 mm). The spectrum of pure potassium bromide previously dried at a temperature of ~600 °C for 6 h was used as a reference spectrum. IR absorption spectra were acquired with the FT-891 Fourier transform infrared spectrometer (SIMECS; Russia) in the 500–4000 cm^{-1} range (number of scans — 32, resolution — 4 cm^{-1}). Baseline correction and normalization of spectra were performed using the ZaIR 3.5 software (SIMECS; Russia). Position and intensity of the absorption bands (AB) were determined in all spectra.

Statistical data processing

Statistical analysis of the results was performed using the Statistica 10.0 software package (StatSoft; USA) by nonparametric methods: Wilcoxon signed-rank test for dependent samples and Mann–Whitney *U* test for independent samples. The sample was described using median (Me) and interquartile range in the form of the 25th and 75th percentiles (L_Q; U_Q). The differences were considered significant at $p < 0.05$.

RESULTS

Our findings have shown that dentinal tubules originate on the dentin inner surface and cross dentin in the outward direction perpendicular to the tangential fibers of the ground substance. The radial and tangential collagen fibers define topographic arrangement and correct orientation of the dentinal tubules. It has been noted that in young people (aged 14–17, 18–21), the dentinal tubules are small, in contrast to the age groups of 22–26 years, 27–31 years, 32–36 years. In the age group of 32–36 years the decrease in the dentinal tubule size is observed that is due to the reduced trophic function and dental hard tissue mineralization, obliteration and emergence of numerous denticles, which adversely affect metabolic processes and can results in the dental hard tissue diseases. As mandibular third molar moves towards the occlusal plane and full eruption, the size of dentinal tubules significantly increases in all age groups (14–17 years, 18–21 years, 22–26 years, 27–31 years) ($p < 0.05$) (Table 1; Fig. 1A–E).

Our studies have demonstrated the increase in mineralization of the dentinal tubule inner layer at the stage of mandibular third molar eruption to the mid-crown of the second molar in the age groups of 21–26 years, 27–31 years, which is consistent with the literature data on the dentinal tubules' varying width [23]. The described ring of the dentinal tubule mineralization is narrower near the pulp and wider near the dentin–enamel junction (Table 1; Fig. 1A–E). Thickening of the dentin layer is reported in all the compared age groups, except for the group aged 32–36, in which its thickness remains unchanged with the mandibular third molar development and its growth to the mid-crown of the second molar. Dentinogenesis proceeds evenly and actively throughout all stages of tooth eruption, which is reflected by statistical analysis of the groups being compared ($p > 0.05$) (Table 1).

The width of prisms in various areas of enamel changes with age and as mandibular third molar eruption proceeds. We have revealed a significant increase in the size of enamel prisms in individuals aged 27–31; no such increase is observed

Table 2. Width of enamel prisms in various enamel layers of mandibular third molars of the surveyed patients during various eruption phases

Age group / Parameter		14–17 years	18–21 years	22–26 years	27–31 years	32–36 years
Width of enamel prisms in the surface layer, nm	1	4.13	4.16	4.25	4.44	4.45
		[4.11; 4.15]	[4.13; 4.19]**	[4.22; 4.29]**	[4.42; 4.46]	[4.42; 4.49]
	2	4.21*	4.29*	4.36*	4.51*	4.53*
		[4.19; 4.23]	[4.26; 4.31]**	[4.34; 4.37]**	[4.49; 4.53]	[4.51; 4.55]
		(p = 0.0002)	(p = 0.001)	(p = 0.0002)	(p = 0.0001)	(p = 0.001)
	3	4.46*	4.49*	4.52*	4.59*	4.61*
		[4.43; 4.48]	[4.45; 4.53]	[4.50; 4.55]**	[4.56; 4.61]	[4.57; 4.64]
		(p = 0.0002)	(p = 0.0002)	(p = 0.001)	(p = 0.001)	(p = 0.0002)
	4	4.35*	4.55	4.59*	4.68*	4.71*
		[4.33; 4.38]**	[4.52; 4.59]	[4.56; 4.62]	[4.65; 4.72]	[4.69; 4.73]
		(p = 0.0001)	(p = 0.58)	(p = 0.0001)	(p = 0.0002)	(p = 0.002)
Width of enamel prisms in the deep layer, nm	1	4.52	4.51	4.55	4.66	4.65
		[4.50; 4.55]	[4.48; 4.54]	[4.53; 4.56]**	[4.63; 4.69]	[4.63; 4.68]
	2	4.61*	4.62*	4.63*	4.78*	4.76*
		[4.60; 4.63]	[4.60; 4.65]	[4.60; 4.67]**	[4.74; 4.82]	[4.73; 4.79]
		(p = 0.002)	(p = 0.001)	(p = 0.0001)	(p = 0.001)	(p = 0.001)
	3	4.71*	4.73*	4.75*	4.92*	4.91*
		[4.68; 4.75]	[4.71; 4.76]	[4.73; 4.77]**	[4.90; 4.95]	[4.87; 4.95]
		(p = 0.002)	(p = 0.002)	(p = 0.001)	(p = 0.001)	(p = 0.001)
	4	4.89*	4.87*	4.82*	5.02*	4.99*
		[4.85; 4.91]	[4.85; 4.91]	[4.80; 4.85]**	[5.00;5.05]	[4.97; 5.02]
		(p = 0.0002)	(p = 0.001)	(p = 0.002)	(p = 0.0001)	(p = 0.02)

Note: * — differences between tooth eruption phases; ** — significant differences between age groups (Mann–Whitney U test, Wilcoxon signed-rank test, Bonferroni corrected at $p < 0.02$). No significant differences in/between age groups have been revealed ($p > 0.05$). 1 — tooth germ phase; 2 — tooth grown to the level of the gum; 3 — tooth grown to the mid-crown of the second molar; 4 — fully erupted tooth.

in individuals over the age of 32 ($p > 0.05$). The rapid increase in the size of prisms in deep layers of enamel was detected during such tooth eruption stages, as tooth germ and tooth grown to the level of the gum, in all groups being compared. The width increase in the enamel surface layer throughout early stages of the mandibular third molar eruption is far behind relative to deep layers in all age groups ($p > 0.05$) (Table 2; Fig. 1E–O).

We have found that growth of prisms in the enamel surface layer significantly increases in the age groups of 18–21 years ($p = 0.001$), 22–26 years ($p = 0.002$) during the stages of tooth germ and tooth grown to the level of the gum, while in deep layers it is increased in the age group of 22–26 years throughout all stages of tooth eruption ($p < 0.05$).

We have revealed significant differences in the mandibular third molar hard tissue water content that characterize metabolic processes and the rate of the molars' maturation on their way to full eruption. The highest enamel water content is observed in the age groups of 18–21 years, 22–26 years at the stage of the mandibular third molar grown to the level of the gum. No significant changes in the enamel water content were revealed at other stages of tooth eruption ($p > 0.05$) (Table 3).

The dentin water content changes with age. The highest dentin water content is observed in the age groups of 18–21 years, 22–26 years throughout all phases of tooth eruption ($p < 0.05$). A significant increase in water content associated with the mandibular third molar full eruption is observed in the above age groups. No significant differences have been revealed in other age groups, however, the water content downward trend has been reported for the age group of 32–36 years (Table 3).

The same changes in this parameter as that reported for dentin have been reported for the dentin–enamel junction, along with positive dynamics of the increase in the age group of 22–26 years throughout all phases of tooth eruption (Table 3).

A total of 19 absorption bands have been identified in the mandibular third molar hard tissue IR spectra: 3239 cm^{-1} (νsO-H); 2963 cm^{-1} (νasCH3); 2922 cm^{-1} (νasCH$_2$); 2855 cm^{-1} (νsCH$_2$); 1769 cm^{-1} (νC=C); 1637 and 1618 cm^{-1} (νC=O); 1546 cm^{-1} (δN-H, νC-N); 1454 cm^{-1} (δasCH3, δCH$_2$); 1418 cm^{-1} (νC-N, δN-H, δC-H); 1384 cm^{-1} (δCH3); 1342 cm^{-1} (CH2); 1249 and 1202 cm^{-1} (δN-H, νC-N); 1106 cm^{-1} (νsPO, νCC, νCO); 1050 cm^{-1} (PO4); 1037 cm^{-1} (νCC, νCO, νCH$_2$OH); 967 cm^{-1} (νPO$_4$); 876 cm^{-1} (δO-C-O) [22].

It has been shown that the set of absorption bands found in the mandibular third molar hard tissue IR spectra qualitatively does not change with age, while intensity of certain absorption bands changes significantly (Fig. 2). Intensity of the absorption bands of the methyl and methylene groups of lipids and proteins decreases with age (2855, 2922 and 2963 cm^{-1}), while that of phosphate groups increases (1050 cm^{-1}). This suggests the higher degree of hard tissue mineralization in the age groups of 27–31 years, 32–36 years. Apparent changes in the dentin–enamel junction structure predominate among age groups (Fig. 2B). Intensity of the dentinal collagen absorption bands (1202, 1249 and 1342 cm^{-1}) decreases with age (Fig. 2C), while that of the enamel increases (Fig. 2A); the dentin–enamel junction occupies an intermediate position and combines the decrease in the 1202 cm^{-1} band intensity with the increase in the 1342 cm^{-1} intensity

Table 3. Water content of the mandibular third molar hard tissues during various eruption phases in the group of surveyed patients

Age group / Parameter		14–17 years	18–21 years	22–26 years	27–31 years	32–36 years
Enamel, %	1	3.97	4.02	4.28	4.18	4.22
		[3.68; 4.09]	[3.94; 4.15]**	[4.19; 4.36]	[4.05; 4.29]	[4.11; 4.34]
	2	4.14	4.43*	4.49*	4.21	4.25
		[4.01; 4.25]**	[4.28; 4.56]	[4.37; 4.65]**	[4.06; 4.29]	[4.13; 4.39]
		(p = 0.54)	(p = 0.02)	(p = 0.02)	(p = 0.94)	(p = 0.94)
	3	4.29	4.58	4.59	4.38	4.41
		[4.18; 4.42]**	[4.46; 4.65]	[4.49; 4.71]	[4.28; 4.50]	[4.29; 4.56]
		(p = 0.78)	(p = 0.88)	(p = 0.84)	(p = 0.92)	(p = 0.95)
	4	4.28	4.59	4.65	4.42	4.39
		[4.15; 4.41]**	[4.46; 4.69]	[4.54; 4.76]	[4.29; 4.58]	[4.25; 4.51]
		(p = 0.79)	(p = 0.48)	(p = 0.81)	(p = 0.96)	(p = 0.83)
Dentin–enamel junction, %	1	–	–	–	–	–
	2	10.23	10.38	10.77	10.19	10.31
		[9.89; 10.43]	[10.03; 10.49]**	[10.56; 10.92]**	[9.91; 10.39]	[10.17; 10.45]
	3	10.56	10.89*	11.32*	10.41	10.43
		[10.12; 10.73]	[10.61; 10.98]**	[11.05; 11.52]**	[10.28; 10.54]	[10.27; 10.59]
		(p = 0.47)	(p = 0.02)	(p = 0.02)	(p = 1.13)	(p = 0.81)
	4	10.65	10.98	11.71*	10.58	10.55
		[10.11; 10.79]	[10.79; 11.14]**	[11.54; 11.96]**	[10.39; 10.76]	[10.36; 10.72]
		(p = 0.87)	(p = 0.45)	(p = 0.02)	(p = 0.74)	(p = 1.91)
Dentin–enamel junction, %	1	–	–	–	–	–
	2	7.93	8.35	8.43	8.05	8.12
		[7.76; 8.11]**	[8.21; 8.56]	[8.29; 8.61]**	[7.89; 8.26]	[8.01; 8.29]
	3	8.15	8.82*	8.91*	8.32	8.23
		[8.02; 8.32]**	[8.65; 8.99]	[8.75; 9.22]**	[8.19; 8.52]	[8.05; 8.44]
		(p = 0.75)	(p = 0.02)	(p = 0.02)	(p = 0.72)	(p = 0.38)
	4	8.43	8.95	9.01	8.44	8.34
		[8.25; 8.63]**	[8.82; 9.19]	[8.81; 9.35]**	[8.23; 8.64]	[8.11; 8.59]
		(p = 0.21)	(p = 0.49)	(p = 0.82)	(p = 0.98)	(p = 0.91)

Note: * — differences between tooth eruption phases; ** — significant differences between age groups (Mann–Whitney *U* test, Wilcoxon signed-rank test, Bonferroni corrected at $p < 0.02$). No significant differences between age groups have been revealed ($p > 0.05$). 1 — tooth germ phase; 2 — tooth grown to the level of the gum; 3 — tooth grown to the mid-crown of the second molar; 4 — fully erupted tooth.

(Fig. 2B). Such findings demonstrate an important role of the dentin–enamel junction being a key link between the enamel and dentin due to metabolic, shock-absorbing, protective, and nutritional functions.

The principal component analysis of the enamel, dentin and dentin–enamel junction samples' IR spectroscopy results in different age groups has shown that no differentiation of groups is reported for enamel and dentin. The vertical axis partially separates the age groups of 14–17 years and 27–31 years from other groups, however, such differentiation is non-significant (p = 0.5298 for enamel and p = 0.4157 for dentin) (Fig. 3A, B). The opposite pattern can be observed for the dentin–enamel junction (Fig. 3C, D). It is clear that the age groups of 14–17 years and 27–31 years are to the left of the vertical axis, while the horizontal axis separates these groups from each other (Fig. 3C). In this case differentiation of the groups is significant (p = 0.0392). The absorption bands of phosphate ions (1050 cm^{-1}; r = 0.7843; $p < 0.0001$), methyl and methylene groups of the lipid or protein carbon skeleton (2963 cm^{-1}; r = 0.7268; $p < 0.0001$), (2855 cm^{-1}; r = 0.6967; p < 0.0001), and collagen (1202 $см^{-1}$; r = 0.6592; $p < 0.0001$) (1249 cm^{-1}; r = 0.4763; $p < 0.0001$) contribute the most to differentiation of age groups (Fig. 3D), as we have earlier reported. A negative correlation coefficient has been obtained for the 1037 cm^{-1} (r = –0.8105; $p < 0.0001$) and 1418 cm^{-1} (r = –0.6498; $p < 0.0001$) absorption bands. As for the second axis, maximum contribution has been reported for the 1454 cm^{-1} absorption band (r = 0.7371; $p < 0.0001$) corresponding to vibrations of the methyl and methylene groups of proteins and the 1249 cm^{-1} collagen absorption band (r = –0.4117; $p < 0.0001$) (Fig. 3D).

The differences in the enamel, dentin, and dentin–enamel junction have been demonstrated at various stages of the mandibular third molar eruption. No significant changes in enamel have been revealed at the tooth germ stage, biochemical processes represent an integrated process. The mandibular third molar movement is associated with significant changes. The 0–0 horizontal axis separates the group with the teeth erupted to the middle of the second molar (above the axis) from the groups with fully erupted teeth (below the axis). The 0–0 vertical axis divides the groups with fully erupted teeth and the groups that are in the tooth germ phase. A more clear delineation of the groups is observed for dentin and dentin–enamel junction.

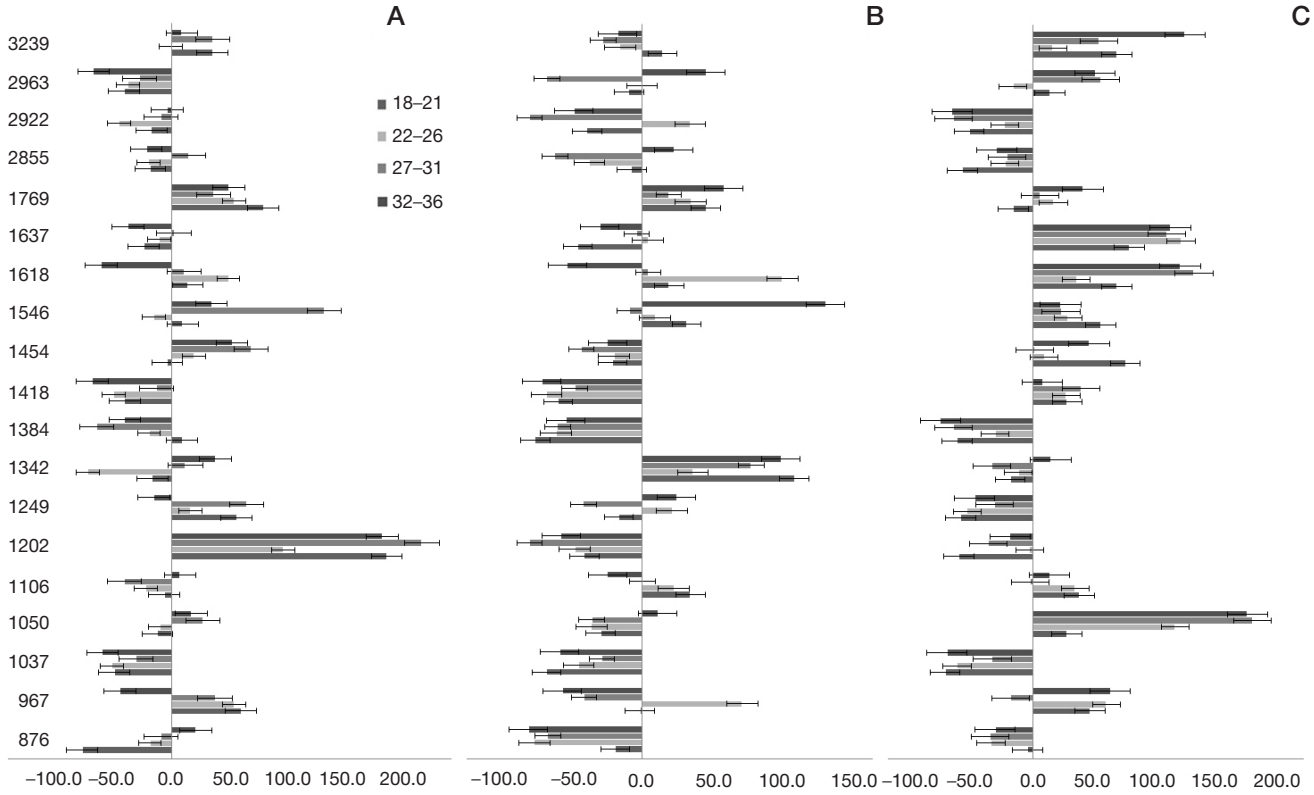

Fig. 2. Relative changes in the intensities of the IR spectra absorption bands: Enamel (**A**), dentin–enamel junction (**B**), dentin in various age groups relative to the group aged 14–17 (%) (**C**)

DISCUSSION

When comparing IR spectra in the comparison groups we agreed that orientation and organization of the collagen fibrils in dentin at early tooth eruption stages defined correct enamel prism packaging. Strong dentin-to-enamel adhesion is achieved due to correct organization of the dentin–enamel junction via a complex system of the tangling collagen fibrils in it [24]. The dentin biochemical alterations can results in abnormal enamel prism maturation, especially at early stages.

It has been noted that collagens are expressed in the dentin–enamel junction and dentin in all age groups. The

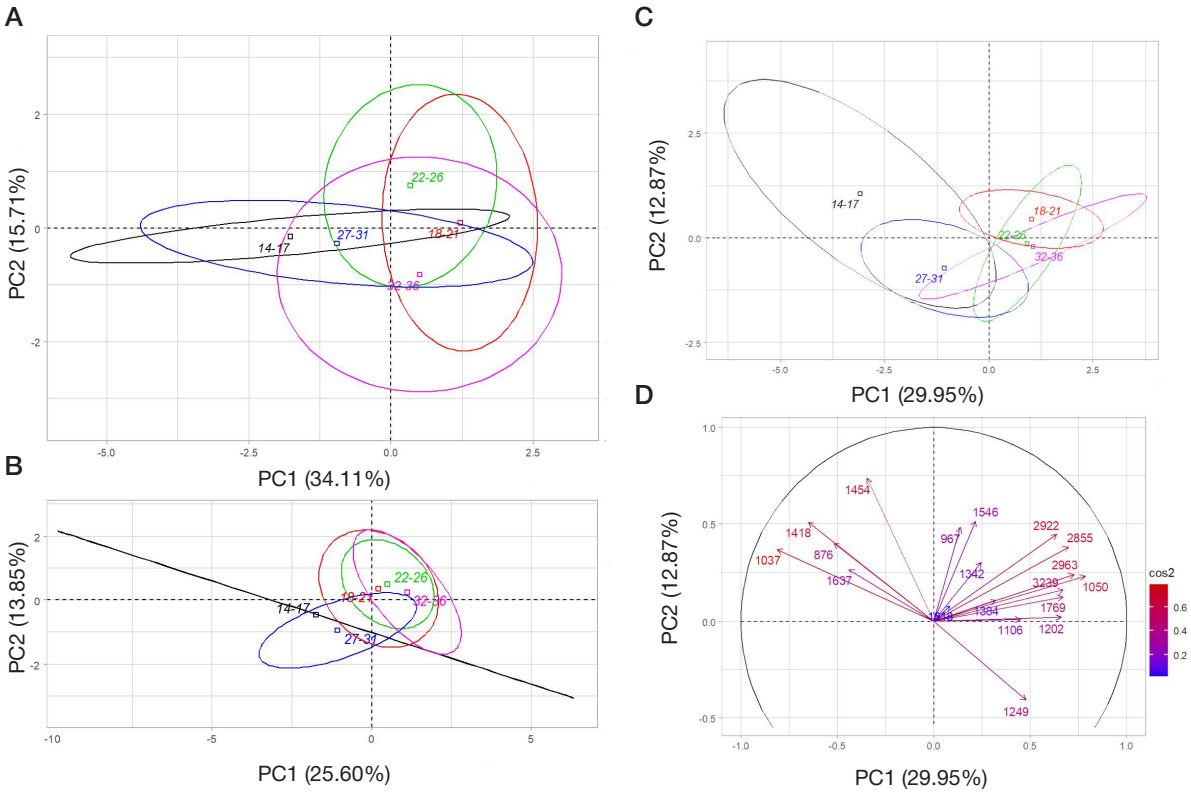

Fig. 3. Principal component analysis of IR spectra of various age groups: enamel (**A**), dentin (**B**); dentin–enamel junction: individual factor chart (**C**), variable factor map (**D**)

significance of such interactions, as amelogenin–collagen and enamelin–collagen, as well as the expansion of dentin collagens into the inner matrix of the deep enamel layer help explain structural, biochemical, and morphofunctional changes of enamel after the mandibular third molar eruption [25, 26].

We have found that sufficiency of the dentin–enamel junction and dentin connective tissue complex provides a strong semi-permeable barrier for intercellular transport of minerals and ions that circulate freely in the enamel matrix, thereby enabling a faster and more full-fledged maturation of mandibular third molars. Our observations complement the data of foreign researchers on the enamel crystal growth induced by the collagen fibrils of the dentin–enamel junction and dentin [27]. The enamel heterogeneity and integrity depend on the dentin–enamel junction and dentin biochemical and morphological state. The presence of congenital or acquired disorder or condition can impair the collagen structure, thereby causing major alterations of the dentin–enamel layer and enamel [28, 29].

The facts, that clinical material was collected from residents of one region only (Omsk Region), from women, mandibular third molars were the object of the study and no other groups of teeth were studied, and the samples of patients in the studied group were small, can be considered the study limitations. This necessitates further research in this area.

CONCLUSIONS

The results of the mandibular third molar hard tissue morphological and biochemical assessment confirm the existing data that mandibular third molars start changing their position at the tooth germ stage, when the pronounced changes in packaging and orientation of the dentin–enamel junction and dentin collagen fibrils and fibers, as well as their expansion into deep enamel layers affect initial spatial orientation and topographic arrangement of these teeth in the mandible. The data reported can answer the key question that correct orientation of the collagen fibrils in dentin and the dentin–enamel junction, coordinated action of the drainage network between the enamel and dentin via intraprismatic and interprismatic spaces and dentinal tubules that co-produce and increase pressure in the coronal part of the tooth trigger movement and growth of the mandibular third molar germs. This is a working hypothesis that needs in-depth analysis and requires further research.

References

1. Bankole OO, Lawal FB. Teething. Int Q Community Health Educ. 2017; 37 (2): 99–106. DOI: 10.1177/0272684X17701262.
2. Kjær I. Mechanism of human tooth eruption: review article including a new theory for future studies on the eruption process. Scientifica (Cairo). 2014; 2014: 341905. DOI: 10.1155/2014/341905.
3. Yu Y, Cui C, Guan SY, Xu RS, Zheng LW, Zhou XD, et al. Function of orofacial stem cells in tooth eruption: an evolving perspective. Chin J Dent Res. 2021; 24 (3): 143–52. DOI: 10.3290/j.cjdr.b1965049.
4. Marks SC Jr, Schroeder HE. Tooth eruption: theories and facts. Anat Rec. 1996; 245 (2): 374–93. DOI: 10.1002/(SICI)1097-0185(199606)245:2<374::AID-AR18>3.0.CO;2-M.
5. McDermott CL, Hilton K, Park AT, Tooley UA, Boroshok AL, Mupparapu M, et al. Early life stress is associated with earlier emergence of permanent molars. Proc Natl Acad Sci USA. 2021; 118 (24): e2105304118. DOI: 10.1073/pnas.2105304118.
6. Goncharova EI. Rost i razvitie zubov, ih gormonal'naya regulyaciya. Rossijskij stomatologicheskij zhurnal. 2013; 1: 53–56. DOI: 10.17816/dent.39190. Russian.
7. Berkovitz BK, Migdalski A, Solomon M. The effect of the lathyritic agent aminoacetonitrile on the unimpeded eruption rate in normal and root-resected rat lower incisors. Arch Oral Biol. 1972; 17 (12): 1755–63. DOI: 10.1016/0003-9969(72)90239-7.
8. Weintraub H. The MyoD family and myogenesis: redundancy, networks, and thresholds. Cell. 1993; 75 (7): 1241–4. DOI: 10.1016/0092-8674(93)90610-3.
9. Choukroune C. Tooth eruption disorders associated with systemic and genetic diseases: clinical guide. J Dentofacial Anom Orthod. 2017; 20 (4): 402. DOI: 10.1051/odfen/2018129.
10. Maksimovskij YuM. Stroenie i funkcii organov i tkanej polosti rta. Zuby. V knige: Maksimovskij Yu. M., redaktor. Terapevticheskaya stomatologiya. M., 2002; c. 45–50. Russian.
11. Leontev VK. Ehmal' zubov kak biokiberneticheskaya sistema. M.: GEhOTAR-Media, 2016; 72 c. Russian.
12. Shumilovich BR, Vorobeva YuB, Malyhina IE, Chertovskih AV. Sovremennye predstavleniya o kristallicheskoj strukture gidroksiapatita i processah vozrastnyh izmenenij ehmali zuba (issledovanie in vitro). Zhurnal anatomii i gistopatologii. 2015; 4 (1): 77–86.
13. Lacruz RS, Habelitz S, Wright JT, Paine ML. Dental enamel formation and implications for oral health and disease. Physiol Rev. 2017; 97 (3): 939–993. DOI: 10.1152/physrev.00030.2016.
14. Jussila M, Thesleff I. Signaling networks regulating tooth organogenesis and regeneration, and the specification of dental mesenchymal and epithelial cell lineages. Cold Spring Harb Perspect Biol. 2012; 4 (4): a008425. DOI: 10.1101/cshperspect.a008425.
15. McGuire JD, Walker MP, Mousa A, Wang Y, Gorski JP. Type VII collagen is enriched in the enamel organic matrix associated with the dentin-enamel junction of mature human teeth. Bone. 2014; 63: 29–35. DOI: 10.1016/j.bone.2014.02.012.
16. Kashkarov VM, Goloshchapov DL, Rumyantseva AN, Seredin PV, Domashevskaya EP, Spivakova IA, et al. X-ray diffraction and IR spectroscopy investigation of synthesized and biogenic nanocrystalline hydroxyapatite. J Surf Investig. 2011; 5: 1162–7. DOI: 10.1134/S1027451011120068.
17. Horakova L, Dalecka L, Zahradnicek O, Lochovska K, Lesot H, Peterkova R, et al. Eda controls the size of the enamel knot during incisor development. Front Physiol. 2023; 13: 1033130. DOI: 10.3389/fphys.2022.1033130
18. Vagner VD, Korshunov AS, Kuryatnikov KN, Rogachev EA, Belskaya LV, Sarf EA, i dr. Harakter obmennyh processov v tverdyh tkanyah zubov cheloveka v zavisimosti ot ih morfologicheskogo stroeniya. Stomatologiya. 2022; 101 (6): 7–13. DOI: 10.17116/stomat20221010617.
19. Silin AV, Terekhov AYu, Andreevskaya MV, Maryanovich AT. Proteins of mineralized dental tissues. Russian Biomedical Research. 2022; 7 (2): 53–68. DOI: 10.56871/1744.2022.70.82.005.
20. Shumilovich BR, Sadovskij VV, Sushhenko AV, Haritonov YuM. Fiziologicheskie izmeneniya morfologii osnovnoj strukturnoj edinicy ehmali — kristalla gidroksiapatita — v processe ego zhiznedeyatel'nosti (issledovanie in vitro). Stomatologiya. 2015; 94 (6): 11–18. DOI: 10.17116/stomat201594611-18. Russian.
21. Korshunov AS, Vagner VD, Kuryatnikov KN, Serov DO, Torohov AL, Shykhalieva DD, et al. Infrared Spectroscopy to Analyze Sexual Dimorphism of Hard Dental Tissue Maturation at Eruption in Patients with Connective Tissue Dysplasia. Appl Spectrosc. 2023; 77 (5): 457–69. DOI: 10.1177/00037028231160145.
22. Korshunov AS, Vagner VD, Kuryatnikov KN, Meloyan AD, Kasiy MN, Sarf EA, et al. IR-spectroscopic analysis of hard tissues of lower “wisdom” teeth at the eruption stage of connective tissue dysplasia. Journal of Applied Spectroscopy. 2022; 89 (4): 689–97. DOI: 10.1007/s10812-022-01410-9
23. Williams C, Wu Y, Bowers DF. ImageJ analysis of dentin tubule

distribution in human teeth. Tissue Cell. 2015; 47 (4): 343–8. DOI: 10.1016/j.tice.2015.05.004.
24. Moradian-Oldak J. Protein-mediated enamel mineralization. Front Biosci (Landmark Ed). 2012; 17 (6): 1996–2023. DOI: 10.2741/4034.
25. Du C, Falini G, Fermani S, Abbott C, Moradian-Oldak J. Supramolecular assembly of amelogenin nanospheres into birefringent microribbons. Science. 2005; 307 (5714): 1450–4. DOI: 10.1126/science.1105675.
26. Iijima M, Moradian-Oldak J. Interactions of amelogenins with octacalcium phosphate crystal faces are dose dependent. Calcif Tissue Int. 2004; 74 (6): 522–31. DOI: 10.1007/s00223-002-0011-3.
27. Bartlett JD. Dental enamel development: proteinases and their enamel matrix substrates. ISRN Dent. 2013; 2013: 684607. DOI: 10.1155/2013/684607.
28. Korshunov A, Vagner V, Konev V, Moskovskiy S, Kuryatnikov K, Skurikhina A, Yakovlev V, Nurakhmetova A. Research of connective tissue dysplasia influence on teething. Saudi Dent J. 2022; 34 (5): 385–89. DOI: 10.1016/j.sdentj.2022.05.002.
29. Josic U, Maravic T, Bossù M, Cadenaro M, Comba A, Ierardo G, et al. Morphological Characterization of Deciduous Enamel and Dentin in Patients Affected by Osteogenesis Imperfecta. Applied Sciences. 2020; 10 (21): 7835. DOI: 10.3390/app10217835.

Литература

1. Bankole OO, Lawal FB. Teething. Int Q Community Health Educ. 2017; 37 (2): 99–106. DOI: 10.1177/0272684X17701262.
2. Kjær I. Mechanism of human tooth eruption: review article including a new theory for future studies on the eruption process. Scientifica (Cairo). 2014; 2014: 341905. DOI: 10.1155/2014/341905.
3. Yu Y, Cui C, Guan SY, Xu RS, Zheng LW, Zhou XD, et al. Function of orofacial stem cells in tooth eruption: an evolving perspective. Chin J Dent Res. 2021; 24 (3): 143–52. DOI: 10.3290/j.cjdr.b1965049.
4. Marks SC Jr, Schroeder HE. Tooth eruption: theories and facts. Anat Rec. 1996; 245 (2): 374–93. DOI: 10.1002/(SICI)1097-0185(199606)245:2<374::AID-AR18>3.0.CO;2-M.
5. McDermott CL, Hilton K, Park AT, Tooley UA, Boroshok AL, Mupparapu M, et al. Early life stress is associated with earlier emergence of permanent molars. Proc Natl Acad Sci USA. 2021; 118 (24): e2105304118. DOI: 10.1073/pnas.2105304118.
6. Гончарова Е. И. Рост и развитие зубов, их гормональная регуляция. Российский стоматологический журнал. 2013; 1: 53–56. DOI: 10.17816/dent.39190.
7. Berkovitz BK, Migdalski A, Solomon M. The effect of the lathyritic agent aminoacetonitrile on the unimpeded eruption rate in normal and root-resected rat lower incisors. Arch Oral Biol. 1972; 17 (12): 1755–63. DOI: 10.1016/0003-9969(72)90239-7.
8. Weintraub H. The MyoD family and myogenesis: redundancy, networks, and thresholds. Cell. 1993; 75 (7): 1241–4. DOI: 10.1016/0092-8674(93)90610-3.
9. Choukroune C. Tooth eruption disorders associated with systemic and genetic diseases: clinical guide. J Dentofacial Anom Orthod. 2017; 20 (4): 402. DOI: 10.1051/odfen/2018129.
10. Максимовский Ю. М. Строение и функции органов и тканей полости рта. Зубы. В книге: Максимовский Ю. М., редактор. Терапевтическая стоматология. М., 2002; с. 45–50.
11. Леонтьев В. К. Эмаль зубов как биокибернетическая система. М.: ГЭОТАР-Медиа, 2016; 72 с.
12. Шумилович Б. Р., Воробьева Ю. Б., Малыхина И. Е., Чертовских А. В. Современные представления о кристаллической структуре гидроксиапатита и процессах возрастных изменений эмали зуба (исследование in vitro). Журнал анатомии и гистопатологии. 2015; 4 (1): 77–86.
13. Lacruz RS, Habelitz S, Wright JT, Paine ML. Dental enamel formation and implications for oral health and disease. Physiol Rev. 2017; 97 (3): 939–993. DOI: 10.1152/physrev.00030.2016.
14. Jussila M, Thesleff I. Signaling networks regulating tooth organogenesis and regeneration, and the specification of dental mesenchymal and epithelial cell lineages. Cold Spring Harb Perspect Biol. 2012; 4 (4): a008425. DOI: 10.1101/cshperspect.a008425.
15. McGuire JD, Walker MP, Mousa A, Wang Y, Gorski JP. Type VII collagen is enriched in the enamel organic matrix associated with the dentin-enamel junction of mature human teeth. Bone. 2014; 63: 29–35. DOI: 10.1016/j.bone.2014.02.012.
16. Kashkarov VM, Goloshchapov DL, Rumyantseva AN, Seredin PV, Domashevskaya EP, Spivakova IA, et al. X-ray diffraction and IR spectroscopy investigation of synthesized and biogenic nanocrystalline hydroxyapatite. J Surf Investig. 2011; 5: 1162–7. DOI: 10.1134/S1027451011120068.
17. Horakova L, Dalecka L, Zahradnicek O, Lochovska K, Lesot H, Peterkova R, et al. Eda controls the size of the enamel knot during incisor development. Front Physiol. 2023; 13: 1033130. DOI: 10.3389/fphys.2022.1033130
18. Вагнер В. Д., Коршунов А. С., Курятников К. Н., Рогачев Е. А., Бельская Л. В., Сарф Е. А., и др. Характер обменных процессов в твердых тканях зубов человека в зависимости от их морфологического строения. Стоматология. 2022; 101 (6): 7–13. DOI: 10.17116/stomat20221010617.
19. Silin AV, Terekhov AYu, Andreevskaya MV, Maryanovich AT. Proteins of mineralized dental tissues. Russian Biomedical Research. 2022; 7 (2): 53–68. DOI: 10.56871/1744.2022.70.82.005.
20. Шумилович Б. Р., Садовский В. В., Сущенко А. В., Харитонов Ю. М. Физиологические изменения морфологии основной структурной единицы эмали — кристалла гидроксиапатита — в процессе его жизнедеятельности (исследование in vitro). Стоматология. 2015; 94 (6): 11–18. DOI: 10.17116/stomat201594611-18.
21. Korshunov AS, Vagner VD, Kuryatnikov KN, Serov DO, Torohov AL, Shykhalieva DD, et al. Infrared Spectroscopy to Analyze Sexual Dimorphism of Hard Dental Tissue Maturation at Eruption in Patients with Connective Tissue Dysplasia. Appl Spectrosc. 2023; 77 (5): 457–69. DOI: 10.1177/00037028231160145.
22. Korshunov AS, Vagner VD, Kuryatnikov KN, Meloyan AD, Kasiy MN, Sarf EA, et al. IR-spectroscopic analysis of hard tissues of lower “wisdom” teeth at the eruption stage of connective tissue dysplasia. Journal of Applied Spectroscopy. 2022; 89 (4): 689–97. DOI: 10.1007/s10812-022-01410-9
23. Williams C, Wu Y, Bowers DF. ImageJ analysis of dentin tubule distribution in human teeth. Tissue Cell. 2015; 47 (4): 343–8. DOI: 10.1016/j.tice.2015.05.004.
24. Moradian-Oldak J. Protein-mediated enamel mineralization. Front Biosci (Landmark Ed). 2012; 17 (6): 1996–2023. DOI: 10.2741/4034.
25. Du C, Falini G, Fermani S, Abbott C, Moradian-Oldak J. Supramolecular assembly of amelogenin nanospheres into birefringent microribbons. Science. 2005; 307 (5714): 1450–4. DOI: 10.1126/science.1105675.
26. Iijima M, Moradian-Oldak J. Interactions of amelogenins with octacalcium phosphate crystal faces are dose dependent. Calcif Tissue Int. 2004; 74 (6): 522–31. DOI: 10.1007/s00223-002-0011-3.
27. Bartlett JD. Dental enamel development: proteinases and their enamel matrix substrates. ISRN Dent. 2013; 2013: 684607. DOI: 10.1155/2013/684607.
28. Korshunov A, Vagner V, Konev V, Moskovskiy S, Kuryatnikov K, Skurikhina A, Yakovlev V, Nurakhmetova A. Research of connective tissue dysplasia influence on teething. Saudi Dent J. 2022; 34 (5): 385–89. DOI: 10.1016/j.sdentj.2022.05.002.
29. Josic U, Maravic T, Bossù M, Cadenaro M, Comba A, Ierardo G, et al. Morphological Characterization of Deciduous Enamel and Dentin in Patients Affected by Osteogenesis Imperfecta. Applied Sciences. 2020; 10 (21): 7835. DOI: 10.3390/app10217835.

ANTIBACTERIAL, ANTI-ADHESIVE AND ANTI-BIOFILM-FORMING ACTIVITY OF PLANT COMPLEXES AGAINST PERIODONTOPATHOGENIC BACTERIA *IN VITRO*

Nosova MA[1], Latif II[2], Kraeva LA[2,3], Khamdulaeva GN[3], Sharov AN[4] ✉, Kopetskiy IS[5], Eremin DA[4], Postnikova EV[6], MA Postnikov[1]

[1] Samara State Medical University, Samara, Russia
[2] Military Medical Academy named after S.M.Kirov, St. Petersburg, Russia
[3] Saint-Petersburg Pasteur Institute, St. Petersburg, Russia
[4] ROMASHKA dental shop, department of scientific research, St. Petersburg, Russia
[5] Pirogov Russian National Research Medical University, Moscow, Russia
[6] Korolev Samara State University, Samara, Russia

Periodontitis is a problem urgent in Russia and throughout the world in general. Because of the dynamically changing flora causing this diseases, the treatment methods designed against it should be adapted on a regular basis. The classic approach to arresting development of the acute process relies on 0.2–0.12% chlorhexidine, a chemical antiseptic, but after 3 weeks of use, its efficacy drops drastically because pathogenic flora adjusts thereto. In the recent years, plant-based complexes with antiseptic properties have shown their capacity to challenge the classic approach. Obviously, efficacy of active ingredients depends on the form of the final product. The marker of periodontitis in the oral cavity is *Staphylococcus aureus*. *Klebsiella pneumoniae*, *Pseudomonas aeruginosa*, *Acinetobacter baumannii* have virulence markers that are copathogens for periodontitis. This study aimed to find plant-based preparations capable of eliminating the said microbes and *Streptococcus mitis*, *Streptococcus oralis*, *Streptococcus salivarius*, *Enterococcus faecalis*. We compared antibacterial, adhesion and biofilm formation preventing properties of Phytodent plant-based products in various forms: water solution, water-alcohol solution, oil solution, gel. Long exposure form — gel — proved to be the most effective in terms of the properties tested. Products with synthetic and plant-based antiseptics, as well as those with plant-based antiseptics in maximum concentration (elixir), had comparable efficacy. Water and oil solutions are less effective because of the lower active ingredient concentration and relatively brief exposure. Our results support the results of clinical studies dedicated to the use of Phytodent products as oral care products in the context of periodontitis prevention and treatment. We recommend conducting further studies comparing compositions, cross- and comparative studies investigating the effect of frequency of application and time of exposure, such studies registering titers of active ingredient concentrations, and with subjects thereof including mixed biofilms.

Keywords: periodontitis, copper derivatives of chlorophyll, gel, aspen bark, dihydroquercetin, biofilm formation preventing properties, antimicrobial properties, adhesion prevention properties, Phytodent

Acknowledgements: authors thank SS Astashova, illustrator with the Academy of Chlorophyll and Aspen Bark journal, for preparing photos and tables for this publication.

Author contribution: Kraeva LA, Khamdulayeva GN, Nosova MA — concept and design of the study; Latif II, Sharov AN — literature analysis, data collection and processing; Kraeva LA — statistical processing; Kraeva LA, Sharov AN, Latif II — manuscript drafting; Kopetsky IS, Eremin DA, Postnikova EV, Postnikov MA — editing.

Compliance with ethical standards: the study was approved by the Samara State Medical University's Ethics Committee (Minutes # ... of January 10, 2022)

✉ **Correspondence should be addressed:** Alexey N. Sharov
Nevsky Prospekt, 46, Saint Petersburg, Russia; me@sharovalex.ru

Received: 16.06.2023 **Accepted:** 08.08.2023 **Published online:** 24.08.2023

DOI: 10.24075/brsmu.2023.029

ИССЛЕДОВАНИЕ АНТИБАКТЕРИАЛЬНОЙ, АНТИАДГЕЗИВНОЙ И АНТИБИОПЛЕНКООБРАЗУЮЩЕЙ АКТИВНОСТИ РАСТИТЕЛЬНЫХ КОМПЛЕКСОВ В ОТНОШЕНИИ ПАРОДОНТОПАТОГЕННЫХ БАКТЕРИЙ *IN VITRO*

М. А. Носова[1], И. И. Латиф[2], Л. А. Краева[2,3], Г. Н. Хамдулаева[3], А. Н. Шаров[4] ✉, И. С. Копецкий[5], Д. А. Еремин[4], Е. В. Постникова[6], М. А. Постников[1]

[1] Самарский государственный медицинский университет, Самара, Россия
[2] Военно-медицинская академия имени С. М. Кирова, Санкт-Петербург, Россия
[3] Санкт-Петербургский научно-исследовательский институт эпидемиологии и микробиологии имени Пастера, Санкт-Петербург, Россия
[4] Стоматологический магазин «РОМАШКА», отдел научных исследований, Санкт-Петербург, Россия
[5] Российский национальный исследовательский медицинский университет имени Н. И. Пирогова, Москва, Россия
[6] Самарский национальный исследовательский университет имени С. П. Королева, Самара, Россия

Пародонтит — актуальная проблема в России и в мире, требующая регулярной адаптации схем лечения и реабилитации из-за динамично меняющейся пародонтопатогенной флоры. Классическая терапия купирования острого процесса включает использование химического антисептика хлоргексидин 0,2–0,12%, эффективного только до трех недель применения ввиду адаптации патогенной флоры. Растительные комплексы с антисептическим действием в последние годы зарекомендовали себя как способные заместить классическую терапию. Очевидно, что разные формы выпуска имеют разную эффективность. *Staphylococcus aureus* в полости рта служит маркером пародонтита. *Klebsiella pneumoniae*, *Pseudomonas aeruginosa*, *Acinetobacter baumannii* обладают маркерами вирулентности в качестве копатогенов при пародонтите. Целью исследования было выявить растительные препараты для борьбы с перечисленными микробами, а также с *Streptococcus mitis*, *Streptococcus oralis*, *Streptococcus salivarius*, *Enterococcus faecalis*. Проводили сравнительную оценку антибактериальной, антиадгезивной и антибиопленкообразующей активности отечественных средств «Фитодент» из растительного сырья: водных, водно-спиртовых и масляных растворов; гелевых форм. Наибольшая антибактериальная, антиадгезивная и антибиопленочная эффективность обнаружена у форм с длительной экспозицией — гелей, сопоставимая — у средств с синтетическими и с растительными антисептиками, а также у форм с максимальной концентрацией растительных антисептиков — эликсира. Водные и масляные формы за счет меньшей концентрации и сравнительно короткого времени контакта имеют меньшую эффективность. Полученные результаты подтверждают результаты клинических наблюдений за применением средств «Фитодент» в качестве ухода за полостью рта при лечении и профилактике пародонтита. Рекомендованы дальнейшие сравнительные исследования композиций, перекрестные и сравнительные исследования в зависимости от частоты применения и времени воздействия и с титрованием концентраций активных компонентов, в том числе на смешанных биопленках.

Ключевые слова: пародонтит, медные производные хлорофилла, гель, кора осины, дигидрокверцетин, антибиопленкообразующее действие, антимикробное действие, антиадгезивное действие, Фитодент

Благодарности: авторы выражают благодарность С. С. Асташовой, дизайнеру научно-практического журнала «Академия хлорофилла и коры осины» за подготовку фотографий и таблиц для публикации.

Вклад авторов: Л. А. Краева, Г. Н. Хамдулаева, М. А. Носова — концепция и дизайн исследования; И. И. Латиф, А. Н. Шаров — анализ литературы, сбор и обработка данных; Л. А. Краева — статистическая обработка; Л. А. Краева, А. Н. Шаров, И. И. Латиф — подготовка черновика рукописи; И. С. Копецкий, Д. А. Еремин, Е. В. Постникова, М. А. Постников — редактирование.

Соблюдение этических стандартов: исследование одобрено этическим комитетом СамГМУ (протокол № 7 от 10 января 2022 г.).

✉ **Для корреспонденции:** Алексей Николаевич Шаров
Невский пр., д. 46, г. Санкт-Петербург, Россия; me@sharovalex.ru

Статья получена: 16.06.2023 **Статья принята к печати:** 08.08.2023 **Опубликована онлайн:** 24.08.2023

DOI: 10.24075/vrgmu.2023.029

Periodontitis (P) is an extremely urgent oral cavity problem in Russia and the entire world in general [1–4]. Almost all medicines with proven effectiveness against it, those that arrest acute infectious and inflammatory processes, contain a chemical antiseptic, 0.12–0.2% chlorhexidine in most cases, regardless of the form of the product [5-8]. However, bacterial flora can grow resistant to chemical antiseptics, which makes them effective only for a limited period of time. In the recent years, plant-based complexes with antiseptic properties proved they are a viable alternative to the standard antiseptic therapy products, with which these complexes are comparable in terms of the range of action and efficacy [9–12]. Obviously, different forms of products, be they water solutions, water-alcohol solutions, oil solutions, or gels, have different efficacy, which is conditioned by the time the product remains on periodontal tissues, and subsequently, frequency of its use, time needed to arrest the acute process and, ultimately, the time of compensated stable remission of the patient [13–14]. There is evidence confirming antibacterial properties of phytoncides of coniferous plants, extracts from aspen bark, Japanese and sugar kelp. The results of their application have been known for a long time, and various combined forms are used in dentistry in a cosmopolitan manner. However, the evidence base is fragmentary, and its key components are clinical, not fundamental [15–18]. The preferred form of anti-periodontitis drugs is gel, which ensures prolonged exposure of periodontal tissues to active ingredients. The gels currently available to a periodontist contain either an antiseptic or substrates for tissue repair. There is no gel acting in all the directions needed, i.e. eliminating toxins and biological debris, promoting metabolism in periodontal tissues, producing a non–specific immunomodulatory effect, normalizing respiration and trophism in the periodontium, and, as a result, inducting autoregeneration [19].

Oral cavity is a habitat for a large number of different microorganisms. Most of them are commensals. However, a number of bacterial species directly or indirectly drive development of P and other inflammatory processes. For example, Streptococcus sanguinis promotes formation of biofilm on teeth that includes *Fusobacterium nucleatum*, which is one of the bacteria causing P [20], with one of the possible consequences thereof being endocarditis [21]. Many researchers seek for preparations, plant-based or synthesized from substances of natural origin, that would combat cariesogenic and periodontal bacteria *Streptococcus mitis*, *Streptococcus oralis*, *Streptococcus salivarius*, *Enterococcus faecalis* [22–25]. Detection of *Staphylococcus aureus* and its metabolites in the oral cavity can indicate a certain stage of P [26]. The "oral cavity — intestine" pathogenetic axis allows considering a number of bacteria, especially those with virulence markers, as copathogens in periodontitis: *Klebsiella pneumoniae*, *Pseudomonas aeruginosa*, *Acinetobacter baumannii* [27–29]. Therefore, we considered these pathogens in this work. The purpose of this study was to evaluate antibacterial, adhesion and biofilm formation preventing properties of various forms of products combining plant-based and synthetic components factoring in the vectors of their effect on flora causing periodontitis.

METHODS

The study was conducted at the Department of New Technologies of the Pasteur Research Institute in October 2021 – April 2022.

We used the patented gel composition that includes copper derivatives of chlorophyll, aspen bark, sodium alginate and dihydroquercetin (DHQ); this gel meets the requirements for complex therapy of P and has the necessary antibacterial properties [30]. The study has shown positive clinical results of application of gel with copper derivatives of chlorophyll, aspen bark, sodium alginate and DHQ against P [31] and gingivitis concomitant with P [32].

Compositions of active ingredients

The elixir is a water-alcohol concentrate of active ingredients: water, 20% ethyl alcohol, sodium-copper chlorophyllin, aspen bark extract, kelp extract, cocamidopropyl betaine, natural flavor "Mint", polyvinylpyrrolidone.

The mouthwash is a water concentrate of active ingredients: water, sodium-copper chlorophyllin, aspen bark extract, kelp extract, cocamidopropyl betaine, natural flavor "Mint", polyvinylpyrrolidone, sodium benzoate.

Phytolon oil is an oil solution of active ingredients: refined peach pit or olive oil, sodium-copper chlorophyllin.

Provitam oil is an oil solution of active ingredients: refined peach pit or olive oil, spruce concentrate with provitamins.

Gel 1 with chlorhexidine is a gel composition of active ingredients: sorbitol, water, hydrogenated castor oil, hydroxyethyl cellulose, sodium alginate, chlorhexidine hydrochloride, d-panthenol, allantoin, methylparaben, methyl salicylate, flavor "Pectral", menthol, fir extract, sodium-copper chlorophyllin, eugenol, pectin.

Gel 2 with aspen bark and DHQ is a gel composition of active ingredients: sorbitol, water, hydrogenated castor oil, hydroxyethyl cellulose, sodium alginate, dihydroquercetin, d-panthenol, allantoin, aspen bark extract, methylparaben, methyl salicylate, spruce extract complex, menthol, flavor "Pectral", citric acid, sodium-copper chlorophyllin, eugenol.

Gel 3 with chlorhexidine is a gel composition of active ingredients: sorbitol, water, hydrogenated castor oil, hydroxyethyl cellulose, sodium alginate, d-panthenol, chlorhexidine hydrochloride, allantoin, methylparaben, methyl salicylate, Pectral flavor, menthol, fir extract, sodium-copper chlorophyllin, eugenol, pectin; the product was 2 years expired.

Bacterial strains

Reference bacterial strains:
Staphylococcus aureus ATCC № 25923
Enterococcus faecalis ATCC № 29212
Klebsiella pneumoniae ATCC № 13883
Pseudomonas aeruginosa ATCC № 27853
Acinetobacter baumannii ATCC № 19606
Bacterial strains from the laboratory's collection of microorganisms:
Streptococcus sanguinis № 2111
Streptococcus mitis № 2118
Streptococcus oralis № 2114
Streptococcus salivarius № 2107

Research methods

We used the bacteriological method of research to study the effect of plant-based complexes on the bacteria's capability to survive, adhere to surfaces and form biofilms.

Investigation of antibacterial properties of plant-based complexes

We prepared microbial suspensions of 24-hour bacterial cultures in saline, initial content — 1×10^8 CFU/ml. Tenfold dilutions brought the content down to 1×10^5 CFU/ml. For the last

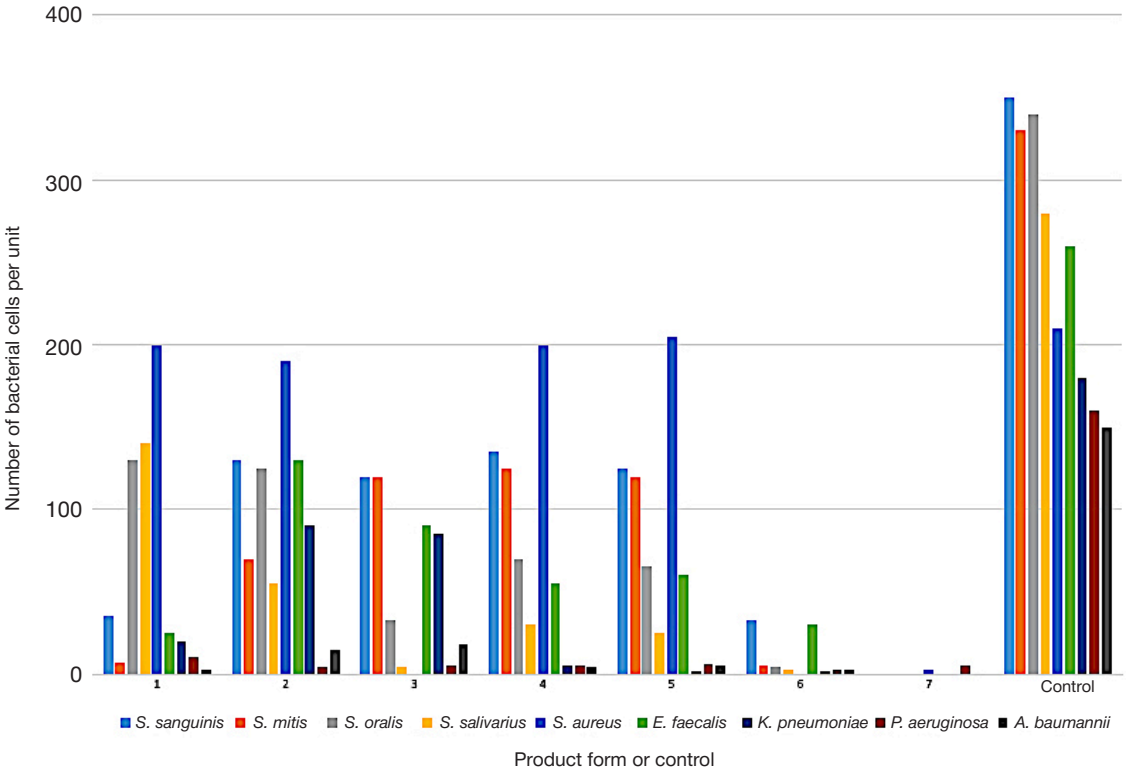

Fig. 1. Investigation of antibacterial properties of plant-based complexes. 1 — mouthwash; 2 — gel with chlorophyll, aspen bark and DHQ (Gel 2); 3 — gel with chlorophyll and chlorhexidine (Gel 1); 4 — oil with chlorophyll (Phytolone oil); 5 — oil with carotenoids from fir needles (Provitam oil); 6 — gel with chlorophyll and chlorhexidine (Gel 3); 7 — dental elixir with aspen bark extract and chlorophyll (Elixir)

dilution, we used meat peptone broth. Microbial suspensions were transferred to twenty four 1 ml tubes. One ml of each plant-based complex was added to 3 test tubes containing 1 ml of microbial suspension (final concentration), and the remaining 2 test tubes received 1 ml of saline. All test tubes were kept in the thermostat at +37 °C for 30 minutes. Then, we plated 10 mcl from each tube onto nutrient agar: blood agar for streptococci, meat peptone agar for other bacteria. Plating followed the lawn pattern. Petri dishes were incubated in a thermostat at +37 °C for 24 hours. Next, we counted colonies on dish and calculated simple mean for each plant ingredient sample.

Investigation of adhesion preventing properties of plant-based complexes

For this investigation, we applied A.S. Blagonravova's method [33] and used cells of buccal epithelium. The cells were washed three times from the indigenous microflora in buffered saline solution at pH 7.2–7.4, speed of 35 g, for 10 minutes. Then the cells were put into test tubes, 0.5 ml of bacterial suspension containing 3×10^8 CFU/ml of S.sanguinis and 0.5 ml of each plant-based complex into each tube. One test tube contained only buccal epithelium and was used as control (natural colonization). We did three cycles of all experiments and controls. Next, the tubes with all the components were intensively shaken and put into a thermostat to incubate at +37 °C for 30 minutes. After that, we washed out non-attached microorganisms, prepared smears on slides, fixed and Gram stained the bacteria. The adhesion index was calculated by the formula:

$$AI = AB50/50E, (1)$$

where AI is the adhesion index, AB50 is the number of bacterial cells that attached to 50 epithelial cells, and 50E is the 50 studied epithelial cells.

Investigation of biofilm formation preventing properties of plant-based complexes

In the context of this investigation, we registered microcolonies of bacteria forming on a dense nutrient medium. First, we applied the 0.5 McFarland turbidity standard to the daily bacterial culture of the studied strains. Then we reduced concentration of cells to 1×10^6 CFU/ml by serial dilutions, added each plant-based complex to each resulting solution at a ratio of 1 : 10, and spread the resulting mixture on a sterile slide. As a control, we used an inoculum of bacteria in a nutrient broth without the drug. Next, the samples were placed in a thermostat to incubate at +37 °C for 3 hours. After that, the slides were examined under an Axio Scope A1 microscope (Zeiss; Germany) at a magnification of x400. The photos were taken with a professional stationary digital camera AxioCam HRc Rev3 (Zeiss; Germany). We noted the number of bacterial microcolonies that had grown on control and experimental slides on several camera coverages. Whenever the number of microcolonies was twofold or more smaller on experimental slides than on control slides, the respective plant-based complex, in the given form, was considered to produce strong biofilm growth preventing effect.

For statistical analysis of the data, we used MS Excel 2010 (Microsoft; USA), and applied Student's t-test to the results. The results were considered significant at $p < 0.05$.

RESULTS

Investigation of antibacterial properties

Table 1 and Figure 1 present the results of investigation of antibacterial properties.

Description of the results:

1. The most effective product against bacterial flora was

Table 1. Investigation of antibacterial properties of plant-based complexes

Studied object (microorganism)	Number of colonies grown in samples with plant-based complexes (CFU/ml), (M + *m*)							Number of colonies grown in control samples (CFU/ml)
	1	2	3	4	5	6	7	
S. sanguinis	35 ± 5	130 ± 13	120 ± 11	135 ± 15	125 ± 14	33 ± 5	0 ± 1	350 ± 28
S. mitis	7 ± 2	70 ± 6	120 ± 14	125 ± 11	120 ± 9	5 ± 2	0 ± 1	330 ± 31
S. oralis	130 ± 13	125 ± 11	33 ± 5	70 ± 6	65 ± 6	4 ± 1	0 ± 1	340 ± 24
S. salivarius	140 ± 8	55 ± 5	4 ± 2	30 ± 4	25 ± 3	3 ± 1	0 ± 1	280 ± 18
S. aureus	200 ± 18	190 ± 15	0 ± 1	200 ± 17	205 ± 20	0 ± 1	3 ± 1	210 ± 15
E.faecalis	25 ± 4	130 ± 15	90 ± 8	55 ± 6	60 ± 5	30 ± 3	0 ± 1	260 ± 25
K. pneumoniae	20 ± 3	90 ± 6	85 ± 7	5 ± 2	2 ± 1	2 ± 1	0 ± 1	180 ± 15
P. aeruginosa	10 ± 2	4 ± 2	5 ± 2	5 ± 1	6 ± 2	3 ± 1	5 ± 2	160 ± 14
A. baumannii	3 ± 1	15 ± 2	18 ± 3	4 ± 1	5 ± 2	3 ± 1	0 ± 1	150 ± 17

Note: 1 — mouthwash; 2 — gel with chlorophyll, aspen bark and DHQ (Gel 2); 3 — gel with chlorophyll and chlorhexidine (Gel 1); 4 — oil with chlorophyll (Phytolone oil); 5 — oil with carotenoids from fir needles (Provitam oil); 6 — gel with chlorophyll and chlorhexidine (Gel 3); 7 — dental elixir with aspen bark extract and chlorophyll (Elixir)

elixir with 20% of ethyl alcohol (by weight) and maximum concentrations of active ingredients: aspen bark extract, sodium alginate and sodium-copper chlorophyllin.

2. Gel 1 had comparable antibacterial efficacy; its composition includes a chemical antibacterial agent (chlorhexidine) in a bactericidal concentration of 0.12%, and plant-based ingredients (sodium alginate, D-panthenol, allantoin, methyl salicylate, menthol, fir extract, sodium-copper chlorophyllin, eugenol).

3. Gel 3, which had similar but expired 2 years ago, showed average antibacterial activity.

4. Mouthwash and Gel 2 with aspen bark and DHQ were not highly effective against pathogenic flora of periodontium.

5. Oil solutions had poor eliminating effect on the pathogenic flora of periodontium.

Investigation of adhesion preventing properties

Table 2 shows the results of investigation of adhesion preventing properties.

Description of the results:

Elixir and gel with DHQ (Gel 2) showed comparable maximum adhesion preventing effect.

2. Gel with chlorhexidine and mouthwash had an average effect.

3. Oil solutions had poor adhesion preventing effect.

Investigation of biofilm formation preventing properties of plant-based complexes

Figures 2–4 reflect biofilm preventing effect of various forms of products.

Description of the results:

All the products proved to be highly effective in preventing formation of biofilm. Gels (1 and 2) were the most effective.

DISCUSSION

Biofilm tends to change its composition and qualities [1, 8, 20, 21, 23], therefore, it is necessary to evaluate its physical parameters in a particular P patient before starting treatment to more accurately assess the involvement of systemic and general somatic problems, the level of hygienic habits of the patient, personalize treatment plan, factor in phenotypic indicators and achieve the predicted positive clinical result that persists in the long term.

The antibacterial activity of plant-based complexes against pathogenic bacteria of periodontium includes three components: adhesion preventing effect, antibacterial action proper and biolfilm formation preventing effect [2, 8]. Any infectious process of bacterial etiology begins with the adhesion and colonization of the site by microorganisms. Therefore, identification of adhesion preventing capabilities of products used in dental practice translates into the possibility of early prevention, i.e., disallowing adhesion and arrest of colonization. Thus, bacterial invasion is undermined at the first phase of the infectious process, and no biofilm is formed. The studied plant-based complexes were revealed to be highly active against biofilm, such activity significantly reducing the likelihood of appearance of a chronic infection locus in the periodontal area. In turn, direct antibacterial capabilities of the complexes decrease the number of bacteria and renders initiation of the infectious process unlikely [6, 12].

Allegedly, the reasons behind high antiseptic effectiveness of the elixir are 20% of ethyl alcohol in its content (by weight) and high concentrations of plant-based antibacterial components.

Table 2. Investigation of adhesion preventing properties of plant-based complexes

Studied composition	Adhesion index (M + *m*)	
	Control	*S. sanguinis*
1 — Mouthwash	75 + 6	33 + 5
2 — Gel with chlorophyll, aspen bark and DHQ (Gel 2)		24 + 4
3 — Gel with chlorophyll and chlorhexidine (Gel 1)		30 + 5
4 — Oil with chlorophyll (Phytolone oil)		42 + 6
5 — Oil with carotenoids from fir needles (Provitam oil)		37 + 4
6 — Gel with chlorophyll and chlorhexidine (Gel 3)		48 + 5
7 — Elixir with aspen bark extract and chlorophyll (Elixir)		21 + 4

Note: 1 — mouthwash; 2 — gel with chlorophyll, aspen bark and DHQ (Gel 2); 3 — gel with chlorophyll and chlorhexidine (Gel 1); 4 — oil with chlorophyll (Phytolone oil); 5 — oil with carotenoids from fir needles (Provitam oil); 6 — gel with chlorophyll and chlorhexidine (Gel 3); 7 — dental elixir with aspen bark extract and chlorophyll (Elixir).

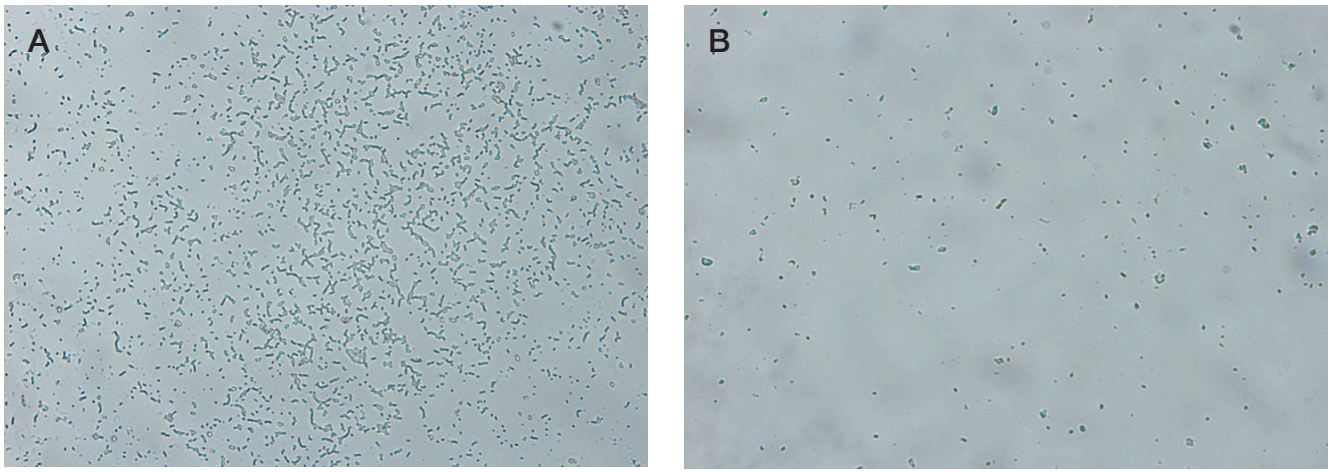

Fig. 2. Biofilm formation preventing properties: Gel 1 vs. *S. sanguinis*. **A**. Colonies of *S. sanguinis* before application of gel with chlorophyll and chlorhexidine. **B**. Colonies of *S. sanguinis* after application of gel with chlorophyll and chlorhexidine (magnification ×400)

The efficacy of Gel 1 is most likely associated with the prolonged release of active ingredients ensured by its unique bioadhesive film-forming base.

As for Gel 3, the expired subject of the experiment, it retained antiseptic properties but its efficacy had decreased compared to the tested gel that had not expired. Likely, the decrease was caused by aging of the components of the base and its rapid degradation, deterioration of the cumulative activity of plant-based complexes, while chlorhexidine remained active as the antiseptic component. This also gives reason to assume the studied composition has a multidirectional combined effect.

Elixir's high adhesion prevention activity is most likely formed by sodium alginate, aspen bark extract and alcohol content, while Gel 2's similar capability stems from sodium alginate, dihydroquercetin and aspen bark extract.

The comparatively lower antiseptic activity of water and oil forms is associated with a low concentration of antibacterial agents (aspen bark extract in the first place) and a short time on the tissues.

The form of the product has a significant effect on the time of exposure of tissues to the active ingredients of plant-based complexes. Gels are the most effective because of the slow and uniform release of the active substances, bioadhesion and development of a film on the gum and mucosa [13–14]. High concentration of active ingredients in water-alcohol solutions also delivers a persistent and long-lasting antibacterial effect, but the time of exposure of periodontal tissues thereto is shorter. The expired gel loses its effect because of the aging of the base due to moisture loss. It is expedient to produce gels in small batches or, in some cases, as a pharmacy-made compounded drug. Base of gels acts in a special way: it adheres to the dried surface of mucosa or gum, remains in the exposure locus for a long time, slowly releases the active ingredients and allows reduction of dosage in the composition; this set of peculiarities calls for additional research.

Thus, the three-stage antibacterial action of plant-based complexes reduces the risk of periodontitis, even in the presence of periodontal pathogenic bacteria in the locus. The use of plant-based complexes in the acute period after professional hygiene, especially if such complexes are part of gels, boosts restoration of the structure and condition of periodontium, normalization of trophism and nutrition, respiration and metabolic processes in the tissues. Used after the arrest of the acute process, plant-based complexes prolong the remission and significantly reduce the risk of repeated exacerbations, their course and repeated tissue damage by infectious agents.

In the acute period, up to days 14 through 21, it is advisable to use a combination of elixir + gel with 0.12% chlorhexidine, and after arrest of the acute process — mouthwash and gel with aspen bark and DHQ [11, 13]. Mouthwash and gel with aspen bark and DHQ can be used to prevent exacerbations in patients with chronic generalized periodontitis since they contain no chemical components bacteria grow resistant to

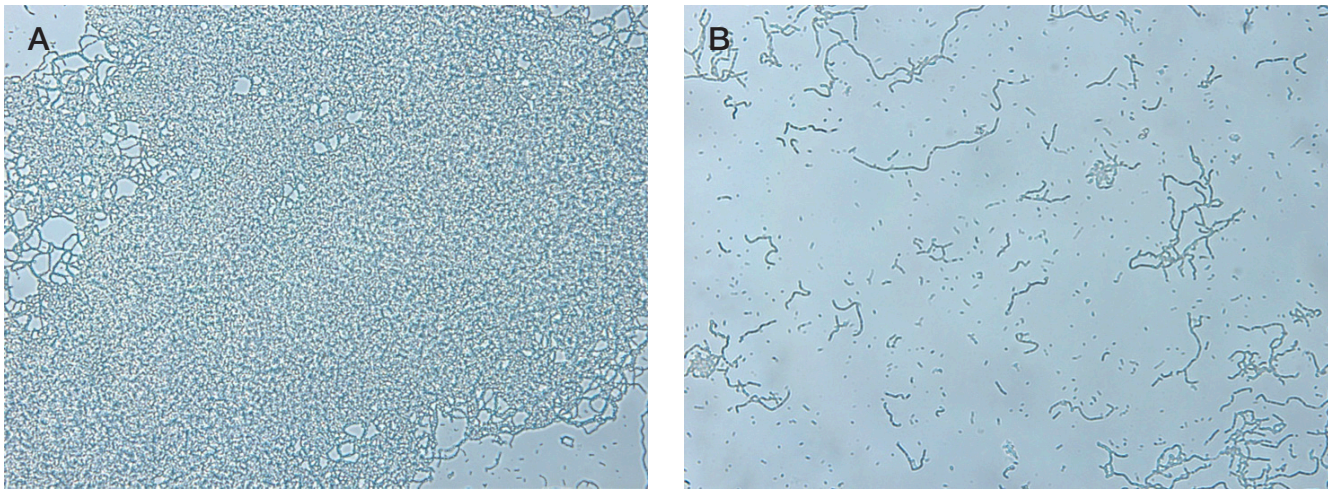

Fig. 3. Biofilm formation preventing properties: mouthwash vs. *S. mitis*. **A**. Colonies of *S. mitis* before use of mouthwash. **B**. Colonies of *S. mitis* after use of mouthwash

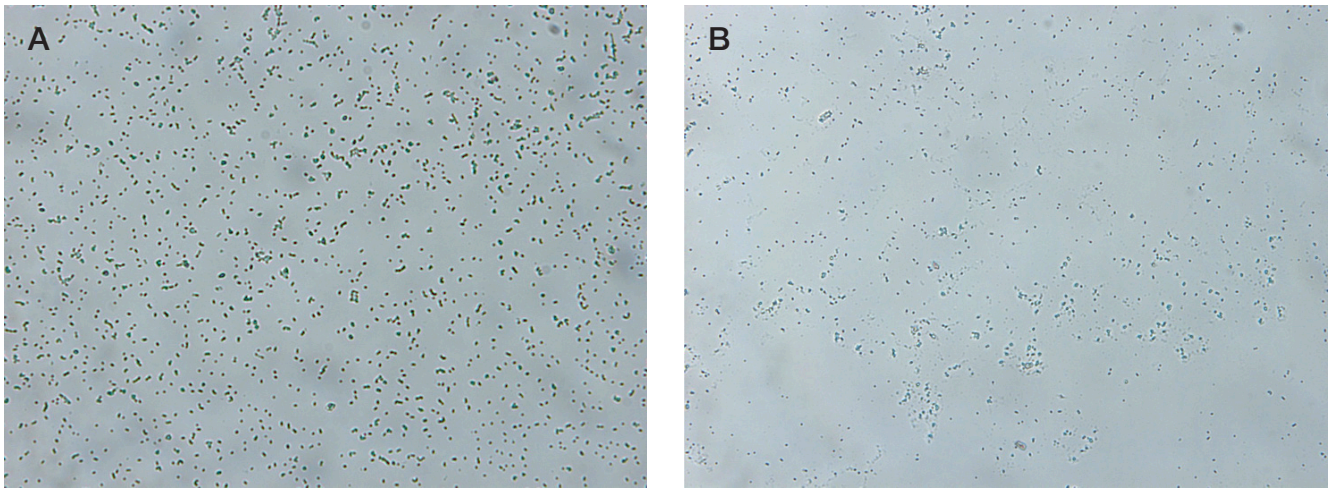

Fig. 4. Biofilm formation preventing properties: Provitam oil vs. *S. oralis*. **A**. Colonies of *S. oralis* before application of oil with fir needle carotenoids. **B**. Colonies of *S. oralis* after application of oil with fir needle carotenoids

while having a non-specific antibacterial effect based on the induced changes in the permeability of bacterial cell wall.

CONCLUSIONS

The studied plant-based complexes in the form of gel have proved to have high antiseptic, adhesion and biofilm formation preventing capabilities. Oil solutions are advisable as part of a complex therapy aimed at diseases of the oral mucosa; elixir and gel with 0.12% chlorophyll and chlorhexidine — as part of a complex therapy of periodontitis; gel with aspen bark and DHQ plus mouthwash — as means of prevention of periodontitis and other gum lesions. It is necessary to continue studying capabilities of plant-based complexes in various forms with titration of concentrations in elixirs compared to mouthwashes, comparison of frequency-dependent effect of application of gels, and determination of when the bacteria become resistant in case of use of gel with a chemical antiseptic. It is important to continue work aimed at *in vitro* evaluation of the biological properties of pathogenic bacteria of periodontium using experimental models of mixed (multi-species) biofilms. Flora of the oral cavity has changed a lot over the past 20 years, with specifics of the regions of residence contributing to the changes. For research activities, it is recommended to first evaluate the actual composition of periodontal pathogenic bacteria in plaque and on the surface of the tooth root, as well as in periodontal fluid.

References

1. Borodulina II, Vasileva LV, Rumakin VP, Kovalevskij AM, Fadeev RA, Grebnev GA. Morfologiya parodontal'nogo karmana pri xronicheskom generalizovannom parodontite srednej stepeni tyazhesti. Medicinskij vestnik Severnogo Kavkaza. 2019; 14: 164–7. Russian.
2. Cepov LM, Goleva NA. Rol' mikroflory v vozniknovenii vospalitel'nyx zabolevanij parodonta. Parodontologiya. 2009; 1: 7–12. Russian.
3. Tonetti, MS, Van Dyke TE. Periodontitis and atherosclerotic cardiovascular disease: consensus report of the Joint EFPA. AP Workshop on Periodontitis and Systemic Diseases. J Periodontol. 2013; 84 (4): 24–29.
4. Kardanova LV, Txazaplizheva MT, Balkarov AO. Nekotorye aspekty mestnogo lecheniya xronicheskix vospalitel'nyx zabolevanij parodonta. Sovremennye problemy nauki i obrazovaniya. 2014; 6: 1048–54. Russian.
5. Iordanishvili AK, Kovalevskij AM. Fakul'tetskaya stomatologiya: rukovodstvo dlya vrachej-stomatologov. M.: SIMK, 2015; 504 s. Russian.
6. Txazaplizheva MT, Batyrbekova FR. Sravnitel'naya ocenka ehffektivnosti izolirovannogo i sochetannogo primeneniya xlorgeksidina i nizkochastotnogo ul'trazvuka v kompleksnom lechenii parodontita srednej stepeni tyazhesti. Materialy V Vsemirnogo kongressa po immunologii i allergii. Allergologiya i immunologiya. 2007; 8 (1): 145. Russian.
7. Barnett ML. The rationale for the daily use of an antimicrobial mouthrinse J Am Dent Assoc. 2006; 137: 16–21.
8. Teles RP, Teles FRF. Antimicrobial agents used in the control of periodontal biofilms: effective adjuncts to mechanical plaque control. Braz Oral Res. 2009; 23 (1): 39–48.
9. Nikolaev AI, Cepov LM. Prakticheskaya stomatologiya: ucheb. posobie. M.: MEDpress-inform, 2018; 928 s. Russian.
10. Kiyun ID. Sravnitel'noe issledovanie otbelivayushhix zubnyx past s umerennoj abrazivnost'yu. Molodoj uchenyj. 2015; 6: 274–7. Russian.
11. Fedorov YuA, Drozhzhina V. A. Profilaktika stomatologicheskix zabolevanij. V kn.: V. A. Kozlov, redaktor. Stomatologiya: uchebnik dlya medicinskix vuzov i posldiplomnoj podgotovki specialistov. SPb.: SpecLit, 2011; 36–67. Russian.
12. Dzhioeva RF. Klinicheskaya ehffektivnost' fitoterapii pri lechenii xronicheskogo generalizovannogo parodontita. Vestnik medicinskogo stomatologicheskogo instituta. 2013; 4 (27): 27–29. Russian.
13. Ulitovskij SB. Poloskaniya dlya rta ili zhidkie sredstva gigieny rta. SPb.: Chelovek, 2017; 192 s. Russian.
14. Ulitovskij SB. Sredstva individual'noj gigieny rta: uchebnik dlya poslediplom. obrazovaniya. M.: Spec. izd-vo med. kn., 2018; 200 s. Russian.
15. Drozhzhina VA, Petrishhev NN, Fedorov YuA. Povyshenie fiziologicheskoj rezistentnosti tkanej parodonta belyx krys pri dejstvii biologicheski aktivnyx veshhestv laminarii. Fiziol. zhurnal. 1995; 81 (2): 126–33. Russian.
16. Blinova KF, Yakovlev GP, redaktory. Botaniko-farmakognosticheskij slovar'. M.: Vysshaya shkola, 1990; 272 s. Russian.
17. Blinova KF, Yakovlev GP, redaktory. Botaniko-farmakognosticheskij slovar'. M.: Vysshaya shkola, 1990; 272 s. Russian.
18. Lobanova IYu, Tureckova VF, Zverev YaF, Talalaeva OS. Izuchenie ostroj toksichnosti i antioksidantnoj aktivnosti ehkstrakta list'ev osiny suxogo. Fundamental'nye issledovaniya. 2012; 9: 308–12. Russian.

19. Belyackaya AV, Kashlikova IM, Elagina AO, Krasnyuk (ml.) II, Krasnyuk II, Stepanova O. I. Nitrofurany dlya naruzhnogo primeneniya. Razrabotka i registraciya lekarstvennyx sredstv. 2019; 8 (2): 38–47. Russian.
20. He X, Hu W, Kaplan CW, Guo L, Shi W, Lux R. Adherence to streptococci facilitates Fusobacterium nucleatum integration into an oral microbial community. Microb Ecol. 2012; 63 (3): 532–42. DOI: 10.1007/s00248-011-9989-2.
21. Zhu B, Macleod LC, Kitten T, Xu P. Streptococcus sanguinis biofilm formation & interaction with oral pathogens. Future Microbiol. 2018; 13 (8): 915–32. DOI: 10.2217/fmb-2018-0043.
22. Kumarasamy B, Manipal S, Duraisamy P, Ahmed A, Mohanaganesh S, Jeevika C. Role of aqueous extract of morinda citrifolia (Indian noni) ripe fruits in inhibiting dental caries-causing streptococcus mutans and streptococcus mitis. J Dent (Tehran). 2014; 11 (6): 703–10.
23. Cabal B, Cafini F, Esteban-Tejeda L, et al. Inhibitory effect on in vitro Streptococcus oralis biofilm of a soda-lime glass containing silver nanoparticles coating on titanium alloy. PLoS One. 2012; 7 (8): e42393. DOI: 10.1371/journal.pone.0042393.
24. Mirpour M, Gholizadeh Siahmazgi Z, Sharifi Kiasaraie M. Antibacterial activity of clove, gall nut methanolic and ethanolic extracts on Streptococcus mutans PTCC 1683 and Streptococcus salivarius PTCC 1448. J Oral Biol Craniofac Res. 2015; 5 (1): 7–10. DOI: 10.1016/j.jobcr.2015.02.002.
25. Wu S, Liu Y, Zhang H, Lei L. Nano-graphene oxide with antisense walR RNA inhibits the pathogenicity of Enterococcus faecalis in periapical periodontitis. J Dent Sci. 2020; 15 (1): 65–74. DOI: 10.1016/j.jds.2019.09.006.
26. Lee J, Lee JB, Song HY, et al. Diagnostic Models for Screening of Periodontitis with Inflammatory Mediators and Microbial Profiles in Saliva. Diagnostics (Basel). 2020; 10 (10): 820. DOI: 10.3390/diagnostics10100820/.
27. Cai Z, Zhu T, Liu F, Zhuang Z, Zhao L. Co-pathogens in Periodontitis and Inflammatory Bowel Disease. Front Med (Lausanne). 2021; 8: 723719. DOI: 10.3389/fmed.2021.723719.
28. Li Q, Wang H, Tan L, et al. Oral Pathogen Fusobacterium nucleatum Coaggregates With Pseudomonas aeruginosa to Modulate the Inflammatory Cytotoxicity of Pulmonary Epithelial Cells. Front Cell Infect Microbiol. 2021; 11: 643913. DOI: 10.3389/fcimb.2021.643913.
29. Richards AM, Abu Kwaik Y, Lamont RJ. Code blue: Acinetobacter baumannii, a nosocomial pathogen with a role in the oral cavity. Mol Oral Microbiol. 2015; 30 (1): 2–15. DOI: 10.1111/omi.12072.
30. Kovalevskij AM, Latif II, Kovalevskij VA, Sharov AN, Nosova MA, Nekrasova VB, avtory; OOO «FITOLON-NAUKA», patentoobladatel'. Kompoziciya v forme gelya dlya uxoda za tkanyami polosti rta. Patent RF # 2733718 ot 06.10.2020. Russian.
31. Nikitenko VV, Kovalevskij AM, Latif II. Ehffektivnost' primeneniya kompozicii v forme gelya s ehkstraktom kory osiny i xlorofillom dlya lecheniya i profilaktiki vospalitel'nyx zabolevanij parodonta. V sbornike: V. V. Nikitenko, V.A. Zheleznyak, redaktory. Materialy nauchno-prakticheskoj konferencii «Aktual'nye voprosy teoreticheskoj i prakticheskoj stomatologii», 7-8 oktyabrya 2021 g. SPb., 2021; 128–33. Russian.
32. Latif II, Kovalevskij AM, Nosova MA, Sharov AN, Kraeva LA. Ocenka ehffektivnosti gelevoj kompozicii dlya uxoda tkanyami polosti rta. Stomatologicheskaya vesna v Belgorode — 2022: sbornik trudov Mezhdunarodnoj nauchno-prakticheskoj konferencii k 100-letiyu MGMSU. Belgorod: «BelGU», 2022; 276 s. Russian.
33. Blagonravova AS, Afonin AN, Vorobeva ON, Shirokova IYu. Sravnitel'nyj analiz adgezivnosti mikroorganizmov, vydelennyx ot bol'nyx i s ob"ektov vneshnej sredy lechebno-profilakticheskix uchrezhdenij. Medicinskij al'manax. 2011; 5 (18): 215–8. Russian.

Литература

1. Бородулина И. И., Васильева Л. В., Румакин В. П., Ковалевский А. М., Фадеев Р. А., Гребнев Г. А. Морфология пародонтального кармана при хроническом генерализованном пародонтите средней степени тяжести. Медицинский вестник Северного Кавказа. 2019; 14: 164–7.
2. Цепов Л. М., Голева Н. А. Роль микрофлоры в возникновении воспалительных заболеваний пародонта. Пародонтология. 2009; 1: 7–12.
3. Tonetti, MS, Van Dyke TE. Periodontitis and atherosclerotic cardiovascular disease: consensus report of the Joint EFPA. AP Workshop on Periodontitis and Systemic Diseases. J Periodontol. 2013; 84 (4): 24–29.
4. Карданова Л. В., Тхазаплижева М. Т., Балкаров А. О. Некоторые аспекты местного лечения хронических воспалительных заболеваний пародонта. Современные проблемы науки и образования. 2014; 6: 1048–54.
5. Иорданишвили А. К., Ковалевский А. М. Факультетская стоматология: руководство для врачей-стоматологов. М.: СИМК, 2015; 504 с.
6. Тхазаплижева, М. Т., Батырбекова Ф. Р. Сравнительная оценка эффективности изолированного и сочетанного применения хлоргексидина и низкочастотного ультразвука в комплексном лечении пародонтита средней степени тяжести. Материалы V Всемирного конгресса по иммунологии и аллергии. Аллергология и иммунология. 2007; 8 (1): 145.
7. Barnett ML. The rationale for the daily use of an antimicrobial mouthrinse J Am Dent Assoc. 2006; 137: 16–21.
8. Teles RP, Teles FRF. Antimicrobial agents used in the control of periodontal biofilms: effective adjuncts to mechanical plaque control. Braz Oral Res. 2009; 23 (1): 39–48.
9. Николаев А. И., Цепов Л. М. Практическая стоматология: учеб. пособие. М.: МЕДпресс-информ, 2018; 928 с.
10. Киюн И. Д. Сравнительное исследование отбеливающих зубных паст с умеренной абразивностью. Молодой ученый. 2015; 6: 274–7.
11. Федоров Ю. А., Дрожжина В. А. Профилактика стоматологических заболеваний. В кн.: В. А. Козлов, редактор. Стоматология: учебник для медицинских вузов и последипломной подготовки специалистов. СПб.: СпецЛит, 2011; 36–67.
12. Джиоева Р. Ф. Клиническая эффективность фитотерапии при лечении хронического генерализованного пародонтита. Вестник медицинского стоматологического института. 2013; 4 (27): 27–29.
13. Улитовский С. Б. Полоскания для рта или жидкие средства гигиены рта. СПб.: Человек, 2017; 192 с.
14. Улитовский С. Б. Средства индивидуальной гигиены рта: учебник для последиплом. образования. М.: Спец. изд-во мед. кн., 2018; 200 с.
15. Дрожжина В. А., Петрищев Н. Н., Федоров Ю. А. Повышение физиологической резистентности тканей пародонта белых крыс при действии биологически активных веществ ламинарии. Физиол. журнал. 1995; 81 (2): 126–33.
16. Блинова К. Ф., Яковлев Г. П., редакторы. Ботанико-фармакогностический словарь. М.: Высшая школа, 1990; 272 с.
17. Дейнеко И. П., Фаустова Н. М. Элементарный и групповой химический состав коры и древесины сосны. Химия растительного сырья. 2015; 1: 51–62.
18. Лобанова И. Ю., Турецкова В. Ф., Зверев Я. Ф., Талалаева О. С. Изучение острой токсичности и антиоксидантной активности экстракта листьев осины сухого. Фундаментальные исследования. 2012; 9: 308–12.
19. Беляцкая А. В., Кашликова И. М., Елагина А. О., Краснюк (мл.) И. И., Краснюк И. И., Степанова О. И. Нитрофураны для наружного применения. Разработка и регистрация лекарственных средств. 2019; 8 (2): 38–47.
20. He X, Hu W, Kaplan CW, Guo L, Shi W, Lux R. Adherence to streptococci facilitates Fusobacterium nucleatum integration into an oral microbial community. Microb Ecol. 2012; 63 (3): 532–42. DOI: 10.1007/s00248-011-9989-2.

21. Zhu B, Macleod LC, Kitten T, Xu P. Streptococcus sanguinis biofilm formation & interaction with oral pathogens. Future Microbiol. 2018; 13 (8): 915–32. DOI: 10.2217/fmb-2018-0043.
22. Kumarasamy B, Manipal S, Duraisamy P, Ahmed A, Mohanaganesh S, Jeevika C. Role of aqueous extract of morinda citrifolia (Indian noni) ripe fruits in inhibiting dental caries-causing streptococcus mutans and streptococcus mitis. J Dent (Tehran). 2014; 11 (6): 703–10.
23. Cabal B, Cafini F, Esteban-Tejeda L, et al. Inhibitory effect on in vitro Streptococcus oralis biofilm of a soda-lime glass containing silver nanoparticles coating on titanium alloy. PLoS One. 2012; 7 (8): e42393. DOI: 10.1371/journal.pone.0042393.
24. Mirpour M, Gholizadeh Siahmazgi Z, Sharifi Kiasaraie M. Antibacterial activity of clove, gall nut methanolic and ethanolic extracts on Streptococcus mutans PTCC 1683 and Streptococcus salivarius PTCC 1448. J Oral Biol Craniofac Res. 2015; 5 (1): 7–10. DOI: 10.1016/j.jobcr.2015.02.002.
25. Wu S, Liu Y, Zhang H, Lei L. Nano-graphene oxide with antisense walR RNA inhibits the pathogenicity of Enterococcus faecalis in periapical periodontitis. J Dent Sci. 2020; 15 (1): 65–74. DOI: 10.1016/j.jds.2019.09.006.
26. Lee J, Lee JB, Song HY, et al. Diagnostic Models for Screening of Periodontitis with Inflammatory Mediators and Microbial Profiles in Saliva. Diagnostics (Basel). 2020; 10 (10): 820. DOI: 10.3390/diagnostics10100820/.
27. Cai Z, Zhu T, Liu F, Zhuang Z, Zhao L. Co-pathogens in Periodontitis and Inflammatory Bowel Disease. Front Med (Lausanne). 2021; 8: 723719. DOI: 10.3389/fmed.2021.723719.
28. Li Q, Wang H, Tan L, et al. Oral Pathogen Fusobacterium nucleatum Coaggregates With Pseudomonas aeruginosa to Modulate the Inflammatory Cytotoxicity of Pulmonary Epithelial Cells. Front Cell Infect Microbiol. 2021; 11: 643913. DOI: 10.3389/fcimb.2021.643913.
29. Richards AM, Abu Kwaik Y, Lamont RJ. Code blue: Acinetobacter baumannii, a nosocomial pathogen with a role in the oral cavity. Mol Oral Microbiol. 2015; 30 (1): 2–15. DOI: 10.1111/omi.12072.
30. Ковалевский А. М., Латиф И. И., Ковалевский В. А., Шаров А. Н., Носова М. А., Некрасова В. Б., авторы; ООО «ФИТОЛОН-НАУКА», патентообладатель. Композиция в форме геля для ухода за тканями полости рта. Патент РФ № 2733718 от 06.10.2020.
31. Никитенко В. В., Ковалевский А. М., Латиф И. И. Эффективность применения композиции в форме геля с экстрактом коры осины и хлорофиллом для лечения и профилактики воспалительных заболеваний пародонта. В сборнике: В. В. Никитенко, В. А. Железняк, редакторы. Материалы научно-практической конференции «Актуальные вопросы теоретической и практической стоматологии», 7-8 октября 2021 г. СПб., 2021; 128–33.
32. Латиф И. И., Ковалевский А. М., Носова М. А., Шаров А. Н., Краева Л. А. Оценка эффективности гелевой композиции для ухода тканями полости рта. Стоматологическая весна в Белгороде — 2022: сборник трудов Международной научно-практической конференции к 100-летию МГМСУ. Белгород: «БелГУ», 2022; 276 с.
33. Благонравова А. С., Афонин А. Н., Воробьева О. Н., Широкова И. Ю. Сравнительный анализ адгезивности микроорганизмов, выделенных от больных и с объектов внешней среды лечебно-профилактических учреждений. Медицинский альманах. 2011; 5 (18): 215–8.